frontiers | Research Topics

The strong adaptability of insects shaped by plasticity

Edited by
Jia Fan, Yong Liu, Fengqi Li, Frédéric Francis and Feng Shang

Published in
Frontiers in Physiology

ISSN 1664-8714
ISBN 978-2-8325-3831-9
DOI 10.3389/978-2-8325-3831-9

About Frontiers

Frontiers is more than just an open access publisher of scholarly articles: it is a pioneering approach to the world of academia, radically improving the way scholarly research is managed. The grand vision of Frontiers is a world where all people have an equal opportunity to seek, share and generate knowledge. Frontiers provides immediate and permanent online open access to all its publications, but this alone is not enough to realize our grand goals.

Frontiers journal series

The Frontiers journal series is a multi-tier and interdisciplinary set of open-access, online journals, promising a paradigm shift from the current review, selection and dissemination processes in academic publishing. All Frontiers journals are driven by researchers for researchers; therefore, they constitute a service to the scholarly community. At the same time, the *Frontiers journal series* operates on a revolutionary invention, the tiered publishing system, initially addressing specific communities of scholars, and gradually climbing up to broader public understanding, thus serving the interests of the lay society, too.

Dedication to quality

Each Frontiers article is a landmark of the highest quality, thanks to genuinely collaborative interactions between authors and review editors, who include some of the world's best academicians. Research must be certified by peers before entering a stream of knowledge that may eventually reach the public - and shape society; therefore, Frontiers only applies the most rigorous and unbiased reviews. Frontiers revolutionizes research publishing by freely delivering the most outstanding research, evaluated with no bias from both the academic and social point of view. By applying the most advanced information technologies, Frontiers is catapulting scholarly publishing into a new generation.

What are Frontiers Research Topics?

Frontiers Research Topics are very popular trademarks of the *Frontiers journals series*: they are collections of at least ten articles, all centered on a particular subject. With their unique mix of varied contributions from Original Research to Review Articles, Frontiers Research Topics unify the most influential researchers, the latest key findings and historical advances in a hot research area.

Find out more on how to host your own Frontiers Research Topic or contribute to one as an author by contacting the Frontiers editorial office: frontiersin.org/about/contact

The strong adaptability of insects shaped by plasticity

Topic editors

Jia Fan — State Key Laboratory for Biology of Plant Diseases and Insect Pests, Institute of Plant Protection (CAAS), China

Yong Liu — Shandong Agricultural University, China

Fengqi Li — Guizhou University, China

Frédéric Francis — University of Liège, Belgium

Feng Shang — Southwest University, China

Citation

Fan, J., Liu, Y., Li, F., Francis, F., Shang, F., eds. (2023). *The strong adaptability of insects shaped by plasticity*. Lausanne: Frontiers Media SA.

doi: 10.3389/978-2-8325-3831-9

Table of contents

frontiers | Frontiers in Physiology

TYPE Original Research
PUBLISHED 11 January 2023
DOI 10.3389/fphys.2022.1079328

OPEN ACCESS

EDITED BY
Jia Fan,
Institute of Plant Protection (CAAS), China

REVIEWED BY
Feng Shang,
Southwest University, China
Wenjuan Yu,
Sichuan Academy of Agricultural Sciences, China
Fangmei Zhang,
Xinyang Agriculture and Forestry University, China

*CORRESPONDENCE
Qi Chen,
chenq766@nenu.edu.cn
Bingzhong Ren,
bzren@nenu.edu.cn

SPECIALTY SECTION
This article was submitted to Invertebrate Physiology, a section of the journal Frontiers in Physiology

RECEIVED 25 October 2022
ACCEPTED 29 December 2022
PUBLISHED 11 January 2023

CITATION
Lu Y, Wang Z, Lin F, Ma Y, Kang J, Fu Y, Huang M, Zhao Z, Zhang J, Chen Q and Ren B (2023), Screening and identification of genes associated with flight muscle histolysis of the house cricket *Acheta domesticus*. *Front. Physiol.* 13:1079328. doi: 10.3389/fphys.2022.1079328

Screening and identification of genes associated with flight muscle histolysis of the house cricket *Acheta domesticus*

Ying Lu[1,2], Zizhuo Wang[2], Fei Lin[2], Yuqing Ma[2], Jiangyan Kang[1], Yuying Fu[2], Minjia Huang[2], Zhuo Zhao[3], Junjie Zhang[4], Qi Chen[2]* and Bingzhong Ren[2]*

[1]Key Laboratory of Economical and Applied Entomology of the Education Department of Liaoning Province, College of Plant Protection, Shenyang Agricultural University, Shenyang, China, [2]Jilin Provincial Key Laboratory of Animal Resource Conservation and Utilization, Key Laboratory of Vegetation Ecology, Ministry of Education, School of Life Sciences, Northeast Normal University, Changchun, China, [3]College of Life Sciences, Jilin Normal University, Siping, China, [4]Engineering Research Center of Natural Enemies, Institute of Biological Control, Jilin Agricultural University, Changchun, China

Introduction: Flight muscle histolysis, as an important survival strategy, is a widespread phenomenon in insects and facilitates adaptation to the external environment in various insect taxa. However, the regulatory mechanism underlying this phenomenon in Orthoptera remains unknown.

Methods: In this study, the flight muscle histolysis in the house cricket *Acheta domesticus* was investigated by transcriptomics and RNA interference.

Results: The results showed that flight muscle histolysis in *A. domesticus* was standard and peaked within 9 days after eclosion of adult crickets, and there was no significant difference in the peak time or morphology of flight muscle histolysis between males and females. In addition, the differentially expressed genes between before and after flight muscle histolysis were studied, of which AdomFABP, AdomTroponin T and AdomActin were identified as candidate genes, and after injecting the dsRNA of these three candidates, only the downregulated expression of AdomFABP led to flight muscle histolysis in *A. domesticus*. Furthermore, the expression level of *AdomFABP* was compared between before and after flight muscle histolysis based on RT-qPCR.

Disscussion: We speculated that *AdomFABP* might play a role in the degradation of flight muscle by inhibiting muscle development. Our findings laid a molecular foundation for understanding the flight muscle histolysis.

KEYWORDS

flight muscle histolysis, cricket, transcriptomics, FABP, RNA interference

1 Introduction

In insects, flight muscles are responsible for that power flight movement (Snelling et al., 2012; Ding et al., 2014; Lu et al., 2020). Numerous studies on flight muscle have been reported in various insect taxa, such as oriental armyworm (*Mythimna separata*) and some species of locusts (*Locusta migratoria manilensis*, *Oedaleus asiaticus* and *Calliptamus italicus*) (Luo, 1996; Liu et al., 2008; Dou et al., 2017; Han et al., 2020). The research mainly focused on three aspects. The relationships between flight muscle and flight ability

and between energy accumulation and consumption during flying (Liu et al., 2008; Dou et al., 2017; Cao and Jin, 2020). The relationship between flight muscle development and reproductive system development (Roff and Fairbairn, 2007; Zhao et al., 2010; Chang et al., 2021; Guo et al., 2022), especially the trade-off between flight capability and reproduction in female insects (Ge et al., 2021). (3) The effects of insecticides on flight muscles in the context of pest control (Liu et al., 2017).

Flight muscle histolysis is an important survival strategy for many insects; it allows them to conserve and utilize compounds and energy and adapt to changes in the external environment after their flight muscles have fully developed (Kobayashi and Ishikawa, 1994). Flight muscle histolysis occurs not only after the end of migration but also when wing dimorphism arises, as observed in the cricket *Velarifictorus asperses* and the butterfly *Pieris napi* (Stjernholm and Karlsson, 2008; Zeng et al., 2012; Zhang et al., 2019). Therefore, studying flight muscle histolysis can provide a better understanding of migration patterns, population dynamics, reproductive signals and wing dimorphism in insects.

To date, many studies have focused on the physiological basis of insect flight muscle histolysis through investigations of muscle composition, morphological differences between before and after flight muscle histolysis, physiological significance and other aspects (Stjernholm and Karlsson, 2008; Gibbs and Van Dyck, 2010; Chaulk et al., 2014; Liu et al., 2017; Matte and Bliien, 2021; Kurihara et al., 2022). For example, a decrease in protein content in flight muscle of the pea aphid *Acyrthosiphon pisum* has been found to occur simultaneously with flight muscle histolysis (Kobayashi and Ishikawa, 1994). Other studies have focused on the physiological and molecular mechanisms underlying flight muscle histolysis by investigating the factors affecting flight muscle histolysis, the relationship between flight muscle histolysis and apoptosis, and other aspects (Tanaka, 1994; Domingo et al., 1998; Fyrberg et al., 1998; Nongthomba et al., 2001; Wu and Haunerland, 2001; Zera and Cisper, 2001; Wu et al., 2002; Gajewski et al., 2006; Azizi et al., 2009; Feng et al., 2019; Katti et al., 2021; Bai et al., 2022). For example, the flight muscle histolysis in both the fire ant *Solenopsis invicta* and the wheat aphid *Sitobion avenae* occurs through apoptosis (Azizi et al., 2009; Feng et al., 2019). Juvenile hormone (JH) can affect the development and degradation of flight muscle in *Modicogryllus confirmatus* (Tanaka, 1994), *Gryllus firmus* (Zera and Cisper, 2001), and *Acyrthosiphon pisum* (Bai et al., 2022). Mitochondria, as organelles supplying energy to the body, can also influence and regulate the formation and degradation of flight muscles by regulating their own fusion and fission (Katti et al., 2021). In addition, there are studies that say due to troponin and actin are important structural proteins involved in the assembly and regulation of myofibrillar fibers, so as to the expression of genes encoding troponin and actin can determine the structural and functional integrity of flight muscles (Domingo et al., 1998; Fyrberg et al., 1998; Nongthomba et al., 2001; Gajewski et al., 2006). And lipid-related genes that regulate the expression of lipid substances also play a very important role in the degradation of flight muscle, because of lipids are among the necessary energy substances for insect flight activities (Wu and Haunerland, 2001; Wu et al., 2002). However, since the degradation of flight muscle is affected to varying degrees by a variety of factors, the regulatory pathways of flight muscle histolysis are poorly understood.

The house cricket *Acheta domesticus* Linnaeus (Orthoptera: Gryllidae) is widely distributed worldwide and has a wide range of food habits. *A. domesticus* is an excellent and often used model organism due to its many advantages, such as its small size, ease of rearing, short life cycle, nutrient richness, lack of diapause, high tolerance and ease of handling (Clifford et al., 1977; Crocker and Hunter, 2018). These advantages make this species ideal for research on the development and utilization of edible and forage insects (Patton, 1978; Grossmann et al., 2021; Khatun et al., 2021), immune regulation (Piñera et al., 2013), adult neurogenesis (Cayre et al., 2007), and other topics (Nelson and Nolen, 1997; Fuciarelli and Rollo, 2020; Deban and Anderson, 2021; Li and Rollo, 2021). Moreover, after *A. domesticus* eclosion, their flight muscles degraded, and some but not all individuals shed their hind wings, resulting in wing dimorphism. Therefore, *A. domesticus* is an ideal model organism for studying insect wing dimorphism as well as flight muscle histolysis (Chen et al., 2019). Studies on *A. domesticus* have revealed that flight muscle cell apoptosis could be regulated by hormones and lead to histolysis (Oliver et al., 2007); however, the regulatory pathways and signaling pathways that are activated during flight muscle histolysis and the functions of key genes during this process in *A. domesticus* remain unknown. Therefore, the aim of our study was to investigate the molecular mechanism underlying flight muscle histolysis in the house cricket *A. domesticus* through transcriptomics and RNA interference (RNAi). Our findings provided new insight into flight muscle histolysis in Orthoptera at the gene level.

2 Materials and methods

2.1 Insects

The house cricket *A. domesticus* was obtained from a commercial colony (Beijing, Sanyuanxishuai, China) and reared in the entomology laboratory of Northeast Normal University starting in early 2015 (Changchun, China). After diapause at 2°C–4°C for approximately 1 week, the eggs were incubated in an artificial climate chamber (BIC 300, Boxun, Shanghai) at 25°C. After hatching, the nymphs were reared in an insect culture chamber at 30°C and 30% relative humidity in the dark. Before eclosion, the nymphs were reared in large rearing boxes (53 cm × 38 cm × 33 cm) at a density of 600~700 crickets per box. The nymphs were fed daily with 600 g of carrots and 30 g of mixed nutrient powder (composed of 35% crude wheat bran, 20% corn starch, 20% soybean flour, 15% skim milk powder, 5% active dry yeast and 5% animal liver meal) per box. After eclosion into adults, the crickets were maintained in small rearing boxes (17 cm × 11.5 cm × 6 cm), each containing 20 individuals at a female:male ratio of 1:1. Each box of crickets was provided with 100 g (1 cm^3) of carrots mixed with 5 g of nutrient powder each day.

2.2 Study on flight muscle histolysis of *A. domesticus*

The newly eclosed adults were housed in rearing boxes (17 cm × 11.5 cm × 6 cm), each containing 20 individuals at a female:male ratio of 1:1. In this study, 30 boxes containing a total of 600 adult crickets (ten boxes in a set, with three replicates) were provided with the same adult diet as described above. To maintain a constant rearing density, spare individuals housed under similar conditions were used to replace the dead crickets in the experience groups.

Flight muscle histolysis in *A. domesticus* was observed daily on 0 to 11th days after eclosion, and 10 individual crickets with similar body

sizes were used for observation each day. The crickets selected for observation were frozen at −20°C for 10 min and then thawed at room temperature (25°C) for 2 min. After that, the fore and hind wings were all removed with curved forceps under a stereomicroscope. Then, forceps were used along the end of the abdomen, and all the integument was completely removed up to the pronotum, exposing the dorsal longitudinal muscles (DLMs). The changes in the dorsal and abdominal longitudinal muscles from before to after flight muscle histolysis were evaluated. Each side of the DLMs was approximated as a rectangle. The length, width (at the widest point) and height of each of the left and right DLMs were measured by vernier caliper in this study. Then, the mean volume of the left and right DLMs was calculated and used as the volume of the flight muscle of the house crickets. Finally, according to the daily observations of the DLM volumes of all of the house crickets, the volume changes in the degradation process of flight muscle were obtained. To visualize the volume variation from before to after flight muscle histolysis, this study divided the degradation process of flight muscle of *A. domesticus* into four stages: 0–2 days for non-degradation (Stage I), 3–5 days for early degradation (Stage II), 6–8 days for late degradation (Stage III), and 9–11 days for total degradation (Stage IV). Thirty individual crickets with similar body sizes were used for volume determinations each day, observations were conducted on 3 days for each stage, and a total of 90 individuals were used for volume determinations in each stage.

2.3 Transcriptome sequencing of *A. domesticus* flight muscle

2.3.1 Collection of flight muscle samples

Based on the degradation of flight muscle observed in the previous experiment, two sampling stages were determined: before flight muscle histolysis (day 0 after eclosion, abbreviated as O1) and after flight muscle histolysis (day 10 after eclosion, abbreviated as R1). DLM samples were collected at these two time points using the sampling method described in Section 2.2. After removal of the trachea, the DLMs were cleaned in PBS buffer and then placed in 2 mL sealed lyophilized tubes for storage. After labeling, the lyophilized tubes were frozen in liquid nitrogen for 30 min and finally stored in a −80°C freezer until RNA extraction. A total of at least 2000 female house crickets were raised for sampling in two periods (O1 and R1). All of the house crickets used for transcriptome sequencing were female.

2.3.2 RNA extraction and sequencing of flight muscle samples

According to the above two sampling stages (O1 and R1) and the sampling requirements to determine the developmental status of the DLMs, RNA extraction of the DLM samples was carried out in batches. Total RNA was extracted from each cricket by TRIzol reagent (Invitrogen, Carlsbad, CA, United States). The quality and concentration of the total RNA in each sample were assessed by preliminary purification. Only the samples of extracted RNA that met the sequencing conditions (based on the electrophoresis results) were mailed to Beckman Coulter, Inc. (Biomarker, Beijing) for transcriptome sequencing. After the mRNA was highly purified with magnetic oligo(dT) beads, the NEBNext Ultra RNA Library Prep Kit with six-base random primers (random hexamers) was used for RNA-seq library preparation. Library purification was performed by using AMPure XP Beads. A HiSeq 4000 platform (Illumina, New England Biolabs, Ipswich, MA, United States) was used for high-throughput sequencing with the PE150 read type.

2.4 Data analysis

2.4.1 Sequence assembly and functional annotation

High-quality clean reads were obtained by removing duplicated sequences, adaptor sequences, low-quality reads and ambiguous reads (reads with unknown ('N') nucleotides). Transcriptomes were *de novo* assembled separately using Trinity (http://trinityrnaseq.sourceforge.net/). Assembly version: r20131110. Assembly parameters: the shortest length of the assembled contig is 200; the length of the inserted contig is 500; other values are the default. A total of 36,163 Unigene were obtained by assembly, and the N50 of Unigene was 2,274, showing high assembly integrity. The unigenes were first annotated in the National Center for Biotechnology Information (NCBI) non-redundant protein sequence database (NR), the protein sequence database Swiss-Prot; and the Gene Ontology (GO), Clusters of Orthologous Genes (COG), Eukaryotic Orthologous Groups (KOG), evolutionary genealogy of genes: Non-supervised Orthologous Groups (eggNOG), and Kyoto Encyclopedia of Genes and Genomes (KEGG) databases. In this study, 13,449 annotated unigenes were obtained by selecting BLAST parameter E-value not greater than 1e-5 and HMMER parameter E-value not greater than 1e-10. Then, BLAST searches of the NR database were performed to explore the candidate genes related to flight muscle histolysis in *A. domesticus*.

2.4.2 Differential gene expression analysis

Gene expression was determined by the fragments per kb per million reads (FPKM) method. Differential expression analysis was performed with the help of DESeq (http://www.bioconductor.org/packages/release/bioc/html/DESeq.html), followed by a false discovery rate (FDR) test using the Benjamini-Hochberg (BH) procedure and *p*-value correction for the obtained datasets. The *p*-value correction was applied to Pearson's correlation analyses to confirm the reliability of the replicates. In addition, the analysis of differentially expressed genes (DEGs) between before and after degradation of *A. domesticus* flight muscle was performed by comparing data between the two stages (O1 and R1).

2.5 Identification and validation of candidate genes associated with flight muscle histolysis in *A. domesticus*

2.5.1 Identification of the candidate genes

The transcriptome was sequenced before and after flight muscle histolysis based on the flight muscle histolysis pattern in *A. domesticus*. DEGs were screened according to the transcriptome sequencing results, focusing on the top 200 upregulated genes and the top 200 downregulated genes. Then, functional exploration was first carried out for genes that have been shown to be associated with flight muscle in previous studies among these DEGs and RNAi was applied to verify their functions.

2.5.2 Quantitative reverse transcription polymerase chain reaction (RT-qPCR) of the candidate genes

Twelve samples from different life periods, i.e., the last nymph stage and 0–10th days after eclosion, were used to explore the expression trends of the candidate genes. Five females were selected at each time point for flight muscle dissection and sampling, each as a group of biological replicates. The sampling method was the same as that described in Section 2.3.1. Then 5 groups of replicate samples of each period were mixed to extract RNA. RNA was extracted from flight muscle specimens using TRIzol reagent (Invitrogen, Carlsbad, CA, United States) in batches, and the quality and concentration of RNA were determined. After RNA quality was confirmed, 2 μg RNA was quantified and reverse transcribed into cDNA. The expression of candidate genes was measured by RT-qPCR, which was conducted with a StepOnePlus real-time polymerase chain reaction (PCR) assay system (Bio-Rad, Hercules, CA, United States) and TransStar Tip Top Green qPCR Supermix (TransGen Biotech, Beijing, China). 18S rRNA was used as the reference gene. The PCR conditions were as follows: 94°C for 30 s, followed by 40 cycles of 94°C for 5 s, 60°C for 15 s, and 72°C for 10 s. Then, conditions of 95°C for 15 s, 60°C for 30 s, and 95°C for 15 s were used to construct dissociation curves. The RT-qPCR data were analyzed using the $2^{-\Delta\Delta CT}$ method based on at least three technical replicates. All primers used in this study were designed using Primer Premier 5. The efficiencies of the primers were measured before RT-qPCR. The primers for the candidate genes used in the RT-qPCR assays are listed in Supplementary Table S1.

2.5.3 RNAi of candidate genes

To further identify the genes that determine flight muscle histolysis of *A. domesticus*, DEGs obtained from comparison of the O1 and R1 transcriptome data (before and after flight muscle histolysis) were comprehensively analyzed. The DEGs, namely, *AdomFABP*, *AdomTroponin T* and *AdomActin*, were functionally validated by using double-stranded RNA (dsRNA) targeting green fluorescent protein (GFP) dsGFP as a negative control. The dsRNA was injected into crickets on day 0 after eclosion. The primers for the candidate genes used for RNAi are listed in Supplementary Table S2.

The specific procedure was as follows. *AdomFABP*, *AdomTroponin T* and *AdomActin* and dsGFP were synthesized from the corresponding PCR fragments and amplified with upstream and downstream primers containing the T7 promoter. Due to the high FPKM value of candidate genes at the O1 stage, RNA reverse transcription at this stage was used to produce a cDNA template. dsRNAs were synthesized using the MEGAscript RNAi kit (Ambion, Austin, TX, United States). The synthesized dsRNAs were purified by precipitation with lithium chloride. Each dsRNA pellet was dissolved in 50 μL of nuclease-free water, quantified by a NanoDrop 2000 spectrophotometer and 1% agarose gels with GoldView Nucleic Acid Stain (Dingguo, China) and stored at −80°C before use. dsRNA was injected into crickets on day 0 after eclosion. A final amount of 6 μg targeted dsRNA in a 4 μL volume was injected at the second ventral segment of the abdomen by using a Nanoliter 2000 injector (World Precision Instruments, Sarasota, FL, United States). The dsRNA for each gene was injected into 120 crickets, which were subsequently returned to their original boxes and maintained under the same conditions described above to observe flight muscle histolysis. Six days after each injection, RNA was extracted from the samples, and 2 μg of RNA was quantified and reverse transcribed into cDNA; the interference effect was evaluated using RT-qPCR. RT-qPCR was performed by using the StepOnePlus Real-Time PCR Detection System (Bio-Rad, Hercules, CA, United States) and TransStar Tip Top Green qPCR Supermix (TransGen Biotech, Beijing, China). 18S rRNA was employed as an internal control. The PCR conditions were as follows: 94°C for 30 s, followed by 40 cycles of 94°C for 5 s, 60°C for 15 s, and 72°C for 10 s, followed by melting curve analysis. The RT-qPCR data were analyzed by the $2^{-\Delta\Delta CT}$ method, which is based on at least three repeats. All of the primers employed in this study were designed with Array Designer 4.3 (PREMIER Biosoft, Palo Alto, CA, United States). The efficiencies of the primers were tested before RT-qPCR. The primers for candidate genes used for testing the RNAi effect are listed in Supplementary Table S3.

3 Results

3.1 Flight muscle histolysis in *A. domesticus*

The pattern of flight muscle histolysis was similar between males and females of *A. domesticus*. The flight muscle histolysis mainly occured on the 9th-11th days after eclosion. In addition, by measuring the length, width and height of the dorsal longitudinal flight muscles of *A. domesticus* individuals from 0 to 11 days after eclosion, we found that the length remained almost unchanged over the degradation process, whereas the width gradually decreased (Supplementary Table S4). To visualized the volume variation from before to after flight muscle histolysis, we divided the degradation process of flight muscle of *A. domesticus* into four stages (Figures 1A, B). The flight muscle had degraded to the greatest extent at Stage IV but had not fully disappeared (Figure 1C). LSD and Tukey's B^a tests were both employed to assess the statistical significance of the DLM volume differences among the four stages of flight muscle histolysis. The results showed no significant difference in DLM volume between Stage I and Stage II, but as expected, there was a significant difference between Stage I and Stage III or Stage IV, with that between Stage I and Stage IV being more obvious ($p < .05$). These results indicate that volume changes significantly during the degradation of the flight muscle and tends to decrease. In addition, the color of the dorsal longitudinal flight muscle changed from pinkish-brown to pale, the morphology changed from full and smooth to flabby and thin, and the volume significantly decreased with flight muscle histolysis (Figure 1; Supplementary Table S4). The abdomen of *A. domesticus* was enlarged after flight muscle histolysis (Figure 2), and eggs were visible, suggesting that flight muscle histolysis is closely related to reproduction in *A. domesticus*.

3.2 Transcriptome analyses of *A. domesticus* before and after flight muscle histolysis

3.2.1 Sequence analysis and assembly of flight muscle transcriptome

The flight muscle transcriptome of *A. domesticus* was sequenced, and 13.58 Gb of high-quality, clean read data were obtained after quality control; the percentage of Q30 bases was 94.53%. To completely assemble the low-abundance transcripts, samples from the two stages (O1 and R1) were combined. Transcriptome assembly was accomplished based on the left.fq and right.fq files obtained using Trinity (Grabherr et al., 2011) with min_kmer_cov set to 2 by default and all other parameters set to default. In total, 66,241 transcripts and

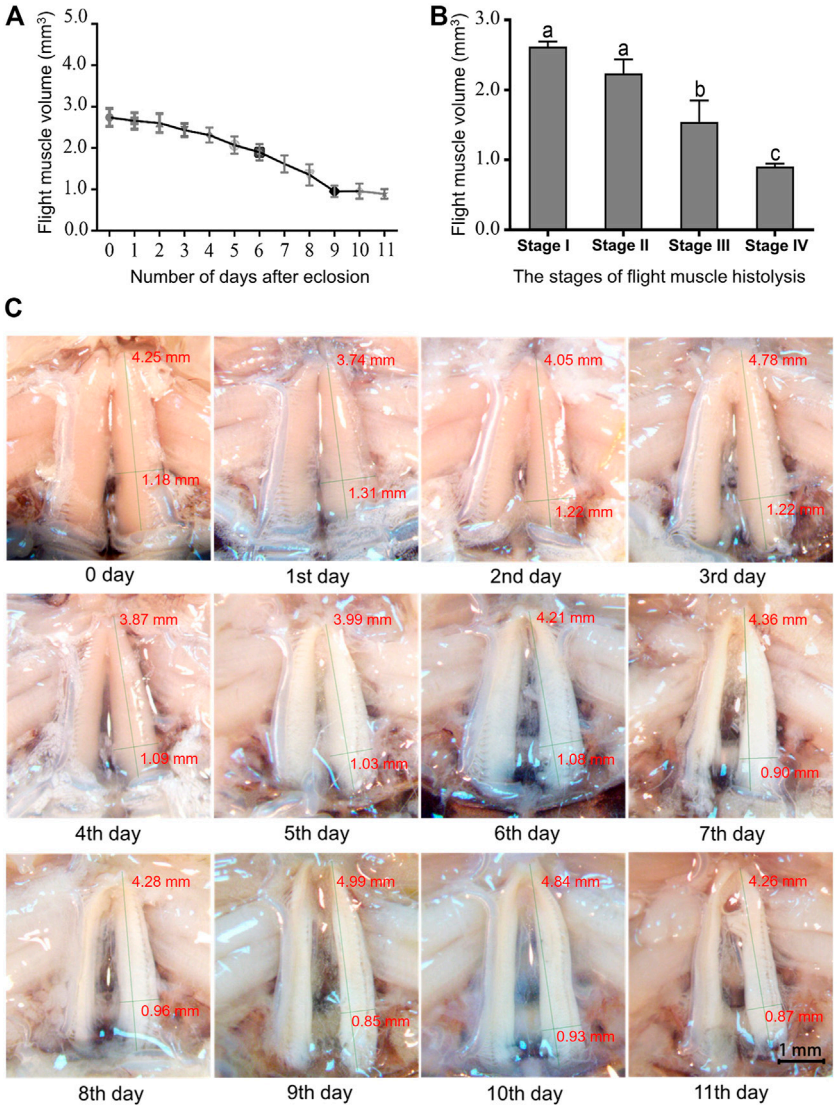

FIGURE 1
Changes in the dorsal longitudinal muscle during flight muscle histolysis in *A. domesticus*. **(A)** Variation in dorsal longitudinal muscle volume during flight muscle histolysis; **(B)** Analysis of the significant of dorsal longitudinal muscle volume changes at various stages of flight muscle histolysis. Stage I: 0–2 days of no degradation of the flight muscle; Stage II: 3–5 days of early degradation of the flight muscle; Stage III: 6–8 days of late degradation of the flight muscle; Stage IV: 9–11 days of total degradation of the flight muscle. **(C)** Morphological changes in the flight muscle during days 0–11 after emergence.

36,163 unigenes were assembled. The N50 length of the transcripts was 3,350 bp, the N50 length of the unigenes was 2,274 bp, and the assembly was largely complete. A total of 36,163 unigenes were filtered; of these, 12,096 unigenes had a length greater than or equal to 1 kb (Supplementary Table S5; Supplementary Figure S1). The clean data from the two stages were compared with the assembled unigene library (Supplementary Table S6).

3.2.2 Functional annotation of genes in the flight muscle transcriptome

A total of 13,449 unigenes were annotated in the flight muscle transcriptome of *A. domesticus*. Among them, 13,246 unigenes were annotated by the NR database, which accounted for the highest proportion of unigene annotations. The number of unigenes annotated by each database is shown in Supplementary Table S7. Comparison of the FPKM values of the samples between the two stages revealed that the FPKM median line of stage R1 (day 10 after eclosion) was higher than that of stage O1 (day 0 after eclosion) (Supplementary Figure S2).

3.2.3 Analysis of DEGs before and after flight muscle histolysis in *A. domesticus*

To investigate the expression of DEGs between before and after flight muscle histolysis in the flight muscle samples from *A. domesticus*, the samples from each stage were compared with those from the other. Prior to differential gene expression analysis, for each sequenced library, the read counts were adjusted by the EBSeq package through an empirical Bayesian approach. Differential expression analysis of two samples was performed using the EBSeq R package. *p*-value < .01 and |log2 (fold change) |>2 was set as the thresholds for significantly differential expression. The results of volcano plots (Supplementary Figure S3A), MA plots (Supplementary Figure S3B) and the heatmap plot (Figure 3)

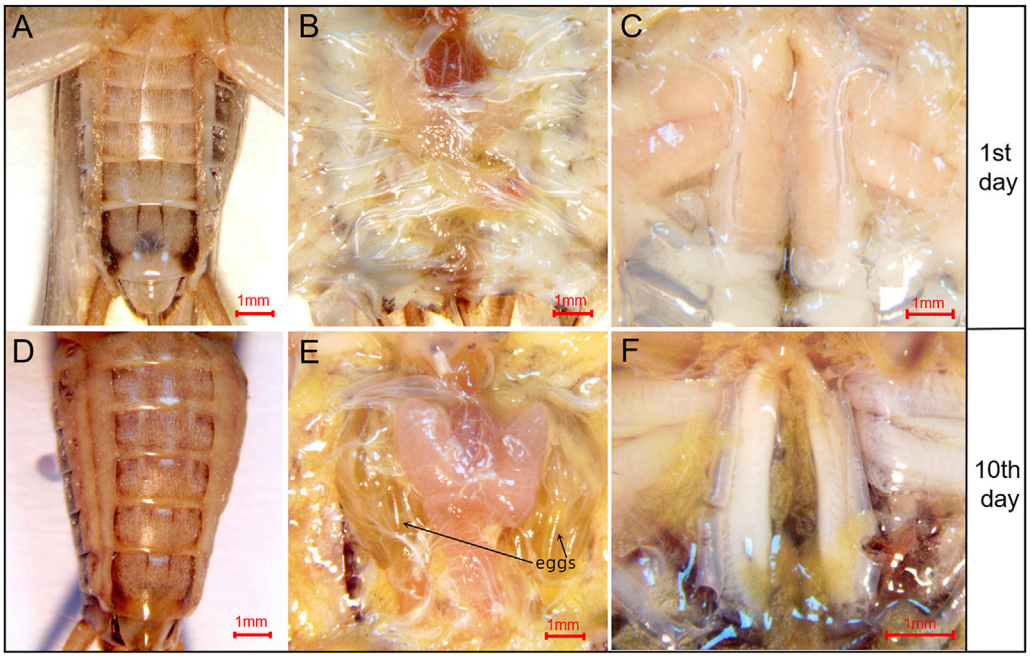

FIGURE 2
Morphological changes in the abdomen of *A. domesticus* females from before to after flight muscle histolysis. **(A)** The anatomy of female crickets on the 1st day after eclosion; **(B)** The abdominal anatomy of female crickets on the 1st day after eclosion; **(C)** The flight muscles of female crickets on the 1st day after eclosion; **(D)** The anatomy of female crickets on the 10th day after eclosion; **(E)** The abdominal anatomy of female crickets on the 10th day after eclosion; mature eggs were clearly observable after abdominal dissection; **(F)** The flight muscles of female crickets on the 10th day after eclosion.

showed that most DEGs were downregulated after flight muscle histolysis. The genes that had altered expression are likely to be key genes in the regulation of flight muscle histolysis in *A. domesticus*. Thus, in this experiment, key genes involved in the regulation of flight muscle histolysis in *A. domesticus* were screened by focusing on DEGs whose expression changed significantly after flight muscle histolysis.

In total, 1,685 DEGs were identified between the two samples, including 118 upregulated genes and 1,567 downregulated genes. To clarify the types and functions of these significantly altered genes, GO analysis was applied to the DEGs related to flight muscle histolysis for functional annotation; other analyses included COG direct homology classification, eggNOG direct homology classification, and KEGG functional annotation. GO functional annotation showed that the DEGs were mainly related to the growth and development of flight muscles (Figure 4). Both results of the COG (Supplementary Figure S4A) and eggNOG (Supplementary Figure S4B) direct homology classification analyses indicated that insect flight energy production, transformation and metabolic activities were increased after flight muscle histolysis in *A. domesticus*. The KEGG functional analysis showed that a large number of DEGs were involved in ribosomal activity during flight muscle histolysis and in the metabolism of sugars, lipids and proteins. In addition, a large number of DEGs were involved in the "fatty acid metabolism" (5.05%) and "fatty acid degradation" (4.73%) pathways, indicating that the fatty acid pathway may play an important role in flight muscle histolysis (Supplementary Figure S5A). The KEGG scatter plot showed that DEGs were mainly enriched in the "fatty acid metabolism", "biosynthesis of amino acids", "ribosome", "fatty acid degradation" pathways and so on (Supplementary Figure S5B). In summary, the GO, COG, eggNOG and KEGG functional analyses of DEGs revealed that the DEGs were mainly involved in pathways related to growth and development, the production and transformation of energy-related substances, protein synthesis and metabolic interactions. The findings show that the analysis of DEGs is a reasonable and feasible entry point for screening candidate genes and identifying pathways related to flight muscle histolysis in *A. domesticus*.

3.3 Screening and functional verification of genes regulating flight muscle histolysis in *A. domesticus*

3.3.1 Screening of candidate genes involved in flight muscle histolysis

The top 200 upregulated genes and top 200 downregulated genes were focused on to identify the DEGs involved in flight muscle histolysis of *A. domesticus*. Based on the genes related to flight muscle development mentioned in existing studies and combined with the analysis results of differences in expression levels, finally decided to screen these genes first from three aspects: fatty acid, troponin and Actin. According to the results of the National Center for Biotechnology Information (NCBI) BLAST and genes functional annotation, three candidate genes were identified, namely, *AdomFABP*, *AdomTroponin T* and *AdomActin* (Supplementary Table S8).

3.3.2 Expression levels of the candidate genes before and after flight muscle histolysis

The RT-qPCR results of the three candidate genes showed that the expression levels of the candidate genes were significantly different between before and after flight muscle histolysis, with those from

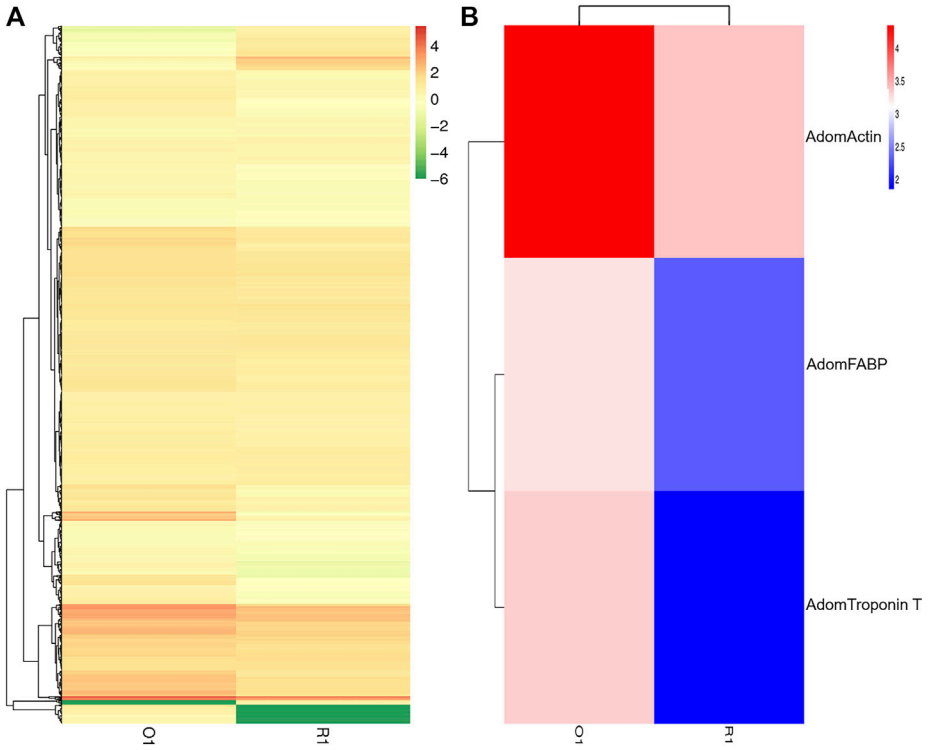

FIGURE 3
Analysis of DEG between before and after flight muscle histolysis in *A. domesticus*. **(A)** Heatmap of the DEGs between before and after flight muscle histolysis in *A. domesticus*. **(B)** Heatmap of *AdomFABP*, *AdomTroponin T* and *AdomActin* expression based on their FPKM values in the two stages in *A. domesticus*.

before histolysis being significantly higher (Figure 5). The expression trends of the candidate genes on days 0 and 10th were consistent with the results of the transcriptomic analysis. In addition, RT-qPCR results showed that the expression of the three candidate genes was upregulated in nymphs within 0–1 days after molting to adulthood. *AdomFABP* was most downregulated on the 2nd day (Figure 5C), which was higher than the other two candidate genes *AdomActin* and *AdomTroponinT* (Figures 5A, B), indicating that AdomFABP might play a key role in the degradation signal transduction pathway.

3.3.3 Detection of RNAi results by RT-qPCR

To further assess whether the three candidate genes play regulatory roles in flight muscle histolysis in *A. domesticus*, the expression of *AdomFABP*, *AdomTroponin T* and *AdomActin* was knocked down by RNAi. On the 6th day of dsRNA injection, candidate gene expression was detected (Figure 6). Compared with the GFP and wild-type groups, the gene injected with ds*AdomFABP* and ds*AdomTroponin T* exhibited significantly lower expression of the corresponding genes ($p < .01$) (Figures 6A, C); the expression of the third candidate gene (*AdomActin*) was not significantly altered in the treated group ($p > .05$), nor was its expression significantly changed in the negative control dsGFP treatment group ($p > .05$) (Figure 6B). Thus, the interference of *AdomFABP* and *AdomTroponin T* was successful. Compared with those of the GFP and wild-type groups, the body condition, growth and development, and physiological status of *A. domesticus* remained unchanged after dsRNA injection (Supplementary Figure S6). This result indicated that the injection volume and quantity in the RNAi experiment were sufficient.

3.3.4 Flight muscle histolysis of *A. domesticus* after RNAi

After RNAi for GFP and the three candidate genes in adult crickets, flight muscle histolysis in each group was anatomically observed from day 3 to day 7. On the 6th after dsRNA injection, flight muscle was significantly degraded in the ds*AdomFABP*-injected group compared with the wild-type (Figures 7A, B) and dsGFP-injected groups ($p = .0031$). This result coincides with the DEG analysis showing that *AdomFABP* was downregulated when flight muscle histolysis occurred in house crickets. Thus, the results of both the transcriptome and RNAi assays revealed that *AdomFABP* was involved in the molecular regulation of flight muscle histolysis of *A. domesticus*. However, there was no significant change in flight muscle histolysis in the group injected with ds*AdomTroponin T* ($p = .1461$) or the group injected with ds*AdomActin* ($p = .8818$) (Figure 7C).

4 Discussion

Flight muscle histolysis is carried out under the control of genes and is a complex process involving multiple genes and multilevel regulation. Although researchers have cloned and analyzed the structural genes and related regulatory genes of flight muscles in various insects, such as fruit flies (Nongthomba et al., 2001), plant hoppers (Vellichirammal et al., 2014), aphids (Kobayashi and Ishikawa, 1994; Ishikawa et al., 2008), and locusts (Liang et al., 2020), but the molecular mechanism of flight muscle tissue degradation has not been fully elucidated, and many related

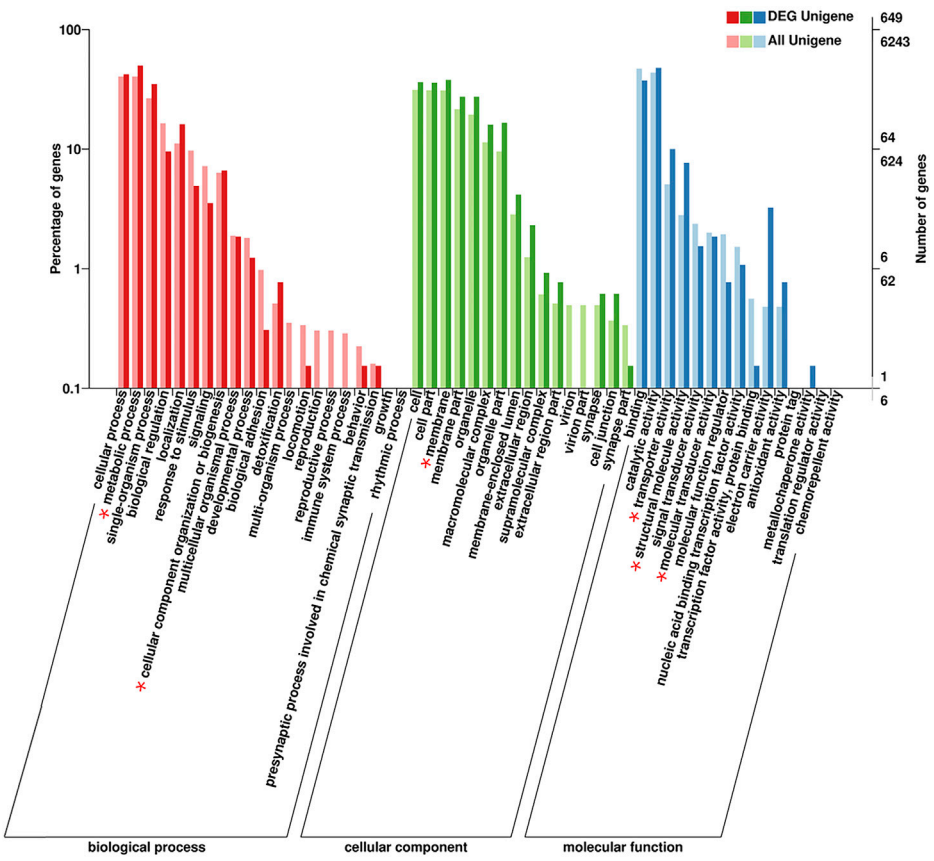

FIGURE 4
GO classification of DEGs related to flight muscle histolysis in *A. domesticus*.

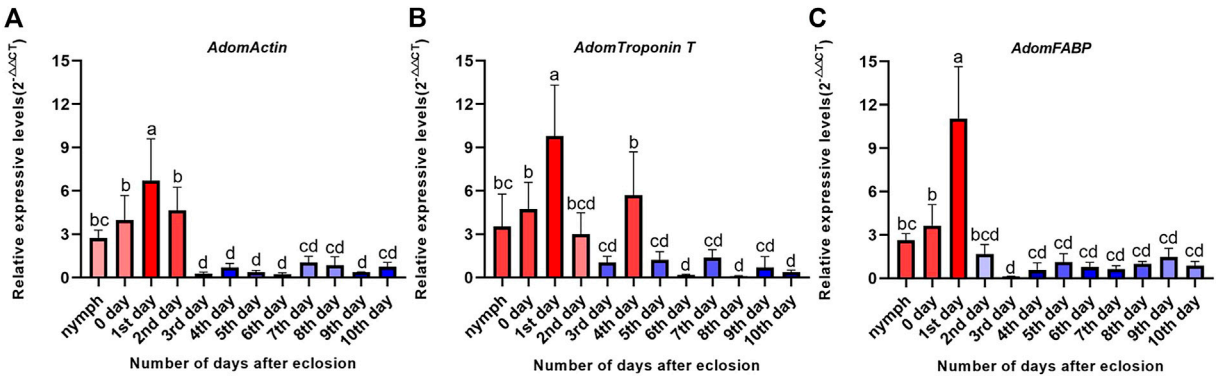

FIGURE 5
Expression levels of three candidate genes during flight muscle development in *A. domesticus*. **(A)** Expression level of *AdomActin* in 12 periods; **(B)** Expression level of *AdomTroponin T* in 12 periods; **(C)** Expression level of *AdomFABP* in 12 periods. Note: The data were analyzed by LSD and Waller-Duncana, b ($p < .05$), and the letters a/b/c/d were used to indicate significance. "nymph" denotes the last nymph age of *A. domesticus*, and the 0–10th days denote the 0–10th days after eclosion.

scientific problems have not yet been addressed. Additionally, beyond research in the fruit fly, which is a model insect employed for the study of flight muscle histolysis because its thoroughly studied genome facilitates the application of gene silencing and other technologies, the study of flight muscle histolysis has mainly focused on insects with migratory ability. However, there are many species of insects that do not have the ability to migrate, but in which flight muscle will degrade to meet the needs of growth and development or adaptation to the environment. The house crickets are one of them, in which the flight muscle histolysis after eclosion is widespread in the population.

Compared with longitudinal flight muscles, transverse flight muscles show no obvious morphological changes during flight muscle histolysis;

10.3389/fphys.2022.1079328

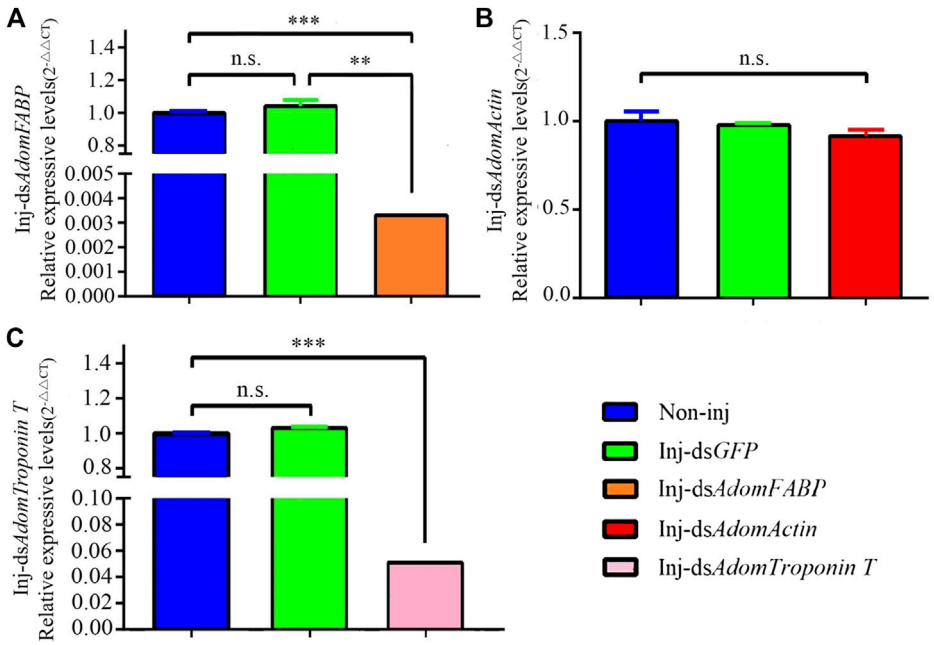

FIGURE 6
RT-qPCR results after RNAi in *A. domesticus*. **(A)** The expression of *AdomFABP* after RNAi; **(B)** The expression of *AdomActin* after RNAi; **(C)** The expression of *AdomTroponin T* after RNAi. Note: T tests were used to analyze gene expression differences; n.s. indicates no significant difference, ** indicates $p < .01$, and *** indicates $p < .001$. The figure displays the mean value, N = 3.

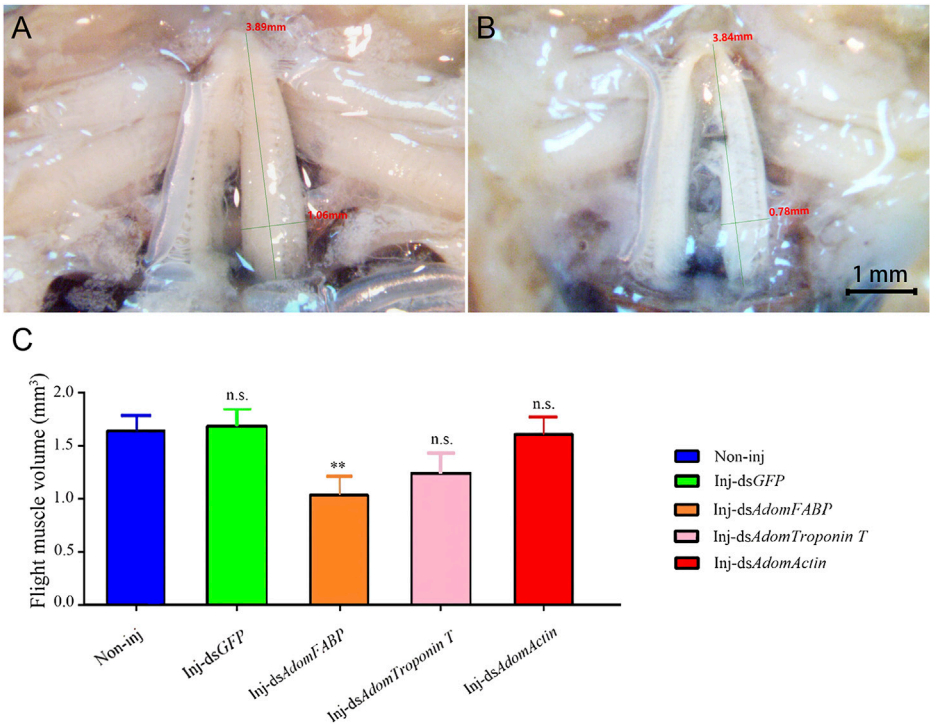

FIGURE 7
Comparison of flight muscle histolysis of *A. domesticus* on the 6th after RNAi. **(A)** The flight muscle morphology of wild-type; **(B)** The flight muscle morphology after ds*AdomFABP* treatment; **(C)** Comparison of flight muscle volume after RNAi.

thus, we focused only on the DLMs in this study. Flight muscle histolysis was observed in *A. domesticus* by dissecting out the DLM and then measuring its length, width and height. The observed changes in the color and morphology of flight muscle were consistent with those of Oliver et al. (2007). In addition, after measuring the wet weight of the tissue, total protein and percentage muscle shortening in the DLM of *A. domesticus*, Oliver et al. (2007) noted that the flight muscle histolysis in *A. domesticus* was complete on 3rd day after adults eclosion. Notably, in the present study, the peak flight muscle histolysis occurred on the 9th to 11th days after eclosion. This difference between studies may be related to study differences in breeding conditions. The feeding temperature and photoperiod in Oliver et al. (2007) were respectively 30°C and L:D = 14:10, but those of this study were 30°C and L:D = 0:24. This could be because environmental factors influence the timing of flight muscle histolysis (Roff, 1990), which in turn affects the pattern of flight muscle histolysis. There was no sexual dimorphism in the peak time of flight muscle histolysis in the crickets. However, the abdomens of females began to swell after flight muscle histolysis, and eggs were visible after dissection. These findings might provide insights into the trade-off between flight muscle maintenance and reproductive activity (Tanaka, 1993).

In this study, through different enrichment analysis of DEGs, it was found that most differentially expressed genes are enriched in the pathway related to energy metabolism, which is consistent with the strong energy metabolism function of flight muscle. Of which, COG and eggNOG enrichment analysis results was performed that many DEGs were enriched in the "Lipid pathway transport and metabolism" pathway; KEGG enrichment analysis also showed that relative majority DEGs were enriched in the "Fatty acid metabolism" and "Fatty acid degradation" pathways. Studies have indicated that fatty acid metabolism is an important metabolic mode for long-distance migration of insects (Arrese and Soulages, 2010; Guo et al., 2022), combined with the pattern of flight muscle histolysis after migration (Feng et al., 2019), it can be inferred that compared with other metabolic pathways, fatty acid metabolic pathway is more likely to be a regulatory pathway involved in and regulating flight muscle histolysis, and fatty acid transporters are more likely to act as regulatory signals than other proteins with fixed metabolic functions due to their properties of transporting fatty acids. In addition, it is reported that FABP has also been reported to be crucial for long-distance migration of migratory locusts (Rajapakse et al., 2019). That is the reason why this study finally focused on it for research.

Our study successfully verified the important regulatory role of AdomFABP in flight muscle histolysis of *A. domesticus*. Downregulation of *AdomFABP* gene expression promotes this process in *A. domesticus*. FABP has been reported to play an important role in lipid uptake and transport in locust flight muscle and is an essential element of skeletal muscle metabolism involved in sustained muscle activity, the absence of which prevents locusts from migrating long distances (Rajapakse et al., 2019). Increased FABP levels are associated with the flight ability of insects (Haunerland, 1997). Flight activity can promote FABP expression in adult locusts, and the expression of FABP in flight muscles has been shown to be upregulated before adults commenced long-distance migration (Chen and Haunerland, 1994). The flight ability of insects mainly depends on the development of their flight muscle structures (Ding et al., 2014). FABP plays an important role in the energy supply of flight muscles and affects flight muscle formation and degradation (Wu et al., 2002). Therefore, it can be inferred that the degradation of flight muscle reduces or prevent flight ability and that the expression of FABP in flight muscle inevitably decrease as well, which supports the results of this study. In addition, in the present study, the expression level of *AdomFABP* was compared between before and after flight muscle histolysis based on RT-qPCR. The results showed that the expression of *AdomFABP* was upregulated in nymphs within 0–1 days after molting to adulthood, indicating that the flight muscles continued to develop and remained intact within 0–1 days after adulthood. However, when crickets entered the 2nd day of adulthood, the expression of *AdomFABP* was significantly downregulated, suggesting that *AdomFABP* might play a role in the degradation of flight muscle by inhibiting muscle development. Similar to the house cricket, many species of locusts show wing dimorphism (with long-winged and short-winged morphs). Wing dimorphism has been proposed as a strategy to balance trade-offs in ecological systems between flight capability and various fitness components (Chen et al., 2019). Long-winged individuals show better migration ability than short-winged individuals, and the transition from the long-winged to the short-winged form is accompanied by flight muscle histolysis. Therefore, the study of flight muscle histolysis in *A. domesticus* could lay a theoretical foundation for the study of wing dimorphism and migration behavior in locusts. However, FABP is a binding protein; thus, the factors that decrease its expression and thereby regulate flight muscle histolysis in *A. domesticus*, as well as other genes and proteins in the FABP pathway that jointly regulate flight muscle histolysis in this insect, need to be identified in future studies.

AdomTroponin and AdomActin may also be involved in flight muscle histolysis. Troponin consists of three subunits, troponin C (TpnC), troponin I (TpnI) and troponin T (TpnT). The different physiological functions of insect muscles can be attributed, at least in part, to specific troponin subunits, and it has been suggested that the acquisition of flight muscle functions (e.g., contraction) may be associated with these subunits (Liang et al., 2020). Actin is a multifunctional protein that regulates muscle contraction. Degradation of actin into two molecular fragments of different sizes can lead to disruption of cell viability and eventually to apoptosis (Mashima et al., 1997); this mechanism is generally considered to be the main mode of flight muscle histolysis. Thus, it is clear that *Actin* is involved in the regulation of flight muscle histolysis. Additionally, *ActinAct88F* is specifically expressed in the indirect flight muscle of adult *Drosophila melanogaster*, and mutations in this gene result in reduced flight ability (Mogami and Hotta, 1981). However, in the present study, when RNAi was used to verify the function of *Troponin T*, it was found that although *Troponin T* was successfully knocked down, the morphology of *A. domesticus* flight muscle was not affected (Figures 6, 7). This result suggests that AdomTroponin T plays only an indirect regulatory role in flight muscle histolysis in *A. domesticus* or has nothing to do with flight muscle histolysis. The RNAi knockdown of AdomActin was not successfully realized, may be due to the special status of AdomActin in flight muscle, which was not easy to be interfered successfully. In addition, it is also possible that the location selection of dsRNA fragments is not appropriate. Therefore, whether the *Actin* is involved in the regulation of flight muscle histolysis further interference and functional studies of *Actin* are needed in the future.

At the hormone level, it has been found that juvenile hormones, prothymosin, etc., are involved in flight muscle histolysis (Feng et al., 2019), but the genes and related pathways involved in the regulation of flight muscle histolysis remain unknown. We will focus on further analyzing the intrinsic regulatory mechanism of flight muscle

histolysis in the future. This study can serve as a reference for the future explorations of the molecular mechanism and physiological significance of flight muscle histolysis in Orthoptera.

Data availability statement

The data presented in the study are deposited in the Sequence Read Archive repository, accession number: SRR22200957 and SRR22200956. The data link: https://www.ncbi.nlm.nih.gov/sra/?term=SRR22200956; https://www.ncbi.nlm.nih.gov/sra/?term=SRR22200957.

Author contributions

Conceptualization, YL and QC; Data curation, ZW, YM, JK, and YF; Formal analysis, ZZ and JZ; Investigation, FL and MH; Writing—original draft, YL and QC; Writing—review and editing, YL, QC, and BR. All authors have read and agreed to the published version of the manuscript.

Funding

This work was supported by the National Natural Science Foundation of China (No. 31172133, BR), the Fundamental Research Funds for the Central Universities (No. 135111010, QC) and the Youth Talent Support Project of Jilin Province (No. QT202121, QC).

Acknowledgments

English-language editing was provided by Prof. Ying Hu (Jilin Agricultural University) and the American Journal Experts editing service.

Conflict of interest

The authors declare that the research was conducted in the absence of any commercial or financial relationships that could be construed as a potential conflict of interest.

Publisher's note

All claims expressed in this article are solely those of the authors and do not necessarily represent those of their affiliated organizations, or those of the publisher, the editors and the reviewers. Any product that may be evaluated in this article, or claim that may be made by its manufacturer, is not guaranteed or endorsed by the publisher.

Supplementary material

The Supplementary Material for this article can be found online at: https://www.frontiersin.org/articles/10.3389/fphys.2022.1079328/full#supplementary-material

References

Arrese, E. L., and Soulages, J. L. (2010). Insect fat body: Energy, metabolism, and regulation. *Annu. Rev. Entomol.* 55, 207–225. doi:10.1146/annurev-ento-112408-085356

Azizi, T., Johnston, J. S., and Vinson, S. B. (2009). Initiation of flight muscle apoptosis and wing casting in the red imported fire ant *Solenopsis invicta*. *Physiol. Entomol.* 34 (1), 79–85. doi:10.1111/j.1365-3032.2008.00655.x

Bai, Y., Pei, X. J., Ban, N., Chen, N., Liu, S. N., Li, S., et al. (2022). Nutrition-dependent juvenile hormone sensitivity promotes flight-muscle degeneration during the aphid dispersal-reproduction transition. *Development* 149 (15), dev200891. doi:10.1242/dev.200891

Cao, T. X., and Jin, J. P. (2020). Evolution of flight muscle contractility and energetic efficiency. *Front. Physiol.* 11, 1038. doi:10.3389/fphys.2020.01038

Cayre, M., Scotto-Lomassese, S., Malaterre, J., Strambi, C., and Strambi, A. (2007). Understanding the regulation and function of adult neurogenesis: Contribution from an insect model, the house cricket. *Chem. Senses.* 32, 385–395. doi:10.1093/chemse/bjm010

Chang, H., Guo, X., Guo, S., Yang, N., and Huang, Y. (2021). Trade-off between flight capability and reproduction in acridoidea (insecta: Orthoptera). *Ecol. Evol.* 11, 16849–16861. doi:10.1002/ece3.8317

Chaulk, A. C., Driscoll, S., Oke, K. B., Coates, P. J., Caravan, H. E., and Chapman, T. W. (2014). Flight muscle breakdown in the soldier caste of the gall-inducing thrips species, Kladothrips intermedius Bagnall. *Insect. Soc.* 61, 57–66. doi:10.1007/s00040-013-0324-4

Chen, Q., Wen, M., Li, J. X., Zhou, H. F., Jin, S., Zhou, J. J., et al. (2019). Involvement of heat shock protein 40 in the wing dimorphism of the house cricket *Acheta domesticus*. *J. Insect Physiol.* 114, 35–44. doi:10.1016/j.jinsphys.2019.02.007

Chen, X. M., and Haunerland, N. H. (1994). Fatty acid binding protein expression in locust flight muscle. Induction by flight, adipokinetic hormone, and low density lipophorin. *Insect biochem. Mol. Biol.* 24 (6), 573–579. doi:10.1016/0965-1748(94)90093-0

Clifford, C. W., Roe, R. M., and Woodring, J. P. (1977). Rearing methods for obtaining house crickets, *Acheta domesticus*, of known age, sex, and instar. *Ann. Entomol. Soc. Am.* 70 (1), 69–74. doi:10.1093/aesa/70.1.69

Crocker, K. C., and Hunter, M. D. (2018). Social density, but not sex ratio, drives ecdysteroid hormone provisioning to eggs by female house crickets (*Acheta domesticus*). *Ecol. Evol.* 8, 10257–10265. doi:10.1002/ece3.4502

Deban, S. M., and Anderson, C. V. (2021). Temperature effects on the jumping performance of house crickets. *J. Exp. Zool.* 335, 659–667. doi:10.1002/jez.2510

Ding, J. T., Adil, S., Zhu, H. F., Yu, F., Alimasiand Luo, L. (2014). Flight capacity of adults of the ber fruit fly, *Carpomya vesuviana* (Diptera: Tephritidae). *Acta Entomol. Sin.* 57 (11), 1315–1320. doi:10.16380/j.kcxb.2014.11.010

Domingo, A., González-Jurado, J., Maroto, M., Díaz, C., Vinós, J., Carrasco, C., et al. (1998). Troponon-T is a calcium-binding protein in insect muscle: *In vivo* phosphorylation, muscle-specific isoforms and developmental profile in *Drosophila melanogaster*. *J. Muscle Res. Cell Motil.* 19, 393–403. doi:10.1023/A:1005349704790

Dou, J., Zhang, R. Y., Liu, M., Qian, X., Xiao, H. W., Jashenko, R., et al. (2017). Comparison of flight muscle and energy consumption of pre- and post-flight in *Caliptamus italicus* (Orthoptera: Acrididae). *Pratac. Sci.* 34 (8), 1721–1726. doi:10.11829/j.issn.1001-0629.2017-0066

Feng, H. L., Guo, X., Sun, H. Y., Zhang, S., Xi, J. H., Yin, J., et al. (2019). Flight muscles degenerate by programmed cell death after migration in the wheat aphid, Sitobion avenae. *BMC Res. Notes.* 12 (672), 1–7. doi:10.21203/rs.2.13011/v3

Fuciarelli, T. M., and Rollo, C. D. (2020). Radiation exposure causes developmental alterations in size and shape of wings and structures associated with song production in male crickets (*Acheta domesticus*). *Entomol. Exp. Appl.* 169, 227–234. doi:10.1111/eea.12999

Fyrberg, E. A., Fyberg, C. C., Biggs, J. R., Saville, D., Beall, C. J., and Ketchum, A. (1998). Functional nonequivalence of *Drosophila* actin isoforms. *Biochem. Genet.* 36 (7/8), 271–287. doi:10.1023/A:1018785127079

Gajewski, K. M., Wang, J., and Schulz, R. A. (2006). Calcineurin function is required for myofilament formation and troponin I isoform transition in *Drosophila* indirect flight muscle. *Dev. Biol.* 289 (1), 17–29. doi:10.1016/j.ydbio.2005.09.039

Ge, S., Sun, X., He, W., Wyckhuys, K. A. G., He, L., Zhao, S., et al. (2021). Potential trade-offs between reproduction and migratory flight in *Spodoptera frugiperda*. *J. Insect Physiol.* 132, 104248. doi:10.1016/j.jinsphys.2021.104248

Gibbs, M., and Van Dyck, H. (2010). Butterfly flight activity affects reproductive performance and longevity relative to landscape structure. *Oecologia* 163, 341–350. doi:10.1007/s00442-010-1613-5

Grabherr, M. G., Haas, B. J., Yassour, M., Levin, J. Z., Thompson, D. A., Amit, I., et al. (2011). Full-length transcriptome assembly from RNA-Seq data without a reference genome. *Nat. Biotechnol.* 29, 644–652. doi:10.1038/nbt.1883

Grossmann, K. K., Merz, M., Appel, D., Araujo, M. M. D., and Fischer, L. (2021). New insights into the flavoring potential of cricket (*Acheta domesticus*) and mealworm (*Tenebrio molitor*) protein hydrolysates and their Maillard products. *Food Chem.* 364, 130336. doi:10.1016/j.foodchem.2021.130336

Guo, P., Yu, H., Xu, J., Li, Y. H., and Ye, H. (2022). Flight muscle structure and flight capacity of females of the long-distance migratory armyworm, *Spodoptera frugiperda*: Effect of aging and reproduction, and trade-offs between flight and fecundity. *Entomol. Exp. Appl.*, 1–11. doi:10.1111/eea.13248

Han, H. B., Gao, S. J., Wang, N., Xu, L. B., Dong, R. W., and Manduhu, N. R. (2020). Ultrastructure of the flight muscle of female adults in the gregarious and solitary phases of the grasshopper, *Oedaleus asiaticus* (Orthoptera: Acrididae). *Plant Prot.* 46 (4), 55–60. doi:10.16688/j.zwbh.2019198

Haunerland, N. H. (1997). Transport and utilization of lipids in insect flight muscles. *Comp. Biochem. Physiol.* 117 (4), 475–482. doi:10.1016/S0305-0491(97)00185-5

Ishikawa, A., Hongo, S., and Miura, T. (2008). Morphological and histological examination of polyphonic wing formation in the pea aphid *Acyrthosiphon pisum* (Hemiptera, Hexapoda). *Zoomorphology* 127, 121–133. doi:10.1007/s00435-008-0057-5

Katti, P., Rai, M., Srivastava, S., Silva, P. D., and Nongthomba, U. (2021). Marf-mediated mitochondrial fusion is imperative for the development and functioning of indirect flight muscles (IFMs) in drosophila. *Exp. Cell. Res.* 399, 112486. doi:10.1016/j.yexcr.2021.112486

Khatun, H., Claes, J., Smets, R., De Winne, A., Akhtaruzzaman, M., and Mik, V. D. B. (2021). Characterization of freeze-dried, oven-dried and blanched house crickets (*Acheta domesticus*) and Jamaican field crickets (*Gryllus assimilis*) by means of their physicochemical properties and volatile compounds. *Eur. Food Res. Technol.* 247, 1291–1305. doi:10.1007/s00217-021-03709-x

Kobayashi, M., and Ishikawa, H. (1994). Mechanisms of histolysis in indirect flight muscles of alate aphid (*Acryrthosiphon pisum*). *J. Insect Physiol.* 40 (1), 33–38. doi:10.1016/0022-1910(94)90109-0

Kurihara, Y., Ogawa, K., Chiba, Y., Hayashi, Y., and Miyazaki, S. (2022). Thoracic crop formation is spatiotemporally coordinated with flight muscle histolysis during claustral colony foundation in *Lasius japonicus* queens. *Arthropod Struct. Dev.* 69, 101169. doi:10.1016/J.ASD.2022.101169

Li, X. B., and Rollo, C. D. (2021). Radiation induces stress and transgenerational impacts in the cricket, *Acheta domesticus*. *Int. J. Radiat. Biol.* 1-8, 1098–1105. doi:10.1080/09553002.2021.1872816

Liang, H. F., Li, J., and Li, X. D. (2020). Identification and characterization of troponin genes in *Locusta migratoria*. *Insect Mol. Biol.* 29, 391–403. doi:10.1111/imb.12644

Liu, H., Li, K. B., Yin, J., Du, G. L., and Cao, Y. Z. (2008). Ultrastructure of the flight muscle of female adults in the gregarious phase and solitary phase of the oriental migratory locust, *Locusta migratoria manilensis* (Meyen) (Orthoptera: Acrididae). *Acta Entomol. Sin.* 51 (10), 1033–1038. doi:10.16380/j.kcxb.2008.10.004

Liu, M. G., Jiang, C. X., Mao, M., Liu, C., Li, Q., Wang, X. G., et al. (2017). Effect of the insecticide dinotefuran on the ultrastructure of the flight muscle of female *Sogatella furcifera* (Hemiptera: Delphacidae). *J. Econ. Entomol.* 110 (2), 632–640. doi:10.1093/jee/tow320

Lu, K. P., Liang, S. B., Han, M. J., Wu, C. M., Song, J. B., Li, C. L., et al. (2020). Flight muscle and wing mechanical properties are involved in flightlessness of the domestic silkmoth, *Bombyx mori*. *Insects* 11 (220), 220. doi:10.3390/insects11040220

Luo, L. Z. (1996). An ultrastructural study on the development of flight muscle in adult oriental armyworm, *Mythimna separata* (Walker). *Acta Entomol. Sin.* 39 (4), 366–374. doi:10.16380/j.kcxb.1996.04.006

Mashima, T., Naito, M., Noguchi, K., Miller, D. K., Nicholson, D. W., and Tsuruo, T. (1997). Actin cleavage by CPP-32/apopain during the development of apoptosis. *Oncogene* 14, 1007–1012. doi:10.1038/sj.onc.1200919

Matte, A., and Bliien, J. (2021). Flight muscle histolysis in *Lasius niger* queens. *Asian Myrmecol* 13, e013003. doi:10.20362/am.013003

Mogami, K., and Hotta, Y. (1981). Isolation of *Drosophila* flightless mutants which affect myofibrillar proteins of indirect flight muscle. *Mol. Gen. Genet.* 183, 409–417. doi:10.1007/BF00268758

Nelson, C. M., and Nolen, T. G. (1997). Courtship song, male agonistic encounters, and female mate choice in the house cricket, *Acheta domesticus* (Orthoptera: Gryllidae). *J. Insect Behav.* 10 (4), 557–570. doi:10.1007/BF02765377

Nongthomba, U., Pasalodos-Sanchez, S., Clark, S., Clayton, J. D., and Sparrow, J. C. (2001). Experssion and function of the *Drosophila* ACT88F actin isoform is not restricted to the indirect flight muscles. *J. Muscle Res. Cell Motil.* 22, 111–119. doi:10.1023/A:1010308326890

Oliver, R. H., Albury, A. N. J., and Mousseau, T. A. (2007). Programmed cell death in flight muscle histolysis of the house cricket. *J. Insect Physiol.* 53, 30–39. doi:10.1016/j.jinsphys.2006.09.012

Patton, R. L. (1978). Growth and development parameters for *Acheta domesticus*. *Ann. Entomol. Soc. Am.* 71 (1), 40–42. doi:10.1093/aesa/71.1.40

Piñera, A. V., Charles, H. M., Dinh, T. A., and Killian, K. A. (2013). Maturation of the immune system of the male house cricket, *Acheta domesticus*. *J. Insect Physiol.* 59, 752–760. doi:10.1016/j.jinsphys.2013.05.008

Rajapakse, S., Qu, D., Ahmed, A. S., Rickers-Haunerland, J., and Haunerland, N. H. (2019). Effects of FABP knockdown on flight performance of the desert locust, *Schistocerca gregaria*. *J. Exp. Biol.* 222, jeb203455. doi:10.1242/jeb.203455

Roff, D. A., and Fairbairn, D. J. (2007). The evolution and genetics of migration in insects. *BioScience* 57, 155–164. doi:10.1641/B570210

Roff, D. A. (1990). The evolution of flightlessness in insects. *Ecol. Monogr.* 60 (4), 389–421. doi:10.2307/1943013

Snelling, E. P., Seymour, R. S., Matthews, P. G. D., and White, C. R. (2012). Maximum metabolic rate, relative lift, wingbeat frequency and stroke amplitude during tethered flight in the adult locust *Locusta migratoria*. *J. Exp. Biol.* 215, 3317–3323. doi:10.1242/jeb.069799

Stjernholm, F., and Karlsson, B. (2008). Flight muscle breakdown in the green-veined white butterfly, *Pieris napi* (Lepidoptera: Pieridae). *Eur. J. Entomol.* 105 (1), 87–91. doi:10.14411/eje.2008.012

Tanaka, S. (1993). Allocation of resources to egg production and flight muscle development in a wing dimorphic cricket, *Modicogryllus confirmatus*. *J. Insect Physiol.* 39 (6), 493–498. doi:10.1016/0022-1910(93)90081-2

Tanaka, S. (1994). Endocrine control of ovarian development and flight muscle histolysis in a wing dimorphic cricket, *Modicogryllus confirmatus*. *Insect Physiol.* 40, 483–490. doi:10.1016/0022-1910(94)90121-X

Vellichirammal, N. N., Zera, A. J., Schilder, R., J., Wehrkamp, C., Riethoven, J. J. M., and Brisson, J. A. (2014). *De novo* transcriptome assembly from fat body and flight muscles transcripts to identify morph-specific gene expression profiles in *Gryllus firmus*. *Plos One* 9 (1), e82129. doi:10.1371/journal.pone.0082129

Wu, Q. W., Chang, W. H., Rickers-Haunerland, J., Higo, T., and Haunerland, N. H. (2002). Characterization of a new fatty acid response element that controls the expression of the locust muscle FABP gene. *Mol. Cell. Biochem.* 239, 173–180. doi:10.1023/A:1020554824176

Wu, Q. W., and Haunerland, N. H. (2001). A novel fatty acid response element controls the expression of the flight muscle *FABP* gene of the desert locust, *Schistocerca gregaria*. *Eur. J. Biochem.* 268, 5894–5900. doi:10.1046/j.0014-2956.2001.02538.x

Zeng, Y., Zhu, D. H., and Zhao, L. Q. (2012). Comparison of flight muscle development, fecundity and longevity between long-winged and short-winged female adults of *Velarifictorus asperses* (Orthoptera: Gryllidae). *Acta Entomol. Sin.* 55 (2), 241–246. doi:10.16380/j.kcxb.2012.02.015

Zera, A. J., and Cisper, G. C. (2001). Genetic and diurnal variation in the juvenile hormone titer in a wing-polymorphic cricket: Implications for the evolution of life histories and dispersal. *Physiol. Biochem. Zool.* 74 (2), 293–306. doi:10.1086/319664

Zhang, C. X., Brisson, J. A., and Xu, H. J. (2019). Molecular mechanisms of wing polymorphism in insects. *Annu. Rev. Entomol.* 64, 297–314. doi:10.1146/annurev-ento-011118-112448

Zhao, L. Q., Zhu, D. H., and Zeng, Y. (2010). Physiological trade-offs between flight muscle and reproductive development in the wing-dimorphic cricket *Velarfictorus ornatus*. *Entomol. Exp. Appl.* 135, 288–294. doi:10.1111/j.1570-7458.2010.00989.x

frontiers | Frontiers in Physiology

TYPE Original Research
PUBLISHED 03 February 2023
DOI 10.3389/fphys.2023.1110998

OPEN ACCESS

EDITED BY
Jia Fan,
Institute of Plant Protection (CAAS), China

REVIEWED BY
Xionbing Tu,
Institute of Plant Protection (CAAS), China
Xiangqun Nong,
Institute of Plant Protection (CAAS), China
Pheophanh Soysouvanh,
MAF, Laos
Yingying Dong,
Aerospace Information Research Institute (CAS), China

*CORRESPONDENCE
Hongmei Li,
h.li@cabi.org

SPECIALTY SECTION
This article was submitted to Invertebrate Physiology, a section of the journal Frontiers in Physiology

RECEIVED 29 November 2022
ACCEPTED 06 January 2023
PUBLISHED 03 February 2023

CITATION
Li H, Zhu J, Cheng Y, Zhuo F, Liu Y, Huang J, Taylor B, Luke B, Wang M and González-Moreno P (2023), Daily activity patterns and body temperature of the Oriental migratory locust, *Locusta migratoria manilensis* (Meyen), in natural habitat.
Front. Physiol. 14:1110998.
doi: 10.3389/fphys.2023.1110998

Daily activity patterns and body temperature of the Oriental migratory locust, *Locusta migratoria manilensis* (Meyen), in natural habitat

Hongmei Li[1,2]*, Jingquan Zhu[3], Yumeng Cheng[1], Fuyan Zhuo[3], Yinmin Liu[1], Jingfeng Huang[4], Bryony Taylor[5], Belinda Luke[5], Meizhi Wang[1] and Pablo González-Moreno[5,6]

[1]MARA-CABI Joint Laboratory for Bio-safety, Institute of Plant Protection, Chinese Academy of Agricultural Science, Beijing, China, [2]CABI East and Southeast Asia, Beijing, China, [3]National Agro-Tech Extension and Service Center, Beijing, China, [4]College of Environment and Resources Science, Zhejiang University, Hangzhou, China, [5]CABI, Egham, United Kingdom, [6]Department of Forest Engineering, ERSAF RNM-360, University of Córdoba, Córdoba, Spain

Current pest management techniques would benefit from understanding the behavioural rhythms of the target pest and its body temperature, a critical aspect not well studied and potentially limiting the effectiveness of biopesticides under natural conditions. This study aims 1) to understand under natural conditions the behavioural patterns of different stages of hoppers and adults of *Locusta migratoria manilensis* and 2) to identify the environmental factors modulating their body temperature through field observation. We carried out an intensive field sampling in two of the main locust breeding regions in China, recording the body temperature (day and night), morphological traits (stage, sex and size) and microhabitat of 953 individuals. The results revealed that locusts preferred the ground as their main activity subhabitat, particularly for hoppers. Adults tended to move upper in the reed canopy at two peaks (10-11 h and 14-15 h). Locusts body temperature during daytime increased with development stage and size, while the opposite pattern occurred during night time. Entompathogenic fungi are more effective if the body temperature of the target pest is in a proper range without too high or too low. Application of biopesticides should focus on younger locusts spraying in the morning or at dusk as the locusts have lower body temperatures.

KEYWORDS

***Locusta migratoria manilensis*, locusts, body temperature, entomopathogenic fungus, body length, position, development**

1 Introduction

Locust plagues cause problems globally in almost all ecosystems except the forest and tundra belts in the north and the equatorial forests. Heavy locust infestations have been often reported in various parts of the world causing enormous damage to agriculture and the environment but without a constant pattern. For instance, locust swarms were reported causing damage to agriculture in New South Wales, Australia in 2015 (Jurd, 2015). Due to the high potential hazard, all countries in West Africa continue maintaining a high standard of reporting that is the basis for the global Desert Locust early warning system. Desert locust, *Schistocerca gregaria* (Forskål), has been causing serious problems in areas about 29 million km^2 from the

Atlantic Ocean in the west to India and Pakistan in the east, and comprising the entire area or parts of 64 countries (Harb, 2009). In China, locust' populations have been stable and no major outbreaks have occurred in recent years. Nevertheless, there are still localised spots of high locust density in marshlands of Jilin, Shanxi and Shandong Provinces (Yang et al., 2018). Specifically, Oriental migratory locust, *Locusta migratoria manilensis*, is one of the key locust species in China occasionally causing destructive outbreaks both in frequency and scale (Xia and Huang, 2002).

Chemical pesticides are the main intervention used against locusts and grasshoppers. Extensive applications of insecticides, particularly organophosphates, have inevitably resulted in the development of resistance in natural populations of the locusts and damage to biodiversity (Zhang, 2011). Preventive management and usage of biopesticides are garnering increasing attention from the government as partial alternatives for chemical pesticides (Ndolo et al., 2019). Many studies of locust biocontrol made great progress, and alternative microbial biopesticides such as those based on entomopathogenic fungus (EPF) greatly reduce the risk of resistance and pollution. *Metarhizium acridum* is an EPF with a narrow host range comprising locusts and grasshoppers, and proofed that *M. acridum* strains had a strong virulence to *L. m. manilensis* (Cao et al., 2016). Strains of *M. acridum* have been developed as biopesticide against locust and grasshoppers worldwide in Africa, Australia, China, Brazil and Mexico (Bateman, 1997; Driver et al., 2000; Peng and Xia, 2011; Maute et al., 2015), including Isolate IMI 330189 marketed as Green Muscle®, IMI189.

Conidia of *M. acridum* require suitable environmental conditions in terms of humidity and temperature to survive and germinate to infect the insect host. The internal temperature of the locust strongly influences the rate of fungal development and the ultimate time to death of the insect (Klass et al., 2007). Studies investigating the relationship between temperature and rate of growth of fungal pathogens have shown that there is a non-linear relation between EPF development and temperature with the lower development threshold for *M. acridum* reported around 10–12°C and the upper around 35–37°C (Smits et al., 2003; Klass et al., 2007; Yao et al., 2007). Above the upper development threshold, growth of the fungus is halted until temperatures fall below the threshold. The optimal growth rate has been shown to be around 28°C. There are many examples of temperature-dependent mortality rates for EPFs used in the biocontrol of insect pests (Doberski, 1981; Carruthers et al., 1985). These findings suggest that environmental conditions are an important factor to the success of microbial control and brings into question the assumption of constant time to death irrespectively of the context. Furthermore, many grasshoppers and locusts can behaviourally regulate their body temperature well above ambient over large parts of the day during sunny conditions (Chappell and Whitam, 1990). This behaviour has been shown to slow disease incubation and confer significant survival advantage (Carruthers et al., 1992; Inglis et al., 1996; Blanford et al., 1998; Blanford and Thomas, 1999a; b). In field trials, mortality does not usually occur earlier than 6 days after spraying and may take longer (Bateman, 1997). Speed of kill is influenced strongly by dose and environmental conditions and their insect hosts, e.g., internal body temperatures of the host insect. Therefore, to encourage the wider use of biopesticides, it is vital to understand how the locust body temperature fluctuates under different habitats and locust characteristics, so that biopesticide spraying can take place when conditions are most favourable to the pathogen.

The body temperature of locusts and grasshoppers is influenced by microclimate, adjacent vegetation, terrain and weather including solar radiation, wind and clouds (Willmer, 1982; Coxwell and Bock, 1995). Moreover, their posture, body colour can also lead to different body temperatures under the same environmental conditions (Stevenson, 1985; Jong et al., 1996; Miller and Denny, 2011). Most insects, such as locusts and grasshoppers, have limited capacity to internally regulate their body temperature and mainly rely on the surrounding environment (Angilletta, 2009). Microhabitat selection is predicted to have the greatest effect on an ectotherm's temperature (Stevenson, 1985). Temperatures of plant canopy exert the principal effect on body temperature of *L. m. manilensis*, especially the ground temperature (Liu et al., 2018).

Although previous laboratory work (Blandford and Thomas, 1999a; Arthurs and Thomas 2000; Yao et al., 2007; Yue et al., 2010; Liu et al., 2019) has expanded our knowledge and provided an invaluable information about the relation between temperature and the effectiveness of EPFs on insect control, there is a need for complementary studies involving more realistic environmental conditions. Behavioural and physiological rhythms in a natural setting remain relatively unexplored for many species, which will provide valuable insights into the precise pest control including time and target location of field treatments (Miyata, 2011). Here, we use *L. m. manilensis* in the main breeding regions of China as a case study to understand daily activity rhythms and behaviour of *L. m. manilensis* under real field conditions *via* the detection of body temperature and locust traits. We conducted extensive field surveys recording locust body characteristics and habitat in two key locust breeding zones, which were lake-reservoir type/wetland and coastal type of locusts breeding habitats on the east coast of China. Specifically, we aimed to answer the following questions: 1) do locust prefer different reed habitat across development stage and location? 2) how body and ambient temperature fluctuates during the day across locations? 3) does body temperature differ across study area, development stage, reed habitat, sex, and body length? Upon the strength of these relations, we could generalize body temperature patterns of locusts across different locations under similar habitat condition. We further discuss how these results may help to tailor the biopesticide product treatment based on environment characteristics, in order to improve the efficacy of the control measures.

2 Materials and methods

2.1 Study zones

Two experimental zones were selected, which represent lake-reservoir type/wetland and coastal type of locusts breeding habitats on the east coast of China (Figure 1): Dagang (DAG) and Dongying (DON). Dagang study area was located in the North Dagang Reservoir area at the southeast of Tianjin City. There is an area of approximately 45,000 ha suitable for locusts (Fan et al., 2010). Dongying study area corresponds to the Yellow River Delta area (Kenli district, Shandong Province, China). This area is a long-known breeding area for locusts in China, and the Kenli district is one of the key locust regions, where there are approximately 148,000 ha suitable for locust occurrence (Hu, 2018). The main soil types in both regions are tidal soil, saline soil and coastal saline. Local farmers will choose slight alkaline land to plant agricultural crops, such as maize, rice, peanut, or establish ponds to culture lotus and feed fish and shrimps in the wetland. These two zones belong to non-agricultural land, and are full of bulrush and

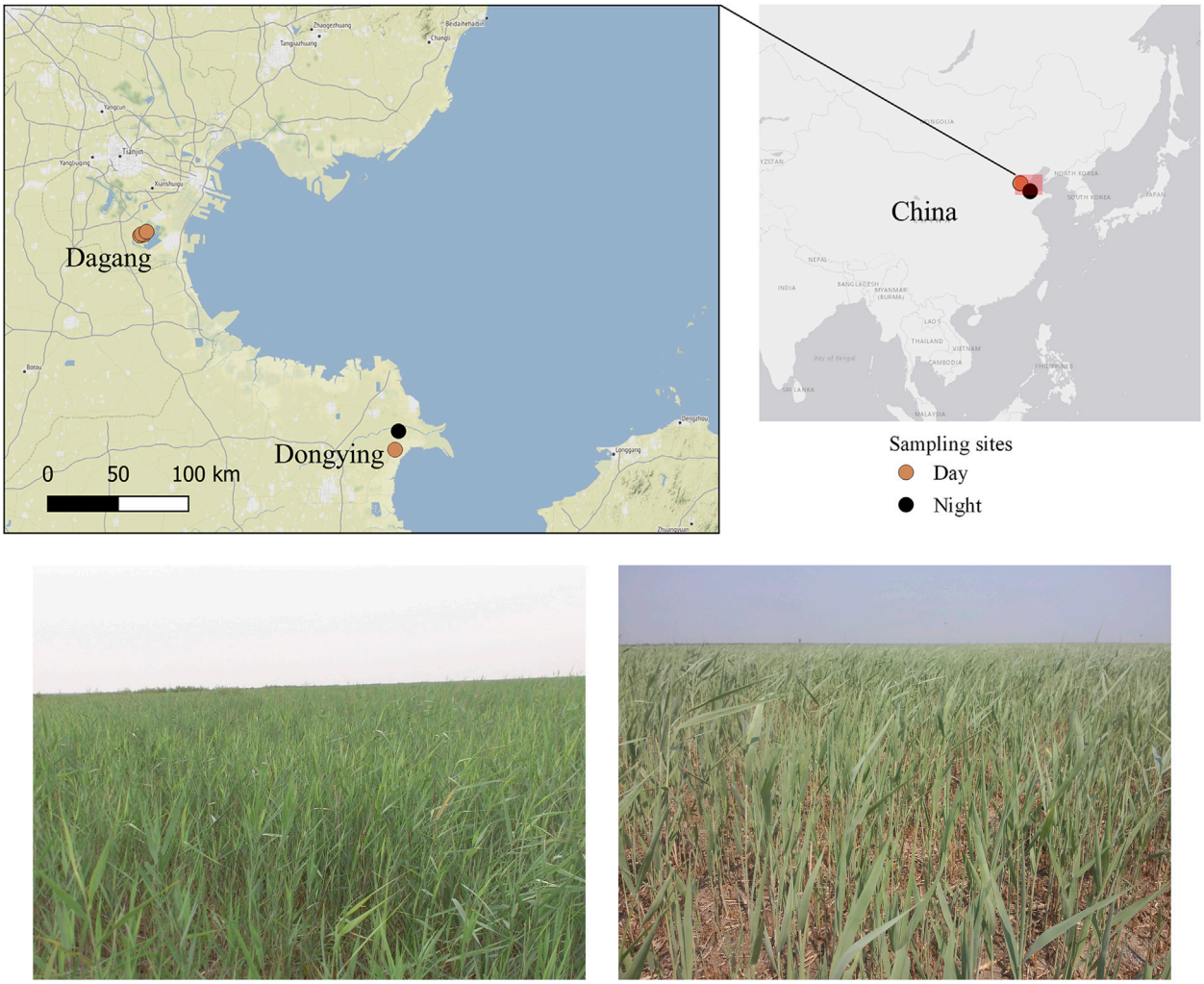

FIGURE 1
Map of study areas (Dagang and Dongying) on the East coast of China.

gramineous vegetations, and the dominant plants in the experimental areas are *Phragmites australis*, mainly associated with *Suaeda glauca*, *Alternanthera sessilis*, *Cynodon dactylon* and *Aster subulatus*. *L. m. manilensis* is the main locust species in both zones producing up to two generations a year. We selected similar sites in terms of vegetation for both zones: four in Dagang and two in Dongying (Figure 1).

2.2 Body temperature and insect traits sampling

Data were collected in Dagang during summer 2016 and in Dongying in summer 2017 (i.e., June, July and August). We conducted two different survey methods, during the day (6:00–18:59) and night time (19:00–5:59). During day time we collected the insects in open field conditions either hand caught or trapped in a small sweep net. Each site was visited weekly until at least five insects were recorded per hour. During the night, due to safety reasons, we were not able to sample in open field conditions. Thus, about 100 locust nymphs were collected in advance during the day and placed in a cage (2 m× 2 m× 2 m) with natural reedbed vegetation at a field station (Figure 1). For practical reasons, we could only carry out this night experiment in Dongying area. A minimum of 10 insects per hour were hand caught randomly chosen from the cage. A total of 645 and 308 locusts were collected during day and night sampling respectively.

In both day and night surveys, internal body temperatures were recorded using a 0.125 mm diameter copper thermocouple connected to a hand-held, fast response, digital thermometer (type 0.1°C resolution, 5 s response time, −0.1 mm diameter; Eutech Instruments). For each insect caught, we made a small hole in its thorax with the tip of a 0.22-mm diameter hypodermic needle (Blandford et al., 1998). A thermocouple was then inserted to a depth of 2 mm and a reading taken at the point the temperature stabilized. Insects were discarded and recordings were not taken when capture and/or length of time for the recording to be taken was felt to have affected the real body temperature (10–12 s after capture). Generally, insects were processed within 5–7 s of capture. Besides internal body temperature, we also recorded the time (H:M) of each record, the ground temperature and position in the vegetation where the insect was collected (Day: ground, canopy, top and flying; Night: ground, canopy, net). Finally, for each insect we recorded the body length, stage (instar three to five and adult), and sex (female, male).

2.3 Data analyses

We studied the subhabitat preference of locust in the reed habitat (e.g., ground, canopy, top and flying) in relation to locust traits (development and sex) and time using contingency tables and conditional extended mosaic plots (Zeileis et al., 2007) using the package vcd in R (Meyer et al., 2006). This type of plot shows an area proportional visualization of a table of expected frequencies. It is composed of boxes, with size proportional to the corresponding frequency entry, given the dimensions of previous splits. The shading in the plots visualizes the Pearson residuals representing the standardized deviations of the observed frequencies from expectations. The blue and red colour show respectively significant deviations ($p < 0.05$) above and below the expected frequencies. Finally, we also computed the sum-of-squares test of independence, based on the permutation distribution of 1000 iterations. Significant test ($p < 0.05$) rejects the null hypothesis of independence (Zeileis et al., 2007).

The linear mixed models were used to understand the relation between body temperature and the factors of interest: study area (only day data), development stage (instar-adult), position in vegetation, sex and body length. Prior to the models, we analysed the correlation between the factors to avoid collinearity. Body length was highly correlated with development stages and sex: higher size for females and older stages (see Appendix). Thus, we performed two sets of models, first with sex and stages and second with body length. For the first set of models, differences of internal body temperature during the day across study area (provinces), position, development stage (instar-adult) and sex was compared in a linear mixed model including as random effects site. We also included ground temperature as fixed effect to control for ambient temperature experiencing each individual locust. The distribution of errors was modelled as a Gaussian function with identity link. A similar linear model was implemented for the night survey but only for the study site available, thus without random effect for site. Significant differences among levels of each factor were tested using a post-hoc normal host z test (asymptotic t test) using Tukey procedure. We repeated the same procedure using a similar structure of linear mixed models for day and night datasets but only including body length instead of sex and development stage. All analyses were performed in R 4.2.1 using packages multcomp, lme4 and lmerTest.

3 Results

3.1 Subhabitat preference of *L. m. manilensis* in natural ecosystem

L. m. manilensis significantly preferred the ground as their major activity subhabitat in both locust breeding regions (Figure 2). Adults showed higher variable preference on their subhabitat significantly preferring higher positions in the vegetation (Figure 2). This pattern was particularly relevant in Dagang while in Dongying most insects preferred the ground irrespectively of their developmental stage (Supplementary Figure S1).

The insect behavior was variable during daytime, although there is a significant trend to prefer ground subhabitat

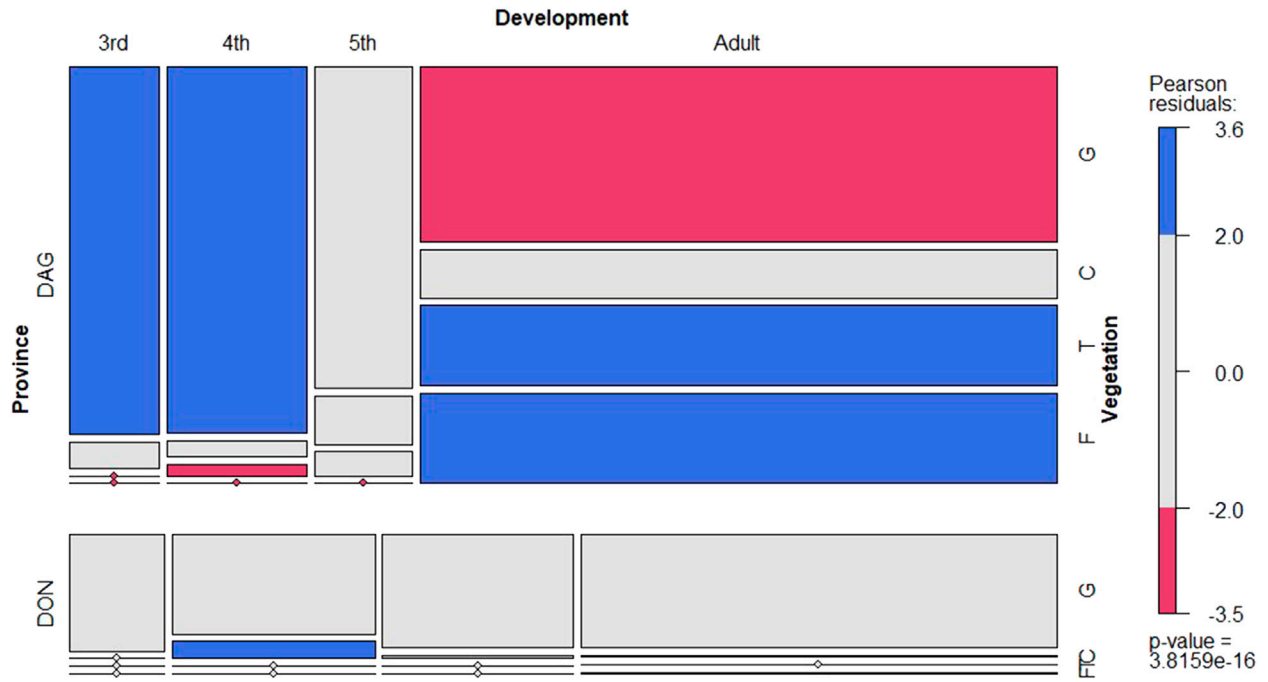

FIGURE 2
Conditional mosaic plot based on the contingency table with the number of locust records in Dagang (top) and Dongying provinces (bottom) per vegetation position (y-axis) and development stage (x-axis) in daytime. The color gradient indicates the Pearson residuals representing the standardized deviations of the observed frequencies from expectations. The blue and red colors indicate the combination of categories statistically significant at 95% confidence level ($\alpha = 0.05$) respectively above and below their expected frequencies. Boxes for the vegetation variable are ordered from ground to flying position (G - ground, C- canopy, T-top and F-flying). The *p*-value at the right bottom corner indicates the χ^2 test of independence, based on the permutation distribution.

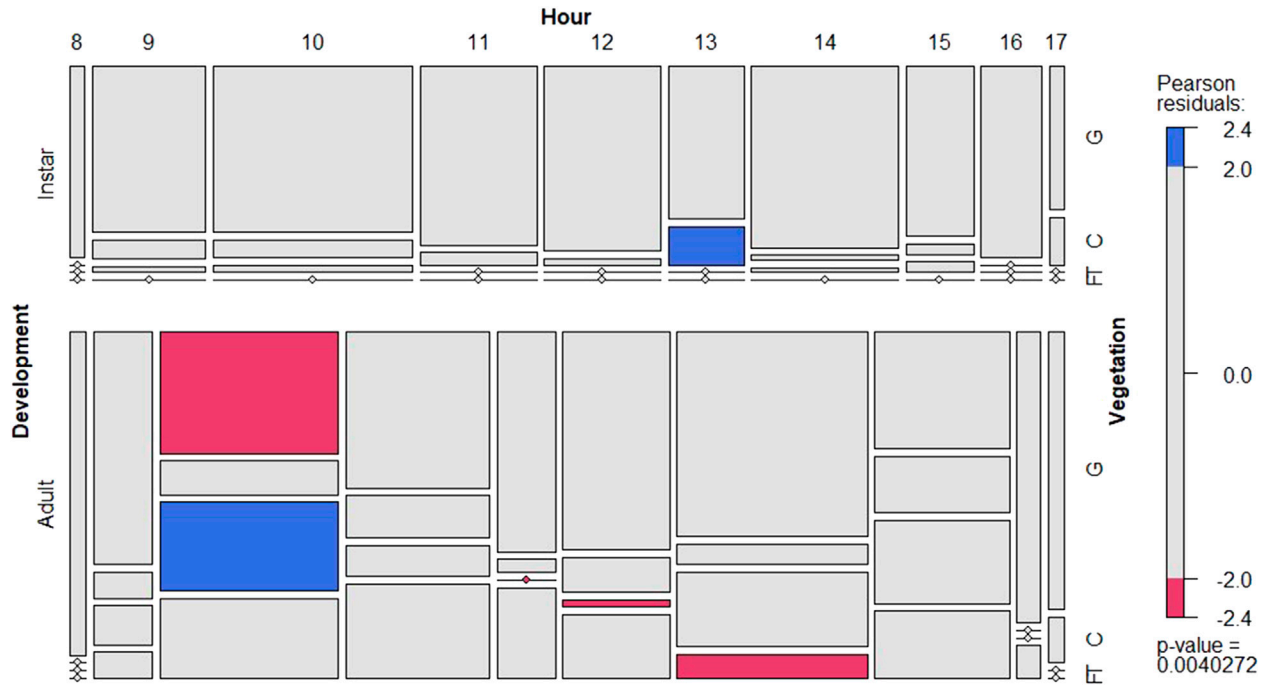

FIGURE 3
Conditional mosaic plot based on the contingency table with the number of locust records for all instars (left figure) and adults (right) in daytime. For each development group it shows the departure from expectations per vegetation position (y-axis) and hour (x-axis). See details in Figure 2.

particularly for instars (Figure 3; Supplementary Figure S2). Adults showed one clear peak of activity at 10:00 showing significantly less preference for the ground subhabitat. Interestingly, adults showed higher flying activity during midday (Figure 3; Supplementary Figure S2). During night time, the preferred subhabitat for locusts was the plant canopy with a sharp increase towards the ground just before sunrise (Supplementary Figure S3).

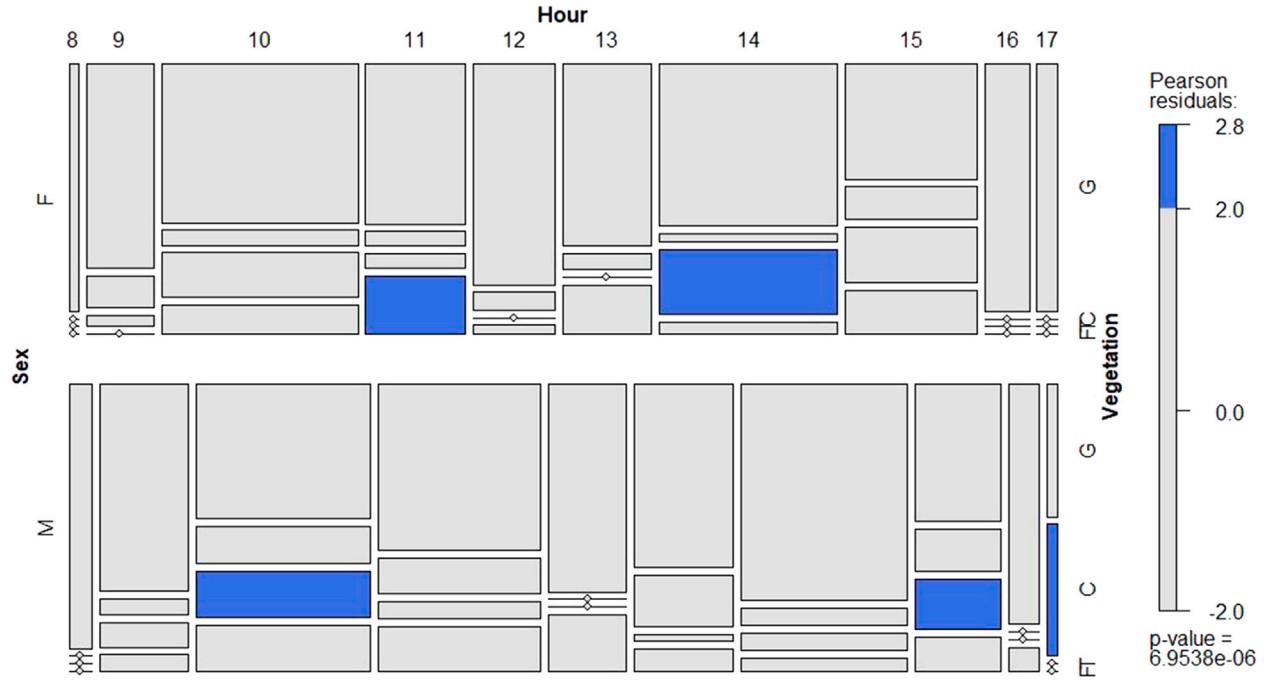

FIGURE 4
Conditional mosaic plot based on the contingency table with the number of locust records for female (left figure) and male (right) in daytime. For each development group it shows the departure from expectations per vegetation position (x-axis) and hour (y-axis). See details in Figure 2.

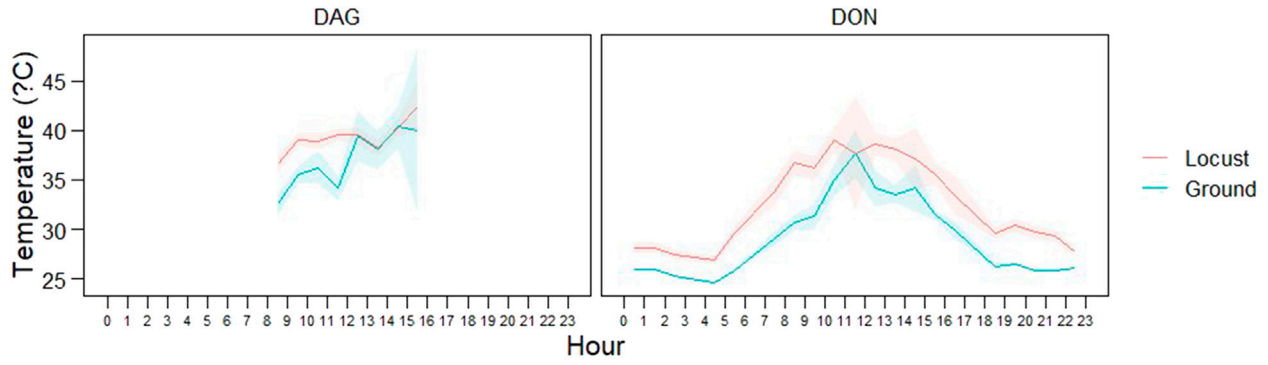

FIGURE 5
Diurnal pattern of locust body temperature (red) and ground temperature (blue) in the two study areas: Dagang (left) and Dongying (right). For each hour the plot indicates the mean (line) and confidence intervals (i.e., standard error).

During day time, both female and male showed a similar behaviour pattern (Figure 4; Supplementary Figure S3). They tended to significantly prefer higher positions in the vegetation at two peaks (10:00–11:00 h and 14:00–15:00 h). Interestingly, males moved up earlier in the morning and later in the afternoon. During night time, both sexes preferred the canopy as their main subhabitat (Supplementary Figure S4).

3.2 The diurnal pattern of internal body temperature of *L. m. manilensis* in two different zones

The mean body temperature during the day was 38.42°C (±3.52 SD; Min: 28.7; Max: 47.2) while during the night body temperature was 28.23°C (±1.65 SD; Min: 24.7; Max: 37.8). Internal body temperature of *L. m. manilensis* showed a characteristic diurnal pattern reaching rather constant minimum temperatures during the night and reaching maximum peaks at mid-day with high variability (Figure 5). Locust body temperature was consistently higher than ground ambient temperature, particularly during night time (Figure 5). This pattern was consistent in both study areas (Figure 5). According to the linear mixed model, body temperature was significantly related to ground temperature ($p < 0.0001$).

3.3 The relationship between locust traits and internal body temperature of *L. m. manilensis*

During day time, mean internal body temperature increased with the development stage of the insect (Figure 6). Adults, 4th and 5th instars showed higher temperature than 3rd instars ($p < 0.05$, Figure 6). In contrast, mean body temperature between locust sex, study areas and position at the vegetation did not show significant differences.

The pattern during night-time was clearly different than for the day (Figure 7). Body temperature decreased with development stage, with adults and 5th instar showing lower temperature than younger instars. Males showed higher body temperature than females, but there was no significantly difference found. Locusts in the canopy showed higher temperature than at ground (Figure 7). Body and ground temperature were positively related for day (beta: 0.34, t value: 18.57, $p < 0.001$) and night sampling (beta: 0.64, t value: 4.05, $p < 0.001$).

Body length was significantly related to body temperature (Figure 8), with a positive trend during the day (beta: 0.55, t value: 4.07, $p < 0.001$) and negative during the night (beta: −1.08, t value: −6.44, $p < 0.001$).

4 Discussion

Ectotherms are intrinsically affected by fluctuations in ambient temperature, as the latter determines the rate of biochemical and physiological reactions including the development of both the host and the pathogen. Thus, the study of body temperature in insects is not only important for ontogeny, but also critical for improvement in the control effect of biopesticide and sustainable pest management. Previously studies implied that the body temperature of *L. m. manilensis* was a similar tendency for variation of natural subhabitat ground temperature (Liu et al., 2018). Similarly, the body temperature of *Oedaleus decorus asiaticus* (Bey-Bienko) increased/decreased with increases/decreases inground temperature, respectively during the daytime (Cheng et al., 2022). This study identified under natural conditions, how subhabitat and species traits modulate *L. m. manilensis* internal body temperature across two separate study breeding regions in China. These results are extremely relevant to improve tailored biopesticide applications taking advantage of habitats frequented and traits that modulate internal body temperature.

The results showed that *L. m. manilensis* preferred the ground as their major activity habitat regardless of the locust breeding regions. Only adults showed a distinct pattern to move upwards in the vegetation during short periods of time during the day. This behaviour is essential to survive as they have limited capacity to internally regulate their body temperature and mainly rely on the surrounding environment (Angilletta, 2009). During the day the Oriental migratory locusts showed two peaks of activity where it tended to climb the vegetation. Specifically, locust chose to move up after sunrise resting at mid and top of the canopy, and then moved back to the shade at noon possibly to avoid injury due to high temperature. Finally, once the ambient temperature was cooling

10.3389/fphys.2023.1110998

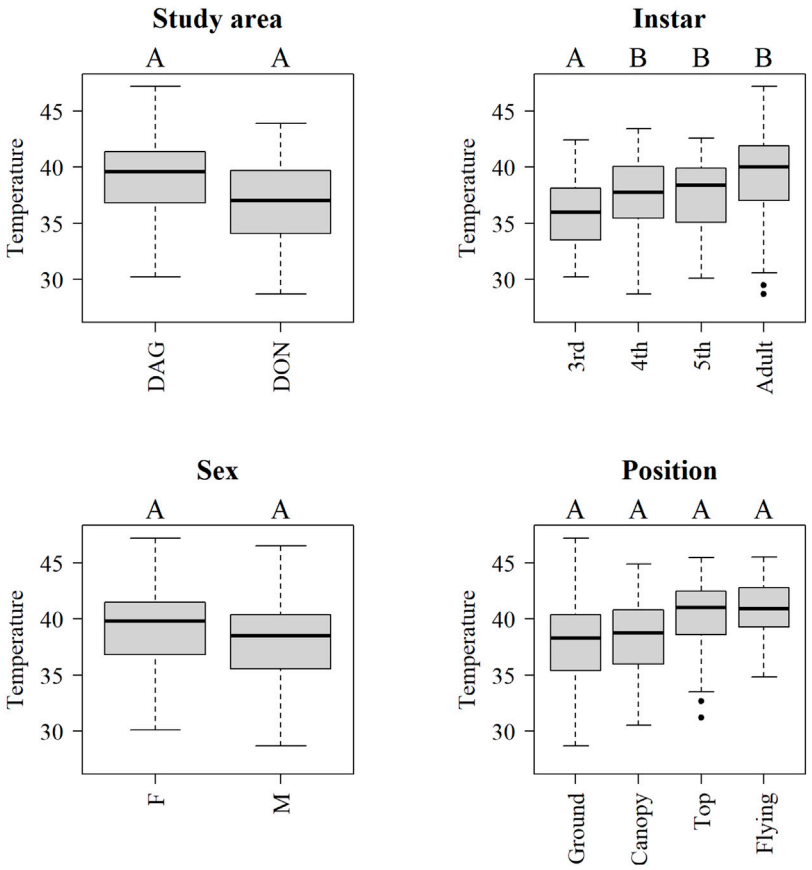

FIGURE 6
Boxplots of internal body temperature of *Locusta migratoria manilensis* across provinces (DAG-Dagang, DON-Dongying), instar, position and sex (F-female, M-male) at daytime (6:00–18:59). Letters above each level indicate significant differences ($p < 0.05$) between levels in a mixed model including all indicated factors and controlling by ambient temperature and site.

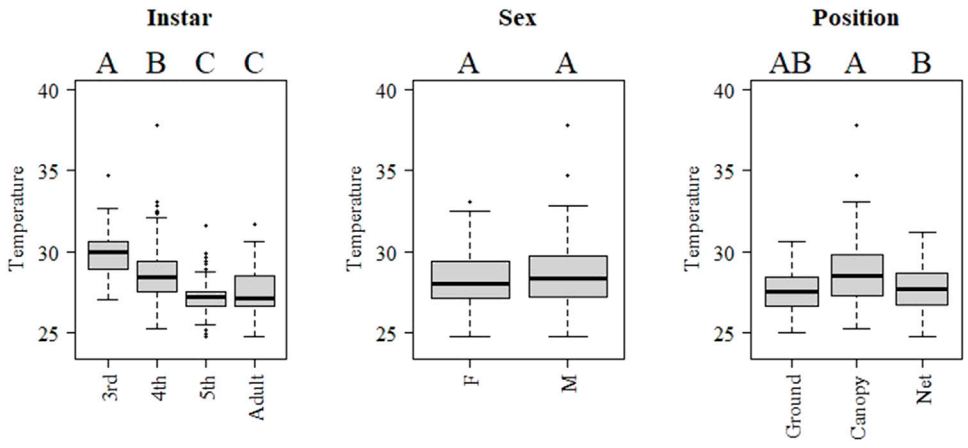

FIGURE 7
Boxplots of internal body temperature of *Locusta migratoria manilensis*, instar, sex and position at night-time (raw data 19:00–05:59). Letters above each level indicate significant differences ($p < 0.05$) between levels in a mixed model including all indicated factors and controlling by hour.

down, the locusts left the ground and moved up in the canopy with a peak around 15:00 h in the afternoon. This behavioural pattern is characteristic of other diurnal insects. For instance, Ellis and Ashall, (1957) noted that bands of hoppers of *S. gregaria* had a definite diurnal pattern of behavior. Before dawn, the hoppers were mainly roosting and again during the hottest part of the day, most of them roosted (Ellis and Ashall, 1957). Chapman (1959) also found a similar pattern for Red locust, *Nomadacris septemfasciata* (Serville). In the morning

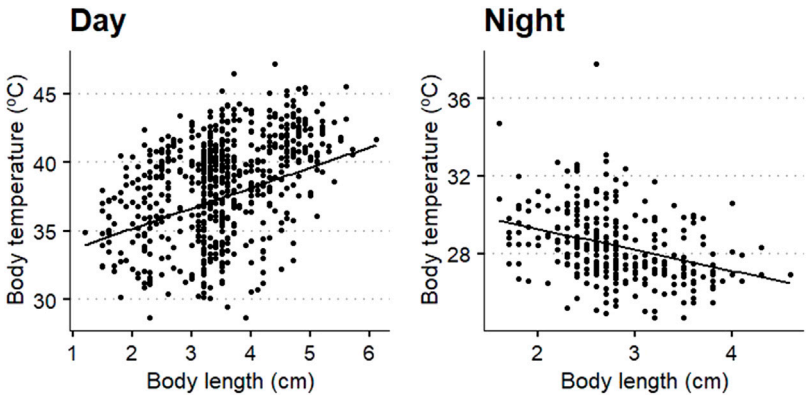

FIGURE 8
Scatterplots of the relation between body temperature of *Locusta migratoria manilensis* and body length at day (left plot) and night (right plot). Black line shows the fitted linear mixed model for the Dongying region and average ground temperature.

and evening, all the locusts inhabit higher plants, which may be related to the increase of light intensity and the decrease of environmental temperature.

During the night, locusts in this study preferred the canopy as main resting habitat. In a similar context to our study, Cheng et al. (2020) found that the position of the Oriental migratory locust was different in different times of the day. In contrast to daytime, locusts at night preferred the canopy as resting subhabitat. Specifically, Cheng et al. (2020) found that during night, the Oriental migratory locust preferred to choose the place higher than 60 cm. Chapman (1959) also found that *N. septemfasciata* inhabited higher plants all night. Similarly, the hoppers of Moroccan locust, *Dociostaurus maroccanus* (Thnb.), remained on or near the ground during the day, moving to the top of the plants at night (Uvarov et al., 1951). In contrast, Senegalese grasshopper, *O. senegalensis* (Krauss), was observed feeding in the evening, and spent the night on the ground in India desert (Chandra, 1983).

Regarding sex differences in habitat preference, this study results implied that both female and male tended to show similar behaviour. However, the proportion of female adults preferred to the lower part of the plant comparing the male adults of *O. d. asiaticus* and *Calliptamus abbreviates* (Ikovnnikov). The female adults of *Euchorthippus unicolor* (Ikonnikov) preferred to choose the upper and top parts of plants more than male adults (Bai et al., 2014). The reason would be related to the different locusts requesting different habitat and hosts. The physiological needs driven their movement. In general, the locusts were plentiful in breeding grounds in the plain where female locusts were ovipositing (Uvarov et al., 1951).

The differences in internal body temperature are mainly related to the species traits (i.e., size and development stage) irrespectively of the breeding region or position preference at reed vegetation. Both selected breeding regions, North Dagang Reservoir area at the southeast of Tianjin City and the Yellow River Delta area, are two of the main areas in east coast China prone to the migratory locust plagues, where the central government and local governments established long-term monitoring and management scheme. Despite the distance between the regions, both areas share similar vegetation, geographical context and availability of natural breeding habitat determining the occurrence of the oriental migratory locust. Thus, the physical process that links ambient and internal body temperature through locust morphological traits seems to be constant across these characteristic locust breeding regions in east coast China. This pattern implied that the comprehensive body temperature of locust in one habitat region may represent the cases in similar habitats, and can provide enough fundamental information to establish the biopesticide model to precisely control.

The main factor affecting the average body temperature of locusts was development stage. At night, position at the vegetation was also a key factor affecting the average body temperature of locusts. These patterns arose once fluctuation in ambient temperature was controlled (i.e., ground temperature) indicating that endogenous traits such as development age have a clear relevance in how locust thermoregulates in relation to the surrounding temperature. Thomas and Blanford. (2003) also identified that some internal characteristics of insects can affect insect thermoregulation, such as body length, age, sex, colour. Similarly, we also identified a significant relation between body length of *L. m. manilensis* and internal body temperature. In fact, body length or size are factors to absorb the energy from the ambient. Body size is a major trait that impacted on nearly all aspects of an individual's life history (Woodward et al., 2005; Brose, 2006). Furthermore, as ectotherms increase in size, solar radiation will raise their body temperature further above the ambient temperature due to the reduced effect of convection on larger organisms (Porter and Gates, 1969; Stevenson, 1985). This explanation is plausible for the pattern observed during daytime, where bigger individuals heated by the Sun light showed higher average body temperature than smaller ones. In adults, the prediction of increased body temperature with increased size has been confirmed by comparison across many different insect species (Willmer and Unwin, 1981). As for developmental size change, early work on the desert locust, *S. gregaria*, suggested increased body temperature between the first and last instars (Stower and Griffiths, 1966), and more recent work on *Manduca sexta* (L.) clearly demonstrates this pattern across all larval stages (Woods, 2013).

We would expect a similar pattern between body temperature and size during the night time. As body size affects the rate of heating and cooling, larger animals should show higher thermal inertia than smaller ones (Stevenson, 1985). Thus, we would expect larger animals that have been heated during the day to keep their

temperature higher than smaller individuals. Nevertheless, the nighttime data showed the opposite pattern, with a decrease in body temperature with body size. A possible explanation for this finding is the behavioural change across development stages. In fact, not only does body size directly affect body temperature (Stevenson, 1985; Woods, 2013), but size should also alter thermoregulatory behaviour, with subsequent indirect changes in body temperature. It is possible that adults, with higher mobility than other instars, are able to track changes in microhabitat temperature moving to specific areas where temperature is more suitable for development or indirectly to escape predators.

The activity pattern may provide the useful information for field spray good timing. We have identified main characteristics in daily variation of *L. m. manilensis* subhabitat preference and the main factors affecting their internal body temperature. Based on these findings, the application of biopesticides should focus on younger locusts at dawn or dusk when temperatures tend to be lower and temperatures more suitable for EFP development. This will help biopesticides play their roles and minimize the risk of outbreak escalation. In addition, the advanced technology against crop insect pests and diseases including the Earth observation, agricultural Apps, generally demanded the ground truth data of the pests. It is not possible to carry out all the collation everywhere, thus the results of this study contribute to the efficacy of biopesticides, and predict such variability in the performance of fungal biopesticides increasing confidence in their use.

Data availability statement

The raw data supporting the conclusions of this article will be made available by the authors, without undue reservation.

Author contributions

All authors conceived the ideas and designed methodology; contributed to the manuscripts and final submission. YC and YL contributed two the field data collection, HL, JH, MW, and PG-M analysed the data and led the writing of the manuscript, JZ, FZ, BT, and BL contributed to the conception and field work design, BT and BL helped to improve the language.

Acknowledgments

We acknowledge financial support from China's Donation to the CABI Development Fund (IVM10051), Newton-UK-China Agri-centres (BBSRC) (Grant No. 104906), National Key R and D Program of China (2017YFE0122400). PG-M was also supported by a "Juan de la Cierva-Incorporación" contract (MINECO, IJCI-2017-31733).

Conflict of interest

The authors declare that the research was conducted in the absence of any commercial or financial relationships that could be construed as a potential conflict of interest.

Publisher's note

All claims expressed in this article are solely those of the authors and do not necessarily represent those of their affiliated organizations, or those of the publisher, the editors and the reviewers. Any product that may be evaluated in this article, or claim that may be made by its manufacturer, is not guaranteed or endorsed by the publisher.

Supplementary material

The Supplementary Material for this article can be found online at: https://www.frontiersin.org/articles/10.3389/fphys.2023.1110998/full#supplementary-material

References

Angilletta, M. J. (2009). *Thermal adaptation*. New York: Oxford University Press.

Arthurs, S., and Thomas, M. B. (2000). Effects of a mycoinsecticide on feeding and fecundity of the Brown locust *Locustana pardalina*. *Biocontrol Sci. Techn.* 10, 321–329. doi:10.1080/09583150050044592

Bai, H., Yao, Y., Sun, W., Dong, H., and Cong, B. (2014). Selection of plant height of three dominant grasshoppers in hilly meadow steppe of Horqin. *J. Shenyang Agric. Univ.* 45, 478–481. doi:10.3969/j.issn.1000-1700.2014.04.018

Bateman, R. P. (1997). The development of a mycoinsecticide for the control of locusts and grasshoppers. *Outlook Agr.* 26, 13–18. doi:10.1177/003072709702600104

Blanford, S., and Thomas, M. B. (1999a). Host thermal biology: The key to understanding host-pathogen interactions and microbial pest control? *Agr. For. Entomol.* 1, 195–202. doi:10.1046/j.1461-9563.1999.00027.x

Blanford, S., Thomas, M. B., and Langewald, J. (1998). Behavioural fever in the Senegalese grasshopper, *Oedaleus senegalensis*, and its implications for biological control using pathogens. *Ecol. Entomol.* 23, 9–14. doi:10.1046/j.1365-2311.1998.00104.x

Blanford, S., and Thomas, M. B. (1999b). Role of thermal biology in disease dynamics. *Asp. Appl. Biol.* 53, 73–82.

Brose, B. (2006). Consumer-resource body-size relationships in natural food webs. *Ecology* 87, 2411–2417. doi:10.1890/0012-9658(2006)87[2411:cbrinf]2.0.co;2

Cao, G., Jia, M., Zhao, X., Wang, L., Zhang, Z., Wang, G., et al. (2016). Different effects of *Metarhizium anisopliae* strains IMI330189 and IBC200614 on enzymes activities and hemocytes of *Locusta migratoria* L. *PLoS ONE* 11, e0155257. doi:10.1371/journal.pone.0155257

Carruthers, R. I., Feng, Z., Robson, D. S., and Roberts, D. W. (1985). *In vivo* temperature-dependent of *Beauveria bassiana* (deuteromycotina: Hyphomycetes) mycosis of the European corn borer, *Ostrinia nubilalis* (Lepidoptera: Pyralidae). *J. Invertebr. Pathol.* 46, 305–311. doi:10.1016/0022-2011(85)90073-4

Carruthers, R. I., Larkin, T. S., Firstencel, H., and Feng, Z. D. (1992). Influence of thermal ecology on the Mycosis of a Rangeland grasshopper. *Ecology* 73, 190–204. doi:10.2307/1938731

Chandra, S. (1983). Some field observations on a small concentration of *Oedaleus senegalensis* Krauss (Orthoptera: Acrididae) in the Indian desert. *Plant Prot. Bull.* 35, 9–13.

Chapman, R. F. (1959). *Field observations of the behaviour of hoppers of the Red locust* (Nomadacris septemfasciata *Serville)*. Ghana: University College of Ghana Press.

Chappell, M. A., and Whitman, D. A. (1990). *Grasshopper thermoregulation in biology of grasshoppers*. New York: Wiley Interscience Wiley.

Cheng, Y., Li, H., Liu, L., Wang, G., Gu, H., and Luke, B. (2022). Sex and body colour affect the variation in internal body temperature of *Oedaleus decorus asiaticus* in natural habitats in Inner Mongolia, China. *Agriculture* 12, 878. doi:10.3390/agriculture12060878

Cheng, Y. M., Li, H. M., Ren, B. Y., Xie, X. H., Zhang, X. J., Liu, Y. M., et al. (2020). Study on factors influencing the selection of the height of plant inhabited by *Locusta migratoria manilensis*. *J. Environ. Entomol.* 42, 545–552. doi:10.3969/j.issn.1674-0858.2020.03.4

Coxwell, C. C., and Bock, C. E. (1995). Spatial variation in diurnal surface temperatures and the distribution and abundance of an alpine grasshopper. *Oecologia* 104, 433–439. doi:10.1007/BF00341340

Doberski, J. (1981). Comparative laboratory studies on three fungal pathogens of the elm bark beetle Scolytus scolytus: Pathogenicity of Beauveria bassiana, Metarhizium anisopliae, and Paecilomyces farinosus to larvae and adults of Scolytus scolytus. *J. Invertebr. Pathol.* 37, 188. doi:10.1016/0022-2011(81)90074-4

Driver, F., Milner, R. J., and Trueman, J. W. H. (2000). A taxonomic revision of *Metarhizium* based on a phylogenetic analysis of rDNA sequence data. *Mycol. Res.* 104, 134–150. doi:10.1017/S0953756299001756

Ellis, P., and Ashall, C. (1957). *Field studies on diurnal behaviour, movement and aggregation in the desert locust (*Schistocerca gregaria Forskål*).* London: Anti-Locust Bull. Press.

Fan, C. B., Dou, C. C., Tian, C. J., Zheng, Y. Q., Wu, H. L., Gao, Y. L., et al. (2010). Control of biological pesticide technology research and application of the *Locusta migratoria* manilensis on Dagang district. *Anhui Agr. Sci. Bull.* 16, 97. doi:10.1371/journal.pone.0206816

Harb, M. F. (2009). *Glossary on desert locust*. Rome: FAO Press.

Hu, P. F. (2018). Management measures against *Locusta migratoria manilensis* in Kenli. *Agr. Technol.* 38, 50.

Inglis, G. D., Dan, L. J., and Goettel, M. S. (1996). Effects of temperature and thermoregulation on Mycosis by *Beauveria bassiana* in grasshoppers. *Biol. Control* 7, 131–139. doi:10.1006/bcon.1996.0076

Jong, P., Gussekloo, S., and Brakefield, P. (1996). Differences in thermal balance, body temperature and activity between non-melanic and melanic two-spot ladybird beetles (*Adalia bipunctata*) under controlled conditions. *J. Exp. Biol.* 199, 2655–2666. doi:10.1242/jeb.199.12.2655

Jurd, T. (2015). Western mag. Available at: https://www.sott.net/article/292984-Locust-swarms-causing-damage-to-crops-in-New-South-Wales-Australia (Accessed February 20, 2015).

Klass, J. I., Blanford, S., and Thomas, M. B. (2007). Development of a model for evaluating the effects of environmental temperature and thermal behaviour on biological control of locusts and grasshoppers using pathogens. *Agr. For. Entomol.* 9, 189–199. doi:10.1111/J.1461-9563.2007.00335.X

Liu, Y. M., Cheng, Y. M., Li, H. M., Nong, X. Q., and Luke, B. (2019). Virulence of *Metarhizium anisopliae* against 3rd instar nymphs of *Locusta migratoria manilensis* under different temperatures. *Chin. J. Biol. Control* 35, 642–647. doi:10.16409/j.cnki.2095-039x.2019.04.021

Liu, Y. M., Yang, J. W., Fan, C. B., Shang, S. Q., Taylor, B., and Li, H. M. (2018). Research on environmental factors regulating body temperature of oriental migratory locust *Locusta migratoria manilensis*. *J. Plant Prot.* 45, 1296–1301. doi:10.13802/j.cnki.zwbhxb.2018.2017018

Maute, K., French, K., Bull, C. M., Story, P., and Hose, G. (2015). Current insecticide treatments used in locust control have less of a short-term impact on Australian arid-zone reptile communities than does temporal variation. *Wildl. Res.* 42, 50–59. doi:10.1071/WR14194

Meyer, D., Zeileis, A., and Hornik, K. (2006). The strucplot framework: Visualizing multi-way contingency tables with vcd. *J. Stat. Softw.* 17 (3), 1–48. doi:10.18637/jss.v017.i03

Miller, L. P., and Denny, M. W. (2011). Importance of behavior and morphological traits for controlling body temperature in Littorinid snails. *Biol. Bull.* 220, 209–223. doi:10.1086/BBLv220n3p209

Miyata, T. (2011). Insect quality control: Synchronized sex, mating system, and biological rhythm. *Appl. Entomol. Zool.* 46, 3–14. doi:10.1007/s13355-010-0017-7

Ndolo, D., Njuguna, E., Adetunji, C. O., Harbor, C., Rowe, A., Breeyen, A. D., et al. (2019). Research and development of biopesticides: Challenges and prospects. *Outlooks Pest Manag.* 30, 267–276. doi:10.1564/v30_dec_08

Peng, G., and Xia, Y. (2011). The mechanism of the mycoinsecticide diluent on the efficacy of the oil formulation of insecticidal fungusfficacy of the oil formulation of insecticidal fungus. *Biocontrol* 56, 893–902. doi:10.1007/s10526-011-9360-z

Smits, N., BriÈRe, J. F., and Fargues, J. (2003). Comparison of non-linear temperature-dependent development rate models applied to *in vitro* growth of entomopathogenic fungi. *Mycol. Res.* 107, 1476–1484. doi:10.1017/S095375620300844X

Stevenson, R. D. (1985). Body size and limits of the daily range of body temperature in terrestrial ectotherms. *Am. Nat.* 125, 102–117.

Stower, W. J., and Griffiths, J. F. (1966). The body temperature of the desert locust (*Schistocerca gregaria*). *Entomol. Exp. Appl.* 9, 127–178. doi:10.1111/j.1570-7458.1966.tb02345.x

Thomas, M. B., and Blanford, S. (2003). Thermal biology in insect-parasite interactions. *Trends Ecol. Evol.* 18, 344–350. doi:10.1016/S0169-5347(03)00069-7

Uvarov, B. P., Chapman, E., Waloff, N., and Waterston, A. R. (1951). Observations on the Moroccan locust (Dociostaurus maroccanus thunberg) in Cyprus. *Anti-Locust Bull.* 10, 4–52. doi:10.1023/A:1009639628627

Willmer, P. G. (1982). Microclimate and the environmental physiology of insects. *Adv. Insect Physiol.* 16, 1–57. doi:10.1016/S0065-2806(08)60151-4

Willmer, P. G., and Unwin, D. M. (1981). Field analyses of insect heat budgets: Reflectance, size and heating rates. *Oecologia* 50, 250–255. doi:10.1007/BF00348047

Woods, H. A. (2013). Ontogenetic changes in the body temperature of an insect herbivore. *Funct. Ecol.* 27, 1322–1331. doi:10.1111/1365-2435.12124

Woodward, G., Ebenman, B., Emmerson, M., Montoya, J. M., Olesen, J. M., Valido, A., et al. (2005). Body size in ecological networks. *Trends Ecol. Evol.* 20, 402–409. doi:10.1016/j.tree.2005.04.005

Xia, J. Y., and Huang, H. (2002). Analysis on the outbreak of *Locusta migratoria manilensis* and its control strategies. *Plant Prot. Technol. Ext.* 22, 7–10. doi:10.3969/j.issn.1672-6820.2002.09.003

Yang, Q. B., Liu, W. C., Huang, C., Zhu, J. Q., Zhang, Z. D., Zhu, J. S., et al. (2018). Occurring analysis on high-density spot of *Locusta migartoria* and suggestions on its monitoring and controlling in China in 2017. *Chin. Plant Prot.* 38, 37–47. doi:10.3969/j.issn.1672-6820.2018.03.007

Yao, J. M., Gu, X. J., Wen, J. Z., Wang, H. H., and Lei, Z. R. (2007). Effect of temperature on biological characters of LA 06 and LD04, two *Metarhizium anisopliae var acridum* isolates. *Wuyi Sci. J.* 23, 6–12. doi:10.3923/pjbs.2006.820.824

Yue, M., Lei, Z. R., Meng, T., Wang, A. Y., and Yao, J. M. (2010). Temperature influence on conidial germination rate, enzyme activity and virulence of *Metarhizium anisopliae* LA isolate. *Plant Prot.* 36, 56–60. doi:10.4028/www.scientific.net/AMM.37-38.1549

Zeileis, A., Meyer, D., and Hornik, K. (2007). Residual-based shadings for visualizing (conditional) independence. *J. Comput. Graph. Stat.* 16, 507–525. doi:10.1198/106186007X237856

Zhang, L. (2011). Advances and prospects of strategies and tactics of locust and grasshopper management. *Chin. J. Appl. Entomol.* 48, 804–810.

frontiers | Frontiers in Physiology

TYPE Original Research
PUBLISHED 02 March 2023
DOI 10.3389/fphys.2023.1102216

OPEN ACCESS

EDITED BY
Feng Shang,
Southwest University, China

REVIEWED BY
Lian-Sheng Zang,
Guizhou University, China
Tian-Xing Jing,
Yangzhou University, China

*CORRESPONDENCE
Shu-Sen Shi,
sss-63@263.net
Jin-Ping Zhang,
j.zhang@cabi.org

SPECIALTY SECTION
This article was submitted to Invertebrate Physiology, a section of the journal Frontiers in Physiology

RECEIVED 18 November 2022
ACCEPTED 14 February 2023
PUBLISHED 02 March 2023

CITATION
Li W-J, Chen J-H, Avila GA, Ali M-Y, Tian X-Y, Luo Z-Y, Zhang F, Shi S-S and Zhang J-P (2023), Performance of two egg parasitoids of brown marmorated stink bug before and after cold storage. *Front. Physiol.* 14:1102216. doi: 10.3389/fphys.2023.1102216

Performance of two egg parasitoids of brown marmorated stink bug before and after cold storage

Wen-Jing Li[1,2], Ju-Hong Chen[2,3], Gonzalo A. Avila[4], Muhammad-Yasir Ali[2], Xin-Yue Tian[1,2], Zheng-Yu Luo[2,5], Feng Zhang[2], Shu-Sen Shi[1]* and Jin-Ping Zhang [2]*

[1]College of Plant Protection, MARA Key Laboratory of Soybean Disease and Pest Control, Jilin Agricultural University, Changchun, China, [2]MARA-CABI Joint Laboratory for Bio-safety, Institute of Plant Protection, Chinese Academy of Agricultural Sciences, Beijing, China, [3]Institute of Entomology, College of Life Sciences, Nankai University, Tianjin, China, [4]The New Zealand Institute for Plant and Food Research Limited, Auckland Mail Centre, Auckland, New Zealand, [5]Hubei Engineering Technology Center for Forewarning and Management of Agricultural and Forestry Pests, Institute of Entomology, College of Agriculture, Yangtze University, Jingzhou, China

Introduction: The genus *Trissolcus* includes a number of egg parasitoids that are known to contribute to the control of *Halyomorpha halys*. The number of progenies, particularly females, is important for the efficient mass rearing of species used in augmentative biological control programs. Cold storage is an important technique for extending the shelf life of natural enemies used in such programs.

Methods: We assessed how fecundity, sex ratio, lifespan, and the number of hosts parasitized within 24 h were affected by host density for *T. japonicus* and *T. cultratus* when offered fresh *H. halys* eggs and how these parameters were affected if adult parasitoids were first placed in cold storage (11°C in the dark) for 19 weeks before being used for propagation.

Results: The fecundity were 110.2 and 84.2 offspring emerged at 25°C, for parasitoids not placed in cold storage; among the offspring that emerged, 82.6% and 85.6% were female for *T. japonicus* and *T. cultratus*, respectively. If first placed in cold storage, *T. japonicus* and *T. cultratus* produced 35.1 and 24.6 offspring per female, respectively, although cold storage significantly extended the shelf life. The survival rates of parasitoids that were placed in cold storage were 90.3% and 81.3% for females, and 3.2% and 0.9% for males of *T. japonicus* and *T. cultratus*, respectively. The number of hosts parasitized within 24 h was not shown to be density dependent, but it was significantly lower after cold storage.

Discussion: This information can be used to estimate the likely production for augmented rearing colonies for use in biological control programs.

KEYWORDS

***Halyomorpha halys*, biological control, *Trissolcus japonicus*, *Trissolcus cultratus*, fecundity, natural enemy, cold storage**

1 Introduction

The brown marmorated stink bug, *Halyomorpha halys* (Stål) (Hemiptera: Pentatomidae), is an invasive and polyphagous pest native to China, Japan, and Korea (Lee et al., 2013). Invasive populations of *H. halys* have been detected in North America (Hoebeke and Carter, 2003), Europe (Wermelinger et al., 2008), and South America (Faúndez and Rider, 2017). Adults and nymphs of *H. halys* feed on economically important crops, including vegetables, fruits, and ornamental trees. The most serious damage is to a number of fruits in crops, such as apple and peach (Acebes-Doria et al., 2016), pear (Bariselli et al., 2016), and kiwifruit (Bernardinelli et al., 2017). This stink bug has been reported to cause losses of 30%–90% in pears and 50% in peaches in China, which are within the insect's native range (Zhao et al., 2019). Because conventional insecticide management of this pest can have negative impacts on the environment (Goff and Giraudo, 2019), the use of environment-friendly control measures based on integrated pest management (IPM) practices is desirable, including the use of egg parasitoids.

Biological control is generally regarded as an environmentally safe method of pest management that aims to reduce targeted pest populations below economic threshold levels by the use of natural enemies (Waage and Greathead, 1988). Natural enemies of *H. halys* include parasitoids and predators. Investigations in Asia, North America, and Europe have focused on native and exotic natural enemies of *H. halys*, especially egg parasitoids. Three families of hymenopteran parasitoids have been found to attack *H. halys* eggs: Scelionidae (*Telenomus* spp., *Trissolcus* spp., and *Gryon* spp.), Eupelmidae (*Anastatus* spp.), and Encyrtidae (*Ooencyrtus* spp.) (Abram et al., 2017; Zhang et al., 2017). The relative prevalence of different parasitoid species associated with *H. halys* eggs seems to be habitat dependent. For example, *Telenomus podisi* Ashmead is the most abundant species in field crops and vegetable crops, while *Anastatus* spp. and *Trissolcus* spp. dominate in ornamentals, forests, and seminatural or urban habitats (Abram et al., 2017). *Trissolcus japonicus* has been identified as the most common parasitoid species attacking *H. halys*, and it is regarded as the most promising natural enemy for classical biological control of *H. halys* (Lara et al., 2019). Adventive populations of *T. japonicus* occur in the United States (Leskey and Nielsen, 2018), Italy (Peverieri et al., 2018), Switzerland (Stahl et al., 2019), and Canada (Abram et al., 2019; Gariepy and Talamas, 2019). *Trissolcus cultratus* is another common egg parasitoid of *H. halys* in China (Yang et al., 2009; Yang et al., 2015), with mean parasitism rates of 84.2% in laboratory choice tests, a level that was not significantly different from that of *T. japonicus* (94.1%) (Yang et al., 2015). However, a Swiss population of *T. cultratus* was found to be unable to attack fresh egg masses of *H. halys*. The Swiss population of this parasitoid is believed to be a different geographical strain of *T. cultratus* from that found attacking *H. halys* in China and other parts of the bug's native range and, therefore, not co-evolved with *H. halys* (Haye et al., 2021). Anyhow, *T. cultratus* is still under consideration as a parasitoid that could contribute to the control *H. halys* in the long-term (Haye et al., 2015). A recent study looking at the abundance and diversity of egg parasitoids of *H. halys* in kiwifruit orchards in China showed that parasitism rates by *T. cultratus* and *T. japonicus* were very similar (Avila et al., 2021). This finding adds further support that parasitoid composition depends on the habitat type and suggests that *T. cultratus* is also a potentially important biological control agent of *H. halys*.

In the development of augmentative biocontrol programs, cold storage is commonly used to stockpile hosts and natural enemies (Colinet and Boivin, 2011; Rathee and Ram, 2018), which can be used to maximize the number of parasitoids available at a given time (Leopold, 2019). Initial studies reported that *T. japonicus* can be reared on previously frozen (−80°C) *H. halys* egg masses (Haye et al., 2015). However, further research found both lethal and sublethal negative effects on parasitism and the production of offspring when using frozen *H. halys* egg masses to rear *T. japonicus*. The use of frozen eggs reduced the number of wasps produced by 56%–65% and increased production time due to slow development compared to fresh eggs (Mcintosh et al., 2019). Parasitism rates and progeny production of *T. japonicus* were higher when host eggs offered for parasitism had been stored at higher temperatures. For example, parasitoid progeny production was higher using host eggs stored at 6°C than that of eggs stored at minus 24°C for up to 2 months prior to exposure to parasitism (Bittau et al., 2021). Similarly, parasitoid emergence from egg masses refrigerated at 8°C for up to 2 months before parasitism was higher than that from frozen egg masses (Wong et al., 2021). A recent study conducted by Cira et al. (2021) reported high mortality for all immature ages of *T. japonicus* when stored at various cold temperatures and for various times, and only adults showed high levels of survival. Qiu (2007) reported that the survival rate of female *T. japonicus* was approximately 90% when stored at 11°C for 19 weeks, and Bittau et al. (2021) reported survival rates of 87.1% when *T. japonicus* adults were stored at 16°C for 12 weeks. Longer duration cold storage of adult *Trissolcus* seems to be the best way to accumulate quantities of this parasitoid and extend the product shelf life of parasitoids reared for field releases. However, little is known about the implications of cold storage for the whole-life fecundity of *T. japonicus* or *T. cultratus* adults. High parasitoid fecundity is important for efficient mass rearing and development of effective biological control programs (Gündüz and Gülel, 2005).

In this study, we compared the survival rate, lifetime fecundity, sex ratio, and the number of hosts parasitized within 24 h (on different host densities) of *T. japonicus* and *T. cultratus* before and after being cold stored at 11°C for 19 weeks.

2 Materials and methods

2.1 *Halyomorpha halys* rearing

The *H. halys* laboratory colony was established using adults collected from an organic kiwifruit orchard located at the Northwest Agriculture and Forestry University kiwifruit experimental field station (34°07′27″N; 107°59′31″E) in Mei County, Baoji city, Shaanxi Province, China. The colony was continuously reared on green beans (*Phaseolus vulgaris* L.) and corn (*Zea mays* L.) in gauze cages (60 × 60 × 60 cm^3) and kept in the laboratory at a constant climatic condition 25°C ± 1°C, 60% ± 1% RH, and a 16:8 h L:D cycle. Food was changed every 3 to 4 days. Newly laid eggs were collected from the cages daily and maintained under the same conditions in separate rearing cages or provided to parasitoids.

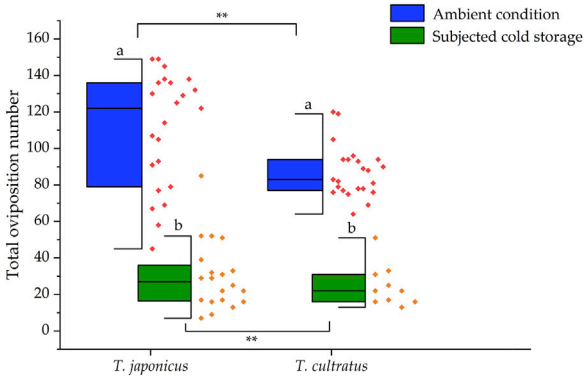

FIGURE 1
Number of parasitoids produced per parental female of *T. japonicus* and *T. cultratus* placed under ambient (25°C) versus subjected to cold storage. Asterisks represent significant differences between *T. japonicus* and *T. cultratus* within the same treatment (**$p < 0.01$). Different letters represent significant differences between ambient temperature (25°C) and subjected to cold storage conditions within each parasitoid species ($p < 0.05$).

2.2 Parasitoid rearing

Trissolcus japonicus and *T. cultratus* colonies were started from field collections of parasitized *H. halys* eggs conducted in the same kiwifruit orchard where the *H. halys* were collected in Mei County, Baoji city, Shaanxi Province. Both populations were reared separately in transparent acrylic rearing cages (25 × 25 × 25 cm^3). Pure honey soaked into cotton wicks was provided weekly for nutrition. For colony production, adult females of either *T. japonicus* or *T. cultratus* were provided with fresh *H. halys* egg masses (preliminary data showed eggs 1 and 3 days old were not distinguished, but fewer eggs were parasitized if host eggs were 5 days old (Yang et al., 2018), and parasitoids were allowed to parasitize eggs for 2 days. After the exposure period, parasitized egg masses were removed from the cages and reared individually per egg mass in a Petri dish (d = 5 cm) at 25°C ± 1°C, 60% ± 1% RH, and a 16: 8 h L:D photoperiod. Egg masses were checked daily for parasitoid emergence. Once female parasitoids emerged (day 1), they were placed with males for 3 days to mate, and pure honey was provided for adult feeding. Identification of individuals from newly established laboratory colonies of *T. japonicus* and *T. cultratus* was verified by E. Talamas (Systematic Entomology Laboratory, USDA/ARS c/o NMNH, Smithsonian Institution, Washington DC.)

2.3 Cold storage of *T. japonicus* and *T. cultratus*

All the mated (males that emerged ahead by one or two days had to wait for females to emerge, and they mated at once when they met during 3 days of mixed rearing) 3-day-old female and male parasitoids were grouped based on each egg mass and placed in a 10-mL tube (16 × 81 mm), and stored in an incubator (Ningbo Haishu Saifu Experimental Instrument Factory, SPX-250, Ningbo city, Zhejiang province) at 11°C ± 1°C, 60% ± 1% RH, and continuous darkness for 19 weeks (133 days). All groups were checked weekly for mortality, and honey droplets in tubes were renewed weekly. The same procedure was carried out for each parasitoid species. The total number was 582 (30 tubes) *T. japonicus* and 563 (28 tubes) *T. cultratus* for cold storage.

2.4 Fecundity bioassays of *T. japonicus* and *T. cultratus*

Fecundity trials were conducted with parasitoids under ambient (non-cold storage) rearing conditions (25°C ± 1°C, 60% ± 5% RH, and 16 h light). Three-day-old mated female parasitoids were randomly selected and placed individually in Petri dishes (d = 5 cm). Honey was provided for adult nutrition, and *H. halys* egg masses (each egg mass of around 28 eggs) were provided for parasitoid oviposition. Egg masses were replaced every 2 days: three egg masses for the first three consecutive times, then one egg mass was provided from the fourth time to refresh host eggs until the female wasp died. Exposed egg masses were placed and reared individually in Petri dishes, under laboratory conditions (as described above) until all eggs produced either parasitoid progeny or stink bug nymphs. In total, 23 replicates (one female parasitoid as one replicate) were conducted for *T. japonicus* and 26 for *T. cultratus*. The numbers of emerging parasitoids or *H. halys* nymphs were recorded. Unhatched eggs were dissected under a stereomicroscope and classified as dead immature parasitoids, dead *H. halys* nymphs, or failed eggs (i.e., nothing found). The proportion of adult parasitoid progeny that were female was calculated, and the average oviposition period and longevity (from parasitoids emergence to death) at 25°C ± 1°C, 60% ± 5% RH, and 16 h light conditions were also recorded. The parasitism rate was defined as (number of emerged parasitoids + number of dead parasitoids within host egg)/total number of *H. halys* eggs × 100. The rate of nymph was defined as (number of emerged nymphs + number of dead nymphs within host egg)/total number of *H. halys* eggs × 100. The rate of egg mortality was defined as number of dead eggs/total number of *H. halys* eggs × 100.

Parasitoid fecundity after cold storage was assessed using the same methods as described for wasps not subject to cold storage. Wasps tested were female parasitoids that had survived 19 weeks of cold storage period. These females were allowed 2 days to adapt to warm ambient conditions before testing. At least ten replicates (one female as a replicate) were run for *T. japonicus* and *T. cultratus*.

2.5 Effect of host numbers on the per-female rate of oviposition

Three-day-old mated females of *T. japonicus* and *T. cultratus* were offered different numbers of *H. halys* egg masses (1, 2, 3, 4, or 5, each with 26–28 eggs). Females (one female per Petri dish) were allowed to oviposit for 24 h at 25°C and were then removed from Petri dishes (d = 5 cm). Exposed egg masses were held and reared individually in Petri dishes, under laboratory conditions (as described above), until all eggs produced either parasitoid progeny, live stink bug nymphs, or failed. The numbers of

TABLE 1 Parameters for *T. japonicus* and *T. cultratus* when reared under normal conditions (25°C) and after a cold storage period of 19 weeks at constant 11°C.

Treatment	Normal condition		After cold storage	
Parasitoid species	*T. japonicus*	*T. cultratus*	*T. japonicus*	*T. cultratus*
Parasitism rate (%)	20.91 ± 4.71 aA	21.49 ± 3.88 aA	5.49 ± 3.39 aB	4.30 ± 1.46 aB
Nymph rate (%)	43.03 ± 1.84 aA	46.80 ± 2.18 aA	75.16 ± 1.69 aB	77.33 ± 1.42 aB
Egg mortality rate (%)	36.06 ± 1.16 aA	31.71 ± 1.93 aA	19.34 ± 0.79 aB	18.37 ± 1.43 aB

Values are mean ± SE. Lowercase letters represent significant differences between the parasitoid species within the same treatment ($p < 0.05$). Capital letters represent significant differences for each parasitoid species between treatments ($p < 0.05$).

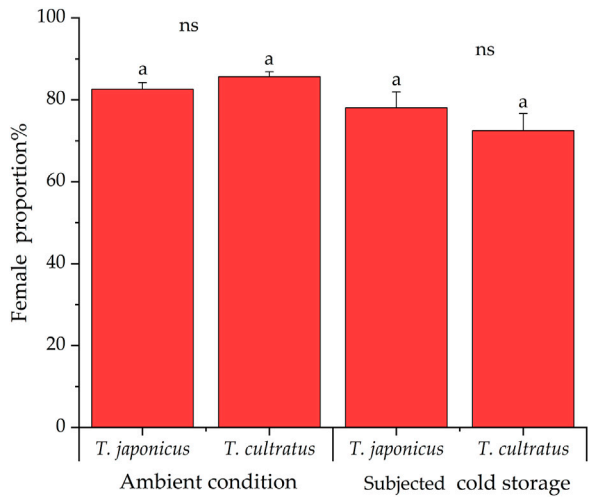

FIGURE 2
Proportion of females produced by *T. japonicus* and *T. cultratus* under ambient rearing conditions (25°C) and after cold storage for 19 weeks at 11°C for offspring. Same marked by lowercase letters represent no significant differences for each parasitoid species between ambient and after cold storage ($p > 0.05$), and ns denotes no significant difference between *T. japonicus* and *T. cultratus* within the same treatment.

emerging parasitoids or *H. halys* nymphs were recorded. Failed eggs were dissected under a stereomicroscope and classified as immature parasitoids, dead *H. halys* nymphs, or failed eggs (i.e., nothing found). Ten replicates were conducted for each treatment. The per-female rate of oviposition was defined as the number of emerged parasitoids + immature parasitoids.

Trissolcus japonicus and *T. cultratus*, after cold storage for 19 weeks, were also parallely tested, and the female rate of oviposition depends on five host densities. The method was the same as that mentioned previously. Three to nine replicates were conducted for each treatment.

2.6 Data analysis

Differences in lifetime fecundity (i.e., number of parasitoids that emerged), the duration of the oviposition period and the parasitoid lifespan, the female proportion of parasitoid offspring, parasitism rate, rate of nymph, rate of egg mortality, and female oviposition rate were compared between the two parasitoids species (*T. japonicus* and *T. cultratus*), and treatments (control wasps and one subjected to cold storage) were analyzed using GLM with Poisson distribution followed by LSD *post-hoc* tests. All statistical analyses were carried out using SPSS 21.0 statistical software. All figures were made using Origin 2022 software.

3 Results

3.1 Fecundity parameters of *T. japonicus* and *T. cultratus* under ambient temperature (25°C) and after cold storage

In tests conducted with parasitoids reared under ambient temperature conditions (25°C), a total of 12,776 and 11,122 host eggs were provided to *T. japonicus* ($n = 23$) and *T. cultratus* ($n = 26$), respectively, to assess the number of parasitoids produced over their lifetime. An average of 555.5 ± 12.4 or 427.8 ± 7.5 fresh *H. halys* eggs were offered to each *T. japonicus* and *T. cultratus* female, respectively. The average number of parasitoids that emerged from *T. japonicus* per parental female was 110.2 ± 6.6, while for *T. cultratus*, it was 84.2 ± 3.2. The former was significantly higher (GLM $\chi^2 = 84.957$, df = 1, $p < 0.001$) (Figure 1).

For tests conducted with female adult parasitoids that survived from cold storage (at 11°C for 19 weeks), a total of 7,171 and 7,327 host eggs were offered to *T. japonicus* ($n = 10$) and *T. cultratus* ($n = 10$), respectively. The number of parasitoids produced per parental females (surviving cold storage) of *T. japonicus* was 35.1 ± 7.4, which was a significant decrease of 68.1% compared to the control (GLM $\chi^2 = 403.379$, df = 1, $p < 0.001$). Similarly, the number of parasitoids produced per parental female of *T. cultratus* was 24.6 ± 3.6, which was a significant decrease of 70.8% compared to the control (females not subject to cold storage) (GLM $\chi^2 = 334.768$, df = 1, $p < 0.001$). There were significant differences in the number of parasitoids produced by *T. japonicus* versus *T. cultratus* after cold storage (GLM $\chi^2 = 18.274$, df = 1, $p < 0.001$) (Figure 1).

At ambient conditions (25°C), there was no significant difference between *T. japonicus* and *T. cultratus* in the parasitism rate (GLM $\chi^2 = 0.231$, df = 1, $p = 0.630$), rate of nymphal (GLM $\chi^2 = 1.767$, df = 1, $p = 0.184$), or the rate of egg mortality (GLM $\chi^2 = 3.636$, df = 1, $p = 0.057$) (Table 1).

However, after a cold storage period, both species of parasitoids experienced a significant decrease in their parasitism rates (*T. japonicus* GLM $\chi^2 = 92.361$, df = 1, $p < 0.001$; *T. cultratus* GLM $\chi^2 = 193.876$, df = 1, $p < 0.001$) and the egg mortality rate (*T. japonicus* GLM $\chi^2 = 87.723$, df = 1, $p < 0.001$; *T. cultratus* GLM $\chi^2 = 17.706$, df = 1, $p < 0.001$)

10.3389/fphys.2023.1102216

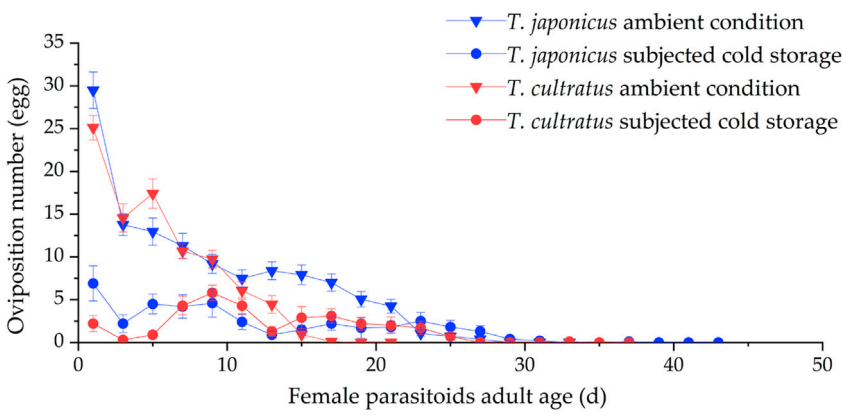

FIGURE 3
Variation in number of ovipositions by *T. japonicus* and *T. cultratus* under ambient rearing condition (25°C) and after cold storage for 19 weeks at 11°C. Values are the mean ± SE.

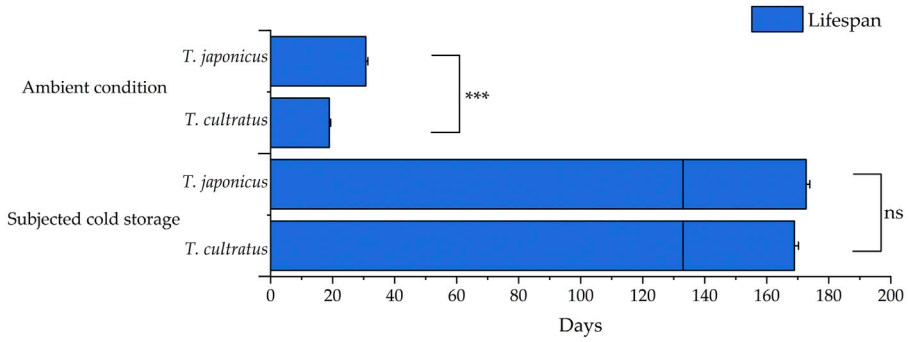

FIGURE 4
Mean lifespan of *T. japonicus* and *T. cultratus* when under ambient rearing conditions (25°C) and extended by cold storage. Values are means ± SE. Asterisks represent statistically significant differences, and ns present no significant difference between *T. japonicus* and *T. cultratus* within the same treatment (***$p < 0.001$).

compared to those in the ambient condition (25°C). Conversely, the nymph rate increased significantly for both parasitoid species after cold storage (*T. japonicus* GLM $\chi^2 = 120.616$, df = 1, $p < 0.001$; T. cultratus GLM $\chi^2 = 74.036$, df = 1, $p < 0.001$) (Table 1).

Between *T. japonicus* and *T. cultratus* after cold storage, there were no significant differences in the parasitism rate (GLM $\chi^2 = 1.163$, df = 1, $p = 0.281$), the nymph rate (GLM $\chi^2 = 1.068$, df = 1, $p = 0.301$), and egg mortality rate (GLM $\chi^2 = 0.391$, df = 1, $p = 0.532$) (Table 1).

3.2 Proportion of female parasitoids

Under ambient rearing conditions, the proportion of female parasitoids produced was 82.6% ± 1.6% and 85.6% ± 1.2% for *T. japonicus* and *T. cultratus*, respectively. After cold storage, the proportion of females parasitoids was 78.0% ± 3.9% of *T. japonicus*, which was not significantly different from wasps reared under ambient conditions (GLM $\chi^2 = 1.769$, $df = 1$, $p = 0.183$). However, the percentage of females produced by *T. cultratus* in the offspring was 72.4% ± 4.2%, which is significantly lower after cold storage than wasps reared under ambient conditions (GLM $\chi^2 = 18.976$, $df = 1$, $p < 0.001$) (Figure 2).

3.3 Oviposition number variation during lifetime of *T. japonicus* and *T. cultratus*

At ambient rearing conditions (25°C), the mean oviposition duration was 21.5 ± 0.9 days for *T. japonicus*, which was significantly different (GLM $\chi^2 = 53.627$, $df = 1$, $p < 0.001$) from that for *T. cultratus* (12.8 ± 0.40 days). The number of ovipositions decreased with female age, and the highest level of oviposition was on the first day of access of new parasitoids to hosts when there were 29.5 ± 2.1 eggs/female/day for *T. japonicus* and 25.1 ± 1.4 eggs for *T. cultratus* (Figure 3).

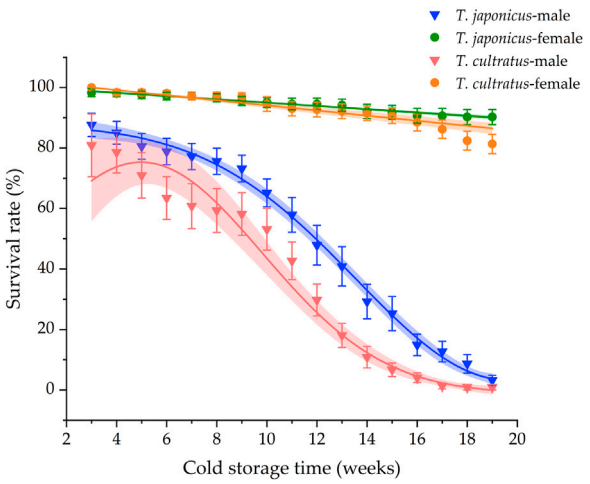

FIGURE 5
Survival rate of *T. japonicus* and *T. cultratus* during 19 weeks of cold storage at 11°C. Values are mean ± SE.

After cold storage, the mean oviposition duration was 24.4 ± 2.0 days for *T. japonicus* and 17.8 ± 1.9 days for *T. cultratus*. Oviposition occurred from the first day that parasitoids were exposed to host eggs. The oviposition duration was significantly different between the two species after cold storage (GLM χ^2 = 10.237, *df* = 1, $p < 0.01$) (Figure 3).

3.4 Effect of cold storage on lifespan of *T. japonicus* and *T. cultratus*

Mean lifespan values for *T. japonicus* and *T. cultratus* females under ambient rearing conditions (25°C) were 30.7 ± 0.7 and 18.9 ± 0.5 days, respectively, which differed significantly between the two species (GLM χ^2 = 67.848, *df* = 1, $p < 0.001$). Adults of both parasitoids were still alive and fertile after 19 weeks of cold storage. The lifespan (period from parasitoid emergence to death) showed no significant difference between the two parasitoid species after cold storage (GLM χ^2 = 1.908, *df* = 1, $p = 0.167$) (Figure 4).

3.5 Survival rates of parasitoids during cold storage

The survival rates declined during cold storage for both parasitoid species (Figure 5). However, survival rates for females were dramatically higher than survival rates of males (*T. japonicus* GLM χ^2 = 883.283, *df* = 1, $p < 0.001$; *T. cultratus* GLM χ^2 = 612.088, *df* = 1, $p < 0.001$), with mean female survival rates of 90.3% ± 1.6% and 81.3% ± 3.1% for *T. japonicus* and *T. cultratus* after 19 weeks of cold storage, respectively. Male survival rates, in contrast, were very low after cold storage, being 3.2% ± 2.5% and 0.9% ± 0.9% for *T. japonicus* and *T. cultratus*, respectively (Figure 5).

3.6 Oviposition number within 24 h at different host densities

At the normal condition, the average oviposition numbers were 27.4 ± 0.40, 23.0 ± 2.61, 22.5 ± 1.84, 23.2 ± 2.56, and 26.0 ± 4.63 eggs when providing one to five egg masses to *T. japonicus*, and there were no significant differences between the different densities tested (GLM χ^2 = 3.321, *df* = 4, $p = 0.506$) (Figure 6A). The oviposition rates of *T. cultratus* were 26.6 ± 0.68, 22.7 ± 4.16, 25.6 ± 4.72, 23.9 ± 4.79, and 26.3 ± 5.11 eggs at five host densities tested, and no differences were observed between different densities (GLM χ^2 = 0.924, *df* = 4, $p = 0.921$) (Figure 6B).

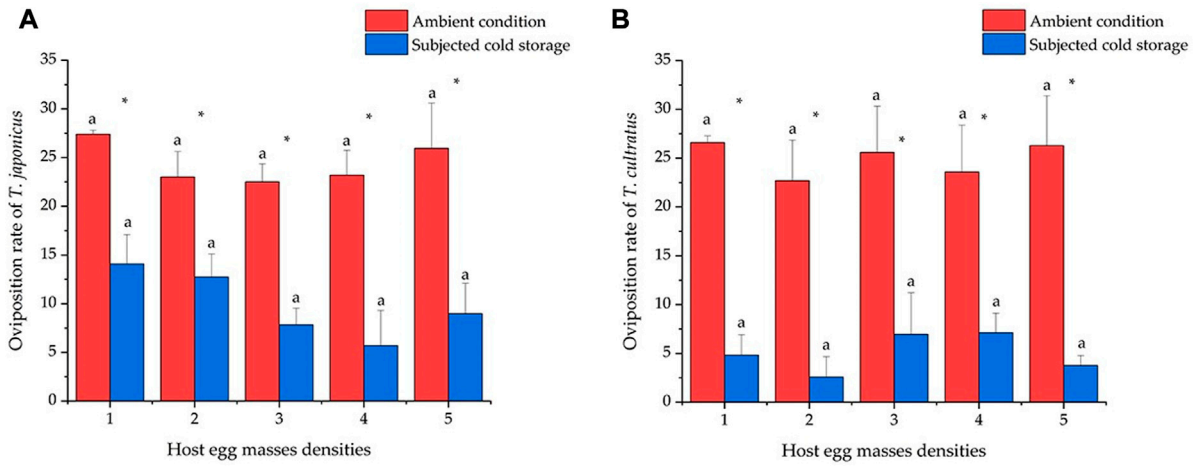

FIGURE 6
Daily per female oviposition rate of *T. japonicus* **(6A)** and *T. cultratus* **(6B)** when individual females were offered one to five host egg masses. Values are means ± SE. Asterisks represent statistically significant differences between wasps placed in ambient conditions (25°C) and wasps subjected to 19 weeks of cold storage (11°C) at the same host density level. Lowercase letters represent no significant difference between different host densities by each parasitoid species ($p > 0.05$).

The oviposition rate significantly decreased after cold storage for both species of parasitoids. The oviposition rates of *T. japonicus* were 14.1 ± 3.01, 12.7 ± 2.37, 7.8 ± 1.69, 5.7 ± 3.60, and 9.0 ± 3.11 eggs for the five host densities, which did not differ significantly (GLM $\chi^2 = 7.871$, $df = 4$, $p = 0.096$) (Figure 6A). The oviposition rates of *T. cultratus* were 4.8 ± 2.07, 2.6 ± 2.09, 7.0 ± 4.25, 7.1 ± 1.99, and 3.8 ± 1.02 eggs for the five host densities and did not differ significantly (GLM $\chi^2 = 3.299$, $df = 4$, $p = 0.509$) (Figure 6B).

Comparisons for the number of oviposition within 24 h between two species after cold storage show that the number of oviposition by *T. japonicus* was significantly higher than *T. cultratus* at low host egg densities, one egg mass (GLM $\chi^2 = 7.944$, $df = 1$, $p < 0.01$), and two egg masses (GLM $\chi^2 = 11.168$, $df = 1$, $p < 0.001$). No significant differences were found between the two species of parasitoids when provided with three, four, and five host egg masses.

4 Discussion

High fecundity and a female-biased progeny sex ratio are important factors for efficient mass rearing to support programs of augmentative biological control (Gündüz and Gülel, 2005). Egg parasitoids in the genera *Trissolcus* are well known as control agents of *H. halys*, especially *T. japonicus*, whose release has been widely recommended to control *H. halys* in field crops, both in its native and adventive ranges. For example, Mi et al. (2017) reported releases of *T. japonicus* and *Anastatus* sp. for suppression of *H. halys* in kiwifruit orchards in China. *T. japonicus* was intentionally released across four eco-regions in Oregon (United States) for investigation of its dispersal capacity (Lowenstein et al., 2019) as part of a classical biocontrol program in North America (Leskey and Nielsen, 2018). Based on a risk analysis of *T. japonicus*, a petition for its release in the field was approved in 2020, with plans to rear and release over 120,000 female *T. japonicus* in Italy (Decreto, 2020; Conti et al., 2021). Research on the fecundity of *T. japonicus* and its cold storage supports the logistics accumulation of enough parasitoids to support field release on such large scales. We found that when the parasitoids *T. japonicus* and *T. cultratus* were reared at 25°C, their lifetime fecundities, respectively, were 110.2 and 84.2, and the proportion female values in their progeny were 82.6% and 85.6%. In addition, we found that the female oviposition number was 22.5 to 27.4 for *T. japonicus* and 22.7 to 26.2 for *T. cultratus* within 24 h on various host densities. We deduced that *T. cultratus* did not perform as well as *T. japonicus* as a potential biological control agent against *H. halys* based on these fecundity and related factors.

The numbers of ovipositions on the first day of life after access to hosts were the highest for both *T. japonicus* (29.5) and *T. cultratus* (25.1). This suggests that one egg mass of *H. halys* (about 28 eggs) per day would be sufficient to support the daily oviposition of *T. japonicus* or *T. cultratus*. Subsequently, daily oviposition declined with female age. Age-related declines in parasitoid fecundity were similarly noted Sabbatini-Peverieri et al. (2020) for *T. japonicus* and *T. mitsukurii*.

T. japonicus are ideally reared on fresh newly laid unfertilized *H. halys* eggs, which leads to the highest parasitoid development rate and fecundity (Gündüz and Gülel, 2005). However, mass-rearing facilities are often constrained by the limited availability of such eggs. Cold storage is an important method for extending the shelf life of parasitoids used as biological control agents (Bittau et al., 2021). Cold storage of each life stage of *T. japonicus* has been studied, and immature parasitoid development on *H. halys* eggs was clearly described (Giovannini et al., 2021). The eggs and larvae of *Trissolcus halyomorphae* (syn *T. japonicus*) could not tolerate storage temperature at either 7 or 11°C. Storage of pupae was feasible, but storage of adult females was optimal, with adult survival being 90% (Qiu, 2007), making cold storage of adults a viable method to extend parasitoid lifespan and match the timing of *T. japonicus* production with release needs (Cira et al., 2021). Storage of adults of *T. japonicus* at 8°C and short photoperiod (8L:14D) resulted in lower realized fertility of stored females and fewer female progeny than those in storage at 13°C and 18°C (Gündüz and Gülel, 2005). Lee and Denlinger (2010) reported that low temperatures affected insects differently based on the severity of the cold and the duration of exposure. Photoperiod during storage can also affect parasitoid fitness but was not investigated in our present study. In our study, female parasitoid adults were stored at 11°C for nearly 5 months (19 weeks) in darkness, and those conditions reduced fecundity by 31.9% for *T. japonicus* and 29.2% for *T. cultratus* compared to rearing at 25°C without cold storage. We deduced that *T. cultratus* did not perform as well as *T. japonicus* as a potential biological control agent against *H. halys* based on these fecundity and related factors. One more positive aspect is that the proportion of female offspring was not low level, 78.0% and 72.4% for *T. japonicus* and *T. cultratus* after storage. So, we deduced that the triple number of storage *T. japonicus* would be of equal efficiency with the non-cold stored one, both for calculating accumulation numbers during mass rearing and parasitism in field biological control.

For male parasitoids of both species, survival rates declined quickly after 9 weeks of storage, suggesting that 9 weeks may be a better storage time for stockpiling parasitoids at 11°C. The general pattern of high survival rates for females of *T. japonicus* and *T. cultratus* and low survival rates for males, after 19 weeks of cold storage, agrees with results from previous studies (Qiu, 2007). Further research is warranted to assess additional combinations of cold storage temperatures, storage duration, and light regimes to determine the optional condition for stockpiling *T. japonicus* and *T. cultratus* without a significant decline in the reproductive rate.

5 Conclusion

Lifetime fecundity of *T. japonicus* and *T. cultratus* were 110.2 and 84.2, respectively, when reared at 25°C, 16L:8D, 60% ± 1% RH (ambient conditions). The lifespan of both species was significantly extended by cold storage at 11°C for 19 weeks. Both parasitoid species remained fertile after cold storage, although the lifetime fecundity was significantly reduced to around one-third of that of wasps not subjected to cold storage. Under ambient conditions (no cold storage), both wasp species laid about 28 eggs within 24 h of contact with hosts, but this value was much lower (less than 14.1) after cold storage.

Data availability statement

The original contribution presented in the study is included in the article/Supplementary Material; further inquiries can be directed to the corresponding authors.

Author contributions

J-PZ, S-SS, FZ, and W-JL conceived and designed the experiments. W-JL, J-HC, X-YT, and Z-YL conducted experiments. W-JL, J-HC, and M-YA analyzed data. GA, J-PZ, and S-SS wrote the original draft. FZ, M-YA, and GA reviewed and edited the manuscript. All authors read and approved the manuscript.

Funding

This research was funded by China's donation to the CABI Development Fund, grant number VM10051.

Acknowledgments

CABI is an international intergovernmental organization and we gratefully acknowledge the core financial support from our member countries (and lead agencies) including the United Kingdom (Department for International Development), China (Chinese Ministry of Agriculture and Rural Affairs), Australia (Australian Centre for International Agricultural Research), Canada (Agriculture and Agri-Food Canada), the Netherlands (Directorate-General for International Cooperation), and Switzerland (Swiss Agency for Development and Cooperation). See https://www.cabi.org/about-cabi/whowe-work-with/key-donors/ for full details.

Conflict of interest

GA was employed by The New Zealand Institute for Plant and Food Research Limited.

The remaining authors declare that the research was conducted in the absence of any commercial or financial relationships that could be construed as a potential conflict of interest.

Publisher's note

References

Abram, P. K., Hoelmer, K. A., Acebes-Doria, A., Andrews, H., Beers, E. H., Bergh, J. C., et al. (2017). Indigenous arthropod natural enemies of the invasive Brown marmorated stink bug in North America and Europe. *J. Pest Sci.* 90, 1009–1020. doi:10.1007/s10340-017-0891-7

Abram, P. K., Talamas, E. J., Acheampong, S., Mason, P. G., and Gariepy, T. D. (2019). First detection of the samurai wasp, *Trissolcus japonicus* (Ashmead) (hymenoptera, Scelionidae), in Canada. *J. Hymenoptera Res.* 68, 29–36. doi:10.3897/jhr.68.32203

Acebes-Doria, A. L., Leskey, T. C., and Bergh, J. C. (2016). Injury to apples and peaches at harvest from feeding by *Halyomorpha halys* (Stål) (Hemiptera: Pentatomidae) nymphs early and late in the season. *Crop Prot.* 89, 58–65. doi:10.1016/j.cropro.2016.06.022

Avila, G. A., Chen, J., Li, W., Alavi, M., Mi, Q., Sandanayaka, M., et al. (2021). Seasonal abundance and diversity of egg parasitoids of *Halyomorpha halys* in kiwifruit orchards in China. *Insects* 12, 428. doi:10.3390/insects12050428

Bariselli, M., Bugiani, R., and Maistrello, L. (2016). Distribution and damage caused by *Halyomorpha halys* in Italy. *Eppo Bull.* 46, 332–334. doi:10.1111/epp.12289

Bernardinelli, I., Malossini, G., and Benvenuto, L. (2017). *Halyomorpha halys*: Risultati preliminari di alcune attività sperimentali condotte in Friuli Venezia Giulia nel 2016. *Not. Ersal* 1, 24–26.

Bittau, B., Dindo, M. L., Burgio, G., Sabbatini-Peverieri, G., Hoelmer, K. A., Roversi, P. F., et al. (2021). Implementing mass rearing of *Trissolcus japonicus* (hymenoptera: Scelionidae) on cold-stored host eggs. *Insects* 12, 840. doi:10.3390/insects12090840

Cira, T., Santacruz, E. N., and Koch, R. L. (2021). Optimization of *Trissolcus japonicus* cold storage methods for biological control of *Halyomorpha halys*. *Biol. Control* 156, 104534. doi:10.1016/j.biocontrol.2021.104534

Colinet, H., and Boivin, G. (2011). Insect parasitoids cold storage: A comprehensive review of factors of variability and consequences. *Biol. Control* 58, 83–95. doi:10.1016/j.biocontrol.2011.04.014

Conti, E., Avila, G., Barratt, B., Cingolani, F., Colazza, S., Guarino, S., et al. (2021). Biological control of invasive stink bugs: Review of global state and future prospects. *Entomologia Exp. Appl.* 169, 28–51. doi:10.1111/eea.12967

Decreto (2020). *Immissione in natura della specie non autoctona* Trissolcus japonicus *quale Agente di Controllo Biologico del fitofago* Halyomorpha halys *ai sensi del Decreto del Presidente della Repubblica 8 settembre 1997*. del 9 giugno 42967n. 357, art. 12. 2020.

Faúndez, E. I., and Rider, D. A. (2017). The Brown marmorated stink bug *Halyomorpha halys* (Stål, 1855) (Heteroptera: Pentatomidae) in Chile. *Arq. Entomolóxicos* 17, 305–307.

Gariepy, T. D., and Talamas, E. J. (2019). Discovery of *Trissolcus japonicus* (hymenoptera: Scelionidae) in ontario, Canada. *Can. Entomologist* 151, 824–826. doi:10.4039/tce.2019.58

Giovannini, L., Sabbatini-Peverieri, G., Tillman, P. G., Hoelmer, K. A., and Roversi, P. F. (2021). Reproductive and developmental biology of *Acroclisoides sinicus*, a hyperparasitoid of scelionid parasitoids. *Biology* 10 (3), 229. doi:10.3390/biology10030229

Goff, G. L., and Giraudo, M. (2019). "Effects of pesticides on the environment and insecticide resistance," in *Olfactory concepts of insect control-alternative to insecticides*. Editor J. F. Picimbon (Cham: Springer), 51–78.

Gündüz, E. A., and Gülel, A. (2005). Investigation of fecundity and sex ratio in the parasitoid *Bracon hebetor Say* (Hymenoptera: Braconidae) in relation to parasitoid age. *Turkish J. Zoology* 29, 291–294.

Haye, T., Fischer, S., Zhang, J., and Gariepy, T. (2015). Can native egg parasitoids adopt the invasive Brown marmorated stink bug, *Halyomorpha halys* (Heteroptera: Pentatomidae), in Europe? *J. Pest Sci.* 88, 693–705. doi:10.1007/s10340-015-0671-1

Haye, T., Zhang, J. P., Risse, M., and Gariepy, T. (2021). A temporal trophic shift from primary parasitism to facultative hyperparasitism during interspecific competition between two co-evolved scelionid egg parasitoids. *Ecol. Evol.* 11, 18708–18718. doi:10.1002/ece3.8483

Hoebeke, E. R., and Carter, M. E. (2003). *Halyomorpha halys* (stål) (heteroptera: Pentatomidae): A polyphagous plant pest from Asia newly detected in North America. *Proc. Entomological Soc. Wash.* 105, 225–237.

Lara, J. R., Pickett, C. H., Kamiyama, M. T., Figueroa, S., Romo, M., Cabanas, C., et al. (2019). Physiological host range of *Trissolcus japonicus* in relation to *Halyomorpha halys* and other pentatomids from California. *BioControl* 64, 513–528. doi:10.1007/s10526-019-09950-4

Lee, D. H., Short, B. D., Joseph, S. V., Bergh, J. C., and Leskey, T. C. (2013). Review of the biology, ecology, and management of *Halyomorpha halys* (Hemiptera: Pentatomidae) in China, Japan, and the Republic of Korea. *Environ. Entomol.* 42, 627–641. doi:10.1603/EN13006

Lee, R., and Denlinger, D. (2010). "Rapid cold-hardening: Ecological significance and underpinning mechanisms," in *Low temperature biology of insects*. Editors D. L. Denlinger and R. E. Lee 2nd ed (Cambridge: Cambridge University Press), 35–58.

Leopold, R. A. (2019). "Cold storage of insects for integrated pest management," in *Temperature sensitivity in insects and application in integrated pest management*. Editors G. J. Hallman and D. L. Denlinger 1st ed (New York: CRC Press), 235–267.

Leskey, T. C., and Nielsen, A. L. (2018). Impact of the invasive Brown marmorated stink bug in North America and Europe: History, biology, ecology, and management. *Annu. Rev. Entomology* 63, 599–618. doi:10.1146/annurev-ento-020117-043226

Lowenstein, D. M., Andrews, H., Hilton, R. J., Kaiser, C., and Wiman, N. G. (2019). Establishment in an introduced range: Dispersal capacity and winter survival of *Trissolcus japonicus*, an adventive egg parasitoid. *Insects* 10 (12), 443. doi:10.3390/insects10120443

Mcintosh, H., Lowenstein, D. M., Wiman, N. G., Wong, J. S., and Lee, J. C. (2019). Parasitism of frozen *Halyomorpha halys* eggs by *Trissolcus japonicus*: Applications for rearing and experimentation. *Biocontrol Sci. Technol.* 29, 478–493. doi:10.1080/09583157.2019.1566439

Mi, Q. Q., Zhang, J. P., Han, Y. X., Yan, Y. C., Zhang, B. X., Li, D. S., et al. (2017). "Releases of *Trissolcus japonicus* and *Anastatus* sp. for suppression of *Halyomorpha halys* in kiwifruit orchards," in *Proceedings of the 5th international symposium on biological control of arthropods*. Editors P. G. Mason, D. R. Gillespie, and C. Vincent (Wallingford UKLangkawi, Malaysia: CABI), 297.

Peverieri, G. S., Talamas, E., Bon, M. C., Marianelli, L., Bernardinelli, I., Malossini, G., et al. (2018). Two Asian egg parasitoids of *Halyomorpha halys* (stål) (Hemiptera, Pentatomidae) emerge in northern Italy: *Trissolcus mitsukurii* (Ashmead) and *Trissolcus japonicus* (Ashmead) (hymenoptera, Scelionidae). *J. Hymenoptera Res.* 67, 37–53. doi:10.3897/jhr.67.30883

Qiu, L. F. (2007). *Studies on biology of the brown marmorated stink bug* Halyomorpha halys *(Stål) (Hemiptera: Pentatomidae), an important pest for pome trees in China and its biological control*. Ph.D thesis (Beijing, China: Chinese Academy of Forestry).

Rathee, M., and Ram, P. (2018). Retracted article: Impact of cold storage on the performance of entomophagous insects: An overview. *Phytoparasitica* 46, 421–449. doi:10.1007/s12600-018-0683-5

Sabbatini-Peverieri, G., Dieckhoff, C., Giovannini, L., Marianelli, L., Roversi, P. F., and Hoelmer, K. (2020). Rearing *Trissolcus japonicus* and *Trissolcus mitsukurii* for biological control of *Halyomorpha halys*. *Insects* 11, 787. doi:10.3390/insects11110787

Stahl, J., Tortorici, F., Pontini, M., Bon, M. C., Hoelmer, K., Marazzi, C., et al. (2019). First discovery of adventive populations of *Trissolcus japonicus* in Europe. *J. Pest Sci.* 92, 371–379. doi:10.1007/s10340-018-1061-2

Waage, J. K., and Greathead, D. J. (1988). Biological control: Challenges and opportunities. Philosophical transactions of the royal society of london. *Biol. Sci.* 318, 111–128.

Wermelinger, B., Wyniger, D., and Forster, B. (2008). First records of an invasive bug in Europe: *Halyomorpha halys* stal (heteroptera: Pentatomidae), a new pest on woody ornamentals and fruit trees? *Mittl. Entomol. Ges.* 81, 1–8.

Wong, W. H., Walz, M. A., Oscienny, A. B., Sherwood, J. L., and Abram, P. K. (2021). An effective cold storage method for stockpiling *Halyomorpha halys* (Hemiptera: Pentatomidae) eggs for field surveys and laboratory rearing of *Trissolcus japonicus* (hymenoptera: Scelionidae). *J. Econ. Entomology* 114, 571–581. doi:10.1093/jee/toaa307

Yang, S. Y., Zhan, H. X., Zhang, F., Babendreier, D., Zhong, Y. Z., Lou, Q. Z., et al. (2018). Development and fecundity of *Trissolcus japonicus* on fertilized and unfertilized eggs of the Brown marmorated stink bug, *Halyomorpha halys*. *J. Pest Sci.* 91, 1335–1343. doi:10.1007/s10340-018-0998-5

Yang, Y. L., Zhong, Y. Z., Zhang, F., Zhou, C. Q., Yang, S. Y., and Zhang, J. P. (2015). Parasitic capacity of *Trissolcus halyomorphae* and *T. flavipes* (hymenoptera: Scelionidae) on eggs of *Halyomorpha halys*. *J. Environ. Entomology* 6, 1257–1262.

Yang, Z. Q., Yao, Y. X., Qiu, L. F., and Li, Z. X. (2009). A new species of *Trissolcus* (Hymenoptera: Scelionidae) parasitizing eggs of *Halyomorpha halys* (Heteroptera: Pentatomidae) in China with comments on its biology. *Ann. Entomological Soc. Am.* 102, 39–47. doi:10.1603/008.102.0104

Zhang, J. P., Zhang, F., Gariepy, T., Mason, P., Gillespie, D., Talamas, E., et al. (2017). Seasonal parasitism and host specificity of *Trissolcus japonicus* in northern China. *J. Pest Sci.* 90, 1127–1141. doi:10.1007/s10340-017-0863-y

Zhao, Y. Q., Li, Z., Chen, M., and Yue, L. Y. (2019). Occurrence regularity and control methods of *Halyomorpha halys* in North China. *Chin. J. Agric. Technol.* 39, 91–92.

frontiers | Frontiers in Physiology

TYPE Original Research
PUBLISHED 07 March 2023
DOI 10.3389/fphys.2023.1136559

OPEN ACCESS

EDITED BY
Jia Fan,
State Key Laboratory for Biology of Plant Diseases and Insect Pests, Institute of Plant Protection (CAAS), China

REVIEWED BY
Huai-Jun Xue,
Nankai University, China
Zhaohuan Xu,
Jiangxi Agricultural University, China

*CORRESPONDENCE
Hongmei Li,
h.li@cabi.org
Aihuan Zhang,
zhangaihuan@126.com

SPECIALTY SECTION
This article was submitted to Invertebrate Physiology, a section of the journal Frontiers in Physiology

RECEIVED 03 January 2023
ACCEPTED 14 February 2023
PUBLISHED 07 March 2023

CITATION
Wang M, Li H, Zhang W, Zhuo F, Li T, Lowry A and Zhang A (2023), Reproduction system development of *Ceracris kiangsu* Tsai female adults and its relationship with fitness characteristics. *Front. Physiol.* 14:1136559. doi: 10.3389/fphys.2023.1136559

Reproduction system development of *Ceracris kiangsu* Tsai female adults and its relationship with fitness characteristics

Meizhi Wang[1,2], Hongmei Li[2,3]*, Wei Zhang[4], Fuyan Zhuo[5], Tianjiao Li[5], Alyssa Lowry[6] and Aihuan Zhang[1]*

[1]College of Bioscience and Resource Environment, Beijing University of Agriculture, Beijing, China, [2]MARA-CABI Joint Laboratory for Bio-safety, Institute of Plant Protection, Chinese Academy of Agricultural Science, Beijing, China, [3]CABI East and Southeast Asia, Beijing, China, [4]Research Institute of Subtropical Forestry/Chinese Academy of Forestry, Fuyang, China, [5]National Agro-Tech Extension and Service Center, Beijing, China, [6]CAB International, Egham, United Kingdom

Research on the ovarian development of insect pests helps provide key information for predicting pest occurrences, and currently, there is very limited information about the reproductive system of *Ceracris kiangsu* Tsai. This study aimed to assess the reproductive fitness of 321 adult female insects by using traditional methods to dissect female adults, measure female ovaries, and assess the process of egg formation. The phenotypic traits including body weight and body length were also measured and used to estimate the model of ovarian developmental stages. Four ovarian developmental stages before the oviposition were identified, and the fundamental ovarian structure of *C. kiangsu* displayed red dots on the matured eggs inside the calyx at ovarian developmental stage V. The accessory glands of *C. kiangsu* had the deepest folds at stage III. Redundancy analysis (RDA) was used to explore the correlation between ovarian development, body weight, and body length. A significant positive correlation was observed for body weight (p = 0.001) and body length (p = 0.009), which varied with the grade of ovarian development evaluated by the ovarian developmental stage, ovarian length, ovarian width, and ovarian cross-sectional area. A partial least square (PLS) regression was used to model the ovarian developmental stage, with a stage-based PLS being identified as the more effective method, which was $y = 1.509x_1 + 0.114x_2$. The model provides a potentially rapid way to identify the population source as either "native" or "immigrant" from the phenotypic traits without dissection. The aforementioned model may be used to estimate adult emergence periods and identify migratory populations from their ovarian development, potentially aiding in implementing proper prevention measures.

KEYWORDS

yellow-spined bamboo locust, phenotypic traits, ovary, grade, migratory pest, dissection

1 Introduction

The monitoring and prediction of insect pests is fundamental to conducting effective pest management. Current measures and approaches for the prediction of pest occurrences include, but is not limited to, light traps, sex pheromone traps, and field monitoring. Another technique that has been used to predict pest population dynamics and occurrences in

migrating species is the dissection of adult female insects (Qi et al., 2011). This technique has been shown to provide information on not only the ovarian development but also the peak oviposition period, which can then be used to estimate the reproductive capacity of the population and the migration potential of the pest (Liu and Huang, 2018). Research studies have been conducted on ovarian structures (Hodge, 1943; Liu and Lu, 1959; Snodgrass, 1993), ovarian developmental stages (Wu and Zhang, 1997; Chen et al., 2005; Ren et al., 2014; Zhang et al., 2020), and the effects of insect hormones and miRNAs on ovarian development. A good example of this is the juvenile hormones of *Locusta migratoria manilensis* (Meyen) in which Let-7 and miRNA-278 have been shown to play a vital role in regulating its reproductive system (Song et al., 2013; Song et al., 2019). However, external factors have also been shown to affect ovarian development; Bhalerao et al. (1987) found that the feeding reduction had a negative effect on the vitellogenesis of *Euscelimena harpago* (Serville) and *Potua sabulosa* Hancock female locusts' ovaries. Chen et al. (2008) found that the host plants had a positive effect on ovarian development and fecundity of *Fruhstorferiola tonkinensis* Willemse. Additionally, mating has also been shown to exert a positive effect on the developmental phenotype of *Eriopis connexa* (Germar) offspring and on the increase in the proportion of mature eggs in female *Aedes taeniorhynchus* (Wiedemann). Mating was also found to accelerate both ovarian development and reproduction abilities of female *Apolygus lucorum* (Meyer-Dür) (Meara and Evans, 1977; Colares et al., 2015; Li et al., 2017). Whilst the extreme temperature and short photoperiod reduced the fecundity of *Drosophila suzukii* (Matsumura) and *Athetis lepigone* Möschler (Everman et al., 2018; Liang et al., 2021), the ovarian development of *Spodoptera mauritia* (Boisduval) has been retarded after being treated with fenoxycarb (Banu and Manogem, 2022). In essence, the study of ovarian development and the effect of biological factors and abiotic factors has become a core component of research around pest prediction and reproductive regulation.

Despite much research on insect ovarian development, relatively little is known about the reproduction system development of the yellow-spined bamboo locust, *Ceracris kiangsu* Tsai (Orthoptera: Arcypteridae). This locust has historically been regarded as the second worst pest species affecting *Phyllostachys heterocycla* (Carr.) and *Indocalamus tessellatus* (Munro). *C. kiangsu* Tsai has been recorded in East Asian and Southeast Asian countries, such as China, Laos, and Vietnam, with the scales and frequency of *C. kiangsu* population outbreaks increasing gradually, attacking agricultural crops including *Zea mays* L., *Sorghum bicolor* (L.), *Oryza sativa* L., and *Musa basjoo* Siebold (Liu et al., 2021; Li et al., 2022). Since 2014, there have been a large number of *C. kiangsu* outbreaks in Laos and subsequent outbreaks from Vietnam to South China in 2019 (Zhuo et al., 2020). Liu et al. (2021) revealed that during this immigration, *C. kiangsu* had characteristics similar to *Schistocerca gregaria* (Forskål), whose recurrent outbreaks have affected farming systems throughout Northern Africa. Currently, high-resolution fully polarimetric insect radars are being used to accurately assess and forecast the migration patterns of *C. kiangsu*; however, this is a costly process and equipment-intensive management strategy. This study aims to investigate the potential of using ovarian development monitoring in order to predict the reproduction ability and the population dynamics of *C. kiangsu*.

To fully understand the ovarian structure and stages of *C. kiangsu*, adult female insects were dissected during different developmental stages after emergence. These adult female insects were collected from both the laboratory and field populations. The rearing temperatures were kept constant (30°C), while the field population was kept at a variable temperature. The laboratory-rearing population may provide relative complete series development information of adult female insects. Meanwhile, adult female insects from the field population may ensure the enough dissection replication as the beneficial complement. Hence, there may be differences in ovarian development between the two populations. Moreover, if we just dissected the field population in this study, the whole ovarian developmental process may be missed. To rapidly get the immigration information of *S. frugiperda*, the ovarian length and width were used to predict the ovarian developmental stages (Zhao et al., 2019). Therefore, it is vital to infer the relationship between the phenotypic traits and the stages of oviposition and pre-oviposition. Thus, the information will contribute to easily mastering phenotypic fitness estimating the ovarian development to further provide the migratory and prediction information of *C. kiangsu*.

2 Materials and methods

2.1 Insect source

C. kiangsu adult female insects were collected from both the laboratory population and natural bamboo forests. The laboratory population was reared in the Institute of Plant Protection, Chinese Academy of Agricultural Sciences (IPPCAAS), Beijing, China. The egg pods were collected from a natural bamboo habitat, Anhua County, Hunan Province, China (28°62′N; 111°35′E), and then placed in vermiculite. Using the method of Fang et al. (2022), the egg pods were incubated in a chamber (MGC-1000HP-2, Shanghai Yiheng Scientific Instruments Co., Ltd., Shanghai, China) at 30°C ± 1°C and 65 ± 5% RH under a 16:8 h L:D photoperiod. Nymphs were transferred gently into nylon mesh cages (35 cm × 35 cm × 35 cm) with a maximum of approximately 300 nymphs each. Then, one female and two male adults were transferred from the aforementioned nylon mesh cages to a plastic cylinder (φ = 9 cm; height = 17.8 cm) covered with a nylon mesh for air ventilation. The nymphs and adults were reared under the same condition as the eggs' hatch and were fed with enough fresh wheat and rice leaves.

The field population of *C. kiangsu* was collected from a bamboo forest in Cha'anpu Town, Taoyuan County, Hunan Province, China (28°42′N; 111°12′E), in late July and early August 2022.

2.2 Measurements of phenotypic traits and classification of ovaries

For the laboratory population, after adult emergence, approximately 1–3 healthy female adults were measured and dissected every 3 days until all female adults were dead (the 81st day after adult emergence). However, for the field population, approximately 10–30 healthy female adults were measured and dissected every day from 27 July 2022 to 6 August 2022. The

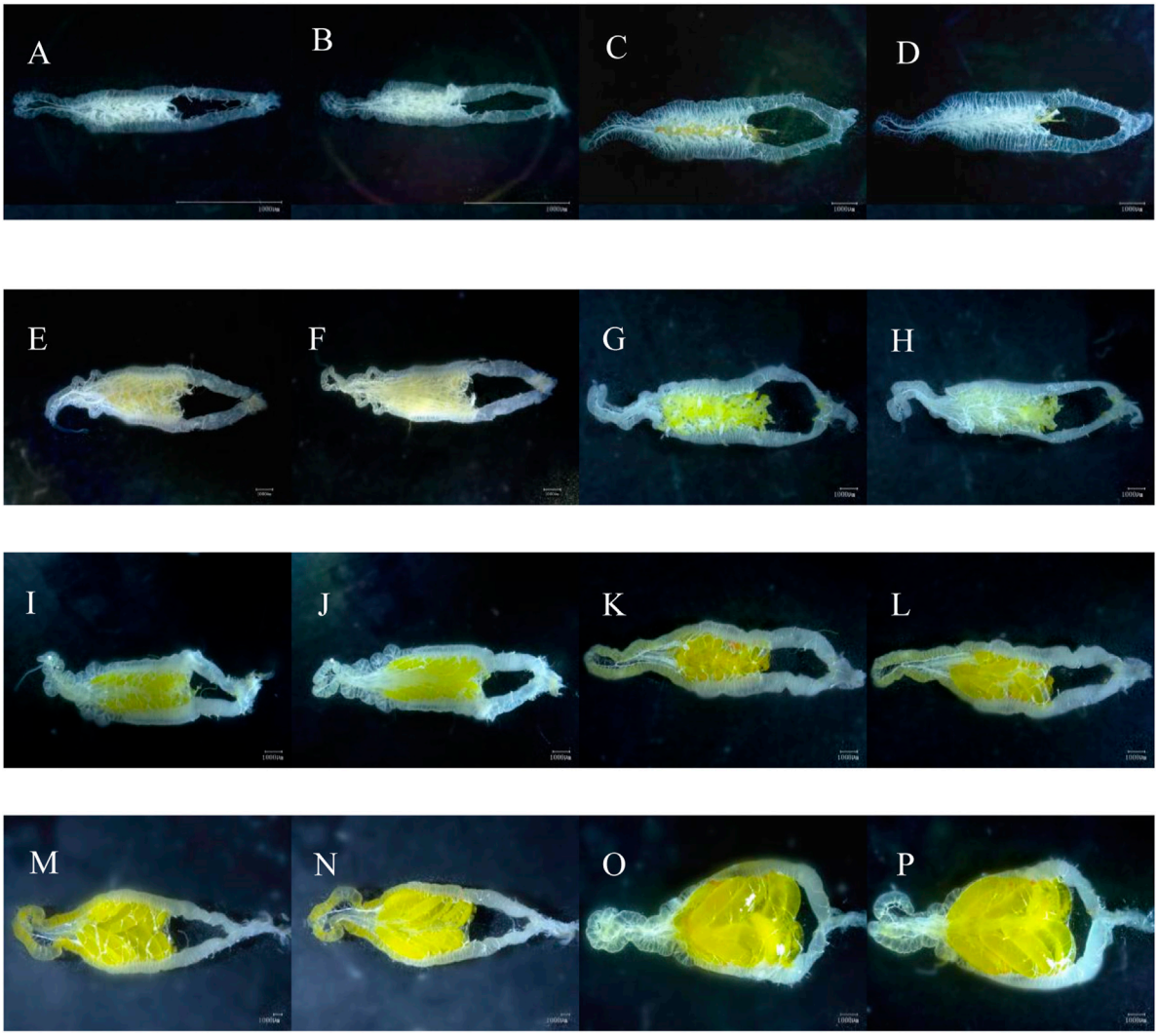

FIGURE 1
Visual view of *C. kiangsu* ovarian morphology. **(A)** Ventral view at stage I, **(B)** dorsal view at stage I, **(C)** ventral view at early-stage II, **(D)** dorsal view at early-stage II, **(E)** ventral view at end-stage II, **(F)** dorsal view at end-stage II, **(G)** ventral view at early-stage III, **(H)** dorsal view at early-stage III, **(I)** ventral view at end-stage III, **(J)** dorsal view at end-stage III, **(K)** ventral view at early-stage IV, **(L)** dorsal view at early-stage IV, **(M)** ventral view at end-stage IV, **(N)** dorsal view at end-stage IV, **(O)** ventral view at stage V, and **(P)** dorsal view at stage V (scale bars = 1,000 μm).

peak data on adult emergence were recorded in advance. In total, 51 and 270 female adults were dissected from the laboratory and field populations, respectively.

The dissection process began with the measurement of the body length and body weight of the female adults by using electronic Vernier calipers (0–150 mm, Shanghai Shenhan Measuring Tools Co., Ltd., Shanghai, China) and the electronic balance (PL203, Mettler-Toledo Instruments Shanghai Co., Ltd., Shanghai, China).

Then, the adult female insects were dissected according to Han et al. (2018). The wings and legs were removed, and the dead locust was placed on a dissecting tray with wax and fixed by means of needles through the thorax. An incision was then made on the middle of sternites using surgical scissors. Approximately 6–8 insect needles were placed through the exoskeleton on the left and right sides of the body and into the wax. Care was taken not to damage the internal organs. Finally, the target organ, ovary, was identified under a stereomicroscope (SZ2-ILST, Olympus Co., Tokyo, Japan) and carefully placed in a Petri dish with saline.

The ovaries were photographed using a super-depth-of-field three-dimensional microscopy system (VHX-2000), and the length, width, and cross-sectional area of the ovaries were also measured. The fundamental ovarian structure was similar to that shown in Liu and Lu (1959), and the ovarian development classification methods were according to Han et al. (2018).

2.3 Statistical analysis

The phenotypic traits and ovarian developmental parameters were evaluated using a one-way ANOVA (Duncan's test; $p < 0.05$; SPSS 22.0).

TABLE 1 Ovarian development characteristics of *C. kiangsu* at different stage standards.

Level	Stage	Characteristics of ovarioles and oviducts	Yolk and egg	Fat body around the ovary	Accessory gland
I	Transparency	Ovarioles appeared transparent and slender	NA	NA	Smooth and thin
II	Vitellogenesis	Ovarioles appeared white. The lateral oviduct and the median oviduct became thickened and widened	Yolk began to appear and gradually increased	Little pale-yellow fat body	Thickening and folds were deepening
III	Egg formation	The calyx formed with the gradually expanding lateral oviducts. The median oviduct became longer	Yolk reduced and eggs appeared	Pale-yellow fat body increased	Folds became deepest
IV	Pre-oviposition	Ovarioles partially encased the eggs. The median oviduct became longer gradually	Eggs arranged neatly	Orange fat body	Thickening and folds spread
V	Oviposition	Ovarioles in the calyx rarely encased eggs	Eggs matured, egg membranes were transparent, and the dark red spots appeared in the calyx	Little orange fat body	The gland appeared the thickest

FIGURE 2
Phenotypic morphology of the *C. kiangsu* abdomen at **(A)** stage IV and **(B)** stage V.

Then, detrended correspondence analysis (DCA; Hill and Gauch, 1980) was used to select the proper constrained ordination method [e.g., redundancy analysis (RDA) and canonical correspondence analysis (CCA)]. Once the axil length of the dataset after DCA is less than 2, RDA can be selected for further analyses according to Nasser et al. (2019). RDA and Pearson's correlation analysis were used to assess and quantify the relationship between the development duration, days after emergence, body length, body weight of female adults, and ovarian development for the optimization of variables. The variance inflation factor (VIF) value indicates the collinearity among every two independent variables. Four independent variables in this study were less than 10, and independent variables with $p < 0.05$ were regarded as significantly contributed to the variance in the process of ovarian development (Grech et al., 2019).

The partial least squares (PLS; Wold, 1975) regression is a powerful method that can be used to extract a few latent variables with information content, which explain as much of the covariance as possible between the dependent variables and independent variables. The optimal number of latent variables (ONLVs) was determined according to the lowest value of the root mean square error of the cross-validation (RMSECV) *via* the leave-one-out cross-validation (LOOCV) method, to avoid overfitting or underfitting. The coefficient of multiple determinations (R^2), the root mean squared error of prediction (RMSEP), and the variance explained (%) and variable importance in the projection (VIP) were used to evaluate PLS models. The

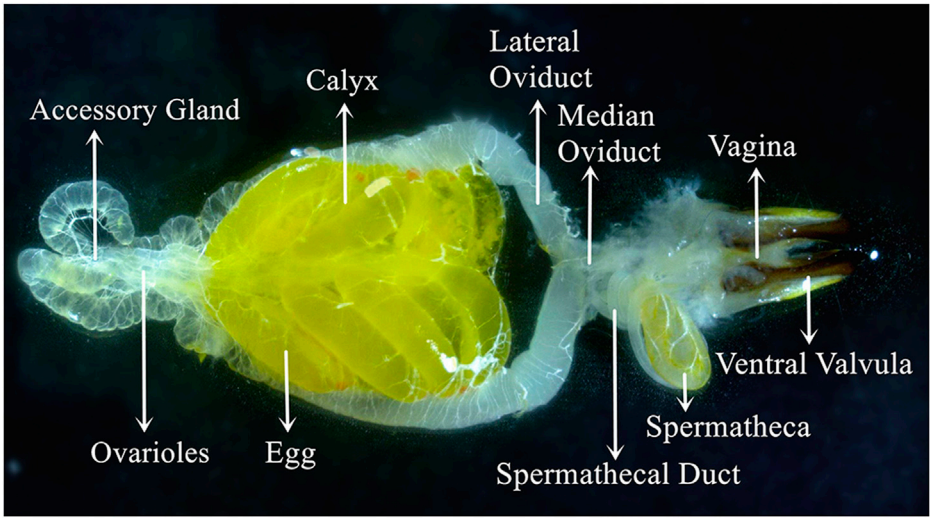

FIGURE 3
Visual view of the *C. kiangsu* ovary at stage V.

higher R^2, variance explained, and VIP means the PLS model fits better; among them, the threshold score of a VIP is 1.0 (Porker et al., 2020; Wise and Dolan, 2020).

RDA (Oksanen et al., 2022), Pearson's correlation analysis (*R* core team, 2022), and PLS (Liland et al., 2022) analysis were carried out using R 4.1.3.

3 Results

3.1 Ovarian development and structure of female adults

In total, 321 adult female insects were dissected over the course of this study. Figure 1 illustrates the development of ovaries with increasing female age. Ovaries shown in Figure 1 were all collected from the laboratory population.

The ovarian development was divided into five stages according to characteristics of ovarioles and oviducts, accessory gland, the number of yolks and eggs, and body fat (Figure 1; Table 1). The main characteristic of ovarian developmental stage I was transparent and thin ovarioles; Figures 1A, B show an ovary from a three-day-old female adult. The main characteristic of ovarian developmental stage II was the appearance of the pale-yellow fat body and yolk, which gradually increased; Figures 1C, D and Figures 1E, F show ovaries from 12-day-old and 18-day-old female adults, respectively. At ovarian developmental stage III, the shape and number of immature eggs appeared and increased in the ovary gradually; Figures 1G, H and Figures 1I, J show ovaries from 27-day-old and 36-day-old female adults, respectively. The main characteristics of stage IV were the proper arrangement of eggs in the calyx and thickening of the accessory gland. The abdominal morphology showed that the intersegmental membranes between the fifth and sixth segments were folded (Figure 2A); Figures 1K–N show ovaries from 27-day-old and 36-day-old female adults, respectively. The eggs matured, the egg membranes were transparent, and dark red spots appeared in the calyx at stage V; Figures 1O, P show the ovary from an 81-day-old female adult. There was an ovipositor located between the eighth and ninth segments. At stage V, the valvulae protruded from the end of the abdomen, and the epiproct lifted up (Figure 2B).

The *C. kiangsu* adult female essential reproductive system (Figure 3) consisted of a pair of ovaries. There was a pair of accessory glands connected to a pair of calyxes and lateral oviducts, and the oviducts jointly form the median oviduct, which led to the vagina. The spermatheca connected with the median oviduct and vagina by the spermatheca duct. There was a suspensory ligament located in the anterior end of the accessory gland, and the suspensory ligament was generally thin and transparent and not shown in Figure 3.

3.2 Phenotype characteristics of different ovarian developmental stages

The analysis indicated that there was an increasing tendency of both ovarian and phenotype characteristics with the progression of ovarian development stages as *C. kiangsu* matured (Figure 4). The ovarian width (7.90 ± 0.47 mm) and cross-sectional area (92.25 ± 10.24 mm^2) at ovarian development stage V were significantly wider and bigger than those at the other four stages, respectively, but there was no significant difference found among the ovarian lengths of ovarian development stages from II to IV. At stage V, the ovarian length was significantly longer than that at stage I (18.95 ± 1.72 mm versus 13.47 ± 1.56 mm).

Similarly, the average body weight and average body length increased proportionally to the ovarian development stage. The average body weight (1.11 ± 0.01 g) and body length (41.49 ±

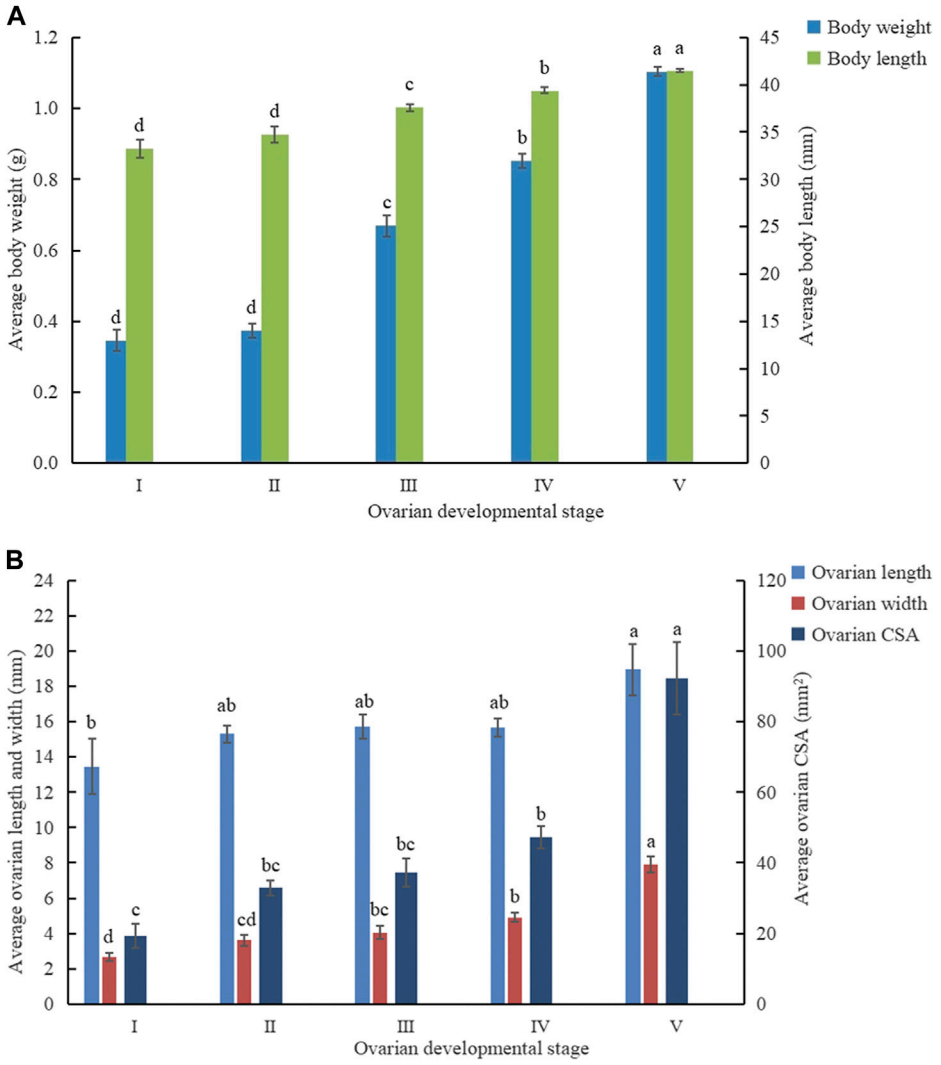

FIGURE 4
Mean value (±SE) at different ovarian developmental stages of **(A)** phenotypic traits and **(B)** ovarian developmental parameters. CSA, cross-sectional area.

0.15 mm) at stage V was significantly heavier and longer than those at the other four stages, respectively.

3.3 Correlation analysis between ovarian developmental parameters and independent variables

Pearson's correlation coefficient analysis and RDA were used to investigate the relationship between body weight and body length during the ovarian development of *C. kiangsu*. Four ovarian developmental parameters were used to evaluate the degree of ovarian development in RDA (stage, ovarian length, ovarian width, and ovarian cross-sectional area).

Pearson's correlation coefficient matrix (Figure 5) showed that body weight and body length were significantly positively correlated with every ovarian development parameter. Furthermore, RDA (Table 2; Figure 6) showed that both body length and body weight were significantly positively correlated with the degree of ovarian development.

RDA showed that body weight and body length accounted for 45.75% of the total variance in the degree of ovarian development, suggesting that the two independent variables had a significant impact on the degree of ovarian development, with Monte Carlo permutation tests with 999 unrestricted permutations (Table 2). The interpretation of the two axes was 44.90% and 0.85%, respectively (Table 3). Therefore, the two axes were selected as the main component axis (Tables 2, 3; Figure 6). From the two independent variables analyzed, the percentage of the total variance explained was the highest for the body weight with 29.47%, which disclosed that body weight had a better

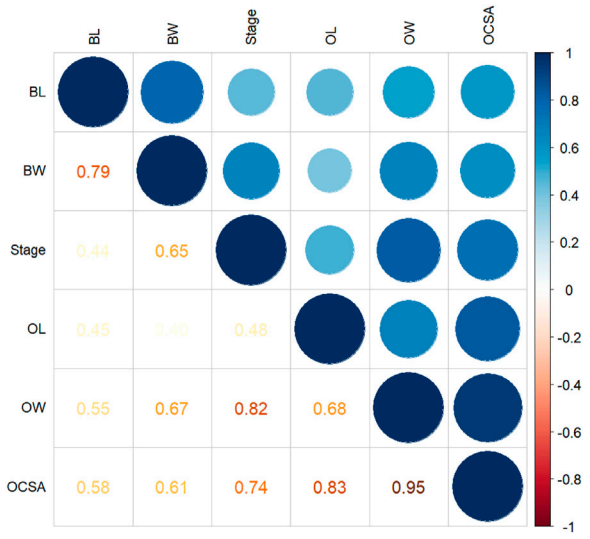

FIGURE 5
Correlation matrix of all variables. The larger the absolute value and the darker the color, the stronger the Pearson's correlation (positive or negative). Circles in different colors represent significant correlation; $p < 0.05$. BL, body length; BW, body weight; OL, ovarian length; OW, ovarian width; OCSA, ovarian cross-sectional area.

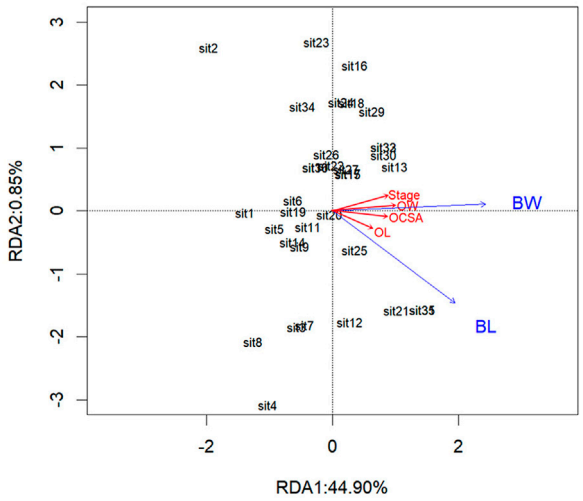

FIGURE 6
Redundancy analysis diagram of correlations between independent variables and the ovarian developmental parameters. The ovarian developmental parameters are indicated by red color arrows: OL, ovarian length; OW, ovarian width; OCSA, ovarian cross-sectional area. The independent variables are indicated by blue color arrows: BL, body length; BW, body weight.

TABLE 2 Forward selection results with the test of variable significance.

	RDA 1	RDA 2	Data variance explained (%)	*p*
Body weight/g	0.999	0.040	29.47	0.001***
Body length/mm	0.797	−0.604	12.99	0.009**

*$p < 0.05$.

explanation of ovarian development than body length (Table 2; Figure 6).

3.4 PLS regression models of ovarian development

All four ovarian developmental parameters were used to model dependent variables. The ONLV first determined the number of latent variables according to the lowest value of the RMSECV. The first latent variable was selected and then fitted in PLS models again. The optimal models based on each dependent variable and their visualization are shown in Figure 7. The latent variable elucidated 92.41% of the stage-based PLS model. R^2, RMSEP, and VIP of the stage-based PLS model were 0.56, 0.67, and 1.00, respectively, which suggested that the stage-based PLS model fitted better (Figure 7).

Furthermore, the VIP of ovarian length-based, ovarian width-based, and ovarian cross-sectional area-based PLS models were all less than 1. Body weight and body length accounted for 56.66% of the total variance explained. The VIP of the stage-based PLS model was greater than 1, which suggests that this PLS model has a relative application in stages' prediction in the ovarian development of *C. kiangsu*. The PLS model was subjected to statistical validation tests, and the SE, *t*-value, and *p*-value of the PLS model are shown in Table 4, which revealed that body weight had a significant effect on the ovarian developmental stage, but there was no significant effect found among body lengths of ovarian development stages by modeling.

4 Discussion

Ovarian development significantly influences the reproduction and expansion capabilities of insect pest populations, and it should be considered when developing sustainable pest management strategies, especially for migratory species (Zhang et al., 2016; Roy et al., 2018). For example, when Masaaki and Seiji (2009) disclosed that the population of *L. m. manilensis* overwintered as adults or eggs by observing the ovarian development on Iheya Island, Japan, it was then this overwinter behavior that provided essential information to better control this population. Similarly, when Elamin et al. (2014) revealed that the ovarian developmental

TABLE 3 Summary of RDA for trapped samples.

Axis	Eigenvalue	Eigenvalues for the unconstrained axis	Interpretation (%)
I	0.050	0.052	44.90
II	0.001	0.001	0.85

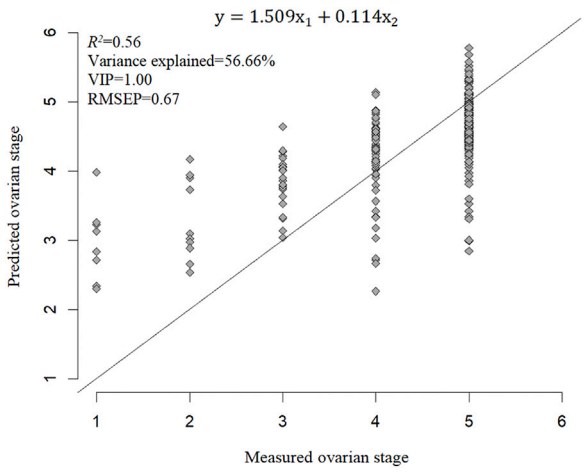

FIGURE 7
PLS prediction of ovarian developmental parameters for Stage. In this model, y was stage, x_1, x_2 were body weight, body length, respectively.

TABLE 4 PLS regression coefficient significance test.

Stage-based PLS model	Regression coefficient		
	SE	*t*	*p*
Body weight	0.079	9.749	***
Body length	0.082	0.153	–

*$p < 0.05$.

stages and the subsequent fecundity of *Oedaleus senegalensis* (Krauss) depended upon the number and function of the ovarioles, this helped improve the pest management operation in North Kordofan State, Sudan. Whilst this study focused on the ovarian development and grade of *C. kiangsu*, it may also help fill the gap by improving basic ovarian development information and thus the pest management strategies for this species. The relationship between the phenotypic traits and ovarian grade can shed light on the population development of *C. kiangsu*.

Overall, the ovarian structure of *C. kiangsu* can be described as similar to *Omocestus viridulus* (L.), *Euchorthippus unicolor* (Ikonn.), *Euchorthippus vittatus* Zheng, etc. (Zhao and Xi, 2005). With five ovarian developmental stages, *C. kiangsu* was found to be similar to *O. decorus asiaticus* (Bey-Bienko). The ovarian developmental duration of *C. kiangsu* was longer than both gregarious and solitary phases of *O. decorus asiaticus* at stages III, IV, and V (Han et al., 2018). The changing trend of the accessory glands was consistent between *C. kiangsu* and *Calliptamus italicus* (L.), whilst the accessory glands folded from stage II to stage IV, and the folds became deepest at stage III (Ren et al., 2014). However, there were unique ovarian features specific to *C. kiangsu* that set it apart from other species. The median oviduct of *C. kiangsu* did not fold during ovarian development, which was different from *O. viridulus*, *E. unicolor*, and *E. vittatus* (Zhao and Xi, 2005). There were also dark red dots observed on the matured eggs inside the calyx at stage V of a *C. kiangsu* ovary, which is not observed in the other species.

In this study, both the ovarian length and width were positively correlated with the ovarian developmental stages, which is similar to *Tomicus yunnanensis Kirkendall & Faccoli* (Liu et al., 2019). In contrast, during the process of ovarian development, the ovarian length of *Telenomus theophilae* Wu et Chen, *L. m. manilensis*, and *Bactrocera cucurbitae* (Coquillett) increased first and then reduced after they had finished laying eggs (Liu et al., 2006; Ouyang et al., 2014; Kwak et al., 2021). After stage IV, the body length rapidly increased with the ovarian development for the *C. kiangsu* adult female insects, as the ovipositor reached out from the abdomen. Furthermore, there was a positive correlation between the body weight and ovarian developmental stage, due to both the yolk continually being transformed into eggs and the increased number of eggs during stages II–V, and this change trend of phenotypic traits on ovarian development was in consistent with *Oxya chinensis* Thunberg and *O. japonica* Thunberg (Wu and Zhang, 1997). The RDA results showed that body weight and body length accounted for 45.75% of the total variance explained in ovarian development, with each factor significantly positively correlating with the ovarian development of *C. kiangsu* ($p < 0.05$). A similar trend has been observed in *Bombus terrestris* L. workers, in which the body weight positively correlated with the ovarian development. (Gosterit et al., 2016).

Generally, during the development of migrating insects, they have been shown to exhibit a delayed ovarian development during migration, which has been classified as reproductive diapause (Qi et al., 2011). However, once they arrived at their destination, the ovaries continued to develop, allowing for successful reproduction (Johnson, 1963). Thus, exploring the ovarian development and mating behaviors of migratory pests has become important in discovering their potential source areas and migratory paths. In order to better implement pest management strategies for *C. kiangsu*, a rapid method to obtain the ovarian developmental stage in the field is fundamental. Previously, PLS was used to predict either continuous or discrete variables (Elsherif et al., 2018); however, it can also be applied to pest management. For example, Xu et al. (2020) used this approach to produce a predictive diagnostic model for cotton aphids based on leaf textural features; the predictive accuracy of up to 91.49% was obtained for this model. In this study, in order to rapidly obtain the degree of ovarian development of *C. kiangsu* without dissection, body weight and body length were used as predictors. The model parameter standards showed that stage-based PLS modeling was the preferred approach, which can

be used in a predictive capacity, and thus, it could potentially be a reference model to identify whether the field populations are "native" or "migratory."

The ovarian development process is highly dynamic (Papaj, 2000). Berger et al. (2008) found that a heavier female insect usually had a higher potential fecundity, and different sizes of female insects indicated different allocation trade-offs between the self-condition and their egg production. However, this phenomenon is found in reproductive systems of not only female insects but also male insects (Leopold, 1976). Chen et al. (2019) showed that the mating rate in the current generation can be reduced through sex pheromone-trapped male adults, which is then reflected by the size of the *Spodoptera litura* male testis. Hence, the observation of the reproductive system of migratory insects is a determining factor in determining the origin and degree of development of migratory insects. The studies can provide information on integrated pest management (IPM) of migrants, but these aforementioned studies of *C. kiangsu* were much less explored.

This study identified the ovarian development process of *C. kiangsu* adult female insects. By grading the ovarian developmental stages, it is easier to identify the transition and critical time between different stages, thus improving the prediction accuracy of the population development of *C. kiangsu*. Moreover, it could be helpful in the study of migratory pathways and predicting the occurrence of pests. It also provides additional information about the further exploration of *C. kiangsu* reproductive systems.

Data availability statement

The raw data supporting the conclusion of this article will be made available by the authors, without undue reservation.

Author contributions

All authors contributed to the manuscript and its final submission. MW and WZ contributed to the field data collection. MW and FZ analyzed the data. MW, HL, and TL contributed to the writing of the manuscript. HL and AZ contributed to the conception and field work design. AL edited and improved the manuscript language.

Acknowledgments

The authors acknowledge the financial support from China's donation to the CABI Development Fund (IVM10051) and the National Key R and D Program of China (2021YFE0194800).

Conflict of interest

The authors declare that the research was conducted in the absence of any commercial or financial relationships that could be construed as a potential conflict of interest.

Publisher's note

All claims expressed in this article are solely those of the authors and do not necessarily represent those of their affiliated organizations, or those of the publisher, the editors, and the reviewers. Any product that may be evaluated in this article, or claim that may be made by its manufacturer, is not guaranteed or endorsed by the publisher.

References

Banu, C. A., and Manogem, E. M. (2022). Development and characterization of *Spodoptera mauritia* ovarian primary cell culture and evaluation of fenoxycarb toxicity. *Vitro Cell. Dev.-An.* 58, 788–797. doi:10.1007/S11626-022-00728-0

Berger, D., Walters, R., and Gotthard, K. (2008). What limits insect fecundity? Body size- and temperature-dependent egg maturation and oviposition in a butterfly. *Funct. Ecol.* 22, 523–529. doi:10.1111/J.1365-2435.2008.01392.X

Bhalerao, A. M., Naidu, N. M., and Paranjape, S. Y. (1987). Some observations on the nutrition-reproduction correlation in grouse locusts (Orthoptera: Tetrigidae). *Proc. Indian Anim. Sci.* 96, 323–327. doi:10.1007/BF03180016

Chen, Q., Zeng, J., Yang, L., Jia, Y., Li, Q., Feng, C., et al. (2019). The structure of day-age of male *Spodoptera litura* moths by sex pheromone trapping in the field. *Sci. China Agricul.* 52, 3819–3827. doi:10.3864/j.issn.0578-1752.2019.21.010

Chen, W., Chen, W., and Wu, W. (2005). Grading ovarian developments of *Fruhstorferiola tonkinensis*. *Chin. Plant Prot.* 25, 5–6. doi:10.3969/j.issn.1672-6820.2005.05.001

Chen, W., Fu, Y., and Wu, W. (2008). Effects of adult feeding on ovarian development and fecundity of *Fruhstorferiola tonkinensis* (Orthoptera: Catantopidae). *Chin. J. Trop. Crops* 29, 89–92. doi:10.3969/j.issn.1000-2561.2008.01.018

Colares, F., Michaud, J. P., Torres, J. B., and Silva-Torres, C. S. A. (2015). Polyandry and male mating history affect the reproductive performance of *Eriopis connexa* (Coleoptera: Coccinellidae). *Ann. Entomol. Soc. Am.* 108, 736–742. doi:10.1093/aesa/sav056

Elamin, A. E. H., Abdalla, A. M., and Naim, A. M. E. (2014). The biology of Senegalese grasshopper (*Oedaleus senegalensis*, Krauss, 1877) (Orthoptera: Acrididae). *Inter. J. Adv. Life Sci. Technol.* 1, 6–15. doi:10.18488/journal.72/2014.1.1/72.1.6.15

Elsherif, L., Heimlich, J. B., Kamthunzi, P., Mafunga, P., Gopal, S., Key, N. S., et al. (2018). Exploratory study of urine metabolomics in sickle cell disease children with albuminuria in Malawi. *Blood* 132 (1), 3680. doi:10.1182/blood-2018-99-120233

Everman, E. R., Freda, P. J., Brown, M., Schieferecke, A. J., Ragland, G. J., and Morgan, T. J. (2018). Ovary development and cold tolerance of the invasive pest *Drosophila suzukii* (Matsumura) in the central plains of Kansas, United States. *Environ. Entomol.* 47, 1013–1023. doi:10.1093/ee/nvy074

Fang, L., Li, Z., Zhang, S., Zhang, W., Shu, J., and Wang, H. (2022). Identification and selection of the internal reference genes of *Ceracris kiangsu* (Orthoptera: Arcypteridae) by RT-PCR. *Sci. Silvae Sin.* 58, 70–77. doi:10.11707/j.1001-7488.20220108

Gosterit, A., Koskan, O., and Gurel, F. (2016). The relationship of weight and ovarian development in *Bombus terrestris* L. workers under different social conditions. *J. Apic. Sci.* 60, 51–58. doi:10.1515/jas-2016-0016

Grech, M. M., Manzo, L. M., Epele, L. B., Laurito, M., Claverie, A. Ñ., Ludueña-Almeida, F., et al. (2019). Mosquito (Diptera: Culicidae) larval ecology in natural habitats in the cold temperate patagonia region of Argentina. *Parasite* 12, 214. doi:10.1186/s13071-019-3459-y

Han, H., Wang, N., Xu, L., Gao, S., Liu, A., and De, Q. (2018). Grading criteria for the ovarian development of *Oedaleus decorus asiaticus* and differences between two types of ovarian development. *Plant Prot.* 44, 135–138. doi:10.16688/j.zwbh.2017094

Hill, M. O., and Gauch, H. G. J. (1980). Detrended correspondence analysis: An improved ordination technique. *Vegetatio* 42, 47–58. doi:10.1007/BF00048870

Hodge, C. (1943). The internal anatomy of *Leptysma marginicollis* (Serv.) and *Opshomala vitreipennis* (Marsch.) (Orthoptera: Acrididae). *J. Morph.* 72, 87–124. doi:10.1002/jmor.1050720104

Johnson, C. G. (1963). Physiological factors in insect migration by flight. *Nature* 198, 423–427. doi:10.1038/198423a0

Kwak, K., Ko, H., Kim, S. Y., Lee, K. Y., and Yoon, H. J. (2021). Developmental characteristics of ovary and egg of migratory locust, *Locusta migratoria* (Orthoptera: Acrididae). *Korean J. Appl. Entomol.* 60, 175–183. doi:10.5656/KSAE.2021.01.1.088

Leopold, R. A. (1976). The role of male accessory glands in insect reproduction. *Ann. Rev. Entomol.* 21, 199–221. doi:10.1146/annurev.en.21.010176.001215

Li, H., Wang, J., Zhuo, F., Zhu, J., Tu, X., Zhang, G., et al. (2022). Review on the occurrence and management technology of *Ceracris kiangsu* in China. *Chin. J. Biol. Control* 38, 531–536. doi:10.16409/j.cnki.2095-039x.2021.05.001

Li, W., Yuan, W., Zhao, X., Li, Y., and Wu, K. (2017). Effects of mating on ovarian development and oviposition of *Apolygus lucorum*. *J. Asia-Pac. Entomol.* 20, 1442–1446. doi:10.1016/j.aspen.2017.10.013

Liang, F., Wang, Z., He, K., Bai, S., and Zhang, T. (2021). Effects of brief exposure to high temperatures on the survival and fecundity of *Athetis lepigone* (Lepidoptera: Noctuidae). *J. Therm. Biol.* 100, 103066. doi:10.1016/J.JTHERBIO.2021.103066

Liland, K. H., Mevik, B. H., and Wehrens, R. (2022). *pls: Partial least squares and principal component regression*. Vienna, Austria: R Foundation for Statistical Computing.

Liu, D., Zhao, S., Yang, X., Wang, R., Cang, X., Zhang, H., et al. (2021). Radar monitoring unveils migration dynamics of the yellow-spined bamboo locust (Orthoptera: Arcypteridae). *Comput. Electron. Agr.* 187, 106306. doi:10.1016/J.COMPAG.2021.106306

Liu, J., Zhao, N., Yang, B., and Li, Z. (2019). Processing morphology change and grading criteria for ovarian development in Tomicus yunnanensis (Coleoptera, Scolytidae). *For. Res.* 32, 74–80. doi:10.13275/j.cnki.lykxyj.2019.01.010

Liu, W., and Huang, C. (2018). Advances in modern crop disease and pest forecast in China. *Plant Prot.* 44, 159–167. doi:10.16688/j.zwbh.2018248

Liu, Y., and Lu, B. (1959). Anatomy and organization of the reproductive system of *Locusta migratoria manilensis* Meyen. *Acta Entomol. Sin.* 9, 1–20. doi:10.16380/j.kcxb.1959.01.001

Liu, Y., Ye, G., and Li, X. (2006). Effects of temperature on the development of ovary and egg of *Bombyx mandarina* Bulter. *Nat. Enemies Insects* 28, 126–131. doi:10.3969/j.issn.1674-0858.2006.03.006

Masaaki, Y., and Seiji, T. (2009). Overwintering biology and morphological characteristics of the migratory locust, *Locusta migratoria* after outbreaks on Iheya Island, Japan. *Appl. Entomol. Zool.* 44, 165–174. doi:10.1303/aez.2009.165

Meara, G. F., and Evans, D. G. (1977). Autogeny in saltmarsh mosquitoes induced by a substance from the male accessory gland. *Nature* 167, 342–344. doi:10.1038/267342a0

Nasser, N. A., Cullen, J., Patterson, C. W., Patterson, R. T., Roe, H. M., and Galloway, J. M. (2019). Inter-annual Arcellinida (testate lobose amoebae) assemblage dynamics within lacustrine environments. *Limnologica* 76, 60–71. doi:10.1016/j.limno.2019.03.006

Oksanen, J., Simpson, G. L., Blanchet, G. F., Kindt, R., Legendre, P., Minchin, P. R., et al. (2022). *vegan: Community ecology package*. Vienna, Austria: R Foundation for Statistical Computing.

Ouyang, Q., Mo, R., and Wu, W. (2014). Classification of ovarian stages of the melon fly, *Bactrocera cucurbitae* (Coquillett) (Diptera: Tephritidae). *J. Biosaf.* 23, 24–29. doi:10.3969/j.issn.2095-1787.2014.01.005

Papaj, D. R. (2000). Ovarian dynamics and host use. *Annu. Rev. Entomol.* 45, 423–448. doi:10.1146/annurev.ento.45.1.423

Porker, K., Coventry, S., Fettell, N. A., Cozzolino, D., and Eglinton, J. (2020). Using a novel PLS approach for envirotyping of barley phenology and adaptation. *Field Crops Res.* 246, 107697. doi:10.1016/j.fcr.2019.107697

Qi, G., Lu, F., Hu, G., Wang, F., Gao, Y., and Lv, L. (2011). The application of ovarian dissection in the research on migratory insects in China. *Chin. Plant Prot.* 31, 18–22. doi:10.3969/j.issn.1672-6820.2011.07.004

Ren, J., Zhao, L., and Ge, Q. (2014). Ovarian development in *Calliptamus italicus* (L.) (Orthoptera: Catantopidae). *Chin. J. Appl. Entomol.* 51, 1280–1288. doi:10.7679/j.issn.2095–1353.2014.152

Roy, S., Saha, T., Zou, Z., and Raikhel, A. S. (2018). Regulatory pathways controlling female insect reproduction. *Annu. Rev. Entomol.* 63, 489–511. doi:10.1146/annurev-ento-020117-043258

Snodgrass, R. E. (1993). *Principles of insect morph*. New York: McGraw-Hill Press.

Song, J., Guo, W., Jiang, F., and Zhou, S. (2013). Argonaute 1 is indispensable for juvenile hormone mediated oogenesis in the migratory locust, *Locusta migratoria*. *Insect biochem. Mol.* 43, 879–887. doi:10.1016/j.ibmb.2013.06.004

Song, J., Li, W., Zhao, H., and Zhou, S. (2019). Clustered miR-2, miR-13a, miR-13b and miR-71 coordinately target *Notch* gene to regulate oogenesis of the migratory locust *Locusta migratoria*. *Insect biochem. Mol. Biol.* 106, 39–46. doi:10.1016/j.ibmb.2018.11.004

Wise, T., and Dolan, R. J. (2020). Associations between aversive learning processes and transdiagnostic psychiatric symptoms in a general population sample. *Nat. Commun.* 11, 4179. doi:10.1038/s41467-020-17977-w

Wold, H. (1975). Soft modelling by latent variables: The non-linear iterative partial least squares (NIPALS) approach. *J. Appl. Probab.* 12, 117–142. doi:10.1017/S0021900200047604

Wu, M., and Zhang, J. (1997). Study on the relationship between ovarian development level and body weight and its application in rice grasshoppers. *Entomol. Knowl.* 34, 257–258.

Xu, J., Lv, X., Lin, J., Zhang, Z., Yao, Q., Fan, X., et al. (2020). The diagnostic model of cotton aphids based on leaf textural features. *Cott. Sci.* 32, 133–142. doi:10.11963/1002-7807.xjclx.20200220

Zhang, L., Cheng, L., Chapman, J. W., Sappington, T. W., Liu, J., Cheng, Y., et al. (2020). Juvenile hormone regulates the shift from migrants to residents in adult oriental armyworm, *Mythimna separata*. *Sci. Rep.* 10, 11626. doi:10.1038/s41598-020-66973-z

Zhang, Y., Zhao, B., Roy, S., Saha, T. T., Kokoza, V. A., Li, M., et al. (2016). MicroRNA-309 targets the Homeobox gene *SIX4* and controls ovarian development in the mosquito *Aedes aegypti*. *Proc. Natl. Acad. Sci. USA.* 113, E4828–E4836. doi:10.1073/pnas.1609792113

Zhao, S., Yang, X., He, W., Zhang, H., Jiang, Y., and Wu, K. (2019). Ovarian development gradation and reproduction potential prediction in *Spodoptera frugiperda*. *Plant Prot.* 45, 28–34. doi:10.16688/j.zwbh.2019413

Zhao, Z., and Xi, G. (2005). The seasonal dynamics of ovarian development of six dominant species of locusts in Siping area of Jilin. *Chin. Bull. Entomol.* 42, 524–527. doi:10.3969/j.issn.0452-8255.2005.05.011

Zhuo, F., Zhu, J., Ren, B., Lv, J., Zhang, L., Chen, A., et al. (2020). Preliminary report on the prevention and control of *Ceracris kiangsu* infestation in Yunnan Province in 2020. *Chin. Plant Prot.* 40, 60–62.

frontiers | Frontiers in Physiology

TYPE Original Research
PUBLISHED 31 March 2023
DOI 10.3389/fphys.2023.1172542

OPEN ACCESS

EDITED BY
Fengqi Li,
Guizhou University, China

REVIEWED BY
Zhongfang Liu,
Shanxi Agricultural University, China
Jianjun Jiang,
Guangxi Academy of Agricultural Sciences, China

*CORRESPONDENCE
Yuqing Wu,
yuqingwu36@hotmail.com
Chuantao Lu,
chuantaolu@qq.com

†These authors have contributed equally to this work and share first authorship

SPECIALTY SECTION
This article was submitted to Invertebrate Physiology, a section of the journal Frontiers in Physiology

RECEIVED 23 February 2023
ACCEPTED 15 March 2023
PUBLISHED 31 March 2023

CITATION
Li T, Jiang Y, Yang X, Li H, Gong Z, Qin Y, Zhang J, Lu R, Wei G, Wu Y and Lu C (2023), The effects of circularly polarized light on mating behavior and gene expression in *Anomala corpulenta* (Coleoptera: Scarabaeidae). *Front. Physiol.* 14:1172542. doi: 10.3389/fphys.2023.1172542

The effects of circularly polarized light on mating behavior and gene expression in *Anomala corpulenta* (Coleoptera: Scarabaeidae)

Tong Li[1†], Yueli Jiang[1†], Xiaofan Yang[2], Huiling Li[1], Zhongjun Gong[1], Yifan Qin[1], Jing Zhang[1], Ruijie Lu[1], Guoshu Wei[3], Yuqing Wu[1*] and Chuantao Lu[1*]

[1]Henan Key Laboratory of Crop Pest Control, Key Laboratory of Integrated Pest Management on Crops in Southern Region of North China, Institute of Plant Protection, Henan Academy of Agricultural Sciences, Zhengzhou, China, [2]Plant Protection Institute, Hebei Academy of Agricultural and Forestry Sciences, Baoding, China, [3]College of Plant Protection, Hebei Agricultural University, Baoding, Hebei, China

Light is an important abiotic factor affecting insect behavior. In nature, linearly polarized light is common, but circularly polarized light is rare. Left circularly polarized (LCP) light is selectively reflected by the exocuticle of most scarab beetles, including *Anomala corpulenta*. Despite our previous research showing that this visual signal probably mediates their mating behavior, the way in which it does so is not well elucidated. In this study, we investigated how LCP light affects not only mating behavior but also gene expression in this species using RNA-seq. The results indicated that disruption of LCP light reflection by females of *A. corpulenta* probably affects the process by which males of *A. corpulenta* search for mates. Furthermore, the RNA-seq results showed that genes of the environmental signaling pathways and also of several insect reproduction-related amino acid metabolic pathways were differentially expressed in groups exposed and not exposed to LCP light. This implies that *A. corpulenta* reproduction is probably regulated by LCP light-induced stress. Herein, the results show that LCP light is probably perceived by males of the species, further mediating their mating behavior. However, this hypothesis needs future verification with additional samples.

KEYWORDS

***Anomala corpulenta*, left circularly polarized light, mating behavior, scarab beetles, light stress**

Introduction

Vision is an important sense that triggers particular behaviors in most animals. In nature, polarized light is generated by atmospheric scattering of unpolarized sunlight and by sunlight reflecting off surfaces like water, leaves, and bodies (Wehner, 2001). Invertebrates, including insects (Horváth and Varjú. (1997); Dacke et al., 2002) and spiders (Dacke et al., 2001), can usually perceive linearly polarized light. However, only a small number of vertebrates are known to use polarization for object-based vision, which exclusively occurs in fish (Kamermans and Hawryshyn, 2011). Polarized light is known to mediate diverse behaviors in insects, including navigation (Labhart and Meyer, 2002), host recognition (Blake et al., 2019), and water avoidance (Shashar et al., 2005). Circularly polarized (CP) light is another form of polarized light that is less common in nature (Heinloth et al., 2018).

Multiple studies have revealed that CP light can be perceived by mantis shrimp and that it affects their mating behavior and defensive behaviors (Chiou et al., 2008; Baar et al., 2014; Gagnon et al., 2015; Templin et al., 2017).

Michelson (1911) initially reported on reflection of polarized light in some scarab beetles (Michelson, 1911), with subsequent studies revealing that their exocuticle selectively reflects left circularly polarized (LCP) light (Finlayson et al., 2017; Bagge et al., 2020). The scarab beetle, *A. corpulenta* Motschulsky, is a destructive agricultural and horticultural pest in China. Its body has a metallic green color and LCP light reflects off its exocuticle. Our previous research showed that the mating behavior of *Anomala corpulenta* is probably regulated by a visual signal (Miao et al., 2015). However, the way in which LCP light affects the mating behavior of *A. corpulenta* has not been thoroughly investigated. In this study, we examine the effects of LCP light on *A. corpulenta* mating behavior. Furthermore, the effects of LCP light on their gene expression are revealed using RNA-seq, and the potential molecular responses to LCP light-induced stress are discussed.

Materials and methods

Insect collection

The *A. corpulenta* adults used in this study were trapped using black lamps in peanut fields in Yuanyang County, Henan Province (35.01 N, 113.69 E), in June 2022. The collected individuals were fed fresh peanut leaves and kept under room conditions of 25 °C with a 16:8 h light:dark regime.

Mating experiments

To uncover the effects of LCP light on the mating behavior of *A. corpulenta*, we disrupted these effects by painting the *A. corpulenta* elytra with green nail enamel, which is similar to their body color. Three experimental groups were established: 1) a group in which only the males were painted, 2) a group in which only the females were painted, and 3) a group in which both males and females were painted. The behavior of these groups was compared in order to reveal the beetles' specific sexual responses to LCP light during mating. A fourth group, consisting of normal (unpainted) *A. corpulenta*, was used as a control. The mating experiments were conducted as previously described (Miao et al., 2015), with a few modifications. First, 10 male and 10 female *A. corpulenta* beetles of one of the experimental groups were placed into a plastic glass pot and kept under natural conditions of <0.3 lx (night) and ~700 lx (day) for 24 h. Five replicates were used for each condition. The number of mating pairs of *A. corpulenta* beetles was counted every half hour. Mating males and females were gently separated after being counted.

Transcriptome sequencing of *Anomala corpulenta*

The effect of LCP light on gene expression in *A. corpulenta* was evaluated using transcriptome sequencing. First, adult beetles were placed into transparent plastic pots and initially kept under a daylight lamp for 3 h, then transferred into a dark room for 3 h. Thereafter, they were divided into an LCP light treatment group (exposed to LCP light at 600 lx for 3 h) and a control group (exposed to darkness (0 lx) for 3 h). A 50 W bromine tungsten lamp (OSRAM, Germany) was used as a light source with LCP light filtered using LCP film (Nitto Denko Corporation, Osaka, Japan). Five *A. corpulenta* pairs (i.e., five males and five females) were subjected to each treatment, and each condition was performed in triplicate. The heads of the individuals were then dissected and subjected to transcriptome sequencing.

Total RNA was extracted using TRIzol reagent (Invitrogen, CA, United States) following the manufacturer's recommendations. The RNA integrity number (RIN) was obtained using the RNA 1000 Nano LabChip Kit on a Bioanalyzer 2100 (Agilent, CA, United States) to evaluate the quantity and purity of total RNA. Samples with RIN <7.0 were excluded from subsequent analyses. mRNA was enriched from ~5 μg total RNA using poly-T oligo-attached magnetic beads with two rounds of purification. Thereafter, the purified mRNA was fragmented using divalent cations under high temperature. Subsequently, the cleaved RNA fragments were reverse-transcribed to create a final cDNA library as per the transcriptome sample preparation kit protocol (Illumina, San Diego, United States). Paired-end sequencing was performed on an Illumina NovaSeq™ 6000 platform. In this study, sequencing libraries were constructed and transcriptome sequencing was conducted by Lc-Bio Technologies Co., Ltd. (Hangzhou, China).

Bioinformatics analyses

The adaptors of the row data were removed using Cutadapt (Version 1.9) (Martin, 2011), and low-quality bases were further trimmed using fqtrim (Version 0.94) (https://ccb.jhu.edu/software/fqtrim/). FastQC (Version 0.10.1) (http://www.bioinformatics.babraham.ac.uk/projects/fastqc/) was used to evaluate the quality of the cleaned data, with low-quality data eliminated for subsequent analyses. *De novo* transcriptome assembly was performed using Trinity (Version 2.4.0) (Grabherr et al., 2011). The longest assembled transcript of a given gene was defined as a unigene. The functions of unigenes were predicted using DIAMOND (Version 0.7.12) (Buchfink et al., 2015) against the non-redundant (Nr) protein sequence database and the Kyoto Encyclopedia of Genes and Genomes (KEGG). An e-value threshold of 1×10^{-5} was used in the searches. GO (Gene Ontology) annotations were mapped to the GO terms in the Gene Ontology database (http://www.geneontology.org/) using Blast2GO (Version 2.3.5) (Conesa et al., 2005). Transcripts per million (TPM) of unigenes were calculated using Salmon (Version 0.8.2) (Patro et al., 2017) to evaluate their expression levels. The edgeR R package (Robinson et al., 2010) was used to help filter differentially expressed genes (DEGs) with a threshold of absolute log2 (FC, fold change) ≥1 and statistical significance (p-value) < 0.05. Principal component analysis (PCA) of the samples was carried out using the gene expression matrix and subsequently visualized using the stats R package.

GO and KEGG enrichment was performed for the DEGs and visualized using the clusterProfiler R package (Yu et al., 2012). The gene–concept network highlighted the interactions between DEGs,

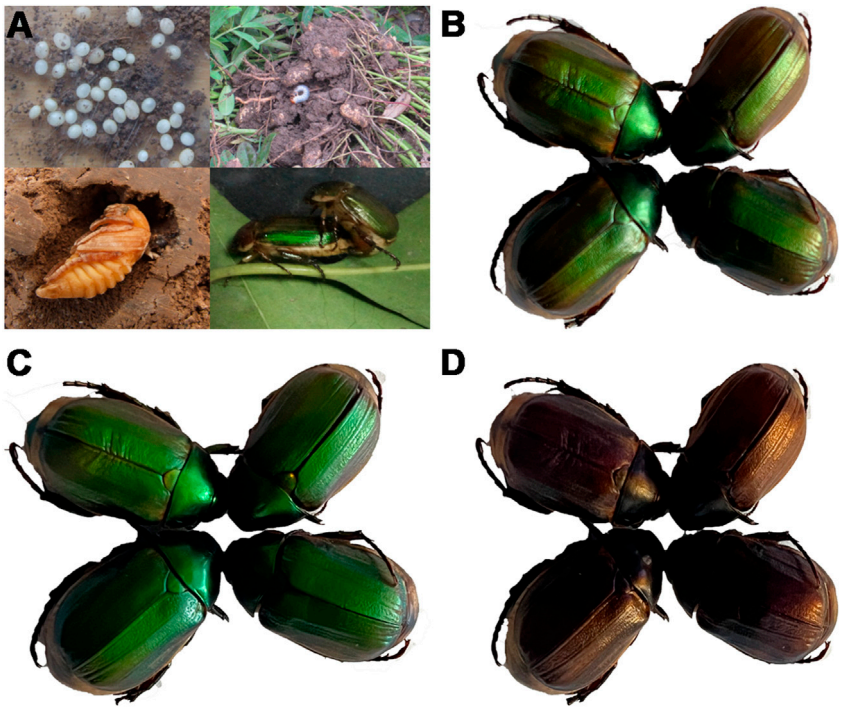

FIGURE 1
Developmental stages of *Anomala corpulenta* and photographs of the beetles under different polarizing films. **(A)** Developmental stages of *A. corpulenta*. **(B)** Photograph showing appearance without polarizing film. **(C)** Photograph showing appearance with left circularly polarizing film. **(D)** Photograph showing appearance with right circularly polarizing film.

with significantly enriched KEGG pathways further constructed using clusterProfiler. The expression patterns of the DEGs among the individuals were visualized using heat maps constructed using TBtools (Chen et al., 2020). The DEGs were further verified by real-time quantitative reverse transcription PCR (RT-qPCR). First, cDNA was synthesized using the First-Strand cDNA Synthesis Kit (Toyobo, Shanghai); RT-qPCR was then performed using the SYBR Green Real-Time PCR Master Mix Kit (Toyobo) on a Mastercycler® ep realplex system (Eppendorf). The relative expression of DEGs was normalized to the *A. corpulenta* β-actin gene as previously described (Livak and Schmittgen, 2001; Bustin et al., 2009). All RT-qPCR assays were conducted with three biological replicates and further analyzed via one-way analysis of variance (ANOVA). The primers used in this study were listed in Supplementary Table S1.

Results

Change in the body color of *Anomala corpulenta* under circularly polarized light

In Henan Province, *A. corpulenta* is one of the major pests of peanut fields (Figure 1A). Under normal light conditions, their body color is green with a little brown (Figure 1B). However, this color is clearly altered by circularly polarized light. In particular, the *A. corpulenta* cuticle selectively reflects LCP light (Figure 1C) rather than right circularly polarized (RCP) light (Figure 1D).

Effects of LCP light on the mating behavior of *Anomala corpulenta*

In this study, to eliminate the effect of body color and evaluate the potential effects of LCP light on the mating behavior of *A. corpulenta*, we colored the elytra of some individuals with green nail enamel (Figure 2A). The results showed that the reflection of circularly polarized light by *A. corpulenta* was greatly disrupted by painting of the elytron (Figures 2B, C). Furthermore, the number of pairs of mating beetles differed significantly between the groups with and without elytron-painting treatment (ANOVA: $F = 4.875$, $p = 0.035$) (Figure 2D). Multiple comparisons indicated that, relative to the control group, the number of pairs of mating beetles was significantly reduced in the group with painted females (LSD test: $p = 0.012$) but there was no significant difference in the case of the group with painted males (LSD test: $p = 0.739$).

Analyses of the *Anomala corpulenta* transcriptome

In this study, we identified 32,619 unigenes with 37.13% GC content assembled in the *A. corpulenta* transcriptome. The N50 of these unigenes was 1,578 bp. We predicted the functions of 15,786 and 10,619 unigenes against the Nr and KEGG databases, respectively. Furthermore, we annotated 11,133 unigenes in the GO predictions. The PCA showed that the LCP light treatment and control groups were well distinguished (Figure 3A). Furthermore,

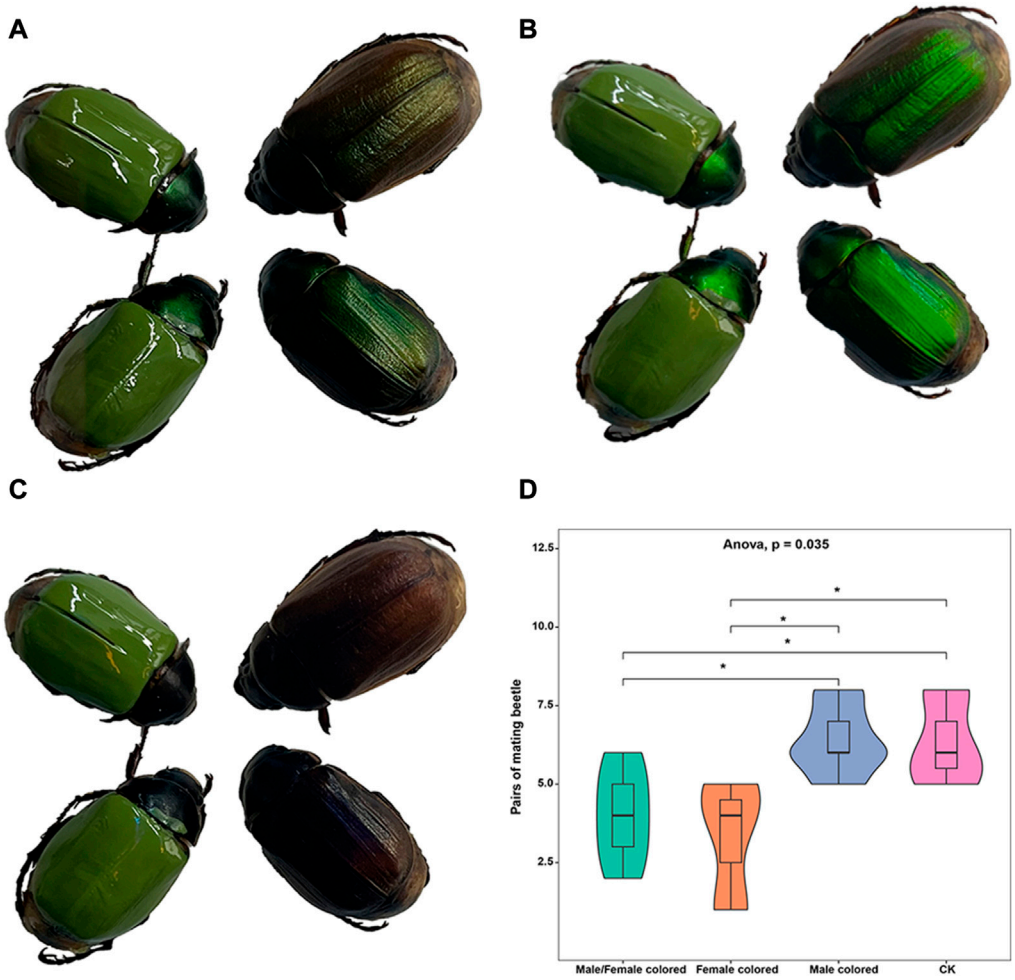

FIGURE 2
Photographs of painted beetles under different polarizing films and results of mating experiment. **(A)** Photograph showing appearance without polarizing film. **(B)** Photograph showing appearance with left circularly polarizing film. **(C)** Photograph showing appearance with right circularly polarizing film. **(D)** Results of the mating experiment with painted and unpainted members of *A. corpulenta*.

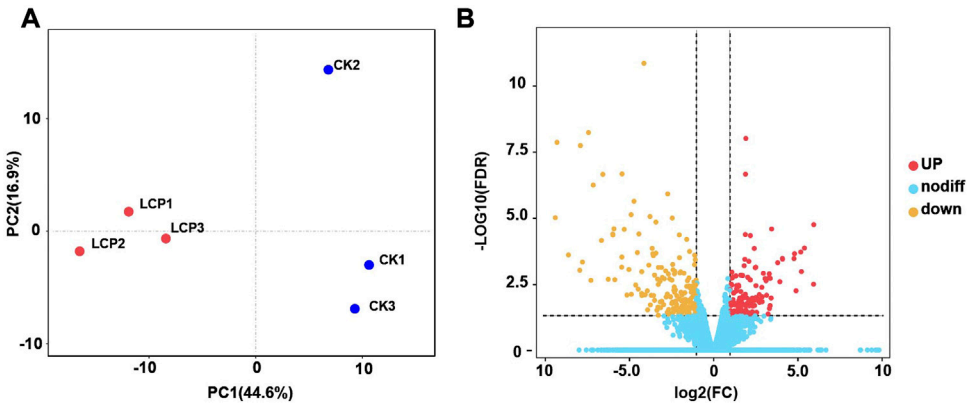

FIGURE 3
Principal component analysis (PCA) and gene expression of *Anomala corpulenta* subjected to left circularly polarized light. **(A)** PCA using the gene expression matrix. **(B)** Volcano plot of gene expression.

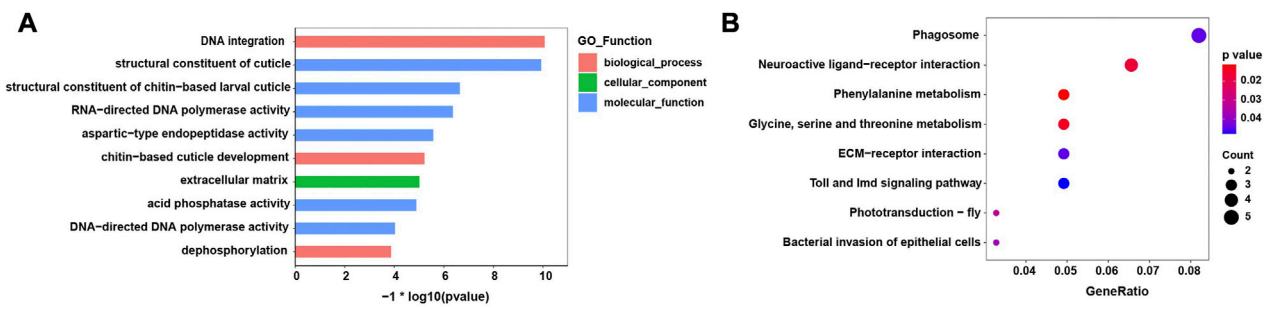

FIGURE 4
Enriched GO terms and KEGG pathways of the differentially expressed genes (DEGs). **(A)** Top ten GO significantly enriched terms (FDR< 0.05) **(B)** KEGG significantly enriched pathways (FDR< 0.05).

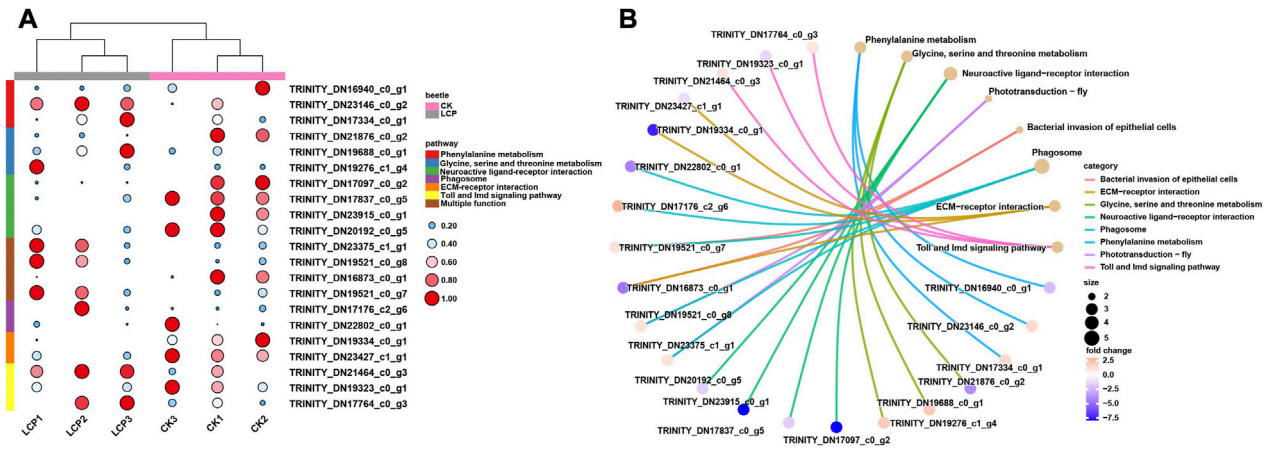

FIGURE 5
Expression patterns and gene−concept network of DEGs. **(A)** Expression patterns of DEGs that related to the significantly enriched pathways. Log2 TPM values are further scaled by row using the zero-to-one method and then indicated by the color and area of the circles. **(B)** Gene−concept network of DEGs among significantly enriched pathways.

315 unigenes were filtered as DEGs, with 176 and 139 being significantly downregulated and upregulated, respectively, at the filtered thresholds (Figure 3B). We also observed similar expression patterns of the representative DEGs *via* RT-qPCR (Supplementary Figure S1), which further confirmed the RNA-seq results.

Predictions of the functions of DEGs

The top 10 enriched GO terms and KEGG pathways are shown in Figure 4. In the GO analysis, most enriched GO terms were clustered under molecular functions. Moreover, the enriched GO terms mainly related to the process of integration and synthesis of DNA, while terms relating to contributions to the structural integrity of the insect cuticle also appeared (Figure 4A). In the KEGG analysis, the significantly enriched pathways were those falling under amino acid metabolism and insect phototransduction, such as glycine, serine, and threonine metabolism and phototransduction−fly (Figure 4B).

Heat maps were also used to visualize differences between the treatment groups in the expression patterns of DEGs in the significantly enriched pathways (Figure 5A). The results showed that the patterns of DEG expression generally clustered by treatment group, and expression patterns varied between groups within the same enriched pathway. In particular, DEGs enriched in the neuroactive ligand−receptor interaction were significantly downregulated in the LCP light group, whereas those enriched in phototransduction were significantly upregulated.

Finally, the interactions between DEGs and significantly enriched pathways are presented in the gene-concept network (Figure 5B). The results show that four DEGs were enriched in multiple pathways. Within these pathways, two DEGs were shared between the phototransduction−fly and phagosome pathways, one DEG was shared between the bacterial invasion of epithelial cells and ECM−receptor interaction pathways, and one DEG was shared between the bacterial invasion of epithelial cells and phagosome pathways.

Discussion

In nature, polarized light is generated by atmospheric scattering of unpolarized sunlight and its reflection off surfaces like water, leaves, and bodies (Wehner, 2001). Polarized light of the form commonly referred to as linearly polarized light plays a role in insect navigation (Wehner, 1976; Krapp, 2007), assists in the predation behaviors of cuttlefish and horseflies (Shashar et al., 1998; Shashar et al., 2000; Meglic et al., 2019), and affects recognition of host and oviposition sites in dragonflies and butterflies, respectively (Wildermuth, 1998; Blake et al., 2019). Circularly polarized light is another form of polarized light that is less common in nature (Heinloth et al., 2018). Previous studies have indicated that circularly polarized light is a covert signal in the intraspecific communication of stomatopod crustaceans (Templin et al., 2017), and that it can alter their mating selections (Chiou et al., 2011; Baar et al., 2014).

Left circularly polarized (LCP) light is selectively reflected by the exocuticle of scarab beetles (Coleoptera: Scarabaeidae) (Finlayson et al., 2017; Bagge et al., 2020). However, its role in beetles has not been thoroughly investigated. Although our previous research showed that the mating behavior of *A. corpulenta* is affected by visual signals, the roles of body color and LCP light in the mate choices of *A. corpulenta* are not well understood (Miao et al., 2015). To investigate how LCP light affects the mating behavior of *A. corpulenta*, we disrupted the reflection of LCP light by members of this species, while retaining their general green body color, by painting their elytra with green nail enamel. The results indicated that, compared with controls, the number of mating pairs of *A. corpulenta* was significantly reduced when LCP light reflection was disrupted in female *A. corpulenta*, but not in male *A. corpulenta*. In beetles, male insects do most of the searching for mates (Muniz et al., 2018). Thus, this finding implies that LCP light reflected by the exocuticle of females of *A. corpulenta* is probably perceived by males of the species, which improves their ability to find mates, as previously reported in *Heliconius* butterflies (Sweeney et al., 2003). However, the circularly polarized light-detecting capability of scarab beetles is debatable. While the jewel scarab, *Chrysina gloriosa*, can distinguish circularly polarized light, another jewel scarab, *C. woodi*, exhibits no phototactic discrimination between linear and circularly polarized light (Brady and Cummings, 2010). Furthermore, in another study, four scarab beetles showed no behavioral response under circularly polarized light treatments (Blaho et al., 2012). Hence, despite the demonstration in this study of potential interactions between LCP light and mating behavior in *A. corpulenta*, firm conclusions cannot be drawn on their LCP light-perceiving capacity. Therefore, further behavioral experiments with more samples are required.

Previous studies indicate that light stress strongly alters the gene expression patterns of insects (Yang et al., 2021; Wang et al., 2023). In this study, we investigated the effect of LCP light on the gene expression patterns of *A. corpulenta*. The results showed that the insect phototransduction pathway was enriched. Phototransduction is a well-known signaling cascade that converts light energy into an electrical signal. In insects, the expression of phototransduction-related genes is significantly modified by exposure to different light environments (Macias-Munoz et al., 2019) and even viral infections (Bhattarai et al., 2018b). Another environmental information signaling pathway, including neuroactive ligand–receptor interaction, was also enriched. Although the neuroactive ligand–receptor interaction pathway is known for responding to diverse environmental stresses (Cao et al., 2013; Yadav et al., 2017; Bhattarai et al., 2018a), it has also been found to be vital in adaptations in invasive beetles (Liu et al., 2021). Furthermore, some amino acid metabolic pathways that regulate insect reproduction were also found to be significantly enriched. Recent studies indicate that phenylalanine metabolism regulates reproduction and mating behavior in flies and mosquitos (Proline et al., 2014; Arya et al., 2021), while glycine, serine, and threonine metabolism are involved in sex pheromone biosynthesis in the oriental fruit fly (Gui et al., 2023). Overall, when *A. corpulenta* beetles were subjected to LCP light stress, not only was the expression of insect environmental signaling pathway-related genes affected, but that of amino acid metabolism pathways related to insect reproduction was also affected. This indicates that LCP light probably regulates reproduction in *A. corpulenta*.

In conclusion, we investigated the effect of LCP light on the mating behavior of *A. corpulenta* and also examined how exposure to this affects gene expression in this species. The results indicated that LCP light probably affects the mate-searching capabilities of male *A. corpulenta* beetles, with multiple insect environmental signaling and reproduction-related pathways being significantly enriched when they are subjected to LCP light-induced stress.

Data availability statement

The datasets presented in this study can be found in online repositories. The names of the repository/repositories and accession number(s) can be found at: NCBI, accession ID: PRJNA907534.

Author contributions

TL, YJ, YW, and CL conceived the study. TL, YJ, XY, and HL drafted the manuscript. ZG, YQ, JZ, and RJL collected and identified the species of the beetles. TL prepared the figures. TL, YJ, GW, YW, and CL revised the manuscript. TL, YJ, YW, and CL designed the entire study and revised the manuscript. All authors read, revised, and approved the manuscript.

Funding

This work was supported by the National Natural Science Foundation of China (Grant No. 32001902), China Agriculture Research System of MOF and MARA (CARS-03), and Henan Scientific and Technical Attack project (12102110460).

Conflict of interest

The authors declare that the research was conducted in the absence of any commercial or financial relationships that could be construed as a potential conflict of interest.

Publisher's note

Supplementary material

The Supplementary Material for this article can be found online at: https://www.frontiersin.org/articles/10.3389/fphys.2023.1172542/full#supplementary-material

SUPPLEMENTARY FIGURE S1
Verification of DEG expression via RT-qPCR.

References

Arya, H., Toltesi, R., Eng, M., Garg, D., Merritt, T. J. S., and Rajpurohit, S. (2021). No water, No mating: Connecting dots from behaviour to pathways. *PLoS One* 16 (6), e0252920. doi:10.1371/journal.pone.0252920

Baar, Y., Rosen, J., and Shashar, N. (2014). Circular polarization of transmitted light by sapphirinidae copepods. *PLoS One* 9 (1), e86131. doi:10.1371/journal.pone.0086131

Bagge, L. E., Kenton, A. C., Lyons, B. A., Wehling, M. F., and Goldstein, D. H. (2020). Mueller matrix characterizations of circularly polarized reflections from golden scarab beetles. *Appl. Opt.* 59 (21), F85–F93. doi:10.1364/AO.398832

Bhattarai, U. R., Katuwal Bhattarai, M., Li, F., and Wang, D. (2018a). Insights into the temporal gene expression pattern in *Lymantria dispar* larvae during the baculovirus induced hyperactive stage. *Virol. Sin.* 33 (4), 345–358. doi:10.1007/s12250-018-0046-x

Bhattarai, U. R., Li, F., Katuwal Bhattarai, M., Masoudi, A., and Wang, D. (2018b). Phototransduction and circadian entrainment are the Key pathways in the signaling mechanism for the baculovirus induced tree-top disease in the Lepidopteran larvae. *Sci. Rep.* 8 (1), 17528. doi:10.1038/s41598-018-35885-4

Blaho, M., Egri, A., Hegedus, R., Josvai, J., Toth, M., Kertesz, K., et al. (2012). No evidence for behavioral responses to circularly polarized light in four scarab beetle species with circularly polarizing exocuticle. *Physiol. Behav.* 105 (4), 1067–1075. doi:10.1016/j.physbeh.2011.11.020

Blake, A. J., Go, M. C., Hahn, G. S., Grey, H., Couture, S., and Gries, G. (2019). Polarization of foliar reflectance: Novel host plant cue for insect herbivores. *Proc. Biol. Sci.* 286 (1915), 20192198. doi:10.1098/rspb.2019.2198

Brady, P., and Cummings, M. (2010). Differential response to circularly polarized light by the jewel scarab beetle *Chrysina gloriosa*. *Am. Nat.* 175 (5), 614–620. doi:10.1086/651593

Buchfink, B., Xie, C., and Huson, D. H. (2015). Fast and sensitive protein alignment using diamond. *Nat. Methods* 12 (1), 59–60. doi:10.1038/nmeth.3176

Bustin, S. A., Benes, V., Garson, J. A., Hellemans, J., Huggett, J., Kubista, M., et al. (2009). The miqe guidelines: Minimum information for publication of quantitative real-time pcr experiments. *Clin. Chem.* 55 (4), 611–622. doi:10.1373/clinchem.2008.112797

Cao, C., Wang, Z., Niu, C., Desneux, N., and Gao, X. (2013). Transcriptome profiling of *Chironomus kiinensis* under phenol stress using solexa sequencing technology. *PLoS One* 8 (3), e58914. doi:10.1371/journal.pone.0058914

Chen, C., Chen, H., Zhang, Y., Thomas, H. R., Frank, M. H., He, Y., et al. (2020). Tbtools: An integrative toolkit developed for interactive analyses of big biological data. *Mol. Plant.* 13 (8), 1194–1202. doi:10.1016/j.molp.2020.06.009

Chiou, T. H., Kleinlogel, S., Cronin, T., Caldwell, R., Loeffler, B., Siddiqi, A., et al. (2008). Circular polarization vision in a stomatopod Crustacean. *Curr. Biol.* 18 (6), 429–434. doi:10.1016/j.cub.2008.02.066

Chiou, T. H., Marshall, N. J., Caldwell, R. L., and Cronin, T. W. (2011). Changes in light-reflecting properties of signalling appendages alter mate choice behaviour in a stomatopod crustacean*Haptosquilla trispinosa*. *Haptosquilla Trispinosa*. *Mar. Freshw. Behav. Physiol.* 44, 1–11. doi:10.1080/10236244.2010.546064

Conesa, A., Gotz, S., Garcia-Gomez, J. M., Terol, J., Talon, M., and Robles, M. (2005). Blast2go: A universal tool for annotation, visualization and analysis in functional genomics research. *Bioinformatics* 21 (18), 3674–3676. doi:10.1093/bioinformatics/bti610

Dacke, M., Doan, T. A., and O'Carroll, D. C. (2001). Polarized light detection in spiders. *J. Exp. Biol.* 204 (14), 2481–2490. doi:10.1242/jeb.204.14.2481

Dacke, M., Nordstrom, P., Scholtz, C. H., and Warrant, E. J. (2002). A specialized dorsal rim area for polarized light detection in the compound eye of the scarab beetle *pachysoma striatum*. *J. Comp. Physiol. A Neuroethol. Sens. Neural. Behav. Physiol.* 188 (3), 211–216. doi:10.1007/s00359-002-0295-9

Finlayson, E. D., McDonald, L. T., and Vukusic, P. (2017). Optically ambidextrous circularly polarized reflection from the chiral cuticle of the scarab beetle *Chrysina resplendens*. *J. R. Soc. Interface.* 14 (131), 20170129. doi:10.1098/rsif.2017.0129

Gagnon, Y. L., Templin, R. M., How, M. J., and Justin, M. N. (2015). Circularly polarized light as a communication signal in Mantis shrimps. *Curr. Biol.* 25, 3074–3078. doi:10.1016/j.cub.2015.10.047

Grabherr, M. G., Haas, B. J., Yassour, M., Levin, J. Z., Thompson, D. A., Amit, I., et al. (2011). Full-length transcriptome assembly from rna-seq data without a reference genome. *Nat. Biotechnol.* 29 (7), 644–652. doi:10.1038/nbt.1883

Gui, S., Yuval, B., Engl, T., Lu, Y., and Cheng, D. (2023). Protein feeding mediates sex pheromone biosynthesis in an insect. *Elife* 12, e83469. doi:10.7554/eLife.83469

Heinloth, T., Uhlhorn, J., and Wernet, M. F. (2018). Insect responses to linearly polarized reflections: Orphan behaviors without neural circuits. *Front. Cell Neurosci.* 12, 50. doi:10.3389/fncel.2018.00050

Horváth, G., and Varjú, D. (1997). Polarization pattern of freshwater habitats recorded by video polarimetry in red, green and blue spectral ranges and its relevance for water detection by aquatic insects. *J. Exp. Biol.* 200 (7), 1155–1163. doi:10.1242/jeb.200.7.1155

Kamermans, M., and Hawryshyn, C. (2011). Teleost polarization vision: How it might work and what it might Be good for. *Philos. Trans. R. Soc. Lond. B. Biol. Sci.* 366 (1565), 742–756. doi:10.1098/rstb.2010.0211

Krapp, H. G. (2007). Polarization vision: How insects find their way by watching the sky. Curr. Biol. *doi J.cub.*, 17, R557, , R560. doi:10.1016/j.cub.2007.05.022

Labhart, T., and Meyer, E. P. (2002). Neural mechanisms in insect navigation: Polarization compass and odometer. *Curr. Opin. Neurobiol.* 12 (6), 707–714. doi:10.1016/s0959-4388(02)00384-7

Liu, Y., Henkel, J., Beaurepaire, A., Evans, J. D., Neumann, P., and Huang, Q. (2021). Comparative genomics suggests local adaptations in the invasive small hive beetle. *Ecol. Evol.* 11 (22), 15780–15791. doi:10.1002/ece3.8242

Livak, K. J., and Schmittgen, T. D. (2001). Analysis of relative gene expression data using real-time quantitative pcr and the 2(-delta delta C(T)) method. *Methods* 25 (4), 402–408. doi:10.1006/meth.2001.1262

Macias-Munoz, A., Rangel Olguin, A. G., and Briscoe, A. D. (2019). Evolution of phototransduction genes in Lepidoptera. *Genome Biol. Evol.* 11 (8), 2107–2124. doi:10.1093/gbe/evz150

Martin, M. (2011). Cutadapt removes adapter sequences from high-throughput sequencing reads. *EMBnet J.* 17 (1), 10–12. doi:10.14806/ej.17.1.200

Meglic, A., Ilic, M., Pirih, P., Skorjanc, A., Wehling, M. F., Kreft, M., et al. (2019). Horsefly object-directed polarotaxis is mediated by a stochastically distributed ommatidial subtype in the ventral retina. *Proc. Natl. Acad. Sci. U. S. A.* 116 (43), 21843–21853. doi:10.1073/pnas.1910807116

Miao, J., Wu, Y.-Q., Li, K.-B., Jiang, Y.-L., Gong, Z.-j., Duan, Y., et al. (2015). Evidence for visually mediated copulation frequency in the scarab beetle *Anomala corpulenta*. *J. Insect Behav.* 28 (2), 175–182. doi:10.1007/s10905-015-9487-3

Michelson, A. A. (1911). LXI. *On metallic colouring in birds and insects*. *Philos. Mag.* 21, 554–567. doi:10.1080/14786440408637061

Muniz, D. G., Baena, M. L., Macias-Ordonez, R., and Machado, G. (2018). Males, but not females, perform strategic mate searching movements between host plants in a leaf beetle with scramble competition polygyny. *Ecol. Evol.* 8 (11), 5828–5836. doi:10.1002/ece3.4121

Patro, R., Duggal, G., Love, M. I., Irizarry, R. A., and Kingsford, C. (2017). Salmon provides fast and bias-aware quantification of transcript expression. *Nat. Methods* 14 (4), 417–419. doi:10.1038/nmeth.4197

Proline, l. a. p. m. i. a. h. d., S., Behrends, V., Bundy, J. G., Crisanti, A., and Nolan, T. (2014). Phenylalanine metabolism regulates reproduction and parasite melanization in the malaria mosquito. *PLoS One* 9 (1), e84865. doi:10.1371/journal.pone.0084865

Robinson, M. D., McCarthy, D. J., and Smyth, G. K. (2010). Edger: A bioconductor package for differential expression analysis of digital gene expression data. *Bioinformatics* 26 (1), 139–140. doi:10.1093/bioinformatics/btp616

Shashar, N., Boal, J. G., and Hanlon, R. T. (2000). Cuttlefish use polarization sensitivity in predation on silvery fish. *Vis. Res.* 40, 71–75. doi:10.1016/S0042-6989(99)00158-3

Shashar, N., Hanlon, R. T., and Petz, A. (1998). Polarization vision helps detect transparent prey. *Nature* 393, 222–223. doi:10.1038/30380

Shashar, N., Sabbah, S., and Aharoni, N. (2005). Migrating locusts can detect polarized reflections to avoid flying over the sea. *Biol. Lett.* 1 (4), 472–475. doi:10.1098/rsbl.2005.0334

Sweeney, A., Jiggins, C., and Johnsen, S. (2003). Insect communication: Polarized light as a butterfly mating signal. *Nature* 423, 31–32. doi:10.1038/423031a

Templin, R. M., How, M. J., Roberts, N. W., Chiou, T. H., and Marshall, J. (2017). Circularly polarized light detection in stomatopod Crustaceans: A comparison of photoreceptors and possible function in six species. *J. Exp. Biol.* 220 (18), 3222–3230. doi:10.1242/jeb.162941

Wang, F. F., Wang, M. H., Zhang, M. K., Qin, P., Cuthbertson, A. G. S., Lei, C. L., et al. (2023). Blue light stimulates light stress and phototactic behavior when received in the brain of *diaphorina citri*. *Ecotoxicol. Environ. Saf.* 251, 114519. doi:10.1016/j.ecoenv.2023.114519

Wehner, R. (2001). Polarization vision--a uniform sensory capacity? *J. Exp. Biol.* 204 (14), 2589–2596. doi:10.1242/jeb.204.14.2589

Wehner, R. (1976). Polarized-light navigation by insects. *Sci. Am.* 235, 106– 115. doi:10.1038/scientificamerican0776-106

Wildermuth, H. (1998). Dragonflies recognize the water of rendezvous and oviposition sites by horizontally polarized light: A behavioural field test. *Naturwissenschaften* 85, 297–302. doi:10.1007/s001140050504

Yadav, S., Daugherty, S., Shetty, A. C., and Eleftherianos, I. (2017). Rnaseq analysis of the *Drosophila* response to the entomopathogenic *nematode Steinernema*. *G3 (Bethesda)* 7 (6), 1955–1967. doi:10.1534/g3.117.041004

Yang, C. L., Meng, J. Y., Yao, M. S., and Zhang, C. Y. (2021). Transcriptome analysis of *Myzus persicae* to uv-B stress. *J. Insect Sci.* 21 (3), 7. doi:10.1093/jisesa/ieab033

Yu, G., Wang, L. G., Han, Y., and He, Q. Y. (2012). Clusterprofiler: An R package for comparing biological themes among gene clusters. *OMICS* 16 (5), 284–287. doi:10.1089/omi.2011.0118

frontiers | Frontiers in Physiology

TYPE Original Research
PUBLISHED 04 April 2023
DOI 10.3389/fphys.2023.1183610

OPEN ACCESS

EDITED BY
Fengqi Li,
Guizhou University, China

REVIEWED BY
Wen Xie,
Insititute of Vegetables and Flowers, Chinese Academy of Agricultural Sciences, China
Man Zhao,
Henan Agricultural University, China

*CORRESPONDENCE
Xiangrui Li,
xrli@ippcaas.cn

SPECIALTY SECTION
This article was submitted to Invertebrate Physiology, a section of the journal Frontiers in Physiology

RECEIVED 10 March 2023
ACCEPTED 21 March 2023
PUBLISHED 04 April 2023

CITATION
Zhang F, Chen Y, Zhao X, Guo S, Hong F, Zhi Y, Zhang L, Zhou Z, Zhang Y, Zhou X and Li X (2023), Antennal transcriptomic analysis of carboxylesterases and glutathione S-transferases associated with odorant degradation in the tea gray geometrid, *Ectropis grisescens* (Lepidoptera, Geometridae). *Front. Physiol.* 14:1183610. doi: 10.3389/fphys.2023.1183610

Antennal transcriptomic analysis of carboxylesterases and glutathione S-transferases associated with odorant degradation in the tea gray geometrid, *Ectropis grisescens* (Lepidoptera, Geometridae)

Fangmei Zhang[1,2], Yijun Chen[1,3], Xiaocen Zhao[1], Shibao Guo[1], Feng Hong[1], Yanan Zhi[1], Li Zhang[1], Zhou Zhou[1], Yunhui Zhang[2], Xuguo Zhou[4] and Xiangrui Li[2]*

[1]College of Agriculture, Xinyang Agriculture and Forestry University, Xinyang, China, [2]State Key Laboratory for Biology of Plant Diseases and Insect Pests, Institute of Plant Protection, Chinese Academy of Agricultural Sciences, Beijing, China, [3]College of Agriculture, Xinjiang Agricultural University, Urumqi, China, [4]Department of Entomology, University of Kentucky, Lexington, KY, United states

Introduction: Carboxylesterases (CXEs) and glutathione S-transferases (GSTs) can terminate olfactory signals during chemosensation by rapid degradation of odorants in the vicinity of receptors. The tea grey geometrid, *Ectropis grisescens* (Lepidoptera, Geometridae), one of the most devastating insect herbivores of tea plants in China, relies heavily on plant volatiles to locate the host plants as well as the oviposition sites. However, CXEs and GSTs involved in signal termination and odorant clearance in *E. grisescens* remains unknown.

Methods: In this study, identification and spatial expression profiles of CXEs and GSTs in this major tea pest were investigated by transcriptomics and qRT-PCR, respectively.

Results: As a result, we identified 28 CXEs and 16 GSTs from female and male antennal transcriptomes. Phylogenetic analyses clustered these candidates into several clades, among which antennal CXEs, mitochondrial and cytosolic CXEs, and delta group GSTs contained genes commonly associated with odorants degradation. Spatial expression profiles showed that most CXEs (26) were expressed in antennae. In comparison, putative GSTs exhibited a diverse expression pattern across different tissues, with one GST expressed specifically in the male antennae.

Disscussion: These combined results suggest that 12 CXEs (EgriCXE1, 2, 4, 6, 8, 18, 20-22, 24, 26, and 29) and 5 GSTs (EgriGST1 and EgriGST delta group) provide a major source of candidate genes for odorants degradation in *E. grisescens*.

KEYWORDS

***Ectropis grisescens*, antennal transcriptome, odorant-degrading enzyme, carboxylesterases, glutathione S-transferases**

1 Introduction

Insects have a highly specific and sensitive chemosensory system, which is extremely critical for sensing various chemical signals and regulating a series of behaviors (Elgar et al., 2018; Fleischer et al., 2018; Kang et al., 2021). Olfactory perception involves various proteins, including odorant binding proteins (OBPs), chemosensory proteins (CSPs), odorant receptors (ORs), gustatory receptors (GRs), ionotropic receptors (IRs), sensory neuron membrane proteins (SNMPs), and odorant degrading enzymes (ODEs) (Fleischer et al., 2018; Sun et al., 2020; Liu et al., 2021). Briefly, odorant molecules are bound and transported by OBPs onto ORs, and then ORs are activated, leading to signal transduction. Soon after, odor molecules are rapidly degraded by various ODEs to terminate the stimulation, ensuring that insect olfactory sensing systems keep stability and sensitivity for odor identity (Leal, 2013; Suh et al., 2014; Li et al., 2018; He et al., 2019).

ODEs, as multiple enzyme families expressed in the sensillar lymph, include carboxylesterases (CXEs) (Liu et al., 2019; Yi et al., 2021), glutathione S-transferases (GSTs) (Liu et al., 2021; Xia et al., 2022), cytochrome P450 monooxygenases (P450s) (Baldwin et al., 2021; Blomquist et al., 2021), UDP-glucuronosyltransferases (UGTs) (Zhang et al., 2017a), alcohol dehydrogenases (ADs) (Huang et al., 2016), and aldehyde oxidases (AOXs) (Zhang et al., 2017b; Wang et al., 2017). The first identified ODE, ApolPDE, a kind of CXE, could effectively degrade sex pheromone E6Z11-160Ac in *Antheraea polyphemus* (Vogt and Riddiford, 1981). Antennal-specific GSTs could quickly remove or degrade the odorants from ORs to maintain chemoreceptor sensitivity (Younus et al., 2014; Durand et al., 2018). The antennal-enriched P450s could degrade plant volatiles, insecticides, and pheromones (Cano-Ramirez et al., 2013; Keeling et al., 2013). Antennal ADs have roles in olfaction, which further necessitated investigating its odorant degradation function (Huang et al., 2016). *In vitro* functional studies clarified the odorant inactivation role of antennal AOXs, such as degrading sex pheromones and plant volatile aldehydes in *Amyelois transitella* (Choo et al., 2013).

Of these ODEs, CXEs and GSTs are the most well-studied and involved in degrading pheromone/odorant degradation and harmful volatile xenobiotics to maintain the sensitivity of the olfactory receptor neurons (ORNs). So far, many insect CXEs and GSTs have been identified, including *Chilo suppressalis* (Liu et al., 2015a), *Drosophila melanogaster* (Chertemps et al., 2015), *Ectropis obliqua* (Sun et al., 2017), *Spodoptera littoralis* (Durand et al., 2018), *Spodoptera exigua* (He et al., 2019), *Plodia interpunctella* (Liu et al., 2019; Liu et al., 2021), *Holotrichia parallela* (Yi et al., 2021), and *Sitophilus zeamais* (Xia et al., 2022), and their functions in insect olfactory perception have been characterized.

CXEs as multifunctional enzymes widely exist in insects, microbes, and plants (Guo and Wong, 2020). In insects, most CXEs are involved in detoxification of exogenous chemicals and are responsible for insecticide resistance and metabolic resistance (Mao et al., 2021). CXEs commonly share conserved active residues, such as the pentapeptide "G-X-S-X-G" (X represents any amino acid), oxyanion hole, glutamate (E), and histidine (H) residues (Godoy et al., 2021). Insect antennal CXEs are characterized as ODEs because they occur in the sensilla and can inactivate odor. They could be divided into ten major clades: mitochondrial and cytosolic esterases, dipteran microsomal α-esterases, cuticular and antennal esterases, β-esterases and pheromone esterases, Lepidopteran juvenile hormone esterases (JHEs), non-Lepidopteran JHEs, moth antennal esterases, neuroligins, neuroreceptors, and gliotactins (Durand et al., 2010a; Oakeshott et al., 2015). To date, many insect antennae CXEs have been identified and functionally characterized for their involvement in the degradation of pheromones or/and plant volatiles. For example, in the genus Spodoptera, two CXEs from *S. littoralis* (SlCXE7 and 10) (Durand et al., 2010b; Durand et al., 2011) and three from *S. exigua* (SexiCXE4, 10, and 14) (He et al., 2014a; He et al., 2014b; He et al., 2015) were functionally characterized and degraded both sex pheromones and plant volatiles. A similar phenomenon was also observed in *D. melanogaster* (EST6) (Chertemps et al., 2012; Chertemps et al., 2015) and *Plutella xylostella* (PxylCCE16c) (Wang et al., 2021). Additionally, a previous study indicated that CXEs modulated insect mating and foraging behaviors through inactivation of sex pheromones and host volatiles, which made them a novel target for pest behavioral inhibition. For example, the knockdown of GmolCXE1 and 5 had an impact on the mating behaviors of male moths of *Grapholita molesta* (Wei et al., 2020). Another CXE gene jhedup (duplication of the Juvenile hormone esterase gene) regulated the electrophysiological response and food-seeking ability by hydrolyzing various ester odorants of jhedup mutant *D. melanogaster* (Steiner et al., 2017).

Similar to CXEs, GSTs also are a diverse family of multifunctional enzymes with conserved amino-terminal domain and carboxyl-terminal domain, which have conserved GSH-binding site (G-site) and hydrophobic substrate (H-site), respectively (Ketterman et al., 2011; Durand et al., 2018). Insect GSTs are divided into six subclasses: delta, epsilon, omega, sigma, theta, and zeta, with some GSTs remaining unclassified, of which the delta- and epsilon-class GSTs are insect-specific (Shi et al., 2012; Labade et al., 2018). Insect GSTs are implicated in the detoxification of xenobiotic compounds (Huang et al., 2011). However, GST expression and their activities demonstrated that they cause signal termination within the olfactory organs (Durand et al., 2018; Tang et al., 2019). For example, in *G. molesta*, the biochemical characterization of GmolGSTD1 had confirmed its high degradation preference for pheromone component (Z)-8-dodecenyl alcohol and the host plant volatile butyl hexanoate, which showed that it could inactivate odorant molecules and maintain sensitivity to olfactory communication of *G. molesta* (Li et al., 2018). The antenna-highly expressed CpomGSTd2 in the codling moth, *Cydia pomonella*, interfered with odorant detection by depredating the odorant (Huang et al., 2017). The antenna-specific SzeaGSTd1 in *S. zeamais* also played a crucial role in host location by degrading the host volatile, capryl alcohol (Xia et al., 2022).

Ectropis grisescens (Lepidoptera, Geometridae), one of the most destructive pests in tea plantations, causing serious economic losses, is more widely distributed in major tea plantations in China than its counterparts (*E. obliqua* Prout) (Zhang et al., 2014; Zhang et al., 2016; Li et al., 2019). At present, control of this pest mainly depends on chemical insecticides, leading to environmental pollution and pest resistance (Pan et al., 2021). Moreover, pesticide residues affect

the safety of drinking tea (Cao et al., 2018), so using insecticides is forbidden on organic tea plantations (Ma et al., 2016). Therefore, development of novel, effective, and environmentally friendly strategies to control this pest is urgently needed. ODEs thus play an important role in the termination of odorant signals and allow restoration of sensitivity of the olfactory system (Li et al., 2018; He et al., 2019). *E. grisescens* mainly depends on plant volatiles to search for host plants and locate oviposition sites. Thus, analyses of its mechanism of signal termination and odorant clearance in these important behaviors are necessary. Previous studies considered antennae CXEs or GSTs as potential molecular targets for developing novel pest management strategies based on the manipulation of chemoreception-driven behaviors (Wei et al., 2020; Xia et al., 2022). However, there is no relative report about CXEs or GSTs in *E. grisescens* yet.

In the present study, we sequenced and analyzed the antennal transcriptome of *E. grisescens* using Illumina sequencing. Then, CXE and GST gene families and subfamilies were identified and cloned; sequence architecture and phylogenetic analysis were carried out; and finally, quantitative real-time PCR (qRT-PCR) was used to profile their expression patterns in various tissues from both sexes. In addition, the potential roles of the identified CXEs and GSTs in signal termination of olfaction or other physiological processes were discussed. Our study on antennae-specific CXEs and GSTs is particularly important for understanding the molecular mechanism underlying odorant inactivation and subsequent development of ODE-based pest control strategies in *E. grisescens*.

2 Materials and methods

2.1 Insect rearing and sample collection

Ectropis grisescens larvae were collected from Mount Zhenlei (32°37′N, 114°42′E), Xinyang, Henan, China, and cultivated on fresh tea leaves in the laboratory under the constant conditions of 24°C ± 1°C, 65% relative humidity, and a 16:8 h L: D photoperiod. Emerged adults were fed with 10% honey solution. Antenna, head (without antennae), thorax, abdomen, wing, and leg tissues from 2-day-old unmated male and female insects were dissected, frozen in liquid nitrogen immediately, and stored at −80°C in a refrigerator.

2.2 RNA extraction, cDNA library construction, and sequencing

Total RNA was extracted from male and female antennae (n = 50, three replicates, respectively) using TRIzol reagent (Life Technologies, Carlsbad, CA, United States). The concentration of RNA samples was determined using a NanoDrop ND-1000 spectrophotometer (Thermo Scientific, Wilmington, DE, United States). RNA integrity was assessed using the RNA Nano 6000 Assay Kit of the Bioanalyzer 2100 system (Agilent Technologies, CA, United States). The cDNA libraries were constructed from RNA samples for Illumina sequencing following the Illumina protocol. Sequencing was carried out on the Illumina Novaseq platform (Novogene Co., Ltd., Beijing), and 150-bp paired-end reads were generated.

2.3 Sequence assembly and functional annotation

Raw data (raw reads) of FASTQ format were first modified into clean data (clean reads) through in-house Perl scripts, and clean data (clean reads) were obtained by removing reads containing adapter, reads containing ploy-N, and low-quality reads from raw data. At the same time, Q20, Q30, and GC content of the clean data was calculated. All the downstream analyses were based on the clean data with high quality.

Transcriptome assembly was performed using Trinity with min_kmer_cov set to 2 (Grabherr et al., 2011) by default and all other parameters set to default. Unigene functions were annotated based on NCBI NR, NT, KO, Swiss-Prot, Pfam, GO, and KEGG using Blastx and Blastn searches (E-value < 10^{-5}), retrieving proteins with the highest sequence similarity for each transcript and their protein functional annotations. KEGG Automatic Annotation Server (KASS) was used to search KEGG with E-value = 10^{-10} (Götz et al., 2008), and Blast2GO v2.5 was used for GO annotation with E-value = 10^{-6} (Moriya et al., 2007).

Coding sequences (CDSs) were predicted through aligning transcriptome sequences to the NR and Swiss-Prot databases or using ESTScan 3.0.3 (Iseli et al., 1999). The read count for each gene was obtained by mapping clean reads to the assembled transcriptome using RSEM (Bowtie2 parameters: mismatch 0). The read count was calculated as Fragments Per Kilobase of transcript per Million mapped reads (FPKM) (Mortazavi et al., 2008).

2.4 Identification and bioinformatics analyses of candidate CXEs and GSTs

Candidate EgriCXEs and EgriGSTs were identified from the transcriptome data. Furthermore, all candidate EgriCXEs and EgriGSTs were manually checked by the BLASTx program at the NCBI. The complete coding regions were predicted by ORF finder (https://www.ncbi.nlm.nih.gov/orffinder/). Putative signal peptides were predicted with SignalP 5.0 (http://www.cbs.dtu.dk/services/SignalP). The isoelectric point (pI) and molecular weight (Mw) were computed by the ExPASy tool (https://web.expasy.org/compute_pi/). Multiple sequence alignment of the EgriCXE protein was performed using the Clustal program in the Jalview (v2.11.20) software with default parameters (Waterhouse et al., 2009). Phylogenetic trees were constructed in MEGA 11. 0 software using the neighbor-joining method with 1000-fold bootstrap resampling (Kumar et al., 2018). The phylogenetic tree image was created by EvolView online software (https://www.evolgenius.info/).

2.5 Tissue expression analysis by qRT-PCR

Total RNA was extracted separately from antennae (n = 50), heads (without antennae; n = 10), thoraxes (n = 5), abdomens (n = 5), wings (n = 5), and legs (n = 10) from both sexes using TRIzol reagent (Life Technologies, Carlsbad, CA, United States). cDNA was synthesized by using TransScript One-Step gDNA Removal and

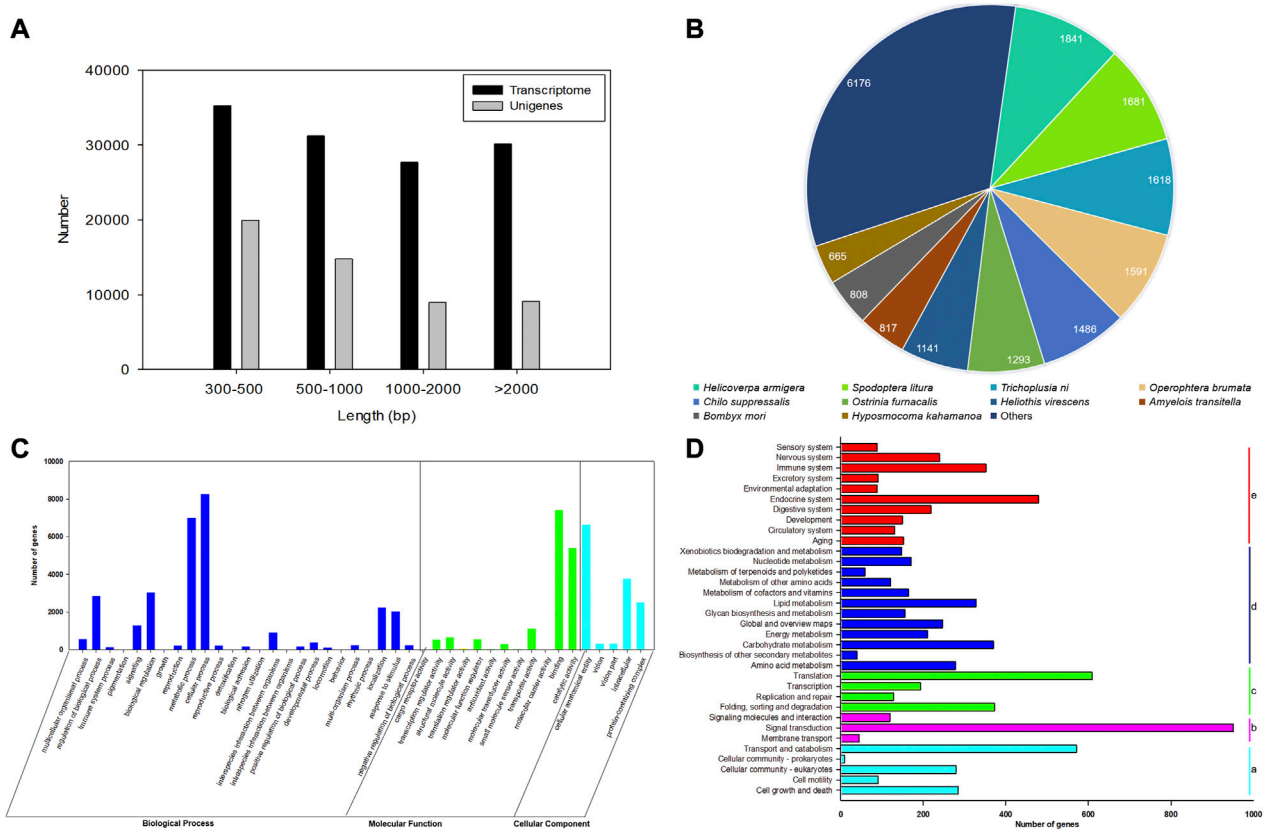

FIGURE 1
Characterization and transcriptome analysis of RNA sequences from antennae of *E. grisescens*. **(A)** Length distributions of the transcriptome and unigenes of *E. grisescens*. **(B)** Species distribution from the Blastx results of *E. grisescens* unigenes in the NR database. **(C)** GO classifications of *E. grisescens* unigenes. **(D)** KEGG classifications of *E. grisescens* unigenes; a: cellular processes, b: environmental information processing, c: genetic information processing, d: metabolism, e: organismal systems.

cDNA Synthesis SuperMix (Tiangen, Beijing, China) following the manufacturer's instructions. Primers specific for EgriCXEs and EgriGSTs were designed using Primer Premier 5.0 software (Premier Biosoft International, Palo Alto, CA, United States; Supplementary Table S1) and synthesized by Sangon Biotech (Shanghai, China).

The reaction volume of 20 μL was prepared using TB Green Premix Ex Taq (Tli RNase H Plus) (TaKaRa, Beijing) by following instructions from the manual. qRT-PCR was conducted using an Applied Biosystems 7500 Fast Real-Time PCR System (Applied Biosystems, Carlsbad, CA) under the following conditions: 95°C for 30 s, then 40 cycles of 95°C for 5 s and 60°C for 34 s, last 95°C for 15 s, 60°C for 1 min, 95°C for 15 s followed by the melting curve analysis. Three biological replicates and three technical replications were carried out. The housekeeping gene glyceraldehyde-3-phosphate dehydrogenase (GAPDH) was used as an internal control to normalize the data.

2.6 Statistical analysis

The relative quantification was calculated by the comparative $2^{-\Delta\Delta CT}$ method (Livak and Schmittgen, 2001). The significance of each candidate EgriCXEs and EgriGSTs among various tissues was determined using a one-way analysis of variance (ANOVA). The significances of EgriCXEs and EgriGSTs from different tissues between female and male adult insects were assessed using a two-sample *t*-test in SAS statistical software 9.2 (SAS Institute Inc., Cary, NC, United States), with thresholds set at a $p < 0.05$.

3 Results

3.1 Transcriptome analysis and assembly

After filtering the low-quality and adapter reads, a total of 21,733,434 (97.27%), 23,300,358 (97.54%), 22,180,396 (96.87%), 22,713,765 (96.91%), 22,797,995 (98.15%), and 22,378,252 (97.27%) clean reads were generated from three replicates of female and male antennal libraries of *E. grisescens* (Supplementary Table S2). The total bases of sequence data were approximately 6.52–6.99 Gb from male and female samples. The average error rates of the sequences were 0.03%. The Q20 and Q30 values for each library exceeded 97% and 92%, respectively, with a GC content of 42.68%–45.79% (Supplementary Table S2). After merging and clustering, the 124,287 transcripts and

TABLE 1 CXE identification and bioinformatics analysis of *E. grisescens* antennal transcriptomes.

Gene name	GenBank accession	ORF (aa)	SP	MW (KDa)	pI	BLASTX best hit		
						(Name/species)	Accession number	Identity (%)
EgriCXE1	OQ296948	565	Yes	63.56	7.17	Putative antennal esterase CXE1 [*Ectropis obliqua*]	ARM65372.1	98.05
EgriCXE2	OQ296949	518	Yes	59.51	6.14	Putative antennal esterase CXE2 [*Ectropis obliqua*]	ARM65373.1	97.30
EgriCXE3	OQ296950	535	No	59.94	5.94	Putative antennal esterase CXE3 [*Ectropis obliqua*]	ARM65374.1	99.07
EgriCXE4	OQ296951	516	Yes	57.92	8.30	Putative antennal esterase CXE4 [*Ectropis obliqua*]	ARM65375.1	97.68
EgriCXE5	OQ296952	595	Yes	66.35	6.65	Putative antennal esterase CXE5 [*Ectropis obliqua*]	ARM65376.1	98.15
EgriCXE6	OQ296953	558	Yes	60.95	5.36	Putative antennal esterase CXE6 [*Ectropis obliqua*]	ARM65377.1	98.92
EgriCXE8	OQ296954	429	No	48.31	6.03	Putative antennal esterase CXE8 [*Ectropis obliqua*]	ARM65379.1	57.24
EgriCXE9	OQ296955	558	No	64.01	7.54	Putative antennal esterase CXE9 [*Ectropis obliqua*]	ARM65380.1	97.67
EgriCXE11	OQ296956	523	No	58.24	5.89	Putative antennal esterase CXE11 [*Ectropis obliqua*]	ARM65382.1	96.75
EgriCXE13	OQ296957	560	Yes	62.12	6.32	Putative antennal esterase CXE13 [*Ectropis obliqua*]	ARM65384.1	98.57
EgriCXE15	OQ296958	401	No	45.25	9.60	Putative antennal esterase CXE15 [*Ectropis obliqua*]	ARM65386.1	98.58
EgriCXE17	OQ296959	495	No	56.05	5.81	Putative antennal esterase CXE17 [*Ectropis obliqua*]	ARM65388.1	97.72
EgriCXE18	OQ296960	542	No	61.16	6.43	Putative antennal esterase CXE18 [*Ectropis obliqua*]	ARM65389.1	99.08
EgriCXE19	OQ296961	609	Yes	69.13	5.30	Putative antennal esterase CXE19 [*Ectropis obliqua*]	ARM65390.1	99.84
EgriCXE20	OQ296962	501	No	56.55	6.13	Putative antennal esterase CXE20 [*Ectropis obliqua*]	ARM65391.1	97.92
EgriCXE21	OQ296963	564	Yes	62.68	5.37	Putative antennal esterase CXE21 [*Ectropis obliqua*]	ARM65392.1	98.70
EgriCXE22	OQ296964	568	Yes	63.42	5.93	Putative antennal esterase CXE22 [*Ectropis obliqua*]	ARM65393.1	97.71
EgriCXE24	OQ296965	567	No	63.76	8.70	Putative antennal esterase CXE24 [*Ectropis obliqua*]	ARM65395.1	97.88
EgriCXE25	OQ296966	570	No	64.10	8.72	Putative antennal esterase CXE25, partial [*Ectropis obliqua*]	ARM65396.1	97.71
EgriCXE26	OQ296967	523	No	59.26	6.02	Putative antennal esterase CXE26 [*Ectropis obliqua*]	ARM65397.1	99.24
EgriCXE27	OQ296968	567	No	53.99	6.53	Putative antennal esterase CXE27 [Ectropis obliqua]	ARM65398.1	95.83
EgriCXE29	OQ296969	569	Yes	63.78	5.83	Putative antennal esterase CXE29 [*Ectropis obliqua*]	ARM65400.1	96.74
EgriCXE30	OQ296970	438	No	49.61	5.50	Putative antennal esterase CXE30 [*Ectropis obliqua*]	ARM65401.1	98.59
EgriCXE32	OQ296971	620	No	65.60	6.42	Putative antennal esterase CXE32 [*Ectropis obliqua*]	ARM65403.1	99.22

(Continued on following page)

TABLE 1 (*Continued*) CXE identification and bioinformatics analysis of *E. grisescens* antennal transcriptomes.

Gene name	GenBank accession	ORF (aa)	SP	MW (KDa)	pI	BLASTX best hit		
						(Name/species)	Accession number	Identity (%)
EgriCXE33	OQ296972	555	Yes	62.35	5.12	Putative antennal esterase CXE33 [*Ectropis obliqua*]	ARM65404.1	99.02
EgriCXE34	OQ296973	563	No	63.95	5.38	Putative antennal esterase CXE34 [*Ectropis obliqua*]	ARM65405.1	98.76
EgriCXE36	OQ296974	532	No	59.13	5.42	Esterase FE4 [*Bombyx mori*]	XP_004932947.1	64.98
EgriCXE37	OQ296975	615	No	69.63	6.69	Carboxylesterase 1C [*Helicoverpa armigera*]	XP_021188868.2	60.93

52,856 unigenes with a mean length of 1,518 and 1,233 bp, with N50 length of 2,552 and 2,170 bp, were identified, respectively (Supplementary Table S3). The length of transcriptomes and unigenes ranged from 301 to 30,857 bp, with an average length of 1,518 and 1,233 bp, respectively (Figure 1A, Supplementary Table S3).

3.2 Functional annotation

A total of 15,500 (29.32%), 7,321 (13.85%), 11,512 (21.77%), 14,325 (27.10%), 14,323 (27.09%), and 6,119 (11.57%) had BLASTn hits in the NT, KO, Swiss-Prot, PFAM, GO, and KOG databases, respectively (Supplementary Table S4). BLASTx results showed 19,118 (36.16%) unigenes had the best hits in the non-redundant protein (NR) database. Moreover, most of the annotated unigenes closely matched to Lepidoptera insect sequences (16,780), including *Helicoverpa armigera* (1,841), *Spodoptera litura* (1,681), *Trichoplusia ni* (1,618), *Heliothis virescens* (1,591), *C. suppressalis* (1,486), *Ostrinia furnacalis* (1,293), *H. virescens* (1,141), *Amyelois transitella* (817), *Bombyx mori* (808), and *Hyposmocoma kahamanoa* (665), as shown in Figure 1B.

Based on the GO annotations, 60,045 unigenes could be annotated into three functional categories: biological processes (50.37%), molecular function (26.98%), and cellular components (22.65%) (Figure 1C). A total of 42 GO terms were identified based on GO level 2, including the odorant recognition process, e.g., binding, catalytic activity, and transporter activity in the molecular function ontology, and localization, signaling, and response to stimulus in the biological process ontology. In the KEGG annotation, 7,936 unigenes were divided into five metabolic pathways: cellular processes, environmental information processing, genetic information processing, metabolism, and organismal systems. Most unigenes were assigned to signal transduction (11.98%), signaling molecules and interaction (1.51%), and environment adaptation (1.11%) involved in recognizing olfaction in insects (Figure 1D).

3.3 Identification of CXEs in *E. grisescens*

A total of 28 candidate EgriCXEs were identified from the antennal transcriptome of *E. grisescens*. The sequences were named EgriCXE1–6, 8–9, 11, 13, 15, 17–22, 24–27, 29–30, 32–34, and 36–37 according to their presumptive orthologs of *E. obliqua* (Sun et al., 2017) and were deposited in the GenBank database under accession numbers OQ296948 to OQ296975 (Table 1). All putative EgriCXEs shared relatively high identities (>60.93%) with their respective orthologs from other species, particularly its counterpart *E. obliqua*. The amino acid identity between these EgriCXEs ranged from 7.84% to 60.11% (Supplementary Table S5). EgriCXE sequences encoded 401 to 620 amino acid residues with molecular weight ranging from 45.25 to 69.63 kDa and the pI from 5.12 to 9.60. Furthermore, 11 EgriCXEs (EgriCXE1–2, 4–6, 13, 19, 21–22, 29, and 33) were predicted to have putative N-terminal signal peptides (Table 1). Multiple sequence alignment analyses showed that a conserved pentapeptide Gly–X–Ser–X–Gly motif ("X" represents any residue) and more variable oxyanion hole residues (Gly–Gly–Ala), conserved serine (S) residues, and glutamate (E) and histidine (H) residues of the catalytic triad were found (Supplementary Table S6).

3.4 Identification of GSTs in *E. grisescens*

A total of 16 candidate EgriGSTs were identified and named EgriGSTe1 to EgriGSTu1, and they were deposited in the GenBank database under the accession numbers OQ296976 to OQ296991 (Table 2). EgriGSTs encoded 179 to 298 amino acid residues, with molecular weight ranging from 20.06 to 33.67 kDa and the pI from 4.95 to 9.46. Blastx search of the best hits showed that all EgriGST sequences shared relatively high sequence identities (53.14%–100.00%) with their respective orthologs from other insects (Table 2). The sequence identities of these EgriGSTs range from 5.50% to 86.76% (Supplementary Table S7). Multiple sequence alignment analyses of the EgriGSTs showed that a conserved G-site can be found in the N-terminal domain and a more variable H-site can be observed with a low sequence identity in the C-terminal domain (Supplementary Figure S1).

3.5 Phylogenetic analysis

The phylogenetic tree of EgriCXEs was constructed with 127 CXE sequences from six kinds of Lepidoptera insects: *E. obliqua*, *S. littoralis*, *P. interpunctella*, *S. exigua*, *S. litura*, and

TABLE 2 GST identification and bioinformatics analysis of *E. grisescens* antennal transcriptomes.

Clade	Gene name	GenBank accession	ORF (aa)	MW (KDa)	pI	BLASX best hit		
						Name/species	Accession number	Identity (%)
Epsilon	EgriGSTe1	OQ296976	179	19.69	4.64	Glutathione S-transferase 1 isoform X2 [*Helicoverpa armigera*]	XP_021180950.2	55.93
	EgriGSTe2	OQ296977	229	26.22	8.74	Glutathione S-transferase 1-like [*Galleria mellonella*]	XP_031763098.1	69.33
	EgriGSTe3	OQ296978	179	20.06	5.57	Glutathione S-transferase 10 [*Streltzoviella insularis*]	QLI62206.1	55.31
	EgriGSTe4	OQ296979	218	25.11	5.83	Glutathione S-transferase 1-like [*Bombyx mandarina*]	XP_028040596.1	53.14
	EgriGSTe5	OQ296980	241	27.64	6.52	Glutathione S-transferase epsilon class [*Spodoptera littoralis*]	AYM01167.1	66.18
Delta	EgriGSTd1	OQ296981	215	24.16	4.95	Glutathione S-transferase 1-1-like [*Pectinophora gossypiella*]	XP_049871107.1	65.28
	EgriGSTd2	OQ296982	216	24.23	6.17	Glutathione S-transferase 1-like [*Bombyx mandarina*]	XP_028025239.1	79.17
	EgriGSTd3	OQ296983	298	33.67	9.46	Glutathione S-transferase delta 3 [*Ostrinia furnacalis*]	QIC35739.1	64.13
	EgriGSTd4	OQ296984	216	24.25	6.44	Glutathione S-transferase 1 [*Manduca sexta*]	XP_030035460.2	83.80
Sigma	EgriGSTs1	OQ296985	204	24.06	5.50	Glutathione S-transferas-like [*Pectinophora gossypiella*]	XP_049871113.1	60.20
	EgriGSTs2	OQ296986	219	25.14	6.34	Glutathione S-transferase 2-like [*Manduca sexta*]	XP_030022570.1	67.96
	EgriGSTs3	OQ296987	218	25.97	7.72	Glutathione S-transferase Mu 1 isoform 2 [*Mus musculus*]	NP_034488.1	100.00
	EgriGSTs4	OQ296988	204	23.96	5.71	Glutathione S-transferase sigma 3 [*Operophtera brumata*]	KOB62848.1	63.18
Theta	EgriGSTt1	OQ296989	228	26.41	7.76	Glutathione S-transferase theta 1 [*Bombyx mori*]	NP_001108463.1	71.62
Omega	EgriGSTo1	OQ296990	104	12.09	5.07	Glutathione S-transferase omega 1 [*Heortia vitessoides*]	AWX68890.1	90.48
Unclassified	EgriGSTu1	OQ296991	231	26.30	5.73	Unclassified glutathione S-transferase [*Chilo suppressalis*]	AKS40352.1	78.26

Sesamia inferens (Figure 2). The results showed that EgriCXEs were distributed in eight different clades: 1) EgriCXE1, 2, 4, 6, 8, 17–18, and 20–22 were clustered with the moth antennal esterase group; 2) EgriCXE13 and 33 were assigned into β-esterase and pheromone esterase group; 3) EgriCXE5 and 4) EgriCXE32 were distributed into cuticular and antennal esterases and neuroligins, respectively; 5) two EgriCXEs (EgriCXE9 and 37) and 6) four EgriCXEs (EgriCXE 9, 11, 34, and 36) were assigned into neuroreceptor and microsomal α-esterases, respectively; 7) EgriCXE3, 24–27, 29, and 30 were clustered with mitochondrial and cytosolic esterases; 8) EgriCXE15 was assigned into Lepidopteran juvenile hormone esterases.

The phylogenetic tree of EgriGSTs was constructed with 159 GST sequences from eleven insect species: *P. interpunctella*, *P. xylostella*, *C. pomonella*, *B. mori*, *C. suppressalis*, *Acyrthosiphon pisum*, *D. melanogaster*, *Anopheles gambiae*, *Tribolium castaneum*, *G. molesta*, and *S. zeamais* (Figure 3). The results showed that the EgriGSTs were divided into six different GST groups: 1) five epsilon EgriGSTs (EgriGSTe1–5); 2) four delta EgriGSTs (EgriGSTd1–4); 3) four sigma EgriGSTs (EgriGSTs1–4); 4) a theta EgriGSTt1; 5) an omega EgriGSTo1, and 6) an unclassified EgriGSTu1.

3.6 Expression profiles of EgriCXEs and EgriGSTs

qRT-PCR results of EgriCXEs (Figure 4) in antennae, heads, thoraxes, abdomens, legs, and wings of both sexes showed that 26 EgriCXEs (*EgriCXE1–6*, *8–9*, *11*, *13*, *17–22*, *24*, *26–27*, *29–30*, *32–34*, and *36–37*) displayed significant antennal bias expression pattern, except for *EgriCXE15* and *EgriCXE25*. Of them, *EgriCXE1–2*, *4*, *8*, *11*, *13*, *18*, *20–22*, *24*, *26*, *29*, *32*, *34*, and *36–37*

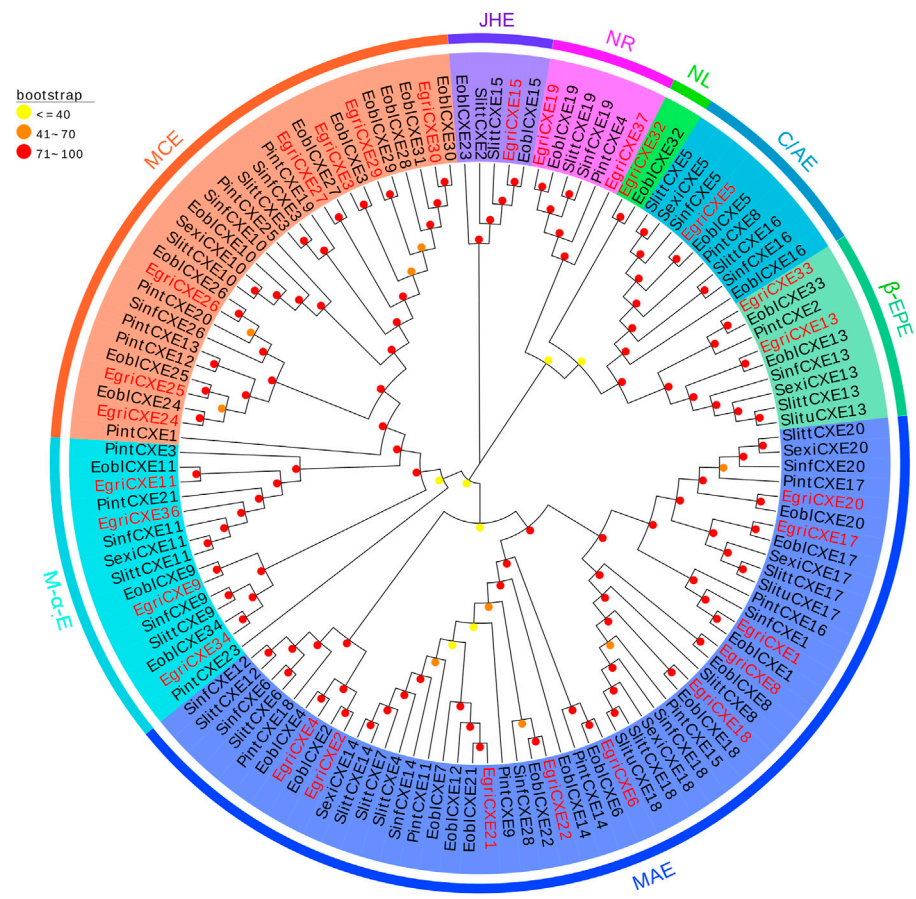

FIGURE 2
Phylogenetic analysis of candidate EgriCXEs with other insect CXEs. MCEs: mitochondrial and cytosolic esterases; JHEs: Lepidopteran juvenile hormone esterases; NR: neuroreceptor; NL: neuroligin; C/AEs: cuticular and antennal esterases; β-EPEs: β-esterases and pheromone esterases; MAEs: moth antennal esterases; M-α-Es: microsomal α-esterases. Egri, *Ectropis grisescens* (N = 28); Eobl, *Ectropis obliqua* (N = 34); Slitt, *Spodoptera littoralis* (N = 19); Pint, *Plodia interpunctella* (N = 19); Sexi, *Spodoptera exigua* (N = 8); Slitu, *Spodoptera litura* (N = 3); Sinf, *Sesamia inferens* (N = 16). Candidate EgriCXEs are indicated by red. The GenBank accession numbers of the 127 CXEs protein used in the phylogenetic analysis are listed in Supplementary Table S8.

were significantly highly expressed in female antennae compared to the male antennae ($t_{EgriCXE1} = 17.21$, $p < 0.0001$; $t_{EgriCXE2} = 38.90$, $p < 0.0001$; $t_{EgriCXE4} = 12.52$, $p = 0.0002$; $t_{EgriCXE8} = 7.20$, $p = 0.0020$; $t_{EgriCXE11} = 9.48$, $p = 0.0007$; $t_{EgriCXE13} = 12.77$, $p = 0.0002$; $t_{EgriCXE18} = 4.67$, $p = 0.0095$; $t_{EgriCXE20} = 3.71$, $p = 0.0207$; $t_{EgriCXE21} = 5.06$, $p = 0.0072$; $t_{EgriCXE22} = 3.28$, $p = 0.0304$; $t_{EgriCXE24} = 5.66$, $p = 0.0048$; $t_{EgriCXE26} = 4.67$, $p = 0.0095$; $t_{EgriCXE29} = 19.63$, $p < 0.0001$; $t_{EgriCXE32} = 10.92$, $p = 0.0004$; $t_{EgriCXE34} = 8.03$, $p = 0.0013$; $t_{EgriCXE36} = 7.10$, $p = 0.0021$; and $t_{EgriCXE37} = 8.49$, $p = 0.0011$). Only *EgriCXE6* were highly expressed in male antennae, showing male-specific expression ($t_{EgriCXE6} = -8.02$, $p = 0.0013$). Other EgriCXEs (*EgriCXE3*, *5*, *9*, *17*, *19*, *27*, *30*, and *33*) showed no significant difference between the two sexes ($t_{EgriCXE3} = -2.08$, $p = 0.1061$; $t_{EgriCXE5} = 1.98$, $p = 0.1857$; $t_{EgriCXE9} = 0.25$, $p = 0.8130$; $t_{EgriCXE17} = 1.49$, $p = 0.2115$; $t_{EgriCXE19} = -2.19$, $p = 0.0934$; $t_{EgriCXE27} = -0.45$, $p = 0.6873$; $t_{EgriCXE30} = 2.16$, $p = 0.0966$; and $t_{EgriCXE33} = 2.14$, $p = 0.0989$), whereas, *EgriCXE15* and *EgriCXE25* were highly expressed in a non-chemosensory organ, heads and wings of both sexes, respectively. Furthermore, all EgriCXE genes were detected in other non-chemosensory organs with less expression levels.

The putative EgriGSTs showed a wide range of expression patterns (Figure 5): *EgriGSTe1*, *s4*, and *u1* were highly expressed in male thoraxes and female wings, whereas *EgriGSTe2* and *d1* were strongly expressed in female thoraxes and male wings. *EgriGSTe3* was highly expressed in male thoraxes and female abdomens. *EgriGSTe4*, *s2*, *t1*, and *o1* were highly expressed in the wings of both sexes. *EgriGSTd2*, *d3*, and *d4* were strongly expressed in the heads of both sexes. *EgriGSTe5* and *s3* were strongly expressed in the thoraxes of both sexes. *EgriGSTs1* was specifically expressed in male antennae, with a significant difference between the two sexes ($t_{EgriGSTs1} = -26.43$, $p = 0.0014$). Some EgriGSTs were widely distributed and detected in various tissues, e.g., *EgriGSTs2* and *EgriGSTs3*.

4 Discussion

In the present research, we identified 52,856 unigenes with a mean length of 1,233 bp from the male and female *E. grisescens* antennal transcriptome, indicating the high quality and great depth

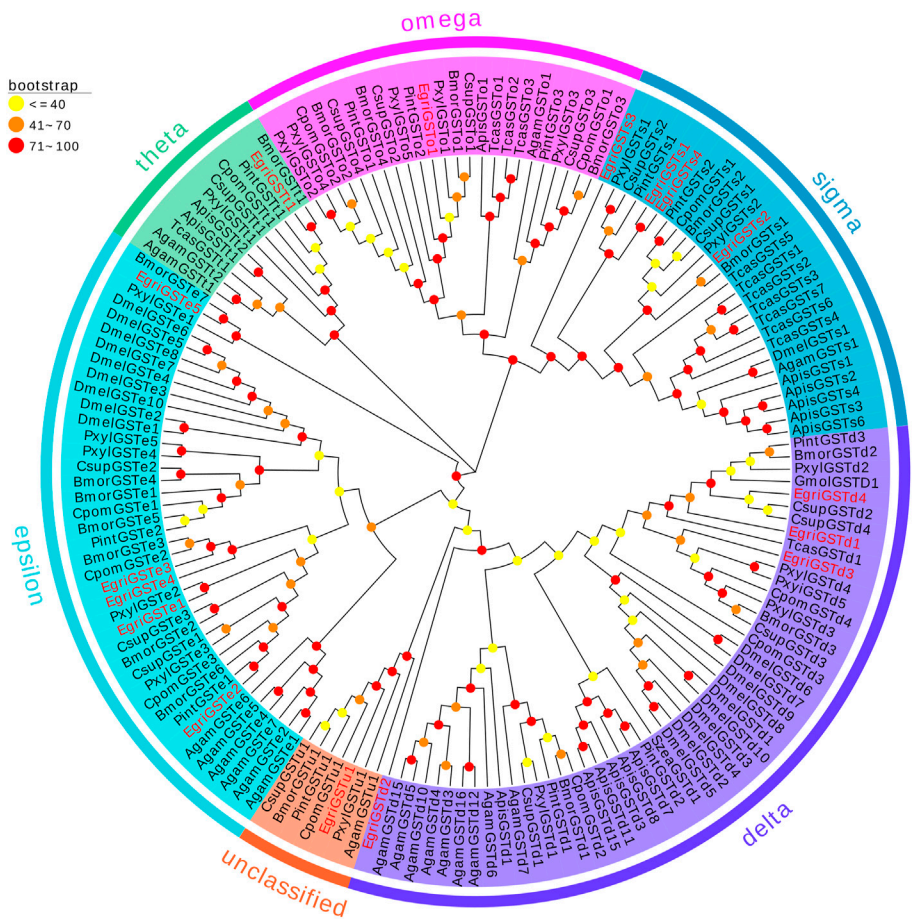

FIGURE 3
Phylogenetic analysis of candidate EgriGSTs with other insect GSTs. Egri, *Ectropis grisescens* (N = 16); Pint, *Plodia interpunctella* (N = 12); Pxyl, *Plutella xylostella* (N = 19); Cpom, *Cydia pomonella* (N = 11); Bmor, *Bombyx mori* (N = 18); Csup, *Chilo suppressalis* (N = 15); Apis, *Acyrthosiphon pisum* (N = 14); Dmel, *Drosophila melanogaster* (N = 20); Agam, *Anopheles gambiae* (N = 16); Tcas, *Tribolium castaneum* (N = 12); Gmol, *Grapholita molesta* (N = 1); Szea, *Sitophilus zeamais* (N = 1). Candidate EgriGSTs are indicated by red. The GenBank accession numbers of the 159 GSTs protein used in the phylogenetic analysis are listed in Supplementary Table S9.

of sequencing at the transcriptome level. The results of Blastx homology search in the NCBI database revealed that *E. grisescens* unigenes shared relatively high homology with sequences from other Lepidoptera species. Ultimately, 28 candidate CXE genes and 16 candidate GST genes were identified in the *E. grisescens* antennal transcriptome.

In GO annotation of the transcriptome, several annotations were associated with olfaction in insects such as binding, catalytic activity, and transporter activity in the molecular function ontology, localization, signaling, and response to stimulus in the biological process ontology, which are vital steps of odorant recognition in insects (Schmidt and Benton, 2020; Zhang et al., 2020; Rihani et al., 2021; Tian et al., 2021). KEGG pathway analysis also had similar function annotations about recognizing olfaction, such as signal transduction and environment adaptation. The aforementioned results of function annotation were similar to the finding in *Bemisia tabaci* MED (Wang et al., 2017) and *Athetis dissimilis* (Song et al., 2021), which further showed that the identified EgriCXEs and EgriGSTs might participate in various chemical communications of *E. grisescens*.

The number of CXE genes identified in *E. grisescens* was the same as that in *Cnaphalocrocis medinalis* (Zhang et al., 2017b) and *Athetis lepigone* (Zhang et al., 2017c). However, this number was significantly greater than that of CXE genes identified in other species reported, such as *C. pomonella* (12) (Huang et al., 2016), *C. suppressalis* (19) (Liu et al., 2015a), *H. parallela* (20) (Yi et al., 2021), and *A. lepigone* (20) (Zhang et al., 2017c). The difference in gene numbers among different species might depend on the evolution of divergent behaviors in the long term, which resulted in gene duplication and loss (Zhang et al., 2017b; Huang et al., 2021). In addition, the sample preparation and sequencing method/depth might also be a reason. Multiple sequence alignment analyses showed that most EgriCXEs had the oxyanion hole residues Gly–Gly–Ala, the catalytic triad Ser–Glu–His, and the conserved pentapeptide Gly–X–Ser-–X–Gly. These characteristics indicated that most of the identified EgriCXEs might encode functional enzymes and play a vital role in the catalytic activity of CXEs (Oakeshott et al., 2010).

The number of GST genes identified in *E. grisescens* was different from that of *S. zeamais* (13) (Xia et al., 2022), *P. interpunctella* (17) (Liu et al., 2021), *S. littoralis* (33) (Durand et al., 2018), and *C. medinalis* (23) (Liu et al., 2015b). This

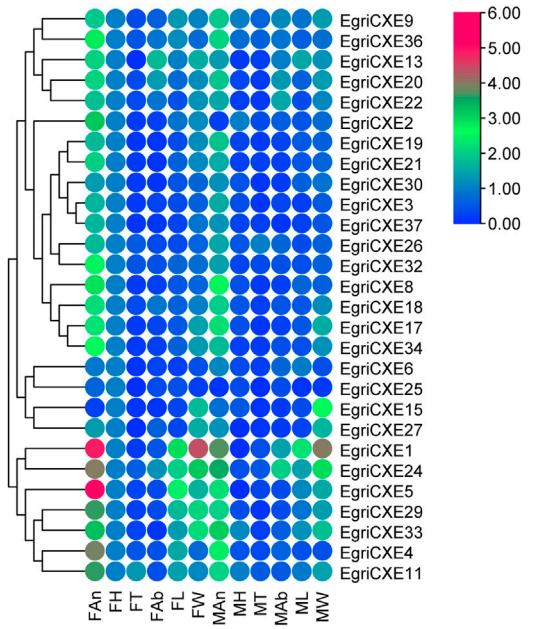

FIGURE 4
Tissue- and sex-specific expression pattern of the EgriCXEs. A total of 28 EgriCXEs were clustered using relative expression values from each of the tissues. Expression values are relative to female head tissue (one-fold), with red and blue representing the highest and the lowest values, respectively. FAn: female antennae; FH: female head; FT: female thorax; FAb: female abdomen; FL: female leg; FW: female wing; MAn: male antennae; MH: male head; MT: male thorax; MAb: male abdomen; ML: male leg; MW: male wing.

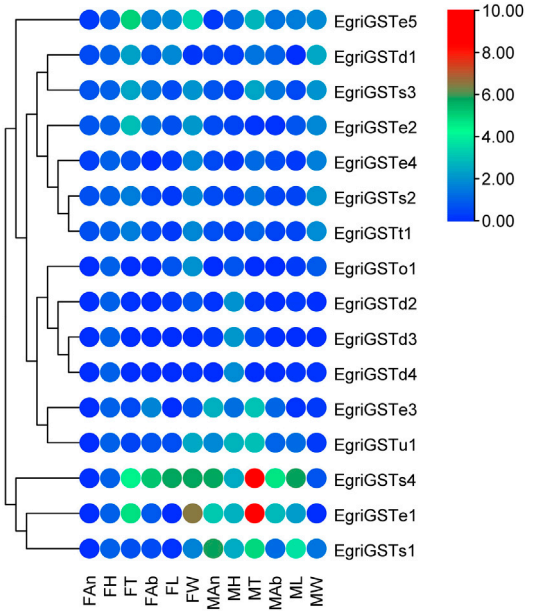

FIGURE 5
Tissue- and sex-specific expression pattern of the EgriGSTs. A total of 16 EgriGSTs were clustered using relative expression values from each of the tissues.

massive increase in the number of of GSTs in insects enables them to detect plant compounds and resist the damage caused by insecticides, as described in some reports (Durand et al., 2018; Liu et al., 2021). The results of the EgriGST sequence analysis showed a conserved G-site can be found in the N-terminal domain, indicating function as GSH-binding. However, a more variable H-site could be observed with a low sequence identity in the C-terminal domain, which enabled GSTs to accommodate various substrate selectivities (Lerksuthirat and Ketterman, 2008). Furthermore, we also found that some full-length EgriCXEs or EgriGSTs had low identities of amino acid sequences, which suggested that these genes evolved rapidly during long-term adaptation to various environmental factors (Campanini and De Brito, 2016).

The phylogenetic tree showed that the EgriCXEs could be divided into eight groups using classifications from the previous studies (Durand et al., 2010a; Oakeshott et al., 2015). The majority of the antennal EgriCXEs were assigned to the clade that contained members of the esterase family. Among them, ten EgriCXEs (EgriCXE1, 2, 4, 6, 8, 17–18, and 20–22) constituted the biggest groups, moth antennal esterase branch, together with the SexiCXE14 of *S. exigua* (He et al., 2014c), and SlittCXE7 of *S. littoralis* (Durand et al., 2011), which caused the degradation of plant volatiles and pheromone compounds. Of them, nine EgriCXEs (EgriCXE1, 2, 4, 6, 8, 18, and 20–22) were significantly expressed in female or male antenna, suggesting these CXEs might have a similar function in odorant degradation. Seven EgriCXEs (EgriCXE3, 24–27, 29, and 30) were clustered into mitochondrial and cytosolic esterase clades with two well-characterized CXEs, SlittCXE10 and SexiCXE10, which were specifically active to plant volatiles pentyl acetate and Z3-6: Ac, respectively (Durand et al., 2010b; He et al., 2015). Of them, three EgriCXEs (EgriCXE 24, 26, and 29) showed high antennal bias, indicating that these EgriCXEs were potentially involved in odorant degradation.

Additionally, two EgriCXEs (EgriCXE13 and 33), along with annotated pheromone and plant volatiles degrading enzymes (like SexiCXE13 for plant volatiles pentyl acetate and the acetate sex pheromone Z9E12-14: Ac, (He et al., 2014a)), were assigned to the β-esterase and pheromone esterase clades. However, the expression pattern of EgriCXE13 and 33 showed no antennal bias in our qRT-PCR. This phenomenon was also observed in the microsomal α-esterase clade, containing four EgriCXEs (EgriCXE9, 11, 34, and 36) without antennal bias and SexiCXE11 which had a high degradation activity against sex pheromones Z9-14: Ac and plant volatile esters pentyl acetate (He et al., 2019). Therefore, functional confirmation of these CXEs would require further functional analyses using *in vitro* and *in vivo* methods.

EgriCXE32 constituted Lepidopteran JHEs, which could control juvenile hormone (JH) titer and regulate larval to adult transition in insects (Gu et al., 2015). Two EgriCXEs (EgriCXE19 and 37) and EgriCXE5 were assigned into neuroreceptor and neuroligins clades, respectively, which were mainly involved in neurological and sensory developmental function (Durand et al., 2017). The cuticular and antennal esterase clade only contained one EgriCXE (EgriCXE15) without antennal-biased expression, and this gene lacked CXE conserved characteristic, the oxyanion hole-

forming residues (Supplementary Table S6), indicating that it might play other roles, such as detoxification of insecticides.

The phylogenetic tree showed that the EgriGSTs could be divided into six groups. The epsilon class group was common GSTs in insects, which was widely recognized to have a detoxification function (Lalouette et al., 2016; Labade et al., 2018), mediating endocrine plasticity (Bigot et al., 2012) and cholesterol transporter activity (Enya et al., 2015). For instance, SlitGSTe1 and SlitGSTe2 in *S. littoralis* antennae were induced by sublethal doses of deltamethrin and were involved in protecting against insecticides (Lalouette et al., 2016). The expression pattern suggested EgriGSTe1–5 was highly expressed in thoraxes, abdomens, and wings, which further verified their function as degraders of non-volatile substances.

Additionally, GSTs of the insect delta group in antennae were commonly associated with odorant degradation, which had been studied and verified in some moths. For example, PintGSTd1 of *P. interpunctella* could efficiently degrade the sex pheromone component Z9-12: Ac and host volatile hexanal (Liu et al., 2021). GmolGSTD1 of *G. molesta* exhibited high degradation activity to the sex pheromone component (Z)-8-dodecenyl alcohol and the host plant volatile butyl hexanoate (Li et al., 2018). SzeaGSTd1 of *S. zeamais* could degrade the volatile of the host capryl alcohol (Xia et al., 2022). Unexpectedly, we found that none of the delta genes in *E. grisescens* was restricted to antenna-based qRT-PCR results, which were mainly expressed in the male heads or ubiquitously expressed in tissues tested. However, phylogenetic tree analysis showed that the delta genes in *E. grisescens* were distributed among the well-defined insect GST clades, together with GmolGSTD1, PintGSTd1, and SzeaGSTd1. Considering this point, we hypothesized that the delta group mediated the degradation of odorants in *E. grisescens*, which needed to be further investigated.

The sigma class genes had diverse functions, e.g., recognizing invasive pathogens (Huang et al., 2011) and detoxifying insecticides (Qin et al., 2012; Qin et al., 2013). The expression pattern showed that the sigma group genes in *E. grisescens* exhibited ubiquitous expression patterns, with the exception of EgriGSTs1, whose expression was almost restricted in the male antennae, suggesting that EgriGSTs1 might play a crucial role in inactivating the chemical signals or pheromone-degrading enzymes (PDEs). Other classes (theta, omega, and unclassified group) were involved in the detoxification of xenobiotics (Qin et al., 2013; Yamamoto and Yamada, 2016; Durand et al., 2018).

In conclusion, we characterized 28 carboxylesterases and 16 glutathione S-transferases encoding odorant-degrading enzymes (ODEs) from *E. grisescens* antennal transcriptome. Furthermore, the expression patterns of carboxylesterases and glutathione S-transferases in different tissues were investigated to identify antennal enriched genes. Finally, 12 EgriCXEs (EgriCXE1, 2, 4, 6, 8, 18, 20–22, 24, 26, and 29) and five GSTs (EgriGST1 and EgriGST delta group) were identified as candidate target genes involved in odorant degradation of *E. grisescens*. The findings of this study revealed the potential involvement of ODEs in the olfactory system of *E. grisescens*.

Data availability statement

The data presented in the study are deposited in the Sequence Read Archive repository, accession number PRJNA784387. The data link: https://www.ncbi.nlm.nih.gov/sra/?term=PRJNA784387.

Author contributions

Conceptualization: FZ and XL; methodology: FH, FZ, and XL; software: YC and FZ; validation: XZ and YZ; investigation: SG; data curation: YC; writing—original draft preparation: YC and FZ; writing—review and editing: XL and XZ; supervision: YZ; project administration: ZZ and LZ; funding acquisition: SG and FZ. All authors have read and agreed to the published version of the manuscript.

Funding

This study was supported by the Natural Science Foundation of Henan Province (No. 212300410229), the Key Project for University Excellent Young Talents of Henan Province (No. 2020GGJS260), the Project of Science and Technology Innovation Team (Nos. XNKJTD-007 and KJCXTD-202001), special funds for Henan Province Scientific and Technological Development guided by the Central Government (Z20221341063), and Youth Foundation (Nos. 2019LG004 and 20200106), Xinyang Agriculture and Forestry University, P.R. China.

Acknowledgments

The authors would like to thank Y Tang and T Zhang (Institute of Plant Protection, Hebei Academy of Agriculture and Forestry Sciences, Baoding, Hebei, China) for their help during data analysis.

Conflict of interest

The authors declare that the research was conducted in the absence of any commercial or financial relationships that could be construed as a potential conflict of interest.

The reviewer WX declared a shared parent affiliation with the authors YZ and XL to the handling editor at the time of review.

Publisher's note

Supplementary material

The Supplementary Material for this article can be found online at: https://www.frontiersin.org/articles/10.3389/fphys.2023.1183610/full#supplementary-material

References

Baldwin, S. R., Mohapatra, P., Nagalla, M., Sindvani, R., Amaya, D., Dickson, H. A., et al. (2021). Identification and characterization of CYPs induced in the Drosophila antenna by exposure to a plant odorant. *Sci. Rep.* 11 (1), 20530. doi:10.1038/s41598-021-99910-9

Bigot, L., Shaik, H. A., Bozzolan, F., Party, V., Lucas, P., Debernard, S., et al. (2012). Peripheral regulation by ecdysteroids of olfactory responsiveness in male Egyptian cotton leaf worms, *Spodoptera littoralis*. *Insect biochem. Mol. Biol.* 42 (1), 22–31. doi:10.1016/j.ibmb.2011.10.003

Blomquist, G. J., Tittiger, C., MacLean, M., and Keeling, C. I. (2021). Cytochromes P450: Terpene detoxification and pheromone production in bark beetles. *Curr. Opin. Insect Sci.* 43, 97–102. doi:10.1016/j.cois.2020.11.010

Campanini, E. B., and De Brito, R. A. (2016). Molecular evolution of odorant-binding proteins gene family in two closely related Anastrepha fruit flies. *BMC Evol. Biol.* 16 (1), 198. doi:10.1186/s12862-016-0775-0

Cano-Ramirez, C., Lopez, M. F., Cesar-Ayala, A. K., Pineda-Martinez, V., Sullivan, B. T., and Zúñiga, G. (2013). Isolation and expression of cytochrome P450 genes in the antennae and gut of pine beetle *Dendroctonus rhizophagus* (Curculionidae: Scolytinae) following exposure to host monoterpenes. *Gene* 520 (1), 47–63. doi:10.1016/j.gene.2012.11.059

Cao, P., Yang, D. J., Zhu, J. H., Liu, Z. P., Jiang, D. G., and Xu, H. B. (2018). Estimated assessment of cumulative dietary exposure to organophosphorus residues from tea infusion in China. *Environ. Health Prev.* 23 (1), 7. doi:10.1186/s12199-018-0696-1

Chertemps, T., François, A., Durand, N., Rosell, G., Dekker, T., Lucas, P., et al. (2012). A carboxylesterase, Esterase-6, modulates sensory physiological and behavioral response dynamics to pheromone in Drosophila. *BMC Biol.* 10, 56. doi:10.1186/1741-7007-10-56

Chertemps, T., Younus, F., Steiner, C., Durand, N., Coppin, C. W., Pandey, G., et al. (2015). An antennal carboxylesterase from *Drosophila melanogaster*, esterase 6, is a candidate odorant-degrading enzyme toward food odorants. *Front. Physiol.* 6, 315. doi:10.3389/fphys.2015.00315

Choo, Y. M., Pelletier, J., Atungulu, E., and Leal, W. S. (2013). Identification and characterization of an antennae-specific aldehyde oxidase from the navel orangeworm. *PLoS One* 8 (6), e67794. doi:10.1371/journal.pone.0067794

Durand, N., Carot-Sans, G., Bozzolan, F., Rosell, G., Siaussat, D., Debernard, S., et al. (2011). Degradation of pheromone and plant volatile components by a same odorant-degrading enzyme in the cotton leafworm, *Spodoptera littoralis*. *PLoS One* 6 (12), e29147. doi:10.1371/journal.pone.0029147

Durand, N., Carot-Sans, G., Chertemps, T., Bozzolan, F., Party, V., Renou, M., et al. (2010a). Characterization of an antennal carboxylesterase from the pest moth *Spodoptera littoralis* degrading a host plant odorant. *PLoS One* 5 (11), e15026. doi:10.1371/journal.pone.0015026

Durand, N., Carot-Sans, G., Chertemps, T., Montagné, N., Jacquin-Joly, E., Debernard, S., et al. (2010b). A diversity of putative carboxylesterases are expressed in the antennae of the noctuid moth *Spodoptera littoralis*. *Insect Mol. Biol.* 19 (1), 87–97. doi:10.1111/j.1365-2583.2009.00939.x

Durand, N., Chertemps, T., Bozzolan, F., and Maïbèche, M. (2017). Expression and modulation of neuroligin and neurexin in the olfactory organ of the cotton leaf worm *Spodoptera littoralis*. *Insect Sci.* 24 (2), 210–221. doi:10.1111/1744-7917.12312

Durand, N., Pottier, M. A., Siaussat, D., Bozzolan, F., Maïbèche, M., and Chertemps, T. (2018). Glutathione-S-Transferases in the olfactory organ of the Noctuid moth *Spodoptera littoralis*, diversity and conservation of chemosensory clades. *Front. Physiol.* 9, 1283. doi:10.3389/fphys.2018.01283

Elgar, M. A., Zhang, D., Wang, Q., Wittwer, B., Thi Pham, H., Johnson, T. L., et al. (2018). Insect antennal morphology: The evolution of diverse solutions to odorant perception. *Yale J. Biol. Med.* 91 (14), 457–469.

Enya, S., Daimon, T., Igarashi, F., Kataoka, H., Uchibori, M., Sezutsu, H., et al. (2015). The silkworm glutathione S-transferase gene noppera-bo is required for ecdysteroid biosynthesis and larval development. *Insect biochem. Mol. Biol.* 61, 1–7. doi:10.1016/j.ibmb.2015.04.001

Fleischer, J., Pregitzer, P., Breer, H., and Krieger, J. (2018). Access to the odor world: Olfactory receptors and their role for signal transduction in insects. *Cell Mol. Life Sci.* 75 (3), 485–508. doi:10.1007/s00018-017-2627-5

Godoy, R., Machuaca, J., Venthur, H., Quiroz, A., and Mutis, A. (2021). An overview of antennal esterases in Lepidoptera. *Front. Physiol.* 12, 643281. doi:10.3389/fphys.2021.643281

Götz, S., García-Gómez, J. M., Terol, J., Williams, T. D., Nagaraj, S. H., Nueda, M. J., et al. (2008). High-throughput functional annotation and data mining with the Blast2GO suite. *Nucleic Acids Res.* 36 (10), 3420–3435. doi:10.1093/nar/gkn176

Grabherr, M. G., Haas, B. J., Yassour, M., Levin, J. Z., Thompson, D. A., Amit, I., et al. (2011). Full-length transcriptome assembly from RNA-Seq data without a reference genome. *Nat. Biotechnol.* 29 (7), 644–652. doi:10.1038/nbt.1883

Gu, X., Kumar, S., Kim, E., and Kim, Y. (2015). A whole genome screening and RNA interference identify a juvenile hormone esterase-like gene of the diamondback moth, Plutella xylostella. *Plutella Xylostella. J. Insect Physiol.* 80, 81–87. doi:10.1016/j.jinsphys.2015.02.001

Guo, S., and Wong, S. M. (2020). A conserved carboxylesterase inhibits tobacco mosaic virus (TMV) accumulation in *Nicotiana benthamiana* Plants. *Viruses* 12 (2), 195. doi:10.3390/v12020195

He, P., Li, Z. Q., Liu, C. C., Liu, S. J., and Dong, S. L. (2014a). Two esterases from the genus Spodoptera degrade sex pheromones and plant volatiles. *Genome* 57 (4), 201–208. doi:10.1139/gen-2014-0041

He, P., Mang, D. Z., Wang, H., Wang, M. M., Ma, Y. F., Wang, J., et al. (2019). Molecular characterization and functional analysis of a novel candidate of cuticle carboxylesterase in *Spodoptera exigua* degradating sex pheromones and plant volatile esters. *Pestic. Biochem. Physiol.* 163, 227–234. doi:10.1016/j.pestbp.2019.11.022

He, P., Zhang, J., Li, Z. Q., Zhang, Y. N., Yang, K., Dong, S. L., et al. (2014b). Functional characterization of an antennal esterase from the noctuid moth, *Spodoptera exigua*. *Arch. Insect Biochem. Physiol.* 86 (2), 85–99. doi:10.1002/arch.21164

He, P., Zhang, Y. N., Li, Z. Q., Yang, K., Zhu, J. Y., Liu, S. J., et al. (2014c). An antennae-enriched carboxylesterase from *Spodoptera exigua* displays degradation activity in both plant volatiles and female sex pheromones. *Insect Mol. Biol.* 23 (4), 475–486. doi:10.1111/imb.12095

He, P., Zhang, Y. N., Yang, K., Li, Z. Q., and Dong, S. L. (2015). An antenna-biased carboxylesterase is specifically active to plant volatiles in *Spodoptera exigua*. *Pestic. Biochem. Physiol.* 123, 93–100. doi:10.1016/j.pestbp.2015.03.009

Huang, C., Zhang, X., He, D. F., Wu, Q., Tang, R., Xing, L. S., et al. (2021). Comparative fenomics provide insights into function and evolution of odorant binding proteins in *Cydia pomonella*. *Front. Physiol.* 12, 690185. doi:10.3389/fphys.2021.690185

Huang, X. L., Fan, D. S., Liu, L., and Feng, J. N. (2017). Identification and characterization of glutathione S-transferase genes in the antennae of codling moth (Lepidoptera: Tortricidae). *Ann. Entomol. Soc. Am.* 110 (4), 409–416. doi:10.1093/aesa/sax041

Huang, X. L., Liu, L., Su, X. J., and Feng, J. N. (2016). Identification of biotransformation enzymes in the antennae of codling moth *Cydia pomonella*. *Gene* 580 (1), 73–79. doi:10.1016/j.gene.2016.01.008

Huang, Y. F., Xu, Z. B., Lin, X. Y., Feng, Q. L., and Zheng, S. C. (2011). Structure and expression of glutathione S-transferase genes from the midgut of the common cutworm, *Spodoptera litura* (Noctuidae) and their response to xenobiotic compounds and bacteria. *J. Insect Physiol.* 57 (7), 1033–1044. doi:10.1016/j.jinsphys.2011.05.001

Iseli, C., Jongeneel, C. V., and Bucher, P. (1999). ESTScan: A program for detecting, evaluating, and reconstructing potential coding regions in EST sequences. *Proc. Int. Conf. Intell. Syst. Mol. Biol.* 7, 138–148.

Kang, Z. W., Liu, F. H., Xu, Y. Y., Cheng, J. H., Lin, X. L., Jing, X. F., et al. (2021). Identification of candidate odorant-degrading enzyme genes in the antennal transcriptome of *Aphidius gifuensis*. *Entomol. Res.* 51 (1), 36–54. doi:10.1111/1748-5967.12489

Keeling, C. I., Henderson, H., Li, M., Dullat, H. K., Ohnishi, T., and Bohlmann, J. (2013). CYP345E2, an antenna-specific cytochrome P450 from the mountain pine beetle, *Dendroctonus ponderosae* Hopkins, catalyses the oxidation of pine host monoterpene volatiles. *Insect biochem. Mol. Biol.* 43 (12), 1142–1151. doi:10.1016/j.ibmb.2013.10.001

Ketterman, A. J., Saisawang, C., and Wongsantichon, J. (2011). Insect glutathione transferases. *Drug Metab. Rev.* 43 (2), 253–265. doi:10.3109/03602532.2011.552911

Kumar, S., Stecher, G., Li, M., Knyaz, C., and Tamura, K. (2018). Mega X: Molecular evolutionary genetics analysis across computing platforms. *Mol. Biol. Evol.* 35 (6), 1547–1549. doi:10.1093/molbev/msy096

Labade, C. P., Jadhav, A. R., Ahire, M., Zinjarde, S. S., and Tamhane, V. A. (2018). Role of induced glutathione-S-transferase from *Helicoverpa armigera* (Lepidoptera: Noctuidae) HaGST-8 in detoxification of pesticides. *Ecotoxicol. Environ. Saf.* 147, 612–621. doi:10.1016/j.ecoenv.2017.09.028

Lalouette, L., Pottier, M. A., Wycke, M. A., Boitard, C., Bozzolan, F., Maria, A., et al. (2016). Unexpected effects of sublethal doses of insecticide on the peripheral olfactory response and sexual behavior in a pest insect. *Environ. Sci. Pollut. Res. Int.* 23 (4), 3073–3085. doi:10.1007/s11356-015-5923-3

Leal, W. S. (2013). Odorant reception in insects: Roles of receptors, binding proteins, and degrading enzymes. *Annu. Rev. Entomol.* 58, 373–391. doi:10.1146/annurev-ento-120811-153635

Lerksuthirat, T., and Ketterman, A. J. (2008). Characterization of putative hydrophobic substrate binding site residues of a Delta class glutathione transferase from *Anopheles dirus*. *Arch. Biochem. Biophys.* 479 (1), 97–103. doi:10.1016/j.abb.2008.08.006

Li, G. W., Chen, X. L., Xu, X. L., and Wu, J. X. (2018). Degradation of sex pheromone and plant volatile components by an antennal glutathione S- transferase in the oriental fruit moth, *Grapholita molesta* Busck (Lepidoptera: Tortricidae). *Arch. Insect Biochem. Physiol.* 99 (4), e21512. doi:10.1002/arch.21512

Li, Z. Q., Cai, X. M., Luo, Z. X., Bian, L., Xin, Z. J., Liu, Y., et al. (2019). Geographical distribution of *Ectropis grisescens* (Lepidoptera: Geometridae) and *Ectropis obliqua* in China and description of an efficient identification method. *J. Econ. Entomol.* 112 (1), 277–283. doi:10.1093/jee/toy358

Liu, H. M., Tang, Y., Wang, Q. Y., Shi, H. Z., Yin, J., and Li, C. J. (2021). Identification and characterization of an antennae-specific Glutathione S-Transferase from the Indian meal moth. *Front. Physiol.* 12, 727619. doi:10.3389/fphys.2021.727619

Liu, H. M., Lei, X. P., Du, L. X., Yin, J. Y., Shi, H. Z., Zhang, T., et al. (2019). Antennae-specific carboxylesterase genes from Indian meal moth: Identification, tissue distribution and the response to semiochemicals. *J. Stored Prod. Res.* 84, 101528. doi:10.1016/j.jspr.2019.101528

Liu, S., Gong, Z. J., Rao, X. J., Li, M. Y., and Li, S. G. (2015a). Identification of putative carboxylesterase and glutathione S-transferase genes from the antennae of the *Chilo suppressalis* (Lepidoptera: Pyralidae). *J. Insect Sci.* 15 (1), 103. doi:10.1093/jisesa/iev082

Liu, S., Rao, X. J., Li, M. Y., Feng, M. F., He, M. Z., and Li, S. G. (2015b). Glutathione S-transferase genes in the rice leaffolder, *Cnaphalocrocis medinalis* (Lepidoptera: Pyralidae): Identification and expression profiles. *Arch. Insect Biochem. Physiol.* 90 (1), 1–13. doi:10.1002/arch.21240

Livak, K. J., and Schmittgen, T. D. (2001). Analysis of relative gene expression data using real-time quantitative PCR and the $2^{-\Delta\Delta CT}$ method. *Methods* 25 (4), 402–408. doi:10.1006/meth.2001.1262

Ma, T., Xiao, Q., Yu, Y. G., Wang, C., Zhu, C. Q., Sun, Z. H., et al. (2016). Analysis of tea Geometrid (*Ectropis grisescens*) pheromone gland extracts using GC-EAD and GC×GC/TOFMS. *J. Agric. Food Chem.* 64 (16), 3161–3166. doi:10.1021/acs.jafc.6b00339

Mao, K. K., Ren, Z. J., Li, W. H., Cai, T. W., Qin, X. Y., Wan, H., et al. (2021). Carboxylesterase genes in nitenpyram-resistant Brown planthoppers, *Nilaparvata lugens*. *Insect Sci.* 28 (4), 1049–1060. doi:10.1111/1744-7917.12829

Moriya, Y., Itoh, M., Okudam, S., Yoshizawam, A. C., and Kanehisa, M. (2007). Kaas: An automatic genome annotation and pathway reconstruction server. *Nucleic Acids Res.* 35, W182–W185. doi:10.1093/nar/gkm321

Mortazavi, A., Williams, B. A., McCue, K., Schaefer, L., and Wold, B. (2008). Mapping and quantifying mammalian transcriptomes by RNA-Seq. *Nat. Methods* 5 (7), 621–628. doi:10.1038/nmeth.1226

Oakeshott, J. G., Claudianos, C., Campbell, P., Newcomb, R., and Russell, R. J. (2015). "Biochemical genetics and genomics of insect esterases," in *Comprehensive molecular insect science*. Editors I. G. Lawrence, I. Kostas, and S. G. Sarjeet (Amsterdam: Elsevier), 309–381.

Oakeshott, J. G., Johnson, R. M., Berenbaum, M. R., Ranson, H., Cristino, A. S., and Claudianos, C. (2010). Metabolic enzymes associated with xenobiotic and chemosensory responses in *Nasonia vitripennis*. *Insect Mol. Biol.* 19, 147–163. doi:10.1111/j.1365-2583.2009.00961.x

Pan, Y. J., Fang, G. Q., Wang, Z. B., Cao, Y. H., Liu, Y. J., Li, G. Y., et al. (2021). Chromosome-level genome reference and genome editing of the tea geometrid. *Mol. Ecol. Res.* 21 (6), 2034–2049. doi:10.1111/1755-0998.13385

Qin, G. H., Jia, M., Liu, T., Zhang, X. Y., Guo, Y. P., Zhu, K. Y., et al. (2013). Characterization and functional analysis of four glutathione S-transferases from the migratory locust, *Locusta migratoria*. *PLoS One* 8 (3), e58410. doi:10.1371/journal.pone.0058410

Qin, G. H., Jia, M., Liu, T., Zhang, X. Y., Guo, Y. P., Zhu, K. Y., et al. (2012). Heterologous expression and characterization of a sigma glutathione S-transferase involved in carbaryl detoxification from oriental migratory locust, *Locusta migratoria* manilensis (Meyen). *J. Insect Physiol.* 58 (2), 220–227. doi:10.1016/j.jinsphys.2011.10.011

Rihani, K., Ferveur, J. F., and Briand, L. (2021). The 40-year mystery of insect odorant-binding proteins. *Biomolecules* 11 (4), 509. doi:10.3390/biom11040509

Schmidt, H. R., and Benton, R. (2020). Molecular mechanisms of olfactory detection in insects: Beyond receptors. *Open Biol.* 10, 200252. doi:10.1098/rsob.200252

Shi, H. X., Pei, L. H., Gu, S. S., Zhu, S. C., Wang, Y. Y., Zhang, Y., et al. (2012). Glutathione S-transferase (GST) genes in the red flour beetle, *Tribolium castaneum*, and comparative analysis with five additional insects. *Genomics* 100 (5), 327–335. doi:10.1016/j.ygeno.2012.07.010

Song, Y. Q., Song, Z. Y., Dong, J. F., Lv, Q. H., Chen, Q. X., and Sun, H. Z. (2021). Identification and comparative expression analysis of odorant-binding proteins in the reproductive system and antennae of *Athetis dissimilis*. *Sci. Rep.* 11 (1), 13941. doi:10.1038/s41598-021-93423-1

Steiner, C., Bozzolan, F., Montagne, N., Maibeche, M., and Chertemps, T. (2017). Neofunctionalization of "juvenile hormone esterase duplication" in Drosophila as an odorant-degrading enzyme towards food odorants. *Sci. Rep.* 7 (1), 12629. doi:10.1038/s41598-017-13015-w

Suh, E., Bohbot, J., and Zwiebel, L. J. (2014). Peripheral olfactory signaling in insects. *Curr. Opin. Insect Sci.* 6, 86–92. doi:10.1016/j.cois.2014.10.006

Sun, D. D., Huang, Y., Qin, Z. J., Zhan, H. X., Zhang, J. P., Liu, Y., et al. (2020). Identification of candidate olfactory genes in the antennal transcriptome of the stink bug *Halyomorpha halys*. *Front. Physiol.* 11, 876. doi:10.3389/fphys.2020.00876

Sun, L., Wang, Q., Wang, Q., Zhang, Y. X., Tang, M. J., Guo, H. W., et al. (2017). Identification and expression patterns of putative diversified carboxylesterases in the tea geometrid *Ectropis obliqua* prout. *Front. Physiol.* 8, 1085. doi:10.3389/fphys.2017.01085

Tang, Q. F., Shen, C., Zhang, Y., Yang, Z. P., Han, R. R., and Wang, J. (2019). Antennal transcriptome analysis of the maize weevil *Sitophilus zeamais*: Identification and tissue expression profiling of candidate odorant-binding protein genes. *Arch. Insect Biochem. Physiol.* 101, e21542. doi:10.1002/arch.21542

Tian, J. H., Zhan, H. X., Dewer, Y., Zhang, B. Y., Qu, C., Luo, C., et al. (2021). Whitefly network analysis reveals gene modules involved in host plant selection, development and evolution. *Front. Physiol.* 12, 656649. doi:10.3389/fphys.2021.656649

Vogt, R. G., and Riddiford, L. M. (1981). Pheromone binding and inactivation by moth antennae. *Nature* 293 (5828), 161–163. doi:10.1038/293161a0

Wang, M. M., Long, G. J., Guo, H., Liu, X. Z., Wang, H., Dewer, Y., et al. (2021). Two carboxylesterase genes in *Plutella xylostella* associated with sex pheromones and plant volatiles degradation. *Pest Manag. Sci.* 77 (6), 2737–2746. doi:10.1002/ps.6302

Wang, R., Li, F. Q., Zhang, W., Zhang, X. M., Qu, C., Tetreau, G., et al. (2017). Identification and expression profile analysis of odorant binding protein and chemosensory protein genes in *Bemisia tabaci* MED by head transcriptome. *PLoS One* 12 (2), e0171739. doi:10.1371/journal.pone.0171739

Waterhouse, A. M., Procter, J. B., Martin, D. M. A., Clamp, M., and Barton, G. J. (2009). Jalview Version 2-a multiple sequence alignment editor and analysis workbench. *Bioinformatics* 25 (9), 1189–1191. doi:10.1093/bioinformatics/btp033

Wei, H. S., Tan, S. Q., Li, Z., Li, J. C., Moural, T. W., Zhu, F., et al. (2020). Odorant degrading carboxylesterases modulate foraging and mating behaviors of *Grapholita molesta*. *Chemosphere* 270, 128647. doi:10.1016/j.chemosphere.2020.128647

Xia, D. S., Zheng, R. W., Huang, J. H., Lu, S. H., and Tang, Q. F. (2022). Identification and functional analysis of Glutathione S-Transferases from *Sitophilus zeamais* in olfactory organ. *Insects* 13 (3), 259. doi:10.3390/insects13030259

Yamamoto, K., and Yamada, N. (2016). Identification of a diazinon-metabolizing glutathione S-transferase in the silkworm, *Bombyx mori*. *Sci. Rep.* 6, 30073. doi:10.1038/srep30073

Yi, J. K., Wang, S., Wang, Z., Wang, X., Li, G. F., Zhang, X. X., et al. (2021). Identification of candidate carboxylesterases associated with odorant degradation in *Holotrichia parallela* antennae based on transcriptome analysis. *Front. Physiol.* 12, 674023. doi:10.3389/fphys.2021.674023

You, Y. C., Xie, M., Ren, N. N., Cheng, X. M., Li, J. Y., Ma, X. L., et al. (2015). Characterization and expression profiling of glutathione S-transferases in the diamondback moth, *Plutella xylostella* (L.). *BMC Genomics* 16 (1), 152. doi:10.1186/s12864-015-1343-5

Younus, F., Chertemps, T., Pearce, S. L., Pandey, G., Bozzolan, F., Coppin, C. W., et al. (2014). Identification of candidate odorant degrading gene/enzyme systems in the antennal transcriptome of *Drosophila melanogaster*. Drosophila melanogaster *Insect Biochem. Mol. Biol.* 53, 30–43. doi:10.1016/j.ibmb.2014.07.003

Zhang, F. M., Merchant, A., Zhao, Z. B., Zhang, Y. H., Zhang, J., Zhang, Q. W., et al. (2020). Characterization of MaltOBP1, a Minus-C odorant-binding protein, from the Japanese pine sawyer beetle, *Monochamus alternatus* Hope (Coleoptera: Cerambycidae). *Front. Physiol.* 11, 212. doi:10.3389/fphys.2020.00212

Zhang, G. H., Yuan, Z. J., Yin, K. S., Fu, J. Y., Tang, M. J., and Xiao, Q. (2016). Asymmetrical reproduce interference between two sibling species of the looper: *Ectropis grisescens* and *Ectropis obliqua*. *Bull. Enotomol. Re.* 11, 1–8. doi:10.1017/S0007485316000602

Zhang, G. H., Yuan, Z. J., Zhang, C. X., Yin, K. S., Tang, M. J., Guo, H. W., et al. (2014). Detecting deep divergence in seventeen populations of tea geometrid (Ectropis obliqua Prout) in China by COI mtDNA and cross-breeding. *PloS One* 9 (6), e99373. doi:10.1371/journal.pone.0099373

Zhang, Y. N., Li, Z. Q., Zhu, X. Y., Qian, J. L., Dong, Z. P., Xu, L., et al. (2017c). Identification and tissue distribution of carboxylesterase (CXE) genes in *Athetis lepigone* (Lepidoptera: Noctuidae) by RNA-seq. *J. Asia Pac. Entomol.* 20 (4), 1150–1155. doi:10.1016/j.aspen.2017.08.016

Zhang, Y. N., Ma, J. F., Xu, L., Dong, Z. P., Xu, J. W., Li, M. Y., et al. (2017a). Identification and expression patterns of UDP-glycosyltransferase (UGT) genes from insect pest *Athetis lepigone* (Lepidoptera: Noctuidae). *J. Asia Pac. Entomol.* 20 (1), 253–259. doi:10.1016/j.aspen.2017.01.008

Zhang, Y. X., Wang, W. L., Li, M. Y., Li, S. G., and Liu, S. (2017b). Identification of putative carboxylesterase and aldehyde oxidase genes from the antennae of the rice leaffolder, *Cnaphalocrocis medinalis* (Lepidoptera: Pyralidae). *J. Asia Pac. Entomol.* 20 (3), 907–913. doi:10.1016/j.aspen.2017.06.001

frontiers | Frontiers in Physiology

TYPE Original Research
PUBLISHED 10 April 2023
DOI 10.3389/fphys.2023.1167174

OPEN ACCESS

EDITED BY
Ettore Tiraboschi,
University of Trento, Italy

REVIEWED BY
Hamadttu Abdel Farag El-Shafie,
University of Khartoum, Sudan
Zhi-Wei Kang,
Hebei University, China

*CORRESPONDENCE
Yong Liu,
liuyong@sdau.edu.cn

†These authors share first authorship

SPECIALTY SECTION
This article was submitted to Invertebrate Physiology, a section of the journal Frontiers in Physiology

RECEIVED 16 February 2023
ACCEPTED 27 March 2023
PUBLISHED 10 April 2023

CITATION
Zhan Y, Wang J, Kong X and Liu Y (2023), Perception and kairomonal response of the coccinellid predator (*Harmonia axyridis*) to the fall armyworm (*Spodoptera frugiperda*) sex pheromone. *Front. Physiol.* 14:1167174. doi: 10.3389/fphys.2023.1167174

Perception and kairomonal response of the coccinellid predator (*Harmonia axyridis*) to the fall armyworm (*Spodoptera frugiperda*) sex pheromone

Yidi Zhan†, Jiaojiao Wang†, Xiaona Kong and Yong Liu*

College of Plant Protection, Shandong Agricultural University, Taian, Shandong, China

Pheromone cues released from hosts or prey are of crucial importance to natural enemies for prey and habitat location. The use of herbivorous insect sex pheromones has long been considered as a potential pest control alternative that is non-toxic and harmless to beneficials. We hypothesized that *Harmonia axyridis* (Pallas) (Coleoptera: Coccinellidae), a major predatory coccinellid beetle of the devastating migratory pest *Spodoptera frugiperda* (Smith) (Lepidoptera: Noctuidae), could perceive and use the sex pheromone of *S. frugiperda* to locate its habitat. Here we tested the electrophysiological and behavioral responses of *H. axyridis* to the two components Z7-12:Ac and Z9-14:Ac of *S. frugiperda* sex pheromone by using electroantennography (EAG) and Y-tube bioassay. The 3D modeling of *H. axyridis* odorant-binding proteins (HaxyOBPs) and molecular docking were also performed. The results showed that both female and male *H. axyridis* exhibited significantly higher electrophysiological and behavioral responses to Z9-14:Ac at the concentrations of 0.001, 0.01, and 0.1 μg/μL, while no significant electrophysiological and behavioral responses of *H. axyridis* were observed to Z7-12:Ac. The blend of Z7-12:Ac and Z9-14:Ac at the ratio of 1:100 had a significant attraction to both male and female *H. axyridis* at the concentrations of 0.01 and 0.1 μg/μL based on electrophysiological and behavioral assays, but no significant behavioral responses were observed at the ratios of 1:9. According to the 3D modeling of HaxyOBPs and molecular docking, HaxyOBP12 has a good affinity with Z9-14:Ac. Z9-14:Ac is bound to the HaxyOBP12 by hydrogen bonding and hydrophobic interactions. However, there were no credible docking results between HaxyOBPs and Z7-12:Ac. Our findings revealed that *H. axyridis* can perceive Z9-14:Ac and could use it as a chemical cue to locate prey habitat. We speculated that Z7-12:Ac, which showed some antagonistic effect toward the response of *H. axyridis* to Z9-14:Ac, could improve the adaptability of *S. frugiperda* in the presence of predators. This study provides new insights into the application of pheromones to manipulate natural enemy behavior for pest control.

KEYWORDS

chemical cue, predatory beetle, Spodoptera frugiperda, odorant-binding protein, population adaptability

1 Introduction

Foraging behavior is a process in which insect natural enemies search for food resources or oviposition sites for survival, growth and reproduction (Kramer, 2001). Natural enemies of herbivores base their foraging decision on chemical cues from plant or herbivorous insects (Kaiser et al., 2017; Peñaflor, 2019). Pheromones released by hosts or prey may serve as kairomonal cues for parasitoids or predators, which can be used as kairomones for natural enemies to locate and control pests (Vaello et al., 2017). Common chemical signals released by the host or prey mainly include sex pheromones (Boo and Yang, 2000; Aukema and Raffa, 2005; Branco et al., 2006; Pekas et al., 2015; Shapira et al., 2018; Wang et al., 2018), alarm pheromones (Pickett et al., 2013; Wang et al., 2019; Liu et al., 2021; Qin et al., 2022), and aggregation pheromones (Kpongbe et al., 2019). To date, pheromone use is a promising way not only to monitor insect pests but to suppress their population growth by improving natural control function in agro-ecosystem.

Insects rely on sensitive olfactory systems to perceive chemical cues. Odorant-binding proteins (OBPs) are responsible for connecting the external environment and odorant receptors (ORs) (Brito et al., 2016). The interaction between OBPs and odor molecules is the first step in insect recognition of chemicals (Leal, 2012). The recognition mechanism of chemical signals of hosts or prey in natural enemies has been investigated within insect olfactory system. For example, aphid alarm pheromone E-β-Farnesene (EβF) was used as a foraging cue for many predators, such as hoverflies (Harmel et al., 2007; Wang et al., 2019), ground beetles (Kielty et al., 1996), green lacewings (Li et al., 2017; Li et al., 2018) and lady beetles (Liu et al., 2014).

Environmentally friendly pest management strategies including the use of natural enemies and pheromones are advocated. For example, slow release of aphid alarm pheromone EβF in wheat fields increases the abundance of mummified aphids by attracting parasitic wasps (Liu et al., 2021). However, the simultaneous use of these two methods may cause synergistic or antagonistic effects. The attraction of natural enemies to pheromones may enhance or interfere with biological control function when the natural enemies are able to generate kairomonal activity towards the pest pheromones (Shapira et al., 2018). Sex pheromone cues may arrest natural enemies to the source and enhance their foraging in the vicinity, thus contributing to the efficiency of pest control (Shapira et al., 2018). Alternatively, sex pheromone may attract natural enemies to the dispensers and reduce their densities in the field, thereby affecting the effectiveness of biological control (Pekas et al., 2015). Knowledge of the kairomonal effects of pheromones on enemies can help to improve lures that recruit and retain natural enemies and to improve the efficiency of biological control of crop pests (Ayelo et al., 2021; Ayelo et al., 2022).

The fall armyworm *Spodoptera frugiperda* (Smith) (*Lepidoptera: Noctuidae*) is a devastating agricultural pest, spreading rapidly in China and causing substantial economic losses (Wang et al., 2020; Wu et al., 2021). Management of *S. frugiperda* relies on the use of chemical insecticides, extracts and metabolites from plants, entomopathogenic bacterium, natural enemies, and sex pheromone traps (Paredes-Sánchez et al., 2021). *Harmonia axyridis* (Pallas) (Coleoptera: Coccinellidae) is a dominant predator that contributes to the suppression of many pests, including various hemipterans, and the larvae and pupae of Coleoptera, Hymenoptera, Diptera, and Lepidoptera (Cheng et al., 2020; Di et al., 2021). *H. axyridis* is a highly voracious predator of the eggs and young larvae of *S. frugiperda*, and can be used as biocontrol agent of this pest (Di et al., 2021). The use of monitoring based on pheromone traps has been shown to be effective to predict the infestation of *S. frugiperda* (Paredes-Sánchez et al., 2021). To date, Z9-14:Ac and Z7-12:Ac are identified as the two principal sex pheromone components of the Yunnan population of *S. frugiperda* (Jiang et al., 2022). However, the functions of these two components on natural enemies remain elusive. So we hypothesized that *H. axyridis* could recognize and detect *S. frugiperda* sex pheromone cues and recruit these cues for prey habitat location and prey location.

Here, we tested the electrophysiological and behavioral responses of *H. axyridis* to the two components Z7-12:Ac and Z9-14:Ac of *S. frugiperda* sex pheromone by using electroantennography (EAG) and Y-tube bioassay. Further tests were performed on the blend of Z7-12:Ac and Z9-14:Ac at the ratios of 1:9 and 1:100 to determine the response of *H. axyridis* to the binary mixture. Subsequently, the binding mechanism between the two pheromone components and *H. axyridis* odorant-binding protein (HaxyOBPs) has been clarified. The potential use of sex pheromone to manipulate the foraging behavior of *H. axyridis* for *S. frugiperda* control in the crops was discussed.

2 Materials and methods

2.1 Insects

Colonies of *H. axyridis* were collected from corn fields at the experimental station of Shandong Agricultural University (Tai'an, Shandong Province, China). Sex determination of *H. axyridis* was based on the labrum pigmentation (female: dark; male: light) and the distal margin of the 5th visible abdominal sternite (female: convex; male: concave) (McCornack et al., 2007). The lady beetles were reared with the wheat aphid *Sitobion miscanthi* (Takahashi) in the laboratory and maintained at 25°C ± 2°C and 65% ± 5% r. h under 12:12 L:D photoperiod. All *H. axyridis* used in this study were naive, and used only once. Before each trial, *H. axyridis* adults were starved for 48 h to enhance their sensitivity to odors.

2.2 Chemicals

(Z)-9-tetradecenal acetate (Z9-14:Ac) and (Z)-7-dodecenyl acetate (Z7-12:Ac) with minimum purity >90% were purchased from Shanghai Yuanye Biotechnology Co., Ltd. n-hexane (≥98%) was purchased from Kaitong Chemical Reagents Co., Ltd., Tianjin, China.

2.3 Comparative EAG responses to the sex pheromone of *S. frugiperda*

The dose-dependent EAG responses of male and female antennae to synthetic standard chemical compounds, Z7-12:Ac,

Z9-14:Ac were investigated. According to AndoLab-PheromoneDatabase, the ratios of the pheromone components of *S. frugiperda* population that broke out in mainland China and east Asia were identified and determined as 1:9 or 1:100, so the blends of Z7-12:Ac and Z9-14:Ac at the ratios of 1:9 and 1:100 were also tested. Five concentrations of each component and the blends (each compound/blend was diluted with n-hexane into solutions of different gradient concentrations at 0.00001 μg/μL, 0.0001 μg/μL, 0.001 μg/μL, 0.01 μg/μL, and 0.1 μg/μL) were tested. Six different antennae were tested as replications for each concentration. Each antenna was stimulated 3 times. The antennae of *H. axyridis* were removed from the base, and the distal tips were also removed. Each dissected antenna was immediately fastened with electrode gel (Spectra 360 Electrode Gel) onto two metal electrodes. Ten microliter of each chemical solution was applied to a piece of filter paper strip (0.8 × 1 cm). The solvent was allowed to evaporate for 1 min, then the paper strip was placed inside a glass Pasteur pipette (5 cm in length, 0.5 cm in internal diameter) in the EAG system directed at the antennal preparation.

The stimuli were provided as 0.5 s puffs of air into a humidified air flow at 0.4 mL/s generated by a stimulus controller. A 15 s interval between successive stimulations was allowed for antennal recovery. EAG response to 10 μL n-hexane was tested as control. Signals were stored and analyzed by using EAG ver. 2.5 software (Synthech, Hilversum, Netherlands).

2.4 Y-tube olfactometer bioassay

The attractiveness of the sex pheromone of *S. frugiperda* to *H. axyridis* was assessed in dual choice assays using a Y-tube olfactometer (common arm, 20.0 cm; arms, 15 cm at 75°angle; internal diameter, 1.5 cm). Air was pumped through an active charcoal filter and re-humidified by passing it through a bottle with distill water before being directed into the two arms of the olfactometer. Chemicals and the blends were prepared in different concentrations (0.00001, 0.0001, 0.001, 0.01 and 0.1 μg/μL) and n-hexane was used as control. An aliquot (10 μL) of each test solution was applied to a filter paper strip (2 × 1 cm^2), and the solvent was allowed to evaporate for 1 min before inserting the strip into an odor-source glass bottle connected to one arm of the olfactometer. The control glass bottle connected to the other arm of the olfactometer contained a filter paper strip treated with 10 μL of hexane. Adult *H. axyridis* was recorded as having made a choice that crossed half of the arm within 5 min. Twenty-five females or males that made a choice were tested for each treatment, individuals making no response to either arm for 5 min were recorded but discarded. The olfactometer was rotated by 90° after each test to avoid any directional bias. The olfactometer was thoroughly washed and rinsed with acetone after five replicates.

2.5 3D modeling and molecular docking

The OBPs sequences of *H. axyridis* were identified by Qu et al. (2021). Two strategies were employed to predict the 3D structure of OBPs. The online program SWISS MODEL (Waterhouse et al., 2018) was used for predicting the OBPs that have >30% homology with the templates in the Protein Data Bank (http://www.rcsb.org/pdb). While the OBPs that have less than 30% homology were generated using a deep residual neural network trRosetta (https://yanglab.nankai.edu.cn/trRosetta; Yang et al., 2020). The final 3D models were assessed by Procheck, Verify_3D and ERRAT (http://services.mbi.ucla.edu/SAVES/).

The binding mode between HaxyOBPs and *S. frugiperda* sex pheromone was performed using Surflex-Dock suit SYBYL X 2.1.1. The results of binding mode were evaluated according to the total score. The PyMOL and LigPlot$^+$ (Laskowski and Swindells, 2011) were used to visualize conformations and interactions.

2.6 Data analysis

Data on EAG responses to each concentration of the sex pheromone components were analyzed using analysis of variance (ANOVA followed by LSD test). Preference numbers of Y-tube olfactory bioassay were evaluated by χ^2 test. Individuals that did not make a choice were excluded from the statistical analysis.

3 Results

3.1 EAG response of *H. axyridis* to *S. frugiperda* pheromone

The dose-EAG responses of male and female antennae of *H. axyridis* to Z7-12:Ac and Z9-14:Ac were measured. Z9-14:Ac elicited higher EAG responses in both females and males than those of Z7-12:Ac (Figure 1). The concentration of 0.0001–0.01 μg/μL Z9-14:Ac caused significantly higher EAG responses in the males than those of Z7-12:Ac and n-hexane (0.0001 μg/μL: $F = 7.072$, $df = 2$, $p = 0.007$; 0.001 μg/μL: $F = 9.884$, $df = 2$, $p = 0.002$; 0.01 μg/μL: $F = 4.971$, $df = 2$, $p = 0.022$; 0.1 μg/μL: $F = 14.782$, $df = 2$, $p < 0.001$) (Figure 1A). Females showed significantly higher EAG responses to Z9-14:Ac at the concentrations of 0.0001 and 0.1 μg/μL than those of Z7-12:Ac and n-hexane (0.0001 μg/μL: $F = 6.956$, $df = 2$, $p = 0.007$; 0.1 μg/μL: $F = 4.682$, $df = 2$, $p = 0.026$) (Figure 1B).

The EAG response of *H. axyridis* to the blend of Z7-12:Ac and Z9-14:Ac at the ratio of 1:100 was higher than that to 1:9 (Figure 2). The responses of male to the ratio of 1:100 were significantly higher than those to 1:9 at the concentration of 0.0001–0.1 μg/μL (0.0001 μg/μL: $F = 5.793$, $df = 2$, $p = 0.012$; 0.001 μg/μL: $F = 6.975$, $df = 2$, $p = 0.007$; 0.01 μg/μL: $F = 7.426$, $df = 2$, $p = 0.006$; 0.1 μg/μL: $F = 9.564$, $df = 2$, $p = 0.002$) (Figure 2A). The female responses to 1:100 were significantly higher than those to 1:9 at the concentrations of 0.001 and 0.1 μg/μL (0.001 μg/μL: $F = 12.157$, $df = 2$, $p = 0.022$; 0.1 μg/μL: $F = 8.472$, $df = 2$, $p = 0.002$) (Figure 2B).

3.2 Olfactory response of *H. axyridis* to *S. frugiperda* pheromone

Behavioral response tests showed that Z7-12:Ac elicited no significant responses of the male and female *H. axyridis* (Figure 3), while *H. axyridis* exhibited strongly attractive response to Z9-14:Ac (Figure 4). At the concentrations ranging from 0.0001 to 0.1 μg/μL, Z9-14:Ac attracted significantly more males than that of n-hexane (Figure 4A), while females showed a

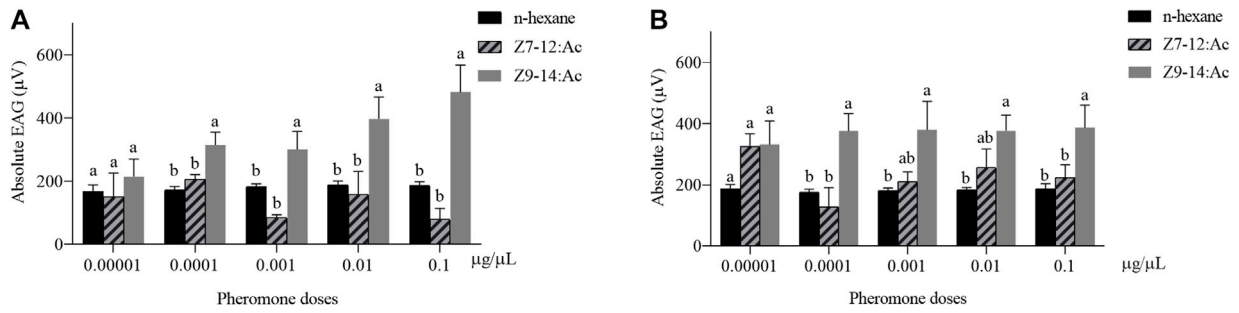

FIGURE 1
Electroantennogram (EAG) responses of male **(A)** and female **(B)** *Harmonia axyridis* to Z7-12:Ac and Z9-14:Ac with various doses (0.00001–0.1 μg/μL). Six different antennae were tested as replications for each concentration. Different letters indicate significant differences between different compounds ($p < 0.05$) at each concentration.

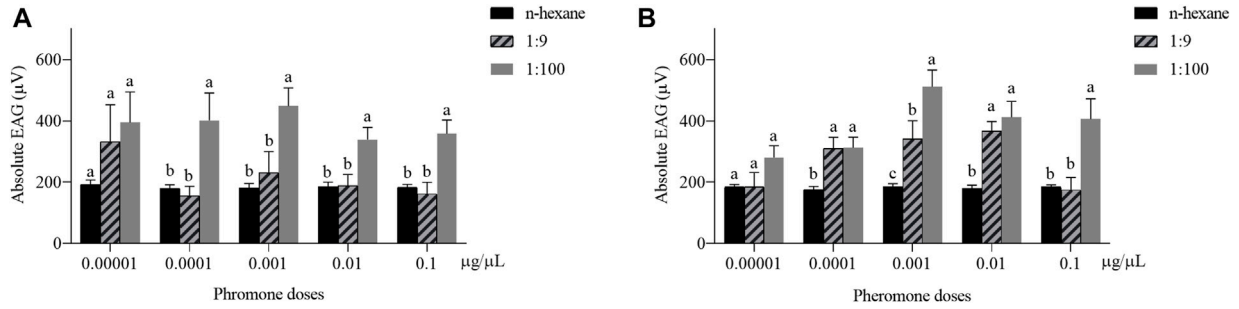

FIGURE 2
Electroantennogram (EAG) responses of male **(A)** and female **(B)** *Harmonia axyridis* to the blend of Z7-12:Ac and Z9-14:Ac at the ratios of 1:100 and 1:9. Six different antennae were tested as replications for each concentration. Different letters indicate significant differences at each concentration ($p < 0.05$).

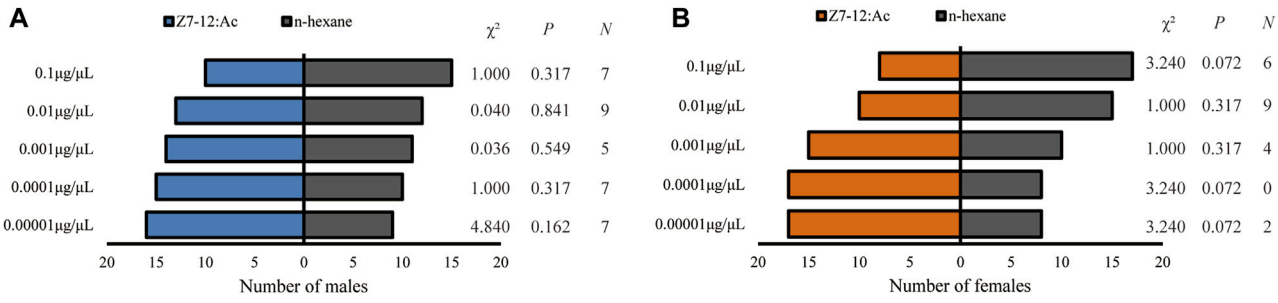

FIGURE 3
Olfactory responses of male **(A)** and female **(B)** *Harmonia axyridis* to Z7-12:Ac in a Y-tube olfactometer. Twenty-five females or males that made a choice were tested for each treatment. N: the number of non-responses.

significant tendency to Z9-14:Ac at the concentrations ranging from 0.001 to 0.1 μg/μL (Figure 4B).

H. axyridis showed completely different olfactory responses to the blends of Z7-12:Ac and Z9-14:Ac at the ratios of 1:9 and 1:100. Neither male nor female showed a preference for a ratio of 1:9 (Figures 5A, B). Males displayed significant preferences for 0.01 and 0.1 μg/μL at the ratio of 1:100 (Figure 5C), and females did for 0.001, 0.01 and 0.1 μg/μL (Figure 5D).

3.3 3D modeling and molecular docking

In order to take insight into the mechanism of the responses of *H. axyridis* to the two components of *S. frugiperda* sex pheromone, 3D modeling of *H. axyridis* odorant-binding protein (HaxyOBPs) and molecular docking were performed. Sequence alignments showed that HaxyOBP12, HaxyOBP13 and HaxyOBP14 shared more than 30% similarity with template proteins

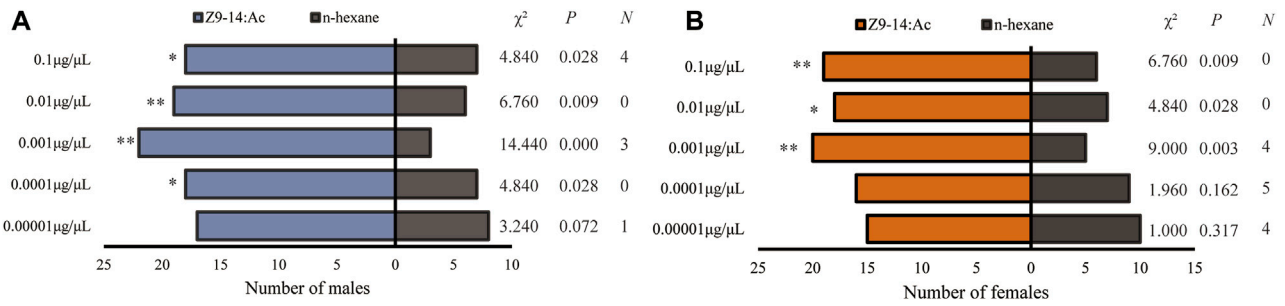

FIGURE 4
Olfactory responses of male **(A)** and female **(B)** *Harmonia axyridis* to Z9-14:Ac in a Y-tube olfactometer. Twenty-five females or males that made a choice were tested for each treatment. N: the number of non-responses. The asterisks indicate significance differences at $p < 0.05$ (*) and $p < 0.01$ (**).

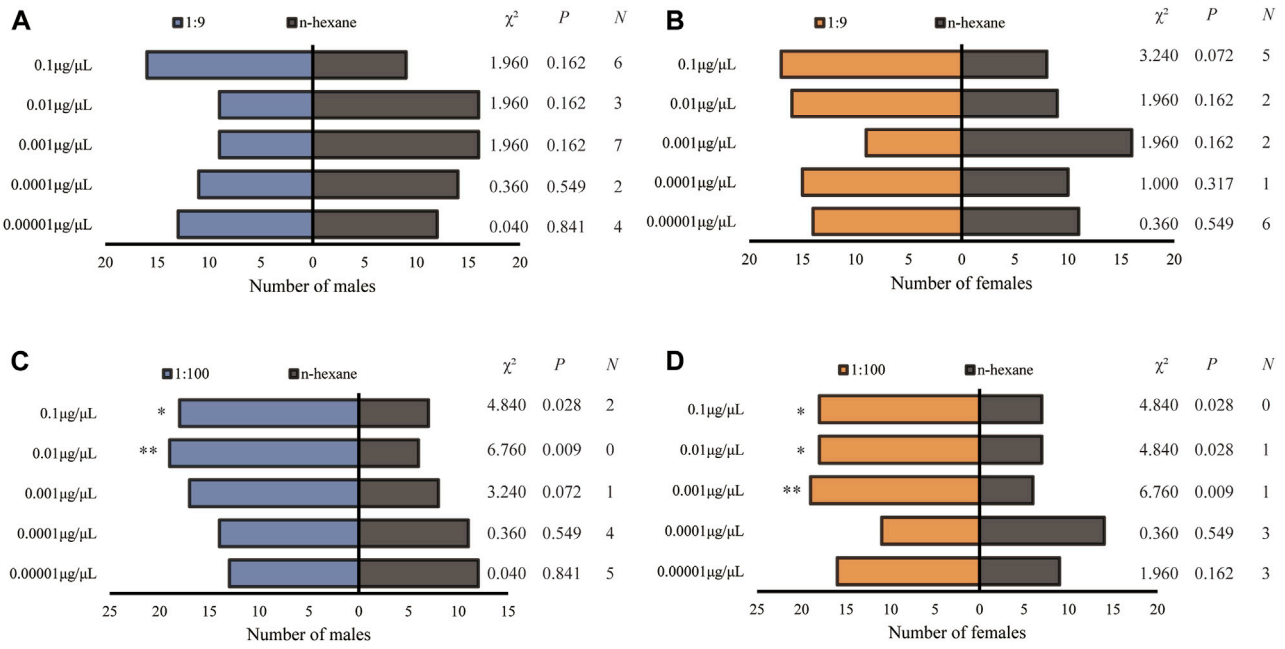

FIGURE 5
Olfactory responses of male and female *Harmonia axyridis* to the blend of Z7-12: Ac and Z9-14: Ac at the ratios of 1:9 (**(A)**: male; **(B)** female) and 1:100 (**(C)**: male; **(D)** female) in a Y-tube olfactometer. Twenty-five females or males that made a choice were tested for each treatment. N: the number of non-responses. The asterisks indicate significance differences at $p < 0.05$ (*) and $p < 0.01$ (**).

(Supplementary Table S1). In addition to these three OBPs, the other 16 OBPs used trRosetta for 3D structure prediction. The predicted results all matched very high (Supplementary Table S2). In order to provide evidence on whether *H. axyridis* could sense and detect *S. frugiperda* sex pheromone Z7-12: Ac and Z9-14: Ac, SYBYL was used to analyze the molecular interactions between identified HaxyOBPs and Z7-12:Ac or Z9-14:Ac respectively. The results revealed that HaxyOBP12 has a good affinity with Z9-14:Ac (Total score = 8.261, C-score = 4). However, there were no credible docking results between HaxyOBPs and Z7-12:Ac (Table 1). Z9-14:Ac bound to HaxyOBP12 by hydrogen bonding interactions and hydrophobic interactions (Figure 6). The Z9-14:Ac was stabilized by a hydrogen bond with Ala119 of HaxyOBP12 (3.00 Å). Additionally, Z9-14:Ac was also buried in tight hydrophobic cavities formed by residues including Thr83, Tyr120, Leu88, Phe121, Ser87, Ala84, Ile72, Gln75, Thr71, Gly68, Leu56, Leu112, Tyr54, Ile80, and Gly68.

4 Discussion

Chemical cues play a key role in mediating the interactions between natural enemies and their hosts or prey. The host or prey can release kairomones that differs from the plant background odors, thus providing the most reliable source of chemical information for natural enemies to detect host and prey in the natural environment (Rodriguez-Saona and Stelinski, 2009; Ayelo et al., 2022). In this study, we examined and determined the kairomonal effect of *S. frugiperda* sex pheromone on the

10.3389/fphys.2023.1167174

TABLE 1 SYBYL docking results.

OBPs	Pheromone	Total score	Crash	Polar	D_score	PMF_score	G_score	Chemscore	C-score
1	Z7	7.4984	−1.3607	0.9609	−113.8115	−6.4901	−213.263	−19.3919	1
	Z9	7.3268	−0.8049	0.8704	−105.3687	26.9388	−222.5839	−18.2059	2
2	Z7	7.5051	−1.3151	0	−108.9621	2.8327	−194.4206	−22.3429	2
	Z9	7.2375	−1.213	1.1738	−102.3625	1.3023	−182.1999	−24.8529	0
3	Z7	5.7676	−2.0033	1.1022	−108.926	7.6937	−186.9444	−18.2901	1
	Z9	6.2581	−2.0055	2.2794	−96.7706	−13.1954	−202.9398	−20.9771	2
4	Z7	4.3342	−0.7624	0	−409.2545	13.2906	−133.6434	−24.8884	3
	Z9	5.0932	−0.5818	1.1844	−425.9345	10.2439	−141.6286	−20.2537	2
5	Z7	7.5756	−0.6529	1.0606	−106.1743	−26.0215	−180.9041	−18.0114	1
	Z9	7.2651	−1.7046	0.6805	−119.396	−1.9989	−227.8684	−23.2066	2
6	Z7	3.5491	−0.7891	1.1178	−77.9468	45.792	−120.6242	−7.3713	2
	Z9	4.4798	−1.1393	2.0942	−73.4433	43.5507	−115.8393	−11.2191	2
7	Z7	7.4842	−0.6505	2.0904	−103.6945	−69.1741	−194.3866	−24.1644	1
	Z9	6.9391	−0.8437	1.3879	−101.1283	−43.8382	−174.9243	−27.272	3
8	Z7	3.339	−1.1489	1.4246	−65.5465	−3.9523	−133.2273	−14.7797	1
	Z9	6.5332	−0.5552	2.5324	−72.0579	−10.2369	−133.3388	−15.2353	1
9	Z7	8.3355	−1.6168	1.3211	−111.1679	−30.8611	−228.47	−20.4871	3
	Z9	8.7695	−1.4592	1.4936	−101.8224	−8.3198	−184.291	−25.9148	1
10	Z7	5.6784	−0.74	1.1019	−90.4941	−33.8735	−162.3957	−19.1104	1
	Z9	5.1383	−1.0542	0	−87.6996	−45.977	−168.931	−23.5797	4
11	Z7	9.2743	−1.0351	0	−121.3123	−54.2514	−227.9555	−27.5486	2
	Z9	8.4632	−2.2112	0	−127.8641	−41.3831	−243.0555	−30.4844	0
12	Z7	7.8721	−3.5849	0	−141.6934	−0.3747	−265.4919	−24.683	3
	Z9	8.261	−2.8121	0.8586	−132.7201	−12.5932	−283.4571	−30.5738	4
13	Z7	7.3845-	−1.8577	2.5499	−94.8605	−7.4795	−184.6	−20.9695	4
	Z9	7.1707	−1.4493	3.4835	−97.4874	−45.7917	−211.037	−29.6366	2
14	Z7	6.9463	−1.2832	0	−96.0042	−22.8851	−203.0978	−17.8821	1
	Z9	5.648	−1.0494	1.0287	−83.3187	−45.7147	−193.2538	−22.8586	2
15	Z7	3.2736	−0.6834	0	−284.6613	−3.0613	−139.3636	−18.6232	2
	Z9	4.8112	−0.8832	1.4739	−304.3181	27.2172	−155.7341	−24.0912	2
16	Z7	7.3746	−1.5197	1.0328	−113.9439	−41.5512	−212.1562	−24.3665	2
	Z9	6.871	−1.563	1.2432	−116.9874	−32.7259	−218.7278	−26.9907	3
17	Z7	6.0605	−1.256	1.171	−97.6921	9.5303	−178.554	−17.05	4
	Z9	5.8333	−0.9551	0.9593	−92.552	7.787	−170.0882	−17.3433	0
18	Z7	5.7515	−2.4271	0	−102.0482	25.0117	−215.5874	−15.5994	0
	Z9	6.2869	−1.1689	1.7872	−91.0506	−5.9071	−154.5452	−21.8616	1
19	Z7	8.0585	−2.0295	0.7858	−118.7177	−24.6058	−232.5992	−23.1932	3
	Z9	7.0481	−1.8582	0	−110.9702	−31.4045	−203.4581	−25.354	3

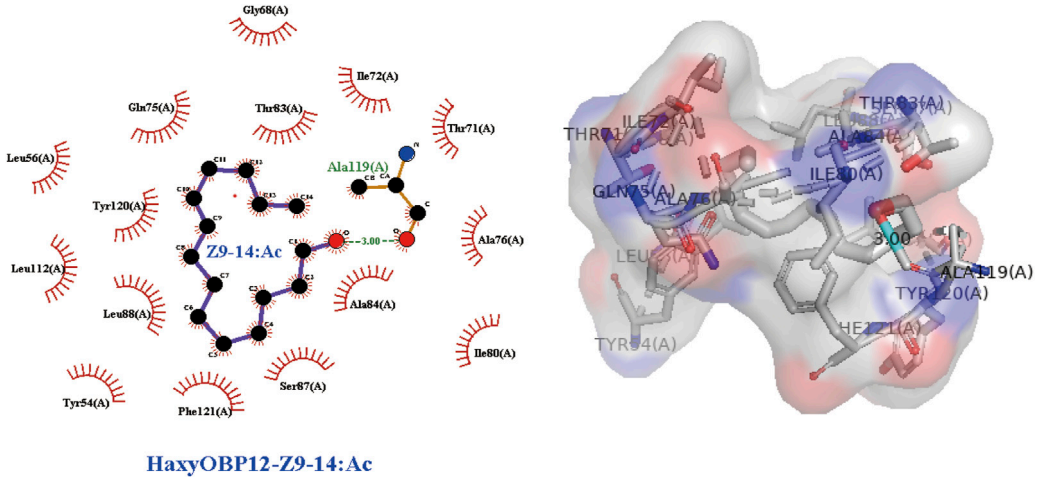

FIGURE 6
Interactions between HaxyOBP12 protein and Z9-14:Ac.

coccinellid predator *H. axyridis*, and the binding properties of *H. axyridis* OBPs to the components of the sex pheromone. Our findings could provide new strategies for the combined application of sex pheromone and natural enemies for *S. frugiperda* control.

The pheromone composition of *S. frugiperda* was inconsistent among different geographic populations (Jiang et al., 2022). To sum up, Z9-14:Ac, Z7-12:Ac, Z9-12:Ac, Z11-16:Ac and E7-12:Ac were employed by different geographic populations (Sekul and Sparks, 1967; Sekul and Sparks, 1976; Tumlinson et al., 1986; Groot et al., 2008; Jiang et al., 2022). The sex pheromone components of the Yunnan population C-strain of *S. frugiperda* are confirmed as Z7-12:Ac and Z9-14:Ac (Jiang et al., 2022). Based on the pre-test of the EAG responses of *S. frugiperda* to the five identified sex pheromone components, we found that Z9-14:Ac and Z7-12:Ac elicited strong electrophysiological responses (Supplementary Figure S1). Therefore, these two components were as the putative candidates for the experiments.

Electrophysiological and olfactory response assays of *H. axyridis* demonstrated that both female and male *H. axyridis* were strongly attracted to Z9-14:Ac. Molecular docking showed that OBP12 and Z9-14:Ac could be closely bonded through hydrogen bonding and hydrophobic interaction, while there was no good docking effect between OBP and Z7-12:Ac. The transcript of *HaxyOBP12* is mainly restricted to adult antennae, implying a potential role in olfactory chemoreception (Qu et al., 2021). These results revealed that *H. axyridis* can sense the stimulation of Z9-14:Ac and transfer the stimulus to its central nervous system. It was suggested that the sex pheromone component Z9-14:Ac of *S. frugiperda* could be recognized by *H. axyridis* and was acted as an important kairomonal signal when *H. axyridis* prey on the eggs and larvae of *S. frugiperda*. Moreover, *HaxyOBP12* is abundant in the larval stage (Qu et al., 2022), indicating that it is also involved in the recognition of Z9-14:Ac by *H. axyridis* in the larval stage to locate prey.

Although *H. axyridis* showed a higher kairomonal response to Z9-14:Ac, further research is needed to determine whether it could be efficient to be used as a pheromone bait to attract and assemble local population of *H. axyridis* in the fields. Several enemies, such as *H. axyridis* (Verheggen et al., 2007), *Coccinella septempunctata* (Ninkovic et al., 2001), the hoverfly *Episyrphus balteatus* (Verheggen et al., 2008), and aphid parasitoids (Liu et al., 2021), are able to perceive the aphid alarm pheromone EβF and show attractant behavior. But in the field, EβF had no effect on the number of predator (Araneae, Opilionidae, Carabidae, Coccinellidae, Staphilinidae, Forficulidae, Syrphidae, Formicidae, Polistinae, Parasitiod, and Chrysopidae) visits to aphid colony or on predator patch residence times (Joachim & Weisser, 2015). Thus, while sex pheromones may have potential for application in agricultural pest management strategies, their ecological role as kairomone in natural settings is worth pondering. The dose-dependent response tests showed that *H. axyridis* seemed to respond to higher concentrations of Z9-14:Ac, suggesting that the potential effect of concentration on natural enemy populations must be taken into consideration when determining the most effective dose to use (Branco et al., 2006).

In addition, *H. axyridis* had a significantly higher response to the mixture of Z7-12:Ac and Z9-14:Ac at the ratio of 1:100 than to 1:9. It suggested that Z7-12:Ac might increase the avoidance effect of Z9-14:Ac on *H. axyridis*. We speculated that insect pest populations have probably evolved in producing a variety of components of sex pheromones with various ratios, thus not only forming reproductive isolation, but also avoiding natural enemy predation or parasite. Therefore, the ratio effect of the two components of *S. frugiperda* sex pheromone on natural enemies should be considered when it is applied for monitoring and control of *S. frugiperda*.

Data availability statement

The original contributions presented in the study are included in the article/Supplementary Material, further inquiries can be directed to the corresponding authors.

Author contributions

YL and JW contributed to the concept and design. JW, YZ, and XK performed the experiments. JW and YZ were involved in

data analysis. YL, YZ, and JW drafted and revised the manuscript. All authors reviewed the manuscript and approved the final manuscript.

Funding

This work was supported by the National Key R&D Program of China (2021YFE0115600).

Conflict of interest

The authors declare that the research was conducted in the absence of any commercial or financial relationships that could be construed as a potential conflict of interest.

Publisher's note

Supplementary material

The Supplementary Material for this article can be found online at: https://www.frontiersin.org/articles/10.3389/fphys.2023.1167174/full#supplementary-material

References

Aukema, B. H., and Raffa, K. F. (2005). Selective manipulation of predators using pheromones: Responses to frontalin and ipsdienol pheromone components of bark beetles in the great lakes region. *Agric. For. Entomol.* 7, 193–200. doi:10.1111/j.1461-9555.2005.00250.x

Ayelo, P. M., Pirk, C. W. W., Yusuf, A. A., Chailleux, A., Mohamed, S. A., and Deletre, E. (2021). Exploring the kairomone-based foraging behaviour of natural enemies to enhance biological control: A review. *Front. Ecol. Evol.* 9, 641974. doi:10.3389/fevo.2021.641974

Ayelo, P. M., Yusuf, A. A., Chailleux, A., Mohamed, S. A., Pirk, C., and Deletre, E. (2022). Chemical cues from honeydew and cuticular extracts of *Trialeurodes vaporariorum* serve as kairomones for the parasitoid *Encarsia formosa*. *J. Chem. Ecol.* 48, 370–383. doi:10.1007/s10886-022-01354-6

Boo, K. S., and Yang, J. P. (2000). Kairomones used by Trichogramma chilonis to find *Helicoverpa assulta* eggs. *J. Chem. Ecol.* 26, 359–375. doi:10.1023/A:1005453220792

Branco, M., Lettere, M., Franco, J. C., Binazzi, A., and Jactel, H. (2006). Kairomonal response of predators to three pine bast scale sex pheromones. *J. Chem. Ecol.* 32, 1577–1586. doi:10.1007/s10886-006-9071-6

Brito, N. F., Moreira, M. F., and Melo, A. (2016). A look inside odorant-binding proteins in insect chemoreception. *J. Insect Physiol.* 95, 51–65. doi:10.1016/j.jinsphys.2016.09.008

Cheng, J., Li, P., Zhang, Y., Zhan, Y., and Liu, Y. (2020). Quantitative assessment of the contribution of environmental factors to divergent population trends in two lady beetles. *Biol. Control* 145, 104259. doi:10.1016/j.biocontrol.2020.104259

Di, N., Zhang, K., Xu, Q., Zhang, F., Harwood, J. D., Wang, S., et al. (2021). Predatory ability of *Harmonia axyridis* (Coleoptera: Coccinellidae) and *Orius sauteri* (Hemiptera: Anthocoridae) for suppression of fall armyworm *Spodoptera frugiperda* (Lepidoptera: Noctuidae). *Insects* 12, 1063. doi:10.3390/insects12121063

Groot, A. T., Marr, M., Schöfl, G., Lorenz, S., Svatos, A., and Heckel, D. G. (2008). Host strain specific sex pheromone variation in *Spodoptera frugiperda*. *Front. Zool.* 5, 20. doi:10.1186/1742-9994-5-20

Harmel, N., Almohamad, R., Fauconnier, M. L., Jardin, P. D., Verheggen, F., Marlier, M., et al. (2007). Role of terpenes from aphid-infested potato on searching and oviposition behavior of *Episyrphus balteatus*. *Insect Sci.* 14, 57–63. doi:10.1111/j.1744-7917.2007.00126.x

Jiang, N. J., Mo, B. T., Guo, H., Yang, J., Tang, R., and Wang, C. Z. (2022). Revisiting the sex pheromone of the fall armyworm *Spodoptera frugiperda*, a new invasive pest in South China. *Insect Sci.* 29 (3), 865–878. doi:10.1111/1744-7917.12956

Joachim, C., and Weisser, W. W. (2015). Does the aphid alarm pheromone (E)-β-farnesene act as a kairomone under field conditions? *J. Chem. Ecol.* 41 (3), 267–275. doi:10.1007/s10886-015-0555-0

Kaiser, L., Ode, P., van Nouhuys, S., Calatayud, P. A., Colazza, S., Cortesero, A. M., et al. (2017). "The plant as a habitat for entomophagous insects," in insect-plant interactions in a crop protection perspective," in *Advances in botanical research*. Editors N. Sauvion, P-A. Calatayud, and D. Thiéry (Londres: Elsevier Ltd.), 179–223. doi:10.1016/bs.abr.2016.09.006

Kielty, J. P., Allen-Williams, L. J., Underwood, N., and Eastwood, E. A. (1996). Behavioral responses of three species of ground beetle (Coleoptera: Carabidae) to olfactory cues associated with prey and habitat. *J. Insect Behav.* 9, 237–250. doi:10.1007/BF02213868

Kpongbe, H., van den Berg, J., Khamis, F., Tamò, M., and Torto, B. (2019). Isopentyl butanoate: Aggregation pheromone of the Brown spiny bug, *Clavigralla tomentosicollis* (Hemiptera: Coreidae), and kairomone for the egg parasitoid *gryon* sp. (Hymenoptera: Scelionidae). *J. Chem. Ecol.* 45, 570–578. doi:10.1007/s10886-019-01081-5

Kramer, D. L. (2001). "Foraging behavior," in *Evolutionary ecology, concepts and cases studies*. Editors C. W. Fox, D. A. Roff, and D. J. Fairbairn (Oxford: Oxford University Press), 232–246.

Laskowski, R. A., and Swindells, M. B. (2011). LigPlot+: Multiple ligand-protein interaction diagrams for drug discovery. *J. Chem. Inf. Model.* 51, 2778–2786. doi:10.1021/ci200227u

Leal, W. S. (2012). Odorant reception in insects: Roles of receptors, binding proteins, and degrading enzymes. *Annu. Rev. Entomol.* 58, 373–391. doi:10.1146/annurev-ento-120811-153635

Li, Z. Q., Zhang, S., Cai, X. M., Luo, J. Y., Dong, S. L., and Cui, J. J. (2017). Three odorant binding proteins may regulate the behavioural response of Chrysopa pallens to plant volatiles and the aphid alarm pheromone (E)-β-farnesene. *Insect Mol. Biol.* 26, 255–265. doi:10.1111/imb.12295

Li, Z. Q., Zhang, S., Cai, X. M., Luo, J. Y., Dong, S. L., and Cui, J. J. (2018). Distinct binding affinities of odorant-binding proteins from the natural predator Chrysoperla sinica suggest different strategies to hunt prey. *J. insect physiol.* 111, 25–31. doi:10.1016/j.jinsphys.2018.10.004

Liu, J. H., Zhao, X. J., Zhan, Y. D., Wang, K., Francis, F., and Liu, Y. (2021). New slow release mixture of E-β-farnesene with methyl salicylate to enhance aphid biocontrol efficacy in wheat ecosystem. *Pest Manag. Sci.* 77, 3341–3348. doi:10.1002/ps.6378

Liu, Y. J., Chi, B. J., Yang, B., Zhu, Y. F., and Yong, L. (2014). Effects of E-β-farnesene release on the spatial distribution patterns of cabbage aphids and lady beetles. *Acta phytophy. Sin.* 41, 754–760.

McCornack, B. P., Koch, R. L., and Ragsdale, D. W. (2007). A simple method for in-field sex determination of the multicolored Asian lady beetle *Harmonia axyridis*. *J. Insect Sci.* 7, 1–12. doi:10.1673/031.007.1001

Ninkovic, V., Al Abassi, S., and Pettersson, J. (2001). The influence of aphid-induced plant volatiles on ladybird beetle searching behavior. *Biol. Control* 21, 191–195. doi:10.1006/bcon.2001.0935

Paredes-Sánchez, F. A., Rivera, G., Bocanegra-García, V., Martínez-Padrón, H. Y., Berrones-Morales, M., Niño-García, N., et al. (2021). Advances in control strategies against *Spodoptera frugiperda*. *A Rev. Mol.* 26, 5587. doi:10.3390/molecules26185587

Pekas, A., Navarro-Llopis, V., Garcia-Marí, F., Primo, J., and Vacas, S. (2015). Effect of the California red scale *Aonidiella aurantii* sex pheromone on the natural parasitism by *Aphytis* spp. in Mediterranean citrus. *Biol. Control* 90, 61–66. doi:10.1016/j.biocontrol.2015.05.016

Peñaflor, M. F. G. V. (2019). "Use of semiochemical-based strategies to enhance biological control," in *Natural enemies of insect pests in neotropical agroecosystems: Biological control and functional biodiversity*. Editors B. Souza, L. L. Vazquez, and R. C. Marucci (Cham: Springer Nature Switzerland), 479–488. doi:10.1007/978-3-030-24733-1_41

Pickett, J. A., Allemann, R. K., and Birkett, M. A. (2013). The semiochemistry of aphids. *Nat. Prod. Rep.* 30, 1277–1283. doi:10.1039/C3NP70036D

Qin, Y. G., Zhang, S. Y., and Li, Z. X. (2022). *Kairomonal effect of aphid alarm pheromones and analogues on the parasitoid* Diaeretiella rapae. PREPRINT (Version 1) available at Research Square. doi:10.21203/rs.3.rs-1706467/v1

Qu, C., Wang, R., Che, W. N., Li, F. Q., Zhao, H. P., Wei, Y. Y., et al. (2021). Identification and tissue distribution of odorant binding protein genes in *Harmonia axyridis* (Coleoptera: Coccinellidae). *J. Integr. Agr.* 20, 2204–2213. doi:10.1016/S2095-3119(20)63297-X

Qu, C., Yang, Z. K., Wang, S., Zhao, H. P., Li, F. Q., Yang, X. L., et al. (2022). Binding affinity characterization of four antennae-enriched odorant-binding proteins from *Harmonia axyridis* (Coleoptera: Coccinellidae). *Front. Physiol.* 13, 829766. doi:10.3389/fphys.2022.829766

Rodriguez-Saona, C., and Stelinski, L. L. (2009). "Behavior-modifying strategies in IPM: Theory and practice," in *Integrated pest management: Innovation and development*. Editor A. K. D. R. Peshin (New York: Springer), 261–312.

Sekul, A. A., and Sparks, A. N. (1976). Sex attractant of the fall armyworm moth. *USDA Tech. Bull.* 1542, 1–6.

Sekul, A. A., and Sparks, A. N. (1967). Sex pheromone of the fall armyworm Moth1: Isolation, identification, and Synthesis23. *J. Econ. Entomol.* 60, 1270–1272. doi:10.1093/jee/60.5.1270

Shapira, I., Keasar, T., Harari, A. R., Gavish-Regev, E., Kishinevsky, M., Steinitz, H., et al. (2018). Does mating disruption of *Planococcus ficus* and *Lobesia botrana* affect the diversity, abundance and composition of natural enemies in Israeli vineyards? *Pest Manag. Sci.* 74, 1837–1844. doi:10.1002/ps.4883

Tumlinson, J. H., Mitchell, E. R., Teal, P. E. A., Heath, R. R., and Mengelkoch, L. J. (1986). Sex pheromone of fall armyworm, *Spodoptera frugiperda* (J.E. Smith). *J. Chem. Ecol.* 12, 1909–1926. doi:10.1007/BF01041855

Vaello, T., Casas, J. L., Pineda, A., de Alfonso, I., and Marcos-García, M. Á. (2017). Olfactory response of the predatory bug *Orius laevigatus* (Hemiptera: Anthocoridae) to the aggregation pheromone of its prey, *Frankliniella occidentalis* (Thysanoptera: Thripidae). *Environ. Entomol.* 46, 1115–1119. doi:10.1093/ee/nvx141

Verheggen, F. J., Arnaud, L., Bartram, S., Gohy, M., and Haubruge, E. (2008). Aphid and plant volatiles induce oviposition in an aphidophagous hoverfly. *J. Chem. Ecol.* 34, 301–307. doi:10.1007/s10886-008-9434-2

Verheggen, F. J., Fagel, Q., Heuskin, S., Lognay, G., Francis, F., and Haubruge, E. (2007). Electrophysiological and behavioral responses of the multicolored Asian lady beetle, *Harmonia axyridis* Pallas, to sesquiterpene semiochemicals. *J. Chem. Ecol.* 33, 2148–2155. doi:10.1007/s10886-007-9370-6

Wang, K., Liu, J., Zhan, Y., and Liu, Y. (2019). A new slow-release formulation of methyl salicylate optimizes the alternative control of *Sitobion avenae* (Fabricius) (Hemiptera: Aphididae) in wheat fields. *Pest Manag. Sci.* 75, 676–682. doi:10.1002/ps.5164

Wang, L., Wang, K., Dong, J., and Liu, Y. (2018). Behavioral responses of *Aphidius avenae* Haliday and *A. gifuensis* Ashmead to the aphid pheromones (E)-β-farnesene and nepetalactone. *Chin. J. Appl. Entomol.* 55, 223–229. doi:10.7679/j.issn.2095-1353.2018.031

Wang, R., Jiang, C., Guo, X., Chen, D., You, C., Zhang, Y., et al. (2020). Potential distribution of *Spodoptera frugiperda* (J.E. Smith) in China and the major factors influencing distribution. *Glob. Ecol. Conserv.* 21, e00865. doi:10.1016/j.gecco.2019.e00865

Waterhouse, A., Bertoni, M., Bienert, S., Studer, G., Tauriello, G., Gumienny, R., et al. (2018). SWISS-MODEL: Homology modelling of protein structures and complexes. *Nucleic Acids Res.* 46 (W1), W296–W303. doi:10.1093/nar/gky427

Wu, Q. L., Jiang, Y. Y., Liu, J., Hu, G., and Wu, K. M. (2021). Trajectory modeling revealed a southwest-northeast migration corridor for fall armyworm *Spodoptera frugiperda* (Lepidoptera: Noctuidae) emerging from the North China Plain. *Insect Sci.* 28, 649–661. doi:10.1111/1744-7917.12852

Yang, J., Anishchenko, I., Park, H., Peng, Z., Ovchinnikov, S., and Baker, D. (2020). Improved protein structure prediction using predicted inter-residue orientations. *Proc. Natl. Acad. Sci. U.S.A.* 117, 1496–1503. doi:10.1073/pnas.1914677117

frontiers | Frontiers in Physiology

TYPE Original Research
PUBLISHED 21 April 2023
DOI 10.3389/fphys.2023.1194370

OPEN ACCESS

EDITED BY
Jia Fan,
Institute of Plant Protection (CAAS), China

REVIEWED BY
Xuexia Miao,
Chinese Academy of Sciences (CAS), China
Letian Xu,
Hubei University, China
Hongjie Li,
Ningbo University, China
Qiuying Huang,
Huazhong Agricultural University, China

*CORRESPONDENCE
Xu-guo Zhou,
xuguozhou@uky.edu
Mu-wang Li,
mwli@just.edu.cn
Qian Wang,
wangqian2017@tongji.edu.cn

RECEIVED 27 March 2023
ACCEPTED 14 April 2023
PUBLISHED 21 April 2023

CITATION
Tang Y-l, Kong Y-h, Qin S, Merchant A, Shi J-z, Zhou X-g, Li M-w and Wang Q (2023), Transcriptomic dissection of termite gut microbiota following entomopathogenic fungal infection. *Front. Physiol.* 14:1194370. doi: 10.3389/fphys.2023.1194370

Transcriptomic dissection of termite gut microbiota following entomopathogenic fungal infection

Ya-ling Tang[1,2], Yun-hui Kong[1], Sheng Qin[1,3], Austin Merchant[4], Ji-zhe Shi[4], Xu-guo Zhou[4]*, Mu-wang Li[1,3]* and Qian Wang[2]*

[1]Jiangsu Key Laboratory of Sericultural Biology and Biotechnology, School of Biotechnology, Jiangsu University of Science and Technology, Zhenjiang, Jiangsu Province, China, [2]Shanghai First Maternity and Infant Hospital, Tongji University School of Medicine, Shanghai, China, [3]Key Laboratory of Silkworm and Mulberry Genetic Improvement, Ministry of Agriculture and Rural Affairs, Sericultural Research Institute, Chinese Academy of Agricultural Science, Zhenjiang, Jiangsu Province, China, [4]Department of Entomology, University of Kentucky, Lexington, KY, United States

Termites are social insects that live in the soil or in decaying wood, where exposure to pathogens should be common. However, these pathogens rarely cause mortality in established colonies. In addition to social immunity, the gut symbionts of termites are expected to assist in protecting their hosts, though the specific contributions are unclear. In this study, we examined this hypothesis in *Odontotermes formosanus*, a fungus-growing termite in the family *Termitidae*, by 1) disrupting its gut microbiota with the antibiotic kanamycin, 2) challenging *O. formosanus* with the entomopathogenic fungus *Metarhizium robertsii*, and finally 3) sequencing the resultant gut transcriptomes. As a result, 142531 transcripts and 73608 unigenes were obtained, and unigenes were annotated following NR, NT, KO, Swiss-Prot, PFAM, GO, and KOG databases. Among them, a total of 3,814 differentially expressed genes (DEGs) were identified between *M. robertsii* infected termites with or without antibiotics treatment. Given the lack of annotated genes in *O. formosanus* transcriptomes, we examined the expression profiles of the top 20 most significantly differentially expressed genes using qRT-PCR. Several of these genes, including APOA2, Calpain-5, and Hsp70, were downregulated in termites exposed to both antibiotics and pathogen but upregulated in those exposed only to the pathogen, suggesting that gut microbiota might buffer/facilitate their hosts against infection by finetuning physiological and biochemical processes, including innate immunity, protein folding, and ATP synthesis. Overall, our combined results imply that stabilization of gut microbiota can assist termites in maintaining physiological and biochemical homeostasis when foreign pathogenic fungi invade.

KEYWORDS

termite, odontotermes formosanus, metarhizium robertsii, *de novo* assembly, innate immunity, gut microbiota

1 Introduction

Microbial symbionts inhabit the guts of many insects, including beetles, silkworms, fruit flies, and termites (Cheng et al., 2017; Garcia-Robles et al., 2020; Li et al., 2021; Vikram et al., 2021). Gut microbiota can be seen as a virtual organ whose existence is indispensable to the life of the host (Gravitz, 2012). Termites possess a wide variety of gut symbionts, including but not limited to bacteria, protists, and fungi, which play many important roles in physiological and biochemical processes such as social alarm, hygienic responses, metabolic capacity, and immunity (Xiong, 2022).

Termites are social insects that live in colonies consisting of three basic caste types: workers, soldiers, and reproductives (He et al., 2018). Because they often live in the soil or in decaying wood, pathogens found in these substrates pose a significant threat to termite colonies (Peterson and Scharf, 2016a). How termites contend with these threats, through mechanisms such as individual and social immunity, has gradually become a new hot spot for research (Avulova and Rosengaus, 2011; Cremer et al., 2018; Hong et al., 2018).

The defensive function of gut microbiota against invading pathogens has been studied in other insects (Zhou et al., 2020; Deng et al., 2022). *Serratia* and other symbionts render mosquitoes resistant to plasmodium infection through activation of the host immune system or by secreting antimalarial enzymes (Xi et al., 2008; Ramirez et al., 2012; Bai et al., 2019; Gao et al., 2021). In *Drosophila*, gut microbiota help flies fight pathogens by mediating the renewal of intestinal epithelial cells, and expression of host immune-related genes is altered after the removal of intestinal microorganisms (Buchon et al., 2009; Douglas, 2018).

The lower termites possess particularly robust defenses against fungal pathogens. Individual workers may ingest a large number of fungal spores while grooming nestmates, which become inactive in the gut and do not germinate (Chouvenc et al., 2009). An antimicrobial peptide with antifungal activity, Termicin, was discovered, in addition to synthesis by gut protozoa of the multifunctional β-1,3-glucanases, which break down fungal cell walls (Rosengaus et al., 2014). Similarly, intestinal symbionts protect lower termites from entomopathogenic fungi by producing antifungal compounds and collaborating with host endogenous compounds containing antifungal peptides or enzymes (Peterson and Scharf, 2016b).

In *Odontotermes formosanus*, a higher termite, only bacterial symbionts are found in the gut (Liu et al., 2013; Hu et al., 2019). Comparably less research has been done on the contributions of bacterial symbionts to termite immunity relative to protists (Peterson and Scharf, 2016a). Previous research on termite immunity has revealed differences in species diversity and relative abundance of the gut microbiota between healthy and pathogen-infected termites (Liu et al., 2015). In addition, the composition and diversity of intestinal symbionts influences gene expression in the termite gut (Xi et al., 2008; Gao et al., 2021). Therefore, it is important to investigate the impacts of bacterial symbionts on termite physiology and immunity.

In this study, we changed the abundance and load of gut microbiota in the hindgut of the higher termite, *O. formosanus*, which is widely distributed in China, with a broad-spectrum antibiotic, kanamycin, a bacterial antibiotic which binds to the bacterial ribosome 30S subunit to inhibit protein synthesis (Shu et al., 2011). In our previous 16s rDNA sequencing experiment, we found kanamycin significantly impacted intestinal composition, especially *Firmicutes* and *Spirochete*. Then, we infected termites with a pathogenic fungus, *Metarhizium robertsii*, and measured the expression changes of genes related to immunity and energy metabolism in intestinal tissue. Analyzing the effects of specific gene expression changes following immune challenge contributes to further understanding of the symbiotic relationship between gut microbiota and their termite hosts and can also provide reference and inspiration for related research in other insects.

2 Materials and methods

2.1 Experimental insects and setup

O. formosanus colonies were collected from Lion Mountain (Huazhong Agricultural University, Wuhan, Hubei, China) in July 2020. Termites were transferred from pieces of rotting wood to 9 cm diameter Petri dishes with filter paper and placed in darkness for 24 h to stabilize the community. Afterwards, termites were maintained in 9 cm diameter Petri dish in 24-h darkness at 25°C ± 1°C and were fed with filter paper soaked with sterile water that was changed once every 2 days. *M. robertsii* ARSEF#2575 was obtained from the Institute of Plant Physiology and Ecology, Chinese Academy of Sciences, Shanghai. *M. robertsii* spores were grown on Potato Dextrose Agar medium (PDA) (200 g potato, 20 g glucose, 15–20 g agar, 1000 mL distilled water) and washed with 0.1% Tween 80 solution. Spore concentration was measured with a hemocytometer, then spores were stored at 4°C as a spore suspension. The concentration of antibiotics used was determined by previous research (Peterson et al., 2015).

Before fungal infestation, we separated termite colonies into four experimental groups (control groups/CT: treated with sterilized water; Kana groups/AT: treated with 5% kanamycin; Kana_ infected groups/IAA: treated with 10^8 spores/mL suspension at 48 h time point after treatment with 5% kanamycin; Infected groups/MI: treated with 10^8 spores/mL suspension at 48 h time point), with every group consisting of three biological replications containing 30 termites each. 5% kanamycin means that the ratio of powder to distilled water is 1:20. Termites were reared on a filter paper soaked with 1 mL of the corresponding solution for their treatment group. Before dissecting, all termite samples were placed on ice and 75% ethanol was used to remove any surface microorganisms. We use anatomical forceps to tear open the abdominal epidermis of termites under a posture microscope, pull out the intestine, and ensure its integrity then transferred to an empty Eppendorf tube. The entire process is immersed in 1× sterile PBS (Phosphate Buffer Solution). All gut samples were stored at −80°C until RNA extraction.

2.2 RNA extraction

All samples were homogenized in Trizol (Ambion/Invitrogen, United States) following the manufacturer's protocol, purified by isopropanol precipitation, and dissolved in DEPC water. Each treatment contains 30 termite samples and sets up 3 biological replicates. RNA concentration was measured using 1% agarose gel electrophoresis and a Nano-Drop 2000 spectrophotometer. RNA

completion was measured using an Agilent 2,100 bioanalyzer. Then, RNA products were stored in a −80°C cryogenic refrigerator.

2.3 Library preparation and sequencing

Library preparation and sequencing were performed by Novogene (Tianjin, China) on an Illumina NovaSeq 6,000 (Illumina Inc., San Diego, United States) platform. mRNA was isolated using Oligo (dT) magnetic beads (Thermo Fisher Scientific, Waltham, Mass., United States). Subsequently, the obtained mRNA was fragmented using NEB Fragmentation Buffer (New England Biolabs (Beijing) LTD., Beijing, China). Using fragmented mRNA as a template and random oligonucleotides as primers, the first strand of cDNA was synthesized using the M-MuLV reverse transcriptase system, and the RNA strand was degraded using RNase H (TAKARA Bio, Beijing, China). In the DNA polymerase I system, dNTPs (TAKARA Bio, Beijing, China) were used as primers to synthesize the second strand of cDNA. The purified double-stranded cDNA underwent end-repair, A-tailing, and ligation of sequencing adapters. AMPure XP beads (Beckman Coulter, Shanghai, China) were used to screen 250-300bp cDNAs, then PCR amplification was performed and AMPure XP beads were used again to purify the PCR products, which constituted the complete library. After the library was constructed, preliminary quantification was carried out using a Qubit2.0 Fluorometer (Thermo Fisher Scientific, Waltham, Mass., United States), then, library concentration was diluted to 1.5 ng/μL. Next, insert size was assessed with an Agilent 2,100 bioanalyzer (Agilent Technologies, Beijing, China). The raw data were submitted to NCBI (National Center for Biotechnology Information) databases (Accession numbers: PRJNA926100).

2.4 De novo assembly and functional annotation

Adapter and low-quality reads were filtered by Fastp (version 0.19.7) (Chen et al., 2018) with default parameters in order to obtain clean data. Clean data was assembled to contigs using Trinity (v2.4.0) software with min_kmer_cov:3 and other default parameters (Grabherr et al., 2011). Based on Trinity splicing, transcripts were aggregated into clusters according to shared reads between transcripts by Corset (v4.6) (Davidson and Oshlack, 2014) with default parameters. Annotation to the NCBI Non-redundant Protein Sequences (NR), Nucleotide (NT), Eukaryotic Orthologous Groups (KOG), Swiss-Prot, Protein Families (PFAM), Gene Ontology (GO), and KEGG Orthology (KO) databases was carried out using BLASTX for all assembled unigenes (E-value≤1e-5) (Altschul et al., 1997; Moriya et al., 2007; Kanehisa et al., 2008; El-Gebali et al., 2019).

2.5 Differential gene expression analysis

The transcripts were assembled using Trinity as reference sequence and clean data were mapped to the reference sequence using RSEM and bowtie2 with default parameters (Li and Dewey, 2011). Then, read counts were obtained by calculating the bowtie2 result and the FPKM value of each gene was derived. Differences in gene expression were analyzed using the DESeq2 R package (1.6.3) with default parameters. Finally, $|\log2FoldChange| > 1$ and P-adj < 0.05 were set as standards to identify differentially expressed genes (DEGs) (Wang et al., 2010; Love et al., 2014).

2.6 KEGG and GO enrichment of DEGs

Enriched GO terms among differentially expressed genes were identified using GOseq (Young et al., 2010) and KOBAS3.0 was used to analyze the statistical enrichment of DEGs among KEGG pathways (Mao et al., 2005).

2.7 Quantitative real-time PCR (qRT-PCR)

A total of 1.0 μg of RNA was reverse-transcribed *in vitro* using a PrimeScript™ RT reagent kit, following the manufacturer's instructions. The cDNA products were used as a template for real-time qPCR. RT-qPCR was used to detect gene expression levels. The primers used in this study were designed by NCBI Primer-BLAST software (https://www.ncbi.nlm.nih.gov/tools/primer-blast/) and are shown in Table 1. The reaction mixtures were prepared using a NovoStart® SYBR qPCR SuperMix Plus kit (Novoprotein Technology Ltd., China), following the manufacturer's instructions. A 10 μL qPCR reaction system was used, including 5 μL of 2 × NovoStart® SYBR qPCR SuperMix Plus, 0.5 μL of upstream and downstream primers, 1.5 μL of the template, and 2.5 μL of ddH2O. The reactions were performed on a LightCycler® 96 System (Roche, Basel, Switzerland). The following qPCR protocol was used: 1 cycle at 95°C for 5 min, followed by 40 cycles at 95°C for 20 s, and 54°C for 40 s. The $2^{-\Delta\Delta CT}$ method was adopted to calculate relative gene expression levels. Each group was repeated three times. β-actin was used as the internal reference gene (Supplementary Table S4).

3 Results

3.1 Kanamycin accelerates termite death by compromising its gut microbiota

To verify which antibiotics can play a significant role in removing termite intestinal microorganisms, we fed termites with four different common antibiotics and measured the change in total bacteria abundance at multiple time points (0, 24, 48, and 72 h) using qRT-PCR (primers shown in Table 1, termite *β-actin* as reference gene). The total bacterial changes in the guts of termites exposed to four different antibiotic treatments are shown in Figure 1. The largest change was observed in the kanamycin-treated individuals, particularly at the 24 h time point ($p < 0.0001$) (Figure 1A a). Based on the results of this assay, kanamycin was ultimately selected as the antibiotic to be used in the following experiments.

TABLE 1 Summary of *de novo* assembled transcriptomes.

Samples	Raw reads	Raw bases (G)	Clean reads	Clean bases (G)	Error rate (%)	Q20 (%)[1]	Q30 (%)[1]	GC (%)
AT-1	29548065	8.9	29066618	8.7	0.03	97.03	91.93	37.25
AT-2	27438745	8.2	27008031	8.1	0.03	97.09	91.95	38.28
AT-3	31207335	9.4	30672455	9.2	0.03	97.31	92.41	38.64
MI-1	28509413	8.6	27855614	8.4	0.03	97.17	92.19	36.94
MI-2	28951294	8.7	28588750	8.6	0.03	97.18	92.19	38.90
MI-3	25660698	7.7	25350768	7.6	0.03	97.17	92.20	37.51
CT-1	29767000	8.9	29024356	8.7	0.03	97.72	93.21	36.46
CT-2	30811690	9.2	29749815	8.9	0.03	97.86	93.65	38.92
CT-3	32076085	9.6	31439083	9.4	0.03	96.85	91.21	36.44
IAA-1	28976224	8.7	27930028	8.4	0.03	97.03	91.77	39.59
IAA-2	3,3562021	10.1	32117335	9.6	0.03	95.99	89.79	40.71
IAA-3	35311566	10.6	34005244	10.2	0.03	96.11	89.93	40.32

[1] Q20/Q30 stands for the percent of bases with quality score [-10 * lg (error rate)] more than 20 and 30 (indicating error rates of 1% and 1‰, respectively).

Moreover, there was no significant difference in the survival rate of kanamycin treated termites at 48 h compared to controls (Figure 1B). At 72 h, mortality was significantly higher in the kanamycin-treated group ($p < 0.0001$). This result suggests that termites remain in a healthy state of life for at least 48 h after intestinal microorganism inhibition. Therefore, we chose to treat termites with antibiotics for 48 h before *M.robertsii* infection in subsequent experiments.

3.2 Transcriptome sequencing, assembly, and annotation

In this study, a total of 108.6 Gb of raw data were obtained from Illumina sequencing. After quality control, a total of 105.8 Gb of clean data was used for further analysis (Table 1). There were 142531 transcripts and 73608 Unigenes obtained by Trinity; their N50 length was 3,655 and 2746bp, respectively (Supplementary Tables S1,S2).

All Unigenes were annotated to NR, NT, KO, Swiss-prot, PFAM, GO, and KOG databases by BLASTx. 52.98% of unigenes were annotated to at least one database. The proportion of unigenes annotated to each of the seven databases was 37.72, 21.94, 13.01, 22.2, 31.31, 31.31, and 11.67%, respectively (Supplementary Table S3).

Annotated genes were placed into one of three groups based on GO classification: BP (biological process), CC (cellular component), or MF (molecular function) (Supplementary Figure S1). Among BP genes, cellular process and metabolic process were the most common classifications. Among CC genes, cellular anatomical entity, intracellular, and protein-containing complex were the most common classifications. Among MF genes, binding and catalytic activity were the most common classifications.

In total, 8,594 genes were annotated to the KOG database across 26 functional categories (Supplementary Figure S2). Over 13% of genes were annotated to the "General function prediction only" category, followed by "Posttranscriptional modification, protein turnover, chaperones" (13.25%), "Translation, ribosomal structure and biogenesis" (11.74%), and "Signal transduction mechanisms" (11.15%). Categories with the fewest annotations included "Extracellular structures" (0.08%), "Defense mechanisms" (0.06%), "Nuclear structure" (0.04%) and "Unnamed protein" (0.002%).

A total of 11300 genes were annotated to the KEGG pathway, distributed among 291 unique KEGG pathways. The highest number of genes were annotated to the "Cellular Processes" (1810, 16.01%), "Environmental Information Processing" (1475, 13.05%), "Genetic Information Processing" (2022, 17.89%), "Metabolism" (3,062, 27.10%) and "Organismal Systems" pathways (2,799, 24.77%) (Figure 2). Additionally, 538 genes (4.76%) were assigned to the immune system.

3.3 Identification of DEGs following antibiotic treatment and/or pathogen exposure

To identify the immune effect of the inhibition of gut microorganisms on termites exposed to entomopathogenic fungi, we used DESeq2 software to analyze differences in gut gene expression between termites from four different treatment groups. A corrected *p*-value of 0.05 and log2fold-change of ±1 was set as thresholds for significant differential expression. Overall, 43 unigenes were upregulated and 57 were downregulated in MI compared to CT termites; 2,204 were upregulated, and 1610 were downregulated in IAA compared to CT termites; 2,711 were upregulated and 2,244 were downregulated in IAA compared to MI termites; 1160 were upregulated and 1133 were downregulated in IAA compared to AT termites; and 125 were upregulated and 204 were downregulated in AT compared to MI termites (Supplementary Figure S3). When termites are infected by *M. robertsii*, their gut microbiota can adapt to the external environment to a certain extent. Similarly, following antibiotics treatment, the impact on uninfected termites is smaller. A total

10.3389/fphys.2023.1194370

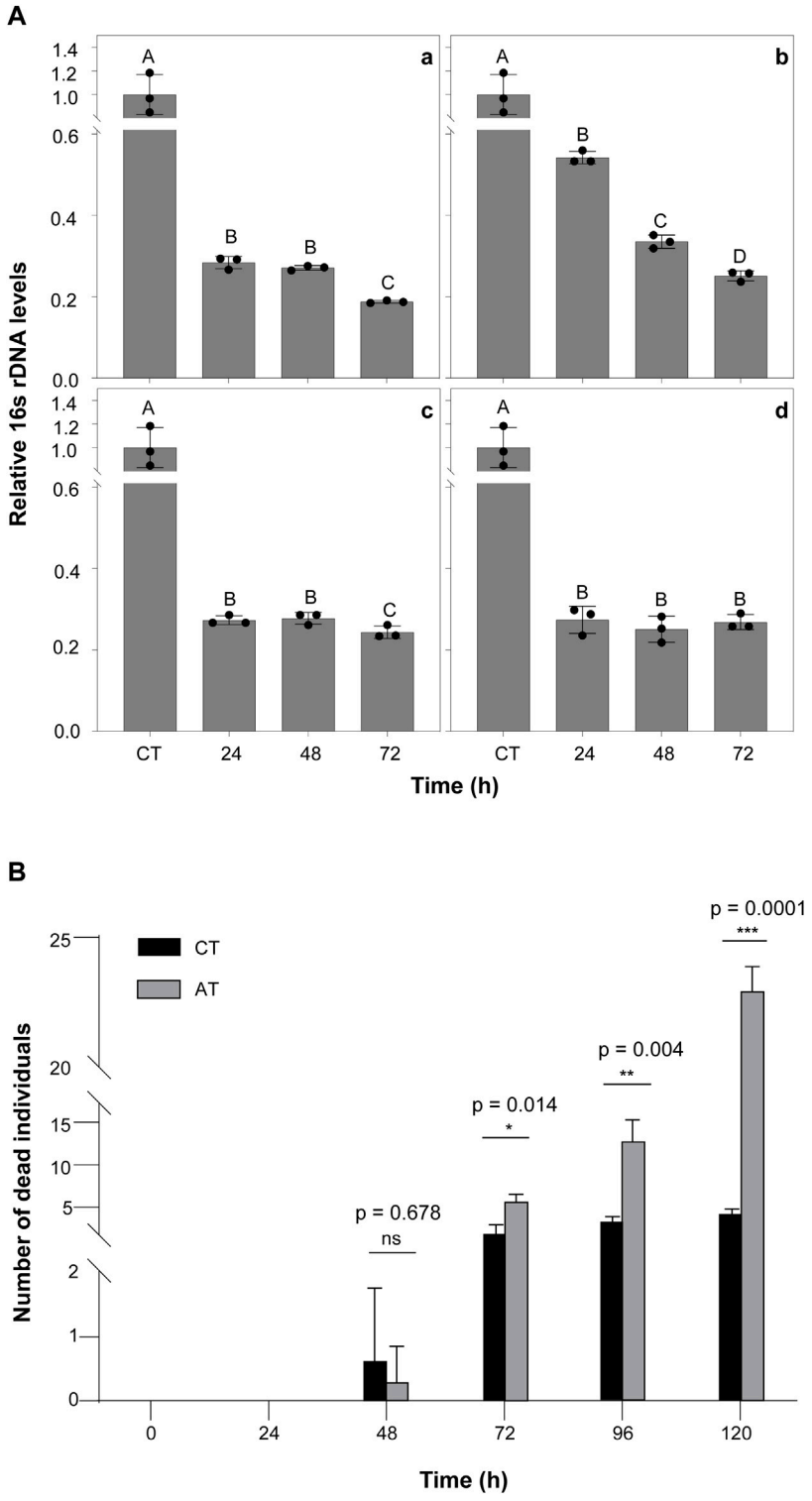

FIGURE 1
The Effect of Antibiotics on Termites **(A)** The effects of antibiotic treatment on bacterial symbiont abundance in the termite gut. The qPCR results for total bacteria in the guts of termites treated with 5% Kanamycin (a), 5% Ampicillin (b), 5% Streptomycin (c), and 2.5% Tetracycline (d). β-actin was used to normalize the data, which are shown as mean ± standard error; the mean was obtained from three independent replications. The $2^{-\Delta\Delta CT}$ method was used to calculate the relative expression level. Statistical differences between time points, determined with an unpaired *t*-test, are shown via GraphPad Prism8. Different letters indicate significant differences (B means $p < 0.0001$, C means $p < 0.05$). **(B)** Number of dead termite individuals fed with 5% kanamycin.AT termites were fed with 5% kanamycin, while CT termites were fed with sterile water. The experiments were performed in three biological replicates. Kanamycin significantly increased mortality compared with the control group after 72 h ($p < 0.05$). The experiments were performed in three biological replicates (n = 30 per replicate). Statistical differences between treatment at every time points, determined with an paired *t*-test, are shown via GraphPad Prism8.

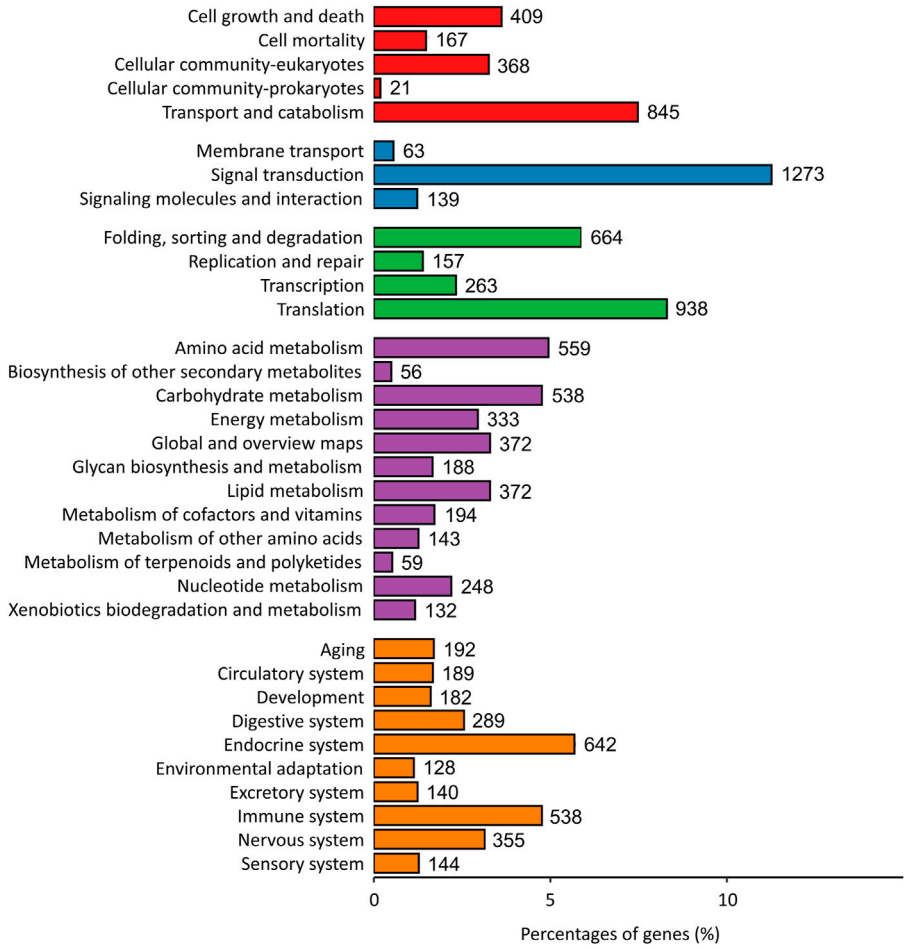

FIGURE 2
KEGG metabolic pathway classification. Annotated genes were assigned into one of five categories based on predicted function (Red bar: Cellular Processes; Blue bar: Environmental Information Processing; Green bar: Genetic Information Processing; Purple bar: Metabolism; Orange bar: Organismal Systems).

FIGURE 3
Venn diagram of DEGs among four pair-wise comparison groups.

of 22 DEGs were identified between the MI: CT group, 115 between the AT: CT group, 555 between the IAA:AT group, and 3,070 between the IAA:MI group (Figure 3).

3.4 Enrichment analysis of DEGs reveals the existence of gut symbionts that maintain termite intestinal stability during fungal invasion

After identifying the numbers of DEGs among different pairs of the four treatment groups, we also examined the placement of these DEGs among KEGG pathways (Figure 4).

When we examined DEGs identified in the AT:CT group, it was found that most metabolic pathways did not change in kanamycin treating 48 h, indicating that antibiotic treatment had no negative effect on gene expression or the physiological status of the termite intestinal tract itself. Examination of DEGs identified in the MI:CT group also yielded a low number of metabolic pathways showing change despite infection by *M. robertsii*. DEGs identified in the IAA:AT and IAA:MI

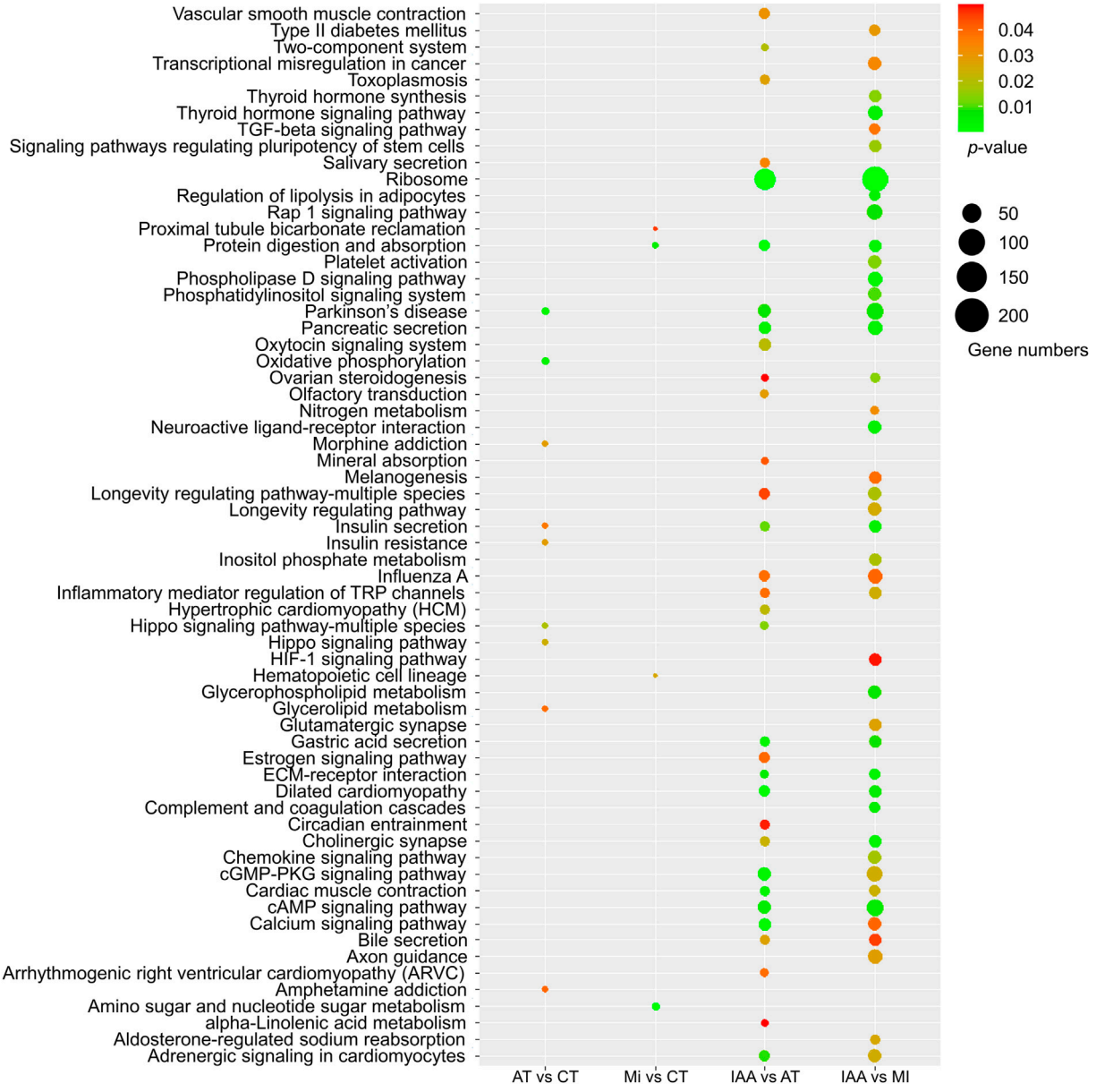

FIGURE 4
KEGG enrichment of DEGs identified in each comparison group. The size of the dot indicates the number of genes, and the *p*-value was derived by hypergeometric tests.

groups suggest significant changes in several metabolic pathways, including the cAMP and calcium signaling pathways. In addition, MAPK signaling pathway were enriched in IAA: CT groups by KEGG enrichment (Supplementary Figure S4A). These results demonstrate that the presence of intestinal microorganisms can alleviate the metabolic effect of fungal invasion to a certain extent.

The GO classification of DEGs identified in each comparison group was also examined (Figure 5). DEGs identified in the AT:CT and MI:CT comparisons showed minimal changes within the CC and MF categories. DEGs placed in the BP category mostly involved membrane-related reactions. DEGs identified in the IAA:AT and IAA:MI comparison groups were spread between all three GO categories.

The results of KEGG and GO enrichment indicate that a change in intestinal symbionts alters host gene expression in the gut and causes the transformation of many metabolic pathways. However, unexpectedly, the main enriched pathways were not directly related to immunity, but indirect pathways such as signal transduction, indicating that gut microorganisms may affect host immunity through other forms of regulation.

3.5 qRT-qPCR analysis

To further evaluate the DEGs identified in the transcriptome and better explain the role of intestinal microorganisms in termite

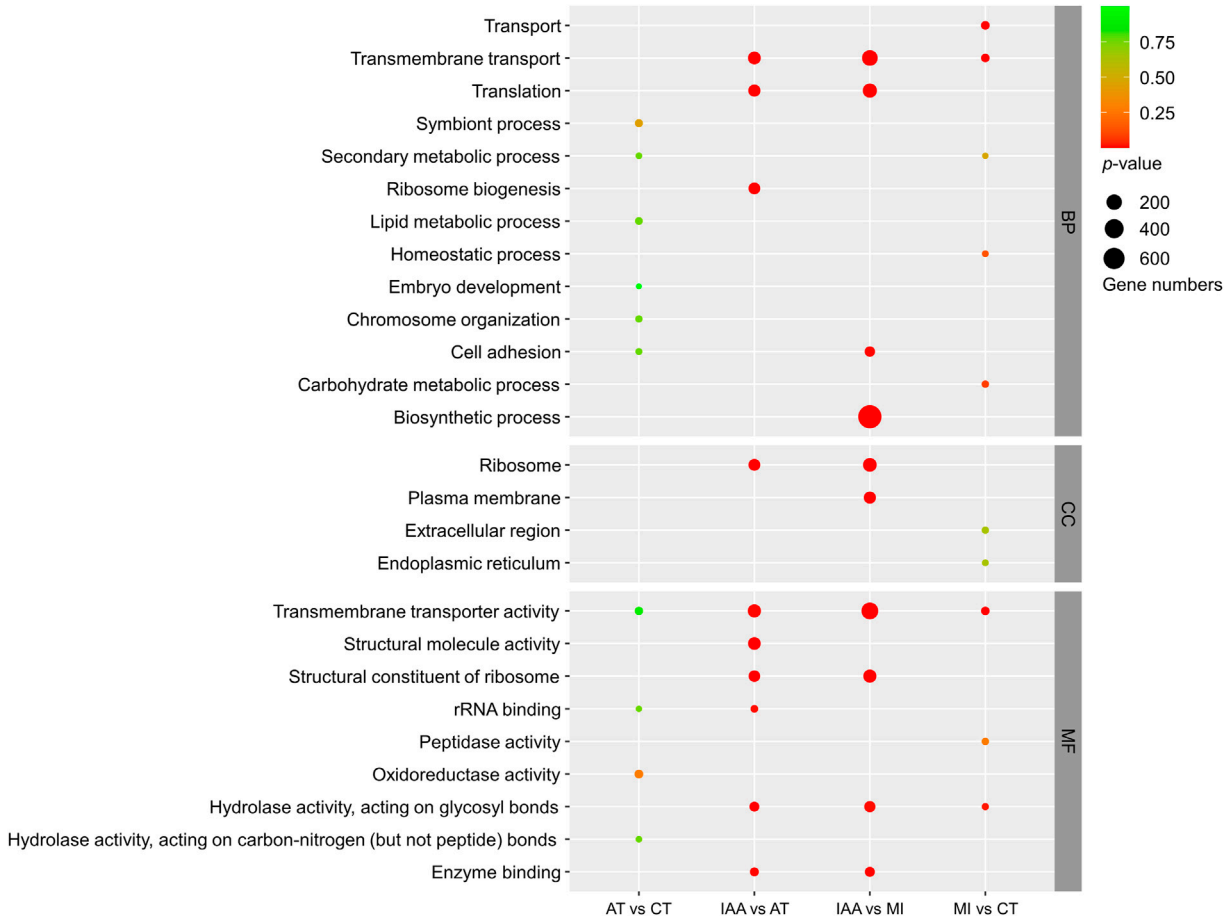

FIGURE 5
GO enrichment of DEGs identified in each comparison group. The size of the dot indicates the number of genes, and the *p*-value was derived by hypergeometric tests. BP: Biological Process; CC: Cellular Component; MF: Molecular Function.

immunity, we carried out real-time fluorescent quantitative PCR validation of the top 20 genes showing the most significant changes in expression among our comparison groups (Figure 6). We chose β-actin as the reference gene for validation. The primers used are listed in Supplementary Table S4 and Blast results are shown in Supplementary Table S5.

Gene expression patterns were divided into five groups. Eight genes showed lower expression in the AT and IAA treatments than in the MI treatment, while expression in the CT and MI treatments was relatively equal (Figure 6A). These eight genes are mainly involved in the process of reverse transcription and cell division. The second group of genes, four in total, showed upregulation in the MI treatment, downregulation in the IAA treatment, and no change in the AT treatment (Figure 6B). These genes included *ApoA2*, *Cal-5-like*, and *Hap*. The third group of genes, three in total, were downregulated in all non-CT treatments and included genes involved in sodium and potassium ion transport (Figure 6C). The change in the internal environment of termites treated with antibiotics and/or pathogens or the influence of external stimuli may inhibit this process. Next, the gene *chitinase5* mainly functions as a chitinase and participates in the decomposition of β-1,4-glucan (Figure 6D), which is the main component of plant cellulose, indicating that the antibiotic treatment does not affect the ability of termites to degrade cellulose at this time point. In addition to the genes that cannot be annotated, in these three genes, *hsp70* showed that all the treatment groups were upregulated. But *ATP-syn* expressed in MI was higher than CT or AT and low expressed in the IAA group.

4 Discussion

Various symbionts inhabit the intestinal tracts of termites, and these symbionts play an indispensable role in the lives of their hosts, aiding in nutrient supply, digestion, nitrogen metabolism, and more (Liu et al., 2013; Peterson and Scharf, 2016a). However, the role of intestinal microorganisms in the immunity of their termite hosts, such as when encountering a fungal pathogen, is unclear (Peterson and Scharf, 2016b). We exposed *O. formosanus* termites to antibiotics, pathogenic *M. robertsii*, or both in sequence, and then measured gut gene expression. Termites exposed to antibiotics followed by a fungal pathogen showed significantly larger changes in gene expression than those exposed only to one or the other (Figure 3), suggesting that gut symbionts can buffer their hosts against foreign pathogens.

10.3389/fphys.2023.1194370

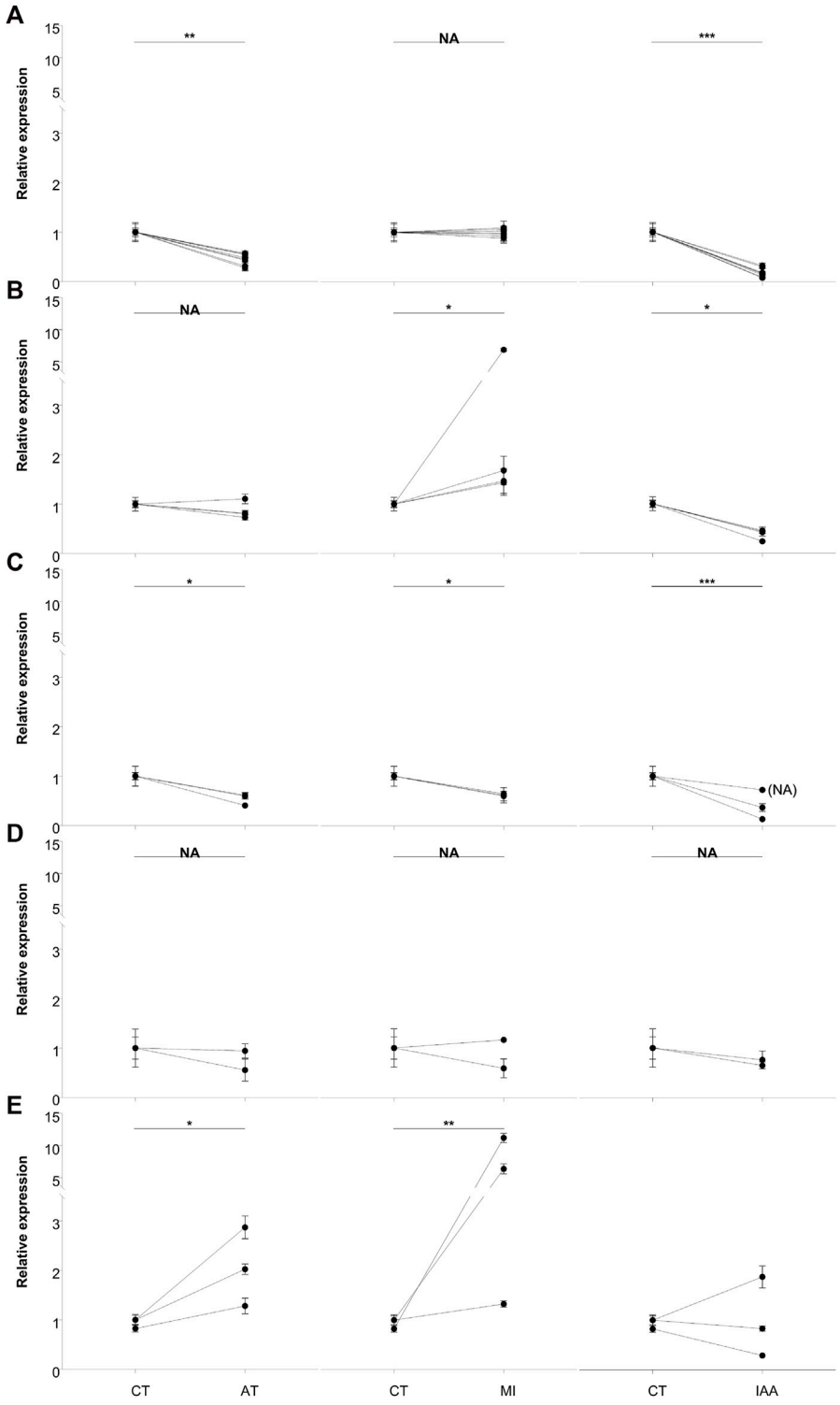

FIGURE 6
qRT-PCR analysis of the top 20 most significantly expressed genes. Based on the expression profiles, DEGs were grouped as flow: **(A)** down-regulated in AT and IAA; **(B)** upregulated in MI but down-regulated in IAA; **(C)** down-regulated in all groups; **(D)** no changed in all groups and **(E)** the remained genes. β-actin was used to normalize the data, which are shown as mean ± standard error; the mean was obtained from three independent repeats. The $2^{-\Delta\Delta CT}$ method was adopted to calculate the relative expression level. The statistical difference relative to the control (CT) group, determined with an unpaired *t*-test, is shown via GraphPad Prism8. Asterisks indicates statistically significant differences (* = $p < 0.05$; ** = $p < 0.01$; *** = $p < 0.001$). (CT: treated with sterilized water as control treatment; AT: treated with 5% kanamycin antibiotic; MI: treated with 108/mL *M. robertsii* conidia suspension at 48-h; IAA: treated with 5% kanamycin, then treated with 108/mL *M. robertsii* conidia suspension at 48 h).

This relationship between gut microbiota and immunity has been demonstrated previously in the lower termite *Reticulitermes flavipes*, which shows greatly increased sensitivity to the fungal pathogen *Beauveria bassiana* following antibiotic treatment (Peterson and Scharf, 2016b). A similar relationship is observed in mosquitoes, which possess midgut microorganisms that mediate host resistance to foreign pathogens, including plasmodium (Dong et al., 2009; Aida et al., 2013; Gao et al., 2021), viruses (Xi et al., 2008), and pathogenic fungi (Wei et al., 2017). Most of these symbionts directly affect the gene expression of the Toll or Imd immune pathway of the host.

The results of our GO and KEGG enrichment analyses indicated that identified DEGs were not involved in direct immune pathways, but rather in signaling pathways, including the calcium signaling pathway (Figures 4, 5). Antibiotics alone are not considered immune activation conditions for termites, so simple antibiotic treatment will not cause immune response in termites. Calcium (Ca^{2+}) is a second messenger that participates in the modulation of various biological processes, including cell survival, cell proliferation, apoptosis, and the immune response (Kong et al., 2021). There is increasing evidence that Ca^{2+} signaling is beneficial for JAK-STAT activation induced by different stimuli and that it plays a vital role in regulating the activation of NF-κB to facilitate gene transcription (Wang et al., 2008; Liu et al., 2016). In addition, we found that the expression of genes related to melanogenesis, which is involved in the innate immunity of insects (Koike and Yamasaki, 2020), changed dramatically in the IAA treatment group (Figure 4). Our GO enrichment analysis also showed a lack of DEGs involved in direct immune pathways (Figure 5). Rather than directly impacting immune pathway gene expression, gut bacteria may contribute to host immunity through other means, such as by affecting host signal transduction and melanogenesis or by changing intestinal oxygen levels at the time of pathogen infestation (Nappi and Vass, 1993; Nappi et al., 2009).

Using qRT-PCR analysis, we measured the gene expression changes of the top 20 most significant DEGs identified from our transcriptomic study (Figure 6). We found that antibiotic treatment did not affect the expression of chitinase in the host (Figure 6D). At the same time, expression of the reverse transcription-related genes *RT-like 1*, *RT-like 2* and *RT-like 3* in the intestinal tract were decreased after antibiotic treatment (Figures 6A,E). Studies have shown that intestinal microbial imbalance can cause cell cancerization and changes in DNA levels, especially in adverse environments (Sobhani et al., 2019). It can be speculated that the presence of pathogenic bacteria does not affect the reverse transcription process of termites, but that the imbalance of intestinal microorganisms leads to this change. Expression of the apolipoprotein gene *APOA2* was upregulated in MI termites but downregulated in IAA termites (Figure 6B). Apolipoproteins participate in the innate immune regulation of insects, demonstrating antibacterial activity and cooperation with antimicrobial peptides (Rahman et al., 2006; Hanada et al., 2011; Feingold and Grunfeld, 2012; Kamareddine et al., 2016). The pattern of expression that was observed in MI and IAA termites suggests that the balance of intestinal microorganisms is necessary for termites to resist pathogen invasion. Interestingly, genes associated with calcium signal pathway were highly enriched in our KEGG analysis, and calpain (Figure 6B) is related to apoptosis and cell division (Shi et al., 2022). Finally, *haptoglobin* (Figure 6B) contains trypsin-like serine protease, which is also related to immunity (Pászti-Gere et al., 2021; Yang et al., 2021). Combined with the above results, we speculate that antibiotic treatment slows down the apoptosis of host cells and increases the expression of apolipoprotein on the surface of cell membranes.

We also measured *HSP70* and *ATP-syn* gene expression in all four treatment groups (Figure 6E). These genes are involved in physiological stress processes, aiding primarily in the folding and stretching of newly synthesized proteins and in the repair of misfolded proteins (Fernández-Fernández and Valpuesta, 2018). Under the stimulation of fungal infection, the expressions of these genes increased. It is speculated that when insects encounter pathogens, *HSP70* is upregulated to protect against cellular injury (Tang et al., 2012). Expression of *ATP-syn* was increased in MI termites, while decreased in IAA termites. We speculate that *M. robertsii* infection led to an increase of protein synthesis in the host, resulting in a large amount of ATP production and consumption. Downregulation of *ATP-syn* in the IAA group suggests that intestinal symbionts play a role in host ATP synthesis during pathogen invasion (Peterson and Scharf, 2016a).

5 Conclusion

In this study, termites exposed to antibiotics followed by a fungal pathogen showed significant changes in gene expression in comparison to those challenged exclusively by one factor. Notably, these changes affected genes associated with calcium signaling pathway and melanization process. These results suggest that intestinal symbionts may play a buffering role when the insect host encounters foreign pathogens, stimulating the expression of immune related genes, such as apolipoprotein. Symbionts may also affect the protein synthesis process and energy supply of the host through *HSP70* and *ATP synthesis*. The gut microbiota provides essential health benefits to its host, particularly by maintaining homeostasis. Disruption of such homeostatic balance can lead to significant adverse impacts, including diseases and lethality. Given that gut microbiota and host immune system have coevolved to maintain homeostasis, genetic underpinnings govern the dialogues between the two is one of the emerging questions warrant immediate attention.

Data availability statement

The datasets presented in this study can be found in online repositories. The names of the repository/repositories and accession number(s) can be found below: https://www.ncbi.nlm.nih.gov/, PRJNA926100.

Author contributions

YT: data curation; formal analysis; investigation; methodology; validation; visualization; writing, original draft; writing, review, and

editing. YK: software; data curation; formal analysis. SQ: software; data curation; formal analysis. AM: writing, review, and editing. JS: data curation; formal analysis. QW: funding acquisition; conceptualization; resources; supervision. ML: supervision; resources; funding acquisition. XZ: supervision, writing, review, and editing.

Funding

This work was supported by the National Natural Science Foundation of China, 32070504 and 31872289, and the Postgraduate Research and Practice Innovation Program of Jiangsu Province (KYCX22_3766).

Acknowledgments

Metarhizium strain used in this study was kindly provided by Cheng-zhu QW from Shanghai Institute of Plant Physiology and Ecology, Chinese Academy of Sciences.

Conflict of interest

The authors declare that the research was conducted in the absence of any commercial or financial relationships that could be construed as a potential conflict of interest.

Publisher's note

Supplementary material

The Supplementary Material for this article can be found online at: https://www.frontiersin.org/articles/10.3389/fphys.2023.1194370/full#supplementary-material

References

Aida, C., Irene, R., Claudia, D., Michela, M., Paolo, R., Patrizia, S., et al. (2013). Interactions between asaia, plasmodium and Anopheles: New insights into mosquito symbiosis and implications in malaria symbiotic control. *Parasites Vectors* 6 (1), 13. doi:10.1186/1756-3305-6-182

Altschul, S. F., Madden, T. L., Schäffer, A. A., Zhang, J., Zhang, Z., Miller, W., et al. (1997). Gapped BLAST and PSI-BLAST: A new generation of protein database search programs. *Nucleic Acids Res.* 25 (17), 3389–3402. doi:10.1093/nar/25.17.3389

Avulova, S., and Rosengaus, R. B. (2011). Losing the battle against fungal infection: Suppression of termite immune defenses during mycosis. *J. Insect Physiol.* 57 (7), 966–971. doi:10.1016/j.jinsphys.2011.04.009

Bai, L., Wang, L., Vega-Rodriguez, J., Wang, G., and Wang, S. (2019). A gut symbiotic bacterium *Serratia marcescens* renders mosquito resistance to plasmodium infection through activation of mosquito immune responses. *Front. Microbiol.* 10, 1580. doi:10.3389/fmicb.2019.01580

Buchon, N., Broderick, N. A., Chakrabarti, S., and Lemaitre, B. (2009). Invasive and indigenous microbiota impact intestinal stem cell activity through multiple pathways in Drosophila. *Genes Dev.* 23 (19), 2333–2344. doi:10.1101/gad.1827009

Chen, S., Zhou, Y., Chen, Y., and Gu, J. (2018). fastp: an ultra-fast all-in-one FASTQ preprocessor. *Bioinformatics* 34 (17), 1884–i890. doi:10.1093/bioinformatics/bty560

Cheng, D., Guo, Z., Riegler, M., Xi, Z., Liang, G., and Xu, Y. (2017). Gut symbiont enhances insecticide resistance in a significant pest, the oriental fruit fly Bactrocera dorsalis (Hendel). *Microbiome* 5 (1), 13. doi:10.1186/s40168-017-0236-z

Chouvenc, T., Su, N. Y., and Robert, A. (2009). Inhibition of Metarhizium anisopliae in the alimentary tract of the eastern subterranean termite Reticulitermes flavipes. *J. Invertebr. Pathol.* 101 (2), 130–136. doi:10.1016/j.jip.2009.04.005

Cremer, S., Pull, C. D., and Furst, M. A. (2018). Social immunity: Emergence and evolution of colony-level disease protection. *Annu. Rev. Entomol.* 63, 105–123. doi:10.1146/annurev-ento-020117-043110

Davidson, N. M., and Oshlack, A. (2014). Corset: Enabling differential gene expression analysis for de novo assembled transcriptomes. *Genome Biol.* 15 (7), 410. doi:10.1186/s13059-014-0410-6

Deng, J., Xu, W., Lv, G., Yuan, H., Zhang, Q. H., Wickham, J. D., et al. (2022). Associated bacteria of a pine sawyer beetle confer resistance to entomopathogenic fungi via fungal growth inhibition. *Environ. Microbiome* 17 (1), 47. doi:10.1186/s40793-022-00443-z

Dong, Y., Manfredini, F., and Dimopoulos, G. (2009). Implication of the mosquito midgut microbiota in the defense against malaria parasites. *PLoS Pathog.* 5 (5), e1000423. doi:10.1371/journal.ppat.1000423

Douglas, A. E. (2018). The Drosophila model for microbiome research. *Lab. Anim. (NY)* 47 (6), 157–164. doi:10.1038/s41684-018-0065-0

El-Gebali, S., Mistry, J., Bateman, A., Eddy, S. R., Luciani, A., Potter, S. C., et al. (2019). The Pfam protein families database in 2019. *Nucleic Acids Res.* 47 (D1), D427–d432. doi:10.1093/nar/gky995

Feingold, K. R., and Grunfeld, C. (2012). Lipids: A key player in the battle between the host and microorganisms. *J. Lipid Res.* 53 (12), 2487–2489. doi:10.1194/jlr.E033407

Fernández-Fernández, M. R., and Valpuesta, J. M. (2018). Hsp70 chaperone: A master player in protein homeostasis. *F1000Res* 7. doi:10.12688/f1000research.15528.1

Gao, H., Bai, L., Jiang, Y., Huang, W., Wang, L., Li, S., et al. (2021). A natural symbiotic bacterium drives mosquito refractoriness to Plasmodium infection via secretion of an antimalarial lipase. *Nat. Microbiol.* 6 (6), 806–817. doi:10.1038/s41564-021-00899-8

Garcia-Robles, I., De Loma, J., Capilla, M., Roger, I., Boix-Montesinos, P., Carrion, P., et al. (2020). Proteomic insights into the immune response of the Colorado potato beetle larvae challenged with Bacillus thuringiensis. *Dev. Comp. Immunol.* 104, 103525. doi:10.1016/j.dci.2019.103525

Grabherr, M. G., Haas, B. J., Yassour, M., Levin, J. Z., Thompson, D. A., Amit, I., et al. (2011). Full-length transcriptome assembly from RNA-Seq data without a reference genome. *Nat. Biotechnol.* 29 (7), 644–652. doi:10.1038/nbt.1883

Gravitz, L. (2012). Microbiome: The critters within. *Nature* 485 (7398), S12–S13. doi:10.1038/485s12a

Hanada, Y., Sekimizu, K., and Kaito, C. (2011). Silkworm apolipophorin protein inhibits *Staphylococcus aureus* virulence. *J. Biol. Chem.* 286 (45), 39360–39369. doi:10.1074/jbc.M111.278416

He, S., Johnston, P. R., Kuropka, B., Lokatis, S., Weise, C., Plarre, R., et al. (2018). Termite soldiers contribute to social immunity by synthesizing potent oral secretions. *Insect Mol. Biol.* 27 (5), 564–576. doi:10.1111/imb.12499

Hong, M., Hwang, D., and Cho, S. (2018). Hemocyte morphology and cellular immune response in termite (Reticulitermes speratus). *J. Insect Sci.* 18 (2), 46. doi:10.1093/jisesa/iey039

Hu, H., da Costa, R. R., Pilgaard, B., Schiott, M., Lange, L., and Poulsen, M. (2019). Fungiculture in termites is associated with a mycolytic gut bacterial community. *mSphere* 4 (3), 001655–e219. doi:10.1128/mSphere.00165-19

Kamareddine, L., Nakhleh, J., and Osta, M. A. (2016). Functional interaction between apolipophorins and complement regulate the mosquito immune response to systemic infections. *J. Innate Immun.* 8 (3), 314–326. doi:10.1159/000443883

Kanehisa, M., Araki, M., Goto, S., Hattori, M., Hirakawa, M., Itoh, M., et al. (2008). KEGG for linking genomes to life and the environment. *Nucleic Acids Res.* 36, D480–D484. doi:10.1093/nar/gkm882

Koike, S., and Yamasaki, K. (2020). Melanogenesis connection with innate immunity and toll-like receptors. *Int. J. Mol. Sci.* 21 (24), 9769. doi:10.3390/ijms21249769

Kong, F., You, H., Zheng, K., Tang, R., and Zheng, C. (2021). The crosstalk between pattern-recognition receptor signaling and calcium signaling. *Int. J. Biol. Macromol.* 192, 745–756. doi:10.1016/j.ijbiomac.2021.10.014

Li, B., and Dewey, C. N. (2011). RSEM: Accurate transcript quantification from RNA-seq data with or without a reference genome. *BMC Bioinforma.* 12, 323. doi:10.1186/1471-2105-12-323

Li, F., Li, M., Zhu, Q., Mao, T., Dai, M., Ye, W., et al. (2021). Imbalance of intestinal microbial homeostasis caused by acetamiprid is detrimental to resistance to pathogenic bacteria in *Bombyx mori*. *Environ. Pollut.* 289, 117866. doi:10.1016/j.envpol.2021.117866

Liu, N., Zhang, L., Zhou, H., Zhang, M., Yan, X., Wang, Q., et al. (2013). Metagenomic insights into metabolic capacities of the gut microbiota in a fungus-cultivating termite (Odontotermes yunnanensis). *PLoS One* 8 (7), e69184. doi:10.1371/journal.pone.0069184

Liu, L., Li, G., Sun, P., Lei, C., and Huang, Q. (2015). Experimental verification and molecular basis of active immunization against fungal pathogens in termites. *Sci. Rep.* 5, 15106. doi:10.1038/srep15106

Liu, X., Berry, C. T., Ruthel, G., Madara, J. J., MacGillivray, K., Gray, C. M., et al. (2016). T cell receptor-induced nuclear factor κB (NF-κB) signaling and transcriptional activation are regulated by STIM1-and orai1-mediated calcium entry. *J. Biol. Chem.* 291 (16), 8440–8452. doi:10.1074/jbc.M115.713008

Love, M. I., Huber, W., and Anders, S. (2014). Moderated estimation of fold change and dispersion for RNA-seq data with DESeq2. *Genome Biol.* 15 (12), 550. doi:10.1186/s13059-014-0550-8

Mao, X., Cai, T., Olyarchuk, J. G., and Wei, L. (2005). Automated genome annotation and pathway identification using the KEGG Orthology (KO) as a controlled vocabulary. *Bioinformatics* 21 (19), 3787–3793. doi:10.1093/bioinformatics/bti430

Moriya, Y., Itoh, M., Okuda, S., Yoshizawa, A. C., and Kanehisa, M. (2007). KAAS: An automatic genome annotation and pathway reconstruction server. *Nucleic Acids Res.* 35, W182–W185. doi:10.1093/nar/gkm321

Nappi, A. J., and Vass, E. (1993). Melanogenesis and the generation of cytotoxic molecules during insect cellular immune reactions. *Pigment. Cell Res.* 6 (3), 117–126. doi:10.1111/j.1600-0749.1993.tb00590.x

Nappi, A., Poirié, M., and Carton, Y. (2009). The role of melanization and cytotoxic by-products in the cellular immune responses of Drosophila against parasitic wasps. *Adv. Parasitol.* 70, 99–121. doi:10.1016/s0065-308x(09)70004-1

Pászti-Gere, E., Pomothy, J., Jerzsele, Á., Pilgram, O., and Steinmetzer, T. (2021). Exposure of human intestinal epithelial cells and primary human hepatocytes to trypsin-like serine protease inhibitors with potential antiviral effect. *J. Enzyme Inhib. Med. Chem.* 36 (1), 659–668. doi:10.1080/14756366.2021.1886093

Peterson, B. F., and Scharf, M. E. (2016a). Lower termite associations with microbes: Synergy, protection, and interplay. *Front. Microbiol.* 7, 422. doi:10.3389/fmicb.2016.00422

Peterson, B. F., and Scharf, M. E. (2016b). Metatranscriptome analysis reveals bacterial symbiont contributions to lower termite physiology and potential immune functions. *BMC Genomics* 17 (1), 772. doi:10.1186/s12864-016-3126-z

Peterson, B. F., Stewart, H. L., and Scharf, M. E. (2015). Quantification of symbiotic contributions to lower termite lignocellulose digestion using antimicrobial treatments. *Insect Biochem. Mol. Biol.* 59, 80–88. doi:10.1016/j.ibmb.2015.02.009

Rahman, M. M., Ma, G., Roberts, H. L., and Schmidt, O. (2006). Cell-free immune reactions in insects. *J. Insect Physiol.* 52 (7), 754–762. doi:10.1016/j.jinsphys.2006.04.003

Ramirez, J. L., Souza-Neto, J., Torres Cosme, R., Rovira, J., Ortiz, A., Pascale, J. M., et al. (2012). Reciprocal tripartite interactions between the *Aedes aegypti* midgut microbiota, innate immune system and dengue virus influences vector competence. *PLoS Negl. Trop. Dis.* 6 (3), e1561. doi:10.1371/journal.pntd.0001561

Rosengaus, R. B., Schultheis, K. F., Yalonetskaya, A., Bulmer, M. S., DuComb, W. S., Benson, R. W., et al. (2014). Symbiont-derived beta-1,3-glucanases in a social insect: Mutualism beyond nutrition. *Front. Microbiol.* 5, 607. doi:10.3389/fmicb.2014.00607

Shi, H., Yu, Y., Liu, X., Yu, Y., Li, M., Wang, Y., et al. (2022). Inhibition of calpain reduces cell apoptosis by suppressing mitochondrial fission in acute viral myocarditis. *Cell Biol. Toxicol.* 38 (3), 487–504. doi:10.1007/s10565-021-09634-9

Shu, G., Ji, Z., and Wang, Z. (2011). "Effect of kanamycin sulfate and gentamicin on growth of probiotics", in: International Conference on Material Engineering, Architectural Engineering and Informatization (MEAEI).

Sobhani, I., Bergsten, E., Couffin, S., Amiot, A., Nebbad, B., Barau, C., et al. (2019). Colorectal cancer-associated microbiota contributes to oncogenic epigenetic signatures. *Proc. Natl. Acad. Sci. U. S. A.* 116 (48), 24285–24295. doi:10.1073/pnas.1912129116

Tang, T., Wu, C., Li, J., Ren, G., Huang, D., and Liu, F. (2012). Stress-induced HSP70 from *Musca domestica* plays a functionally significant role in the immune system. *J. Insect Physiol.* 58 (9), 1226–1234. doi:10.1016/j.jinsphys.2012.06.007

Vikram, S., Arneodo, J. D., Calcagno, J., Ortiz, M., Mon, M. L., Etcheverry, C., et al. (2021). Diversity structure of the microbial communities in the guts of four neotropical termite species. *PeerJ* 9, e10959. doi:10.7717/peerj.10959

Wang, L., Tassiulas, I., Park-Min, K. H., Reid, A. C., Gil-Henn, H., Schlessinger, J., et al. (2008). Tuning' of type I interferon-induced Jak-STAT1 signaling by calcium-dependent kinases in macrophages. *Nat. Immunol.* 9 (2), 186–193. doi:10.1038/ni1548

Wang, L., Feng, Z., Wang, X., Wang, X., and Zhang, X. (2010). DEGseq: an R package for identifying differentially expressed genes from RNA-seq data. *Bioinformatics* 26 (1), 136–138. doi:10.1093/bioinformatics/btp612

Wei, G., Lai, Y., Wang, G., Chen, H., Li, F., and Wang, S. (2017). Insect pathogenic fungus interacts with the gut microbiota to accelerate mosquito mortality. *Proc. Natl. Acad. Sci. U. S. A.* 114 (23), 5994–5999. doi:10.1073/pnas.1703546114

Xi, Z., Ramirez, J. L., and Dimopoulos, G. (2008). The *Aedes aegypti* toll pathway controls dengue virus infection. *PLoS Pathog.* 4 (7), e1000098. doi:10.1371/journal.ppat.1000098

Xiong, W. (2022). Intestinal microbiota in various animals. *Integr. Zool.* 17 (3), 331–332. doi:10.1111/1749-4877.12633

Yang, H., Ji, T., Xiong, H., Zhang, Y., and Wei, W. (2021). A trypsin-like serine protease domain of masquerade gene in crayfish *Procambarus clarkii* could activate prophenoloxidase and inhibit bacterial growth. *Dev. Comp. Immunol.* 117, 103980. doi:10.1016/j.dci.2020.103980

Young, M. D., Wakefield, M. J., Smyth, G. K., and Oshlack, A. (2010). Gene ontology analysis for RNA-seq: Accounting for selection bias. *Genome Biol.* 11 (2), R14. doi:10.1186/gb-2010-11-2-r14

Zhou, F., Xu, L., Wu, X., Zhao, X., Liu, M., and Zhang, X. (2020). Symbiotic bacterium-derived organic acids protect *Delia antiqua* larvae from entomopathogenic fungal infection. *mSystems* 5 (6), 007788–e820. doi:10.1128/mSystems.00778-20

frontiers | Frontiers in Physiology

TYPE Original Research
PUBLISHED 24 April 2023
DOI 10.3389/fphys.2023.1188917

OPEN ACCESS

EDITED BY
Jia Fan,
Institute of Plant Protection (CAAS), China

REVIEWED BY
Haicui Xie,
Hebei Normal University of Science and Technology, China
Jianyang Guo,
Chinese Academy of Agricultural Sciences, China

*CORRESPONDENCE
Fei Zhao,
zhaofei12@126.com

RECEIVED 18 March 2023
ACCEPTED 10 April 2023
PUBLISHED 24 April 2023

CITATION
Xing K, Zhang S-M, Jia M-Q and Zhao F (2023), Response of wheat aphid to insecticides is influenced by the interaction between temperature amplitudes and insecticide characteristics. *Front. Physiol.* 14:1188917. doi: 10.3389/fphys.2023.1188917

Response of wheat aphid to insecticides is influenced by the interaction between temperature amplitudes and insecticide characteristics

Kun Xing[1,2], Shu-Ming Zhang[1,2], Mei-Qi Jia[1,2] and Fei Zhao[1,2]*

[1]Shanxi Key Laboratory of Integrated Pest Management in Agriculture, College of Plant Protection, Shanxi Agricultural University, Taiyuan, China, [2]Shanxi Shouyang Dryland Agroecosystem National Observation and Research Station, Shouyang, China

Introduction: Climate change not only directly affects the phenotype of organisms but also indirectly impacts their physiology, for example, by altering their susceptibility to insecticides. Changed diurnal temperature fluctuations are an important aspect of climate change; ignoring the impact of these fluctuations on the biological effects of various chemical insecticides can lead to inaccurate assessments of insecticide risk under the current and future climate change scenarios.

Methods: In this study, we studied effects of different temperature amplitudes (± 0, ± 6, ± 12°C) at the same mean temperature (22°C) on the life history traits of a globally distributed pest (*Sitobion avenae*, wheat aphid), in response to low doses of two insecticides. The first, imidacloprid shows a positive temperature coefficient; the second, beta-cypermethrin has a negative temperature coefficient.

Results: Compared with the results seen with the constant temperature (22°C), a wide temperature amplitude (± 12°C) amplified the negative effects of imidacloprid on the survival, longevity, and fecundity of *S. avenae*, but significantly increased the early fecundity of the wheat aphid. Beta-cypermethrin positively impacted the wheat aphid at all temperature amplitudes studied. Specifically, beta-cypermethrin significantly increased the survival, longevity, and fecundity of *S. avenae* under medium temperature amplitude (± 6°C). There were no significant differences in the survival, longevity, and the early fecundity of *S. avenae* when it was treated with beta-cypermethrin at the wide temperature amplitude (± 12°C). However, the negative effect of beta-cypermethrin on the intrinsic rate of increase of *S. avenae* decreased gradually with the increase in temperature amplitude.

Discussion: In conclusion, the response of *S. avenae* to positive temperature coefficient insecticides was markedly affected by temperature amplitude, while negative temperature coefficient insecticides increased the environmental adaptability of *S. avenae* to various temperature amplitudes. Our results highlight the importance of the integrated consideration of diurnal temperature fluctuations and different temperature coefficient insecticide interactions in climate-change-linked insecticide risk assessment; these results

emphasize the need for a more fine-scale approach within the context of climate change and poison sensitivity.

KEYWORDS

global warming, insecticides, multiple stress, risk assessment, temperature amplitude, temperature characteristics

1 Introduction

Climate change (Körner and Basler, 2010) and the application of insecticides (Rohr et al., 2011), as two major anthropogenic pressures, have brought developmental and reproductive challenges to a wide array of organisms (Landis et al., 2014). These factors have increased research interest to improve our understanding of the ecophysiological mechanisms that underly the biological responses of organisms to climate change and insecticides (Van den Brink et al., 2018). Currently, there are three different viewpoints with regards to this issue. The first viewpoint suggests that factors related to climate change can increase biological sensitivity to insecticide pollutants, which is referred to as, climate-induced toxicity sensitivity (CITS) (Noyes et al., 2009; Noyes and Lema, 2015). The second viewpoint proposes that exposure to insecticide pollutants can increase biological sensitivity to climate change, known as toxication-induced climate change sensitivity (TICS) (Moe et al., 2013; Janssens et al., 2018). The third viewpoint asserts that these concepts do not exist independently owing to inherent differences between species (De Beeck et al., 2018). Overall, more experimental evidence is necessary to fully understand the biological interactions between climate change and insecticide pollution.

Studies have established that temperature remarkably affects the insecticide mortality of insects. For example, a rise in temperature has been shown to increase insect sensitivity to organophosphorus, nicotine, and benzoylurea (Lydy et al., 1999; Amarasekare and Edelson, 2004). By contrast, a rise in temperature was shown to decrease insect sensitivity to pyrethroids (Harwood et al., 2009; Ma et al., 2011). Moreover, the interaction between temperature and insecticides can significantly affects the life-history traits of insects. For example, these interactions have been shown to increase the mortality of subsequent life stages (Janssens et al., 2018), decrease anti-predation behavior (Tran et al., 2019), and decrease longevity and fecundity (Zuo et al., 2015). However, some studies also found that the interaction between temperature and insecticides may increase adult reproduction (Cheng et al., 2014), alleviate oxidative damage (Janssens et al., 2018), and improve the viral diffusion of disease-carrying insects (Muturi and Alto, 2011). The delayed effect of this interaction effect can even be transmitted across generations, impacting the survival (Tran et al., 2018), development, reproduction (Zuo et al., 2015), and the anti-predation ability of offspring (Tran et al., 2019). Notably, most thermostatic studies ignore the negative effects of daily high temperature, resulting in an overestimation of the ecological adaptation of insects to ambient temperature (Arambourou and Stoks, 2015; Decourten and Brander, 2017); however, studies that focus on short-term heat shock, do not reflect the natural 24-h diurnal temperature fluctuations (Gu et al., 2010; Colinet et al., 2015; Stoks et al., 2017). Furthermore, these studies are not in line with gradual temperature changes that usually characterize most insect habitats (Mitchell and Hoffmann, 2010), and neglects the repair (within the context of thermal damage) that some insects can experience under suitable low temperatures at night (Zhao et al., 2014). Some studies have focused on the effects of temperature fluctuations and insecticide exposure on insects. Compared with a constant temperature, the interaction of temperature fluctuations and insecticides in the context of insect development, growth, insecticide sensitivity, and stage specificity (Delnat et al., 2019a; Verheyen and Stoks, 2019a; Delnat et al., 2019b; Verheyen and Stoks, 2019b) has been shown to have additional (and significant) effects on the ecophysiology of insects. However, these studies mostly focused on insecticides with positive temperature coefficient (such as chlorpyrifos and bioinsecticides), ignored the effect of insecticides with negative temperature coefficient. Furthermore, the number of comparative studies investigating the interaction between temperature fluctuations and the temperature coefficients of insecticides is currently limited. Therefore, these findings may not be sufficient to comprehensively explain the complex effects of temperature fluctuations and insecticide exposure on insects.

Sitobion avenae (Fabricius), one of the most important agricultural pests, is widely distributed globally (Dean, 1970; Winderet al., 1999). Owing to its small size, fast heat conduction, and high metabolic rate, *Sitobion avenae* is extremely sensitive to environmental temperature changes, making it an ideal model organism for studying the impact of environmental changes. With regards to environmental changes, diurnal temperature fluctuations have been shown to significantly impact the development, survival (Xing et al., 2021), longevity, reproduction (Zhao et al., 2014), temperature tolerance (Zhao et al., 2019), and population dynamics (Zhu et al., 2019) of various organisms. Studies examining the interaction between temperature and insecticides have primarily focused on the lethal effects of insecticides under constant temperatures (Pei et al., 2015). However, the potential impacts of interactions between temperature fluctuations and insecticides on insect populations remain poorly understood. The neonicotinoid insecticide imidacloprid (positive temperature coefficient) and the pyrethroid insecticide beta-cypermethrin (negative temperature coefficient) are commonly used in the field control of aphids (Yu et al., 2012; Su et al., 2015). Specifically, these insecticides have been widely used in the wheat-producing regions of China for a long time (Wu et al., 2011; Dong et al., 2020). A better understanding of the combined effects of diurnal temperature fluctuations and insecticides are critical not only for guiding the safe and effective use of insecticides in the context of global warming but also for accurately assessing their potential ecological impacts.

Therefore, herein, we studied the effect of the interaction between temperature amplitudes and different temperature coefficient insecticides (solvent control, imidacloprid, and beta-cypermethrin) on the life history traits of *S. avenae* (i.e., survival, longevity, fecundity, early fecundity and the intrinsic rate of increase).

2 Materials and methods

2.1 Insects

Sitobion avenae was collected in May 2016 from within the wheat experimental field of Shanxi Academy of Agricultural Sciences (116°16′N, 35°55′E). They were then reared on 10–20 cm winter wheat, which was replaced once a week by winter wheat seedlings. The pots with winter wheat were placed inside a breathable and transparent insect-rearing cage (60 cm × 60 cm × 60 cm). The cages were finally placed in the insect rearing room, under the following conditions: 22°C ± 1°C, 50%–60% relative humidity, and 16-h light/8-h dark photoperiod, lights on from 05:00 to 21:00 and lights off from 21:00 to 05:00. *Sitobion avenae* was reared indoors for at least 3 years before the experiment commenced.

2.2 Temperature design

In this study, temperature data from the National Meteorological Information Centre (http://data.cma.cn/en) for May (between 2012 and 2018), which corresponded to the rapid growth period of wheat, in Linfen, northern China were selected. Preliminary analysis of the data revealed that the average daily temperature during the rapid growth period of wheat was approximately 22°C, with a mean diurnal temperature amplitude of ±6°C and a maximum diurnal temperature amplitude of ±12°C (Supplementary Figure S1) (Xing et al., 2021). Therefore, in this study, we used 22°C as the average temperature, while the diurnal temperature variation was set to ±0, ±6, and ±12°C, respectively. The actual temperature and humidity in the artificial climate chambers (RXZ-380B-LED; Ningbo Jiangnan Instrument Factory, Ningbo, China) were automatically recorded at 20-min intervals in each group of variable temperature settings using a Datalogger (Hobo u23-001; Onset Computer Corporation, Bourne, MA, United States) During the experiment, target temperature average and amplitudes are 22 ± 0, 22 ± 6, and 22°C ± 12°C, recorded average temperatures (mean ± SD) are 22.39°C ± 0.13°C, 21.21°C ± 0.26°C and 21.85°C ± 0.20°C, recorded temperature amplitudes (mean ± SD) are 0.89°C ± 0.20°C, 6.89°C ± 0.15°C and 11.93°C ± 0.28°C (Supplementary Table S1, Supplementary Figure S2) (Xing et al., 2021). The photoperiod and relative humidity of the artificial climate chambers, in each group of variable temperature settings, was set as 16-h light/8-h dark, and 50%–60%, respectively. The laboratory temperature was controlled by central air conditioning and kept at a constant temperature of approximately 22°C.

2.3 Insecticide concentration

In this study, a positive temperature coefficient insecticide (PT, imidacloprid), a negative temperature coefficient insecticide (NT, beta-cypermethrin), and a solvent control (SC, distilled water) were selected for wheat aphid control in wheat fields. Imidacloprid and beta-cypermethrin, with a purity grade of >99% for both insecticides, were supplied by Yangzhou Suling Insecticide Chemical Co. Ltd. (Yangzhou, China). We selected the dose at which 10% of the individuals will die (LC_{10}) for these two insecticides for their application. Imidacloprid (6 mg) and cypermethrin (0.5 mg) were dissolved in Tween 80 (0.5 mL) and acetone (4.5 mL), both analytically pure, to obtain 1.2 mg/mL imidacloprid and 0.1 mg/mL cypermethrin stock solutions, respectively, and then diluted with distilled water to obtain their serial dilutions (imidacloprid: 1.2, 3.6, 10.8, 32.4, and 97.2 μg/mL; cypermethrin: 0.1, 0.5, 2.5, 12.5, and 62.5 μg/mL). Using SC as the reference, the toxicity of these insecticides to 9-day-old aphids were measured following a Food and Agriculture Organization of the United Nations (FAO) recommended spotting method, and the number of surviving aphids was recorded after 24 h. Each treatment was replicated three times with 30 insects per replicate. The data were analyzed using probit analysis in the SPSS 21.0 software (SPSS Inc., Chicago, IL, United States). The regression equation of toxicity was obtained as imidacloprid: $y = -0.817 + 1.011x$, $\chi^2 = 1.401$, $df = 5$, $n = 720$; beta-cypermethrin: $y = -0.121 + 0.755x$, $\chi^2 = 1.128$, $df = 5$, $n = 720$. The sublethal concentrations of imidacloprid and beta-cypermethrin were determined as $LC_{10} = 0.347$ μg/mL (95% confidence interval (CI) 0.055–0.895) and $LC_{10} = 0.029$ μg/mL (95% CI 0.003–0.096), respectively.

2.4 Test procedure

A total of 432 nymphs that were born within 4 h were selected and reared individually in a rearing unit consisting of a plastic tube (diameter 15 mm, length 70 mm) sealed using a sponge plug, with a 10 mm slit holding a newly excised wheat leaf (Cao et al., 2021). and maintained at 22°C. On day 9, aphids (most of which had developed into adults) were subjected to three insecticide treatments (i.e., SC, PT, and NT) at three temperature amplitude (22 ± 0, 22 ± 6, and 22°C ± 12°C), with 48 adults per treatment (Figure 1). Individual mortality and reproduction were assessed daily at 08:00, and dead aphids and newly born nymphs were removed until all test aphids were dead, and the experiment was completed. To ensure adequate nutrient supply, wheat leaves in the feeding tubes were replaced every 2 days.

2.5 Statistical analyses

In this study, the longevity is determined as the time from day 10 until death of an adult after treatment; the fecundity is the total number of offspring produced by an adult after day 10 until death; the early fecundity is the proportion of the number of offspring produced in the first 3 days to the total number of offspring. All data were tested for normality using the Shapiro-Wilk test. We found that most of the data were skewed. Therefore, we used the gamma error distribution in generalized linear models for a two-factor analysis of the adult longevity, fecundity and early fecundity (i.e., insecticide, temperature amplitude, and their interactions) and the Fisher's least significant difference procedure for multiple comparisons between treatments. The overall survival of adults was analyzed using a Cox proportional hazard model with two factors (insecticide and temperature amplitude) and their interactions. The survival curves of the adult between treatments under a single factor were analyzed using the Log-rank approach with the Kaplan-Meier analysis, and multiple comparisons between the two were made using the Holm-Sidak method. All data were analyzed using SPSS 21.0 (SPSS Inc., Chicago, IL, United States).

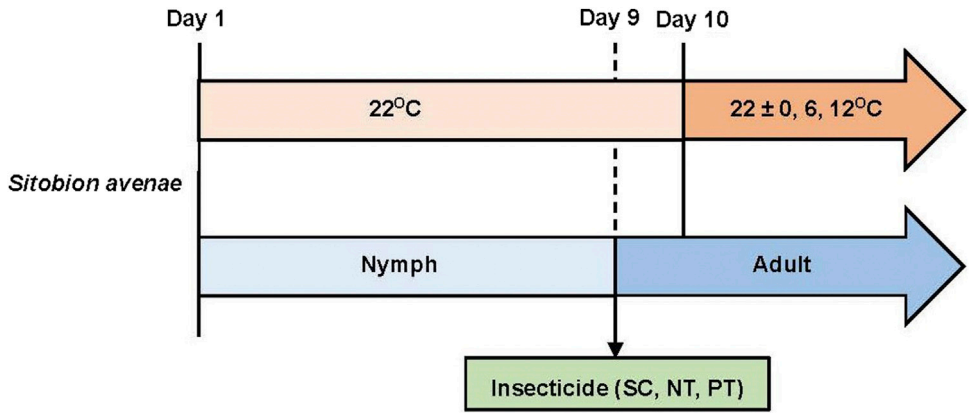

FIGURE 1
The experimental design including treatments and endpoints used.

The intrinsic rate of increase (r_m) was calculated as follows: $R_0 = \sum lx^*mx$, $G = \sum lx^*mx^*X/\sum lx^*mx$, $r_m = \ln(R0)/G$, where "*X*" is the age of the adult, lx is the proportional survival of the adult at age "*X*", and "mx" is the number of offspring per the adult at age "*X*". We used the bootstrap procedure in R to analyze the mean and 95% CI of the intrinsic rate of increase of *S. avenae* population. Kruskal–Wallis multiple comparisons were also performed between treatments using the "Kruskal" function in the "agricolae" data package of R (Zhu et al., 2019).

3 Results

3.1 Effects of interaction between temperature amplitudes and insecticides on survival

Temperature amplitudes (χ^2 = 73.73, *df* = 2, $p < 0.001$) had a significant effect on survival, whereas insecticides (χ^2 = 5.64, *df* = 2, p = 0.060) had no significant effect on survival. However, the interaction of these two factors had a significant effect on survival (χ^2 = 25.78, *df* = 4, $p < 0.001$) (Table 1; Figure 2). Under temperature amplitude ±0°C, insecticides had no significant effect on survival (χ^2 = 6.54, *df* = 2, p = 0.083). However, insecticides significantly affected survival at the temperature amplitude ±6 and ±12°C (χ^2 = 9.36, *df* = 2, p = 0.009; χ^2 = 69.49, *df* = 2, $p < 0.001$), and the survival with the NT treatment was significantly higher than that with the PT treatment. Under SC, NT, and PT treatments, temperature amplitudes had a significant effect on survival (χ^2 = 75.43, *df* = 42, $p < 0.001$; χ^2 = 62.90, *df* = 42, $p < 0.001$; χ^2 = 93.24, *df* = 42, $p < 0.001$, respectively), and survival at the temperature amplitude ± 6°C was significantly higher than that at ± 0 and ± 12°C.

3.2 Effects of interaction between temperature amplitudes and insecticides on longevity

Temperature amplitudes (χ^2 = 333.00, *df* = 2, $p < 0.001$) and insecticides (χ^2 = 47.68, *df* = 2, $p < 0.001$) had significant effects on longevity, whereas their interaction had no significant effect on longevity (χ^2 = 6.27, *df* = 4, p = 0.180) (Table 1; Figure 3). Under the temperature amplitude ± 0°C, insecticides had a significant effect on longevity (χ^2 = 8.79, *df* = 2, p = 0.012). Longevity treated with NT and PT was lower than that treated with SC (0.3 and 2.6 days, respectively). At the temperature amplitude ±6 and ±12°C, insecticides had significant effects on longevity (χ^2 = 11.37, *df* = 2, p = 0.003; χ^2 = 41.13, *df* = 2, $p < 0.001$). Longevity with NT treatment was higher than that with SC treatment (increased by 0.9 and 0.6 days, respectively), and longevity with PT treatment was lower than that with SC treatment (decreased by 3.7 and 5.7 days, respectively). With the SC, NT, and PT treatments, the temperature amplitude had significant effect on longevity (χ^2 = 54.13, *df* = 2, $p < 0.001$; χ^2 = 44.59, *df* = 2, $p < 0.001$; χ^2 = 56.81, *df* = 2, $p < 0.001$, respectively). Moreover, longevity with the SC, NT and PT treatments, under the temperature amplitude ± 6°C was higher than those at the temperature amplitude ± 0°C (9.6, 10.6, 8.5 days, respectively), and longevity at the temperature amplitude ± 12°C was lower than that at temperature amplitude ± 0°C (1.5, 0.6, 4.6 days, respectively).

3.3 Effects of interaction between temperature amplitudes and insecticides on fecundity

Temperature amplitudes (χ^2 = 190.12, *df* = 2, $p < 0.001$) and insecticides (χ^2 = 39.34, *df* = 2, $p < 0.001$) had significant effects on fecundity, whereas their interaction had no significant effect on fecundity (χ^2 = 7.18, *df* = 4, p = 0.127) (Table 1; Figure 4). Under the temperature amplitude ±0°C, insecticides significantly affected fecundity (χ^2 = 17.35, *df* = 2, $p < 0.001$). Fecundity with NT and PT treatment was lower than that with SC treatment (1.8 nymphs/adult and 8.3 nymphs/adult, respectively). At the temperature amplitude ±6°C, insecticides significantly affected fecundity (χ^2 = 7.31, *df* = 2, p = 0.026), and fecundity treated with NT and PT was lower than that treated with SC (1.86 nymphs/adult and 7.5 nymphs/adult, respectively). At the temperature amplitude ±12°C, insecticides significantly affected fecundity

TABLE 1 Results of the temperature amplitude and insecticide effects on *Sitobion avenae*.

Trait	Source	$\chi 2$	*Df*	*p*
Survival	Temperature amplitudes (TA)	73.73	2	<0.001
	Insecticide treatments (IT)	5.64	2	0.060
	TA x IT	25.78	4	<0.001
Longevity	Temperature amplitudes (TA)	333.00	2	<0.001
	Insecticide treatments (IT)	47.68	2	<0.001
	TA x IT	6.27	4	0.180
Fecundity	Temperature amplitudes (TA)	190.12	2	<0.001
	Insecticide treatments (IT)	39.34	2	<0.001
	TA x IT	7.18	4	0.127
Early fecundity	Temperature amplitudes (TA)	189.20	2	<0.001
	Insecticide treatments (IT)	37.65	2	<0.001
	TA x IT	18.63	4	<0.001
Intrinsic rate of increase	Temperature amplitudes (TA)	12820.61	2	<0.001
	Insecticide treatments (IT)	861.48	2	<0.001
	TA x IT	1967.31	4	<0.001

(χ^2 = 29.69, *df* = 2, $p < 0.001$). Fecundity observed under NT treatment was higher than that under SC treatment (increased by 5.4 nymphs/adult), and fecundity observed under PT treatment was lower than that under SC treatment (decreased by 4.4 nymphs/adult). Under the SC, NT, and PT treatments, temperature amplitudes had significant effect on fecundity (χ^2 = 61.93, *df* = 2, $p < 0.001$; χ^2 = 21.28, *df* = 2, $p < 0.001$; χ^2 = 51.02, *df* = 2, $p < 0.001$; respectively). The fecundity under the temperature amplitude ± 6°C, with the SC, NT, and PT treatments, was higher than that under the temperature amplitude ± 0°C (7.5 nymphs/adult, 7.4 nymphs/adult and 8.3 nymphs/adult, respectively), and fecundity treated with temperature amplitude ±12°C was lower than that of temperature amplitude ±0°C (13.7 nymphs/adult, 6.6 nymphs/adult and 9.9 nymphs/adult, respectively).

3.4 Effects of interaction between temperature amplitudes and insecticides on early fecundity

Temperature amplitudes (χ^2 = 189.21, *df* = 2, $p < 0.001$), insecticides (χ^2 = 37.65, *df* = 2, $p < 0.001$), and their interaction (χ^2 = 18.63, *df* = 4, $p < 0.001$) had a significant effect on the early fecundity (Table 1; Figure 5). Under the temperature amplitudes ± 0 and ± 6°C, insecticides had no significant effect on the early fecundity (χ^2 = 5.65, *df* = 2, $p = 0.059$; χ^2 = 2.99, *df* = 2, $p = 0.225$). At ± 12°C, insecticides significantly affected the early fecundity (χ^2 = 23.30, *df* = 2, $p < 0.001$), and the effect of NT treatment was lower than that of SC treatment (1.93% lower), whereas the early fecundity with PT treatment was higher than with SC treatment (27.26% higher). Under the SC, NT, and PT treatments, temperature amplitudes had significant effect on the early fecundity (χ^2 = 57.52, *df* = 2, $p < 0.001$; χ^2 = 36.29, *df* = 2, $p < 0.001$; χ^2 = 51.55, *df* = 2, $p < 0.001$). The early fecundity at the temperature amplitude ± 6°C, with the SC, NT, and PT treatments, was lower than that at the temperature amplitude ± 0°C (decreased by 14.2%, 16.0% and 18.2%, respectively), while the early fecundity at temperature amplitude ±12°C was higher than that at temperature amplitude ±0°C (increased by 18.6%, 10.9%, and 34.1%, respectively).

3.5 Effects of interaction between temperature amplitudes and insecticides on the intrinsic rate of increase

Temperature amplitudes (χ^2 = 12820.61, *df* = 2, $p < 0.001$) and insecticides (χ^2 = 861.48, *df* = 2, $p < 0.001$), including their interaction (χ^2 = 1967.31, *df* = 2, $p < 0.001$), significantly affected the intrinsic rate of increase (Table 1; Figure 6). At the temperature amplitude ±0 and ±6°C, the intrinsic rate of increase was significantly affected by insecticides (χ^2 = 161.702, *df* = 2, $p < 0.001$; χ^2 = 198.620, *df* = 2, $p < 0.001$). The intrinsic rate of increase with the NT treatment was low than that with SC treatment (0.05 and 0.04, respectively), and the intrinsic rate of increase with PT treatment was lower than that with SC treatment (0.06 and 0.03, respectively). At the temperature amplitude ± 12°C, the intrinsic rate of increase was significantly affected by insecticides (χ^2 = 234.90, *df* = 2, $p < 0.001$). The intrinsic rate of increase was higher with PT treatment than with SC treatment (increased by 0.10) and lower with PT treatment than with control SC treatment (decreased by 0.03). Under SC, NT, and PT treatments, the intrinsic rate of increase was significantly affected by temperature amplitudes (χ^2 = 263.11, *df* = 2, $p < 0.001$; χ^2 = 253.21, *df* = 2, $p < 0.001$; χ^2 =

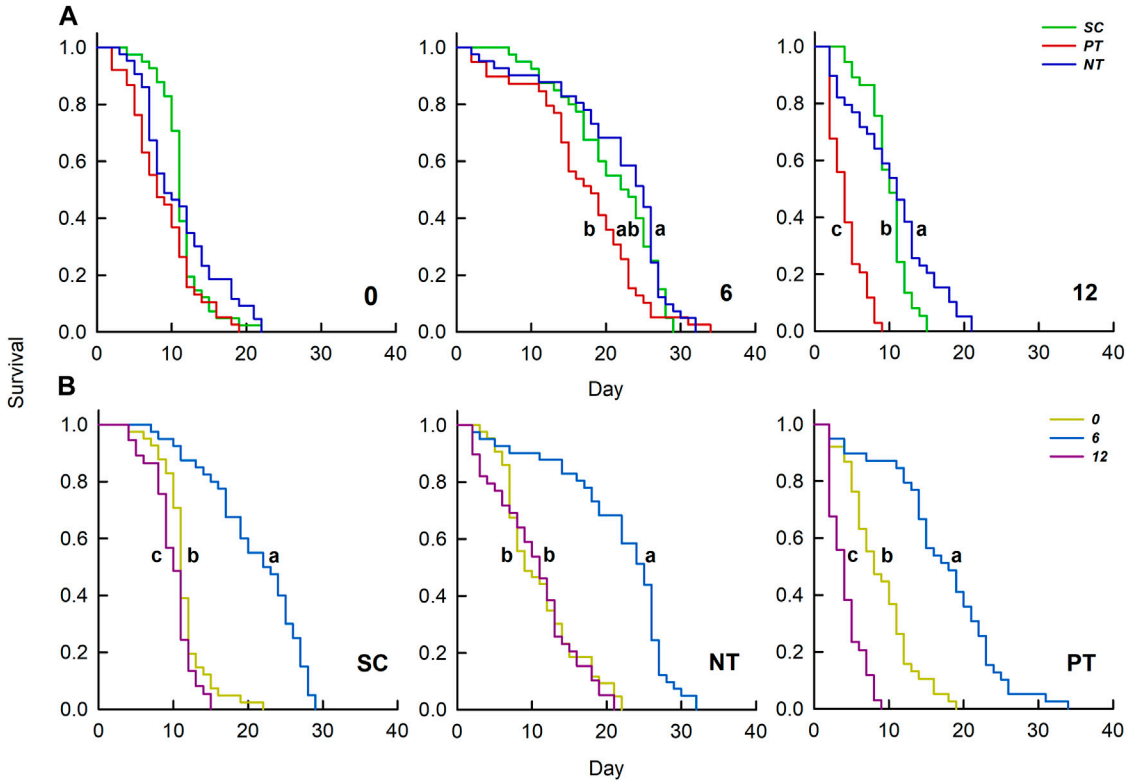

FIGURE 2
Effects of insecticides **(A)** and temperature amplitudes **(B)** on the survival curve. Different letters above the curve indicate significant differences between treatments (p = 0.05); 0, 6, and 12 represent the different temperature amplitudes; SC, NT, and PT represent the control, high chlorine, and imidacloprid treatment, respectively.

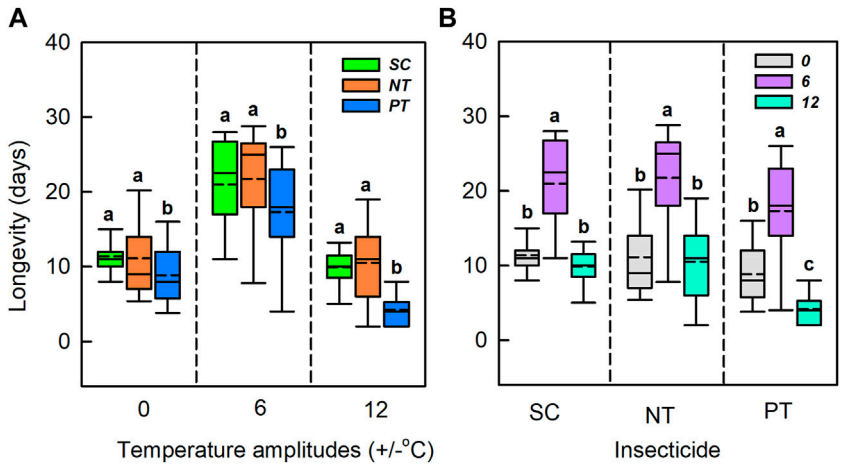

FIGURE 3
Box plot of the longevity under various temperature amplitudes **(A)** and insecticides **(B)**. The upper and lower boundaries of the box indicate the 75th percentile and 25th percentile of the dataset. The black horizontal line and short dash line within the box represent the median and mean values, respectively. Error bars above and below the box indicate the minimum and maximum values, respectively. Different letters above each box indicate significant differences (p < 0.05) among the treatments.

256.80, df = 2, p < 0.001, respectively). The intrinsic rate of increase at the temperature amplitude ± 6°C with SC, NT, PT treatments was lower than that at the temperature amplitude ± 0°C (decreased by 0.19, 0.18, and 0.16, respectively). The intrinsic rate of increase at the temperature amplitude ± 12°C with SC and NT was lower than that at the temperature amplitude ± 0°C (decreased by 0.09,

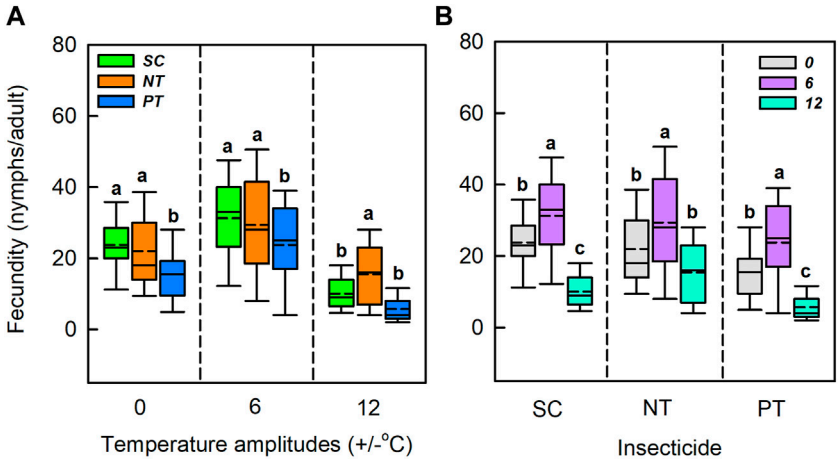

FIGURE 4
Box plot of the fecundity under various temperature amplitudes **(A)** and insecticides **(B)**. The upper and lower boundaries of the box indicate the 75th percentile and 25th percentile of the dataset. The black horizontal line and short dashed-line within the box represent the median and mean values, respectively. Error bars above and below the box indicate the minimum and maximum values, respectively. Different letters above each box indicate significant differences ($p < 0.05$) among the treatments.

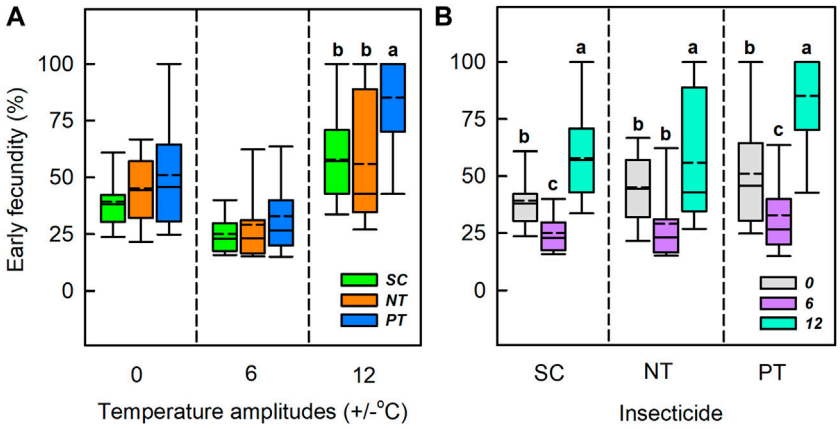

FIGURE 5
Box plot of early fecundity under various temperature amplitudes **(A)** and insecticides **(B)**. The upper and lower boundaries of the box indicate the 75th percentile and 25th percentile of the dataset. The black horizontal line and short dashed-line within the box represent the median and mean values, respectively. Error bars above and below the box indicate the minimum and maximum values, respectively. Different letters above each box indicate significant differences ($p < 0.05$) among the treatments.

0.06 respectively), but the intrinsic rate of increase at the temperature amplitude ± 12°C with PT was higher than that at the temperature amplitude ± 0°C (increased by 0.07).

4 Discussion

4.1 Effects of insecticides alone

Under constant temperature, insecticides had a delayed effect on adult longevity, fecundity, and the intrinsic rate of increase. Overall, these results are consistent with previous studies about the effects of low-dose insecticides on life history traits of insects (Lu et al., 2016; Imelda Martiner et al., 2017). We also found that the delay in the negative effects of imidacloprid on adult longevity and fecundity was much more profound than that of beta-cypermethrin at the same low dose. This may be due to the different correlations between specific insecticides and temperature fluctuations (Nadia et al., 2018). Previous studies have shown that imidacloprid has a positive temperature coefficient and virulence increases with increasing temperature (Gonias et al., 2008; Liu et al., 2016). The toxicity of beta-cypermethrin decreased gradually with an increase in temperature, showing a negative correlation (Musser and Shelton., 2005; Harwood et al., 2009). In this study, the constant

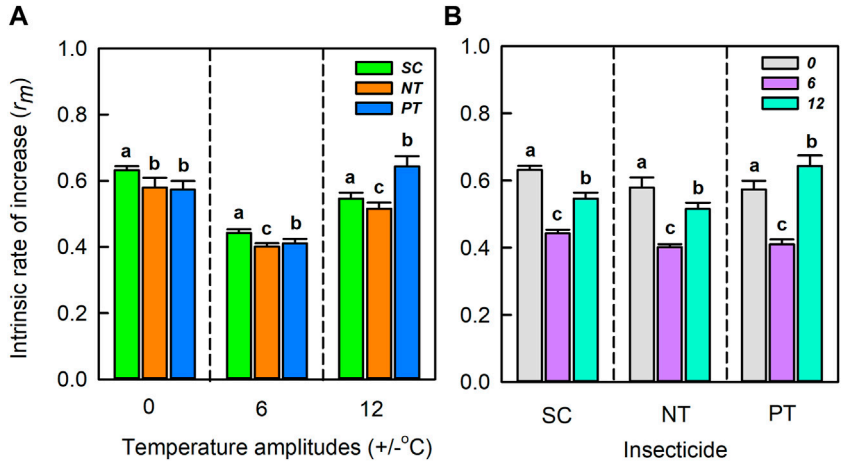

FIGURE 6
The Intrinsic rate of increase (mean ± SD) under temperature amplitudes **(A)** and insecticides **(B)**. Different lowercase letters represent significant differences between different treatments at the p = 0.05 level.

temperature of 22°C may have increased adults' susceptibility to imidacloprid, and it may be closely related to immune gene expression, detoxification enzyme and acetylcholine lipase activity (Fan et al., 2021).

4.2 Effects of temperature amplitudes alone

The temperature amplitude significantly affected the phenotype and population parameter of the adult. Compared with constant temperature and medium temperature amplitude (22°C ± 6°C), the wide temperature amplitude 22°C ± 12°C (maximum daily temperature up to 34°C) reduced adult longevity and fecundity, but the adults still survived long enough to reproduce. This result is discordant with the result of previous studies on the correlation between insect survival and constant temperature. *Sitobion avenae* could not survive at 30°C (Dean, 1974; Jiang et al., 2018). In our experiments, the adult longevity was reduced to 9.9 days and the fecundity was reduced to 10.1 nymphs/adult at the wide temperature amplitude 22°C ± 12°C. These trends show that an adult could still survive and have relatively highly fecundity even when the maximum daily temperature reached 34°C. This may be owing to the repair effect of protective substances such as heat shock proteins, mannitol, and sorbitol accumulated during the suitable recovery temperature after the adults experienced a daily high temperature (Yang and Stamp, 1995). The early fecundity with wide temperature amplitude 22°C ± 12°C was significantly higher than that under the constant temperature (22°C ± 0°C) and medium temperature amplitude (22°C ± 6°C), which may be caused by the response of the adult to high temperature and pressure. High daily temperatures (34°C) with the wide temperature amplitude (22°C ± 12°C) as a temperature-pressure may cause the adult to accelerate reproduction of offspring to maximize fitness, this change in reproductive strategies is adaptive (Javoiš and Tammaru, 2004).

Compared with the constant temperature (22°C ± 0°C) and wide temperature amplitude (22°C ± 12°C), medium temperature amplitude (22°C ± 6°C) increased adult survival, extended the adult longevity, and promoted fecundity. Studies have shown that appropriate temperature amplitudes can accelerate development, improve survival and temperature tolerance, increase fecundity and ability to transmit poison and olfactory response, and so on (Colinet et al., 2015). Our study showed that suitable temperature amplitude significantly increased the survival, extended the longevity, and increased the fecundity. This finding may be explained by the fact that the appropriate temperature amplitude is closely related to the increase in the activity or concentration of key proteins (heat shock proteins), protective agents, and so on, in the metabolic processes of the insects (Colineta et al., 2007; Lalouettea et al., 2011).

4.3 Effects of the interactions between temperature amplitudes and insecticides

The negative effect of imidacloprid on the adult was further intensified under temperature fluctuations. Compared with the results seen with constant temperature, the wide temperature amplitude of 22°C ± 12°C significantly inhibited the survival, longevity, and fecundity of the adult; moreover, medium temperature amplitude (22°C ± 6°C) significantly reduced the increases in the adult phenotypic parameters. This shows the toxicity of insecticides increases as temperature amplitudes increased. Studies have shown that the exposure of organisms to insecticides can increase their biological sensitivity to climate change; this phenomenon is known as TICS (Janssens et al., 2018; Verheyen et al., 2019). This may be due to the conversion of insecticides to more toxic metabolites at wide temperature amplitudes (Harwood et al., 2009), reducing the adult longevity and fecundity. It is also possible that under a high daily temperature, the higher metabolic rate of the adult leads to increased respiration and eating to compensate for energy expenditure. This high uptake of poisons, especially by those with a high metabolic conversion rate, will offset the increased rates of detoxification and excretion at high temperatures, which may precipitate increased toxicity (Hooper et al.,

2013; Hallman and Brooks, 2015). The intrinsic rate of increase includes the contributions of initial reproductive age, reproductive peak, reproductive duration, and population survival. Population dynamics are one of the main factors that predict the growth potential of insect populations. Compared to our results seen with constant temperature, the interaction between temperature amplitudes and imidacloprid markedly affected the intrinsic rate of increase. Under the wide temperature amplitude, imidacloprid was associated with a high intrinsic rate of increase, due to the short adult longevity and increased early fecundity (Ahn and Choi., 2022). In conclusion, both the individual fitness of the adult and the response of population growth to positive temperature coefficient insecticides were considerably affected by the temperature amplitude.

Unexpectedly, we found that beta-cypermethrin profoundly affected adults across the different temperature amplitudes. Specifically, we found that beta-cypermethrin significantly improved survival, longevity, and fecundity of the adult at the medium temperature amplitude (22°C ± 6°C). At the wide temperature amplitude (22°C ± 12°C), the adult treated with beta-cypermethrin was not significantly affected compared to those with SC treatment, and the negative effect of beta-cypermethrin on the intrinsic rate of increase decreased gradually with the increase in temperature amplitudes. This finding disagrees with the results of previous studies, which have shown that wide temperature amplitudes can increase the toxicity of insecticides (Hooper et al., 2013; Van et al., 2014). For example, under high temperature fluctuations, chlorpyrifos increased the mortality of the mosquito (*Culex pipiens*) larvae (Delnat et al., 2019a), and it also increased the mortality of damselfly (*Ischnura elegans*) (Verheyen et al., 2019). However, our results showed that the toxicity of beta-cypermethrin to the adult was very weak at temperature amplitudes (22°C ± 6°C and 22°C ± 12°C). First, there may be a close relationship with the temperature properties of insecticides. Previous studies have shown that the effectiveness of beta-cypermethrin is negatively correlated with increases in the temperature (Harwood et al., 2009). In this study, the daily high temperature increased (up to 34°C) at the wide temperature amplitude (22°C ± 12°C), which greatly limited the effectiveness of beta-cypermethrin. Second, when organisms respond to one stressor by increasing energy expenditure, it may have a synergistic effect on their response to another stressor (Liess et al., 2016). Insecticides and environmental stress can yield coevolution in the target insects (Delnat et al., 2019b). In this study, the daily high temperature reached 34°C at the wide temperature amplitude (22°C ± 12°C), which far exceeded the upper limit of the development threshold of wheat aphid (30°C). When the adult resisted the environmental stress pressure, the synergistic effect of temperature and insecticides might be generated to reduce the toxic effect of high chlorine levels on the adult. In conclusion, in the interaction between the temperature amplitude and the negative temperature coefficient insecticide (beta-cypermethrin), the individual or population fitness of the adult improved, indicating that the negative temperature coefficient insecticide improved the environmental adaptability of insects to the temperature fluctuations.

4.4 Risk assessment of insecticides under climate change

By studying the effects of temperature amplitude and insecticide exposure on insect survival, longevity, fecundity, and population growth, we demonstrated that diurnal temperature fluctuations encountered by most organisms in nature are a key environmental factor that shaped toxicity-linked responses. First, we found that the insecticide toxicity measured at constant temperature is not only inconsistent with the actual conditions in the field but also independent of the interaction of global climate change and ecotoxicology on insects. Second, we demonstrated that insecticides could alter biological sensitivity to climate change and that the temperature amplitude is an important component of TICS. Finally, our study showed that wide temperature amplitude conditions significantly increased the virulence of insecticides with positive temperature coefficients and not of those with negative temperature coefficients. This suggests that the temperature properties of insecticides are also crucial for assessing the risk of insecticide virulence under current and future climate scenarios. Overall, our results highlight the importance of combining the temperature amplitudes with the temperature characteristics of insecticides to improve the accuracy and prediction of insecticide risk assessments under global climate change (Rasmussen et al., 2018; Delnat et al., 2019b; Verheyen et al., 2019).

Data availability statement

The original contribution presented in the study are included in the article/Supplementary Material, further inquiries can be directed to the corresponding author.

Author contributions

Conceptualization, KX; formal analysis, KX and M-QJ; funding acquisition, FZ; methodology, KX; project administration, FZ; writing—original draft, KX and S-MZ; writing—review and editing, KX and FZ. All authors have read and agreed to the published version of the manuscript.

Funding

This research was financially supported by the National Key Research and Development Program (2021YFD1900705-2), the Province Key Research and Development Program of Shanxi (201903D211001-2), and Modern Agro-industry Technology Research System in Shanxi Province (2023CYJSTX03-30, 2023CYJSTX01-19, YMZD202203).

Acknowledgments

We would like to thank Cao Junyu for assistance in completing the experiments.

Conflict of interest

The authors declare that the research was conducted in the absence of any commercial or financial relationships that could be construed as a potential conflict of interest.

Publisher's note

All claims expressed in this article are solely those of the authors and do not necessarily represent those of their affiliated organizations, or those of the publisher, the editors and the reviewers. Any product that may be evaluated in this article, or claim that may be made by its manufacturer, is not guaranteed or endorsed by the publisher.

Supplementary material

The Supplementary Material for this article can be found online at: https://www.frontiersin.org/articles/10.3389/fphys.2023.1188917/full#supplementary-material

References

Ahn, J. J., and Choi, K. S. (2022). Population parameters and growth of *Riptortus pedestris* (Fabricius) (Hemiptera: Alydidae) under fluctuating temperature. *Insects* 13, 113. doi:10.3390/insects13020113

Amarasekare, K. G., and Edelson, J. V. (2004). Effect of temperature on efficacy of insecticides to differential *Grasshopper* (Orthoptera: Acrididae). *J. Econ. Entomol.* 97, 1595–1602. doi:10.1603/0022-0493-97.5.1595

Arambourou, H., and Stoks, R. (2015). Combined effects of larval exposure to a heat wave and chlorpyrifos in northern and southern populations of the damselfly *Ischnura elegans*. *Chemosphere* 128, 148–154. doi:10.1016/j.chemosphere.2015.01.044

Cao, J. Y., Xing, K., and Zhao, F. (2021). Complex delayed and transgenerational effects driven by the interaction of heat and insecticide in the maternal generation of the wheat aphid, Sitobion avenae. *Sitobion Avenae. Pest Manag. Sci.* 77, 4453–4461. doi:10.1002/ps.6480

Cheng, J., Huang, L. J., Zhu, Z. F., Jiang, L. B., Ge, L. Q., and Wu, C. J. (2014). Heat-dependent fecundity enhancement observed in *Nilaparvata lugens* (Hemiptera: Delphacidae) after treatment with triazophos. *Environ. Entomol.* 43, 474–481. doi:10.1603/EN13249

Colinet, H., Sinclair, B. J., Vernon, P., and Renault, D. (2015). Insects in fluctuating thermal environments. *Annu. Rev. Entomol.* 60, 123–140. doi:10.1146/annurev-ento-010814-021017

Colineta, H., Nguyenb, T. T. A., Cloutierb, C., Michaud, D., and Hance, T. (2007). Proteomic profiling of a parasitic wasp exposed to constant and fluctuating cold exposure. *Insect biochem. molec.* 37, 1177–1188. doi:10.1016/j.ibmb.2007.07.004

De Beeck, L. O., Verheyen, J., and Stoks, R. (2018). Competition magnifies the impact of a pesticide in a warming world by reducing heat tolerance and increasing autotomy. *Environ. Pollut.* 233, 226–234. doi:10.1016/j.envpol.2017.10.071

Dean, G. J. (1974). Effect of temperature on the cereal aphids *Metopolophium dirhodum* (WLK.), *Rhopalosiphum padi* (L.) and *Macrosiphum avenae* (F.) (Hem., Aphididae). *B. Entomol. Res.* 63, 401–409. doi:10.1017/S0007485300040888

Dean, G. J. W., and Luuring, B. B. (1970). Distribution of aphids in cereal crops. *J. Appl. Ecol.* 66, 485–496. doi:10.1111/j.1744-7348.1970.tb04628.x

Decourten, B. M., and Brander, S. M. (2017). Combined effects of increased temperature and endocrine disrupting pollutants on sex determination, survival, and development across generations. *Sci. Rep.* 7, 9310. doi:10.1038/s41598-017-09631-1

Delnat, V., Tran, T. T., Janssens, L., and Stoks, R. (2019b). Daily temperature variation magnifies the toxicity of a mixture consisting of a chemical pesticide and a biopesticide in a vector mosquito. *Sci. Total Environ.* 659, 33–40. doi:10.1016/j.scitotenv.2018.12.332

Delnat, V., Tran, T. T., Verheyen, J., Van Dinh, K., Janssens, L., and Stoks, R. (2019a). Temperature variation magnifies chlorpyrifos toxicity differently between larval and adult mosquitoes. *Sci. Total Environ.* 690, 1237–1244. doi:10.1016/j.scitotenv.2019.07.030

Dong, W. Y., Zhang, H. H., Chen, A. Q., Yan, J. H., Wei, Y. H., Ma, K. S., et al. (2020). Resistance levels to five insecticides of wheat aphid field populations from some regions of Gansu and Qinghai Province of China. *Agrochemicals* 59, 532–536. doi:10.16820/j.cnki.1006-0413.2020.07.018

Fan, R. L., Wang, K., Ji, W. N., Chen, X. J., Lin, Z. G., and Ji, T. (2021). Synergistic effects of imidacloprid and ambient temperature on honeybee (*Apis mellifera ligustica*). *J. Environ. Entomol.* 43, 445–452. doi:10.3969/j.issn.1674-0858.2021.02.20

Gonias, E. D., Oosterhuis, D. M., and Bibi, A. C. (2008). Physiologic response of cotton to the insecticide imidacloprid under high temperature stress. *J. Plant Growth Regul.* 27, 77–82. doi:10.1007/s00344-007-9033-4

Gu, X., Tian, S., Wang, D., and Gao, F. (2010). Interaction between short-term heat pretreatment and fipronil on 2nd Instar Larvae of diamondback moth, *Plutella Xylostella* (Linn). *Dose-Response* 8, 331–346. doi:10.2203/dose-response.09-032

Hallman, T. A., and Brooks, M. L. (2015). The deal with diel: Temperature fluctuations asymmetrical warming and ubiquitous metals contaminants. *Environ. Pollut.* 206, 88–94. doi:10.1016/j.envpol.2015.06.005

Harwood, A. D., You, J., and Lydy, M. J. (2009). Temperature as a toxicity identification evaluation tool for pyrethroid insecticides: Toxicokinetic confirmation. *Environ. Toxicol. Chem.* 28, 1051–1058. doi:10.1897/08-291.1

Hooper, M. J., Ankley, G. T., Cristol, D. A., Maryoung, L. A., Noyes, P. D., and Pinkerton, K. E. (2013). Interactions between chemical and climate stressors: A role for mechanistic toxicology in assessing climate change risks. *Environ. Toxicol. Chem.* 32, 32–48. doi:10.1002/etc.2043

Imelda Martínez, M., Lumaret, J. P., Zayas, R. O., and Nassera, K. (2017). The effects of sublethal and lethal doses of ivermectin on the reproductive physiology and larval development of the dung beetle *Euoniticellus intermedius* (Coleoptera: Scarabaeidae). *Can. Entomol.* 149, 461–472. doi:10.4039/tce.2017.11

Janssens, L., Verberk, W., and Stoks, R. (2018). A widespread morphological antipredator mechanism reduces the sensitivity to pesticides and increases the susceptibility to warming. *Sci. Total Environ.* 626, 1230–1235. doi:10.1016/j.scitotenv.2018.01.179

Javoiš, J., and Tammaru, T. (2004). Reproductive decisions are sensitive to cues of life expectancy: The case of a moth. *Anim. Behav.* 68, 249–255. doi:10.1016/j.anbehav.2003.10.022

Jiang, C. Y., Luo, L., Liu, Z. L., Zhang, B., Jiang, H., and Yuan, Z. L. (2018). Effect of temperature on the life table of experimental population of *Sitobion avenae*. *Chin. Plant Prot.* 38, 13–18. doi:10.3969/j.issn.1672-6820.2018.08.002

Körner, C., and Basler, D. (2010). Plant science. Phenology under global warming. *Science* 327, 1461–1462. doi:10.1126/science.1186473

Lalouettea, L., Williams, C. M., Hervant, F., Sinclair, B. J., and Renault, D. (2011). Metabolic rate and oxidative stress in insects exposed to low temperature thermal fluctuations. *Comp. Biochem. Phys.* 158, 229–234. doi:10.1016/j.cbpa.2010.11.007

Landis, W. G., Rohr, J. R., Moe, S. J., Balbus, J. M., Clements, W., Fritz, A., et al. (2014). Global climate change and contaminants, a call to arms not yet heard? *Integr. Environ. Assess. Manage.* 10, 483–484. doi:10.1002/ieam.1568

Liess, M., Foit, K., Knillmann, S., Schäfer, R. B., and Liess, H. D. (2016). Predicting the synergy of multiple stress effects. *Sci. Rep.* 6, 32965. doi:10.1038/srep32965

Liu, J., Lincoln, T. R., An, J. J., Gao, Z. L., Dang, Z. H., Pan, W. L., et al. (2016). The joint toxicity of different temperature coefficient insecticides on *Apolygus lucorum* (Hemiptera: Miridae). *J. Econ. Entomol.* 109, 1846–1852. doi:10.1093/jee/tow082

Lu, Y. H., Zheng, X. S., and Gao, X. W. (2016). Sublethal effects of imidacloprid on the fecundity, longevity, and enzyme activity of *Sitobion avenae* (Fabricius) and *Rhopalosiphum padi* (Linnaeus). *B. Entomol. Res.* 106, 551–559. doi:10.1017/S0007485316000286

Lydy, M. J., Belden, J. B., and Ternes, M. A. (1999). Effects of temperature on the toxicity of m-parathion, chlorpyrifos, and pentachlorobenzene to *Chironomus tentans*. *Arch. Environ. Contam. Toxicol.* 37, 542–547. doi:10.1007/s002449900550

Ma, Y. H., Gao, Z. L., Li, Y. F., Dang, Z. H., and Pan, W. L. (2011). Effect of temperature on the toxicity of several insecticides to the English grain aphid, *Sitobion avenae*. *Chin. J. Appl. Entomol.* 6, 1661–2166. doi:10.7679/j.issn.2095-1353.2011.255

Mitchell, K. A., and Hoffmann, A. A. (2010). Thermal ramping rate influences evolutionary potential and species differences for upper thermal limits in*Drosophila*: *Limited* h^2*and reduced thermal limits in*Drosophila. *Drosoph. Funct. Ecol.* 24, 694–700. doi:10.1111/j.1365-2435.2009.01666.x

Moe, S. J., De Schamphelaere, K., Clements, W. H., Sorensen, M. T., Van den Brink, P. J., and Liess, M. (2013). Combined and interactive effects of global climate change and toxicants on populations and communities. *Environ. Toxicol. Chem.* 32, 49–61. doi:10.1002/etc.2045

Musser, F. R., and Shelton, A. M. (2005). The influence of post-exposure temperature on the toxicity of insecticides to *Ostrinia nubilalis* (Lepidoptera: Crambidae). *Pest Manag. Sci.* 61, 508–510. doi:10.1002/ps.998

Muturi, E. J., and Alto, B. W. (2011). Larval environmental temperature and insecticide exposure alter *Aedes aegypti* competence for arboviruses. *Vector-Borne Zoonot.* 11, 1157–1163. doi:10.1089/vbz.2010.0209

Nadia, S., Lorenzo, T., Andrea, B., and Nicola, M. (2018). Temperature alters the response to insecticides in *Drosophila suzukii* (Diptera: Drosophilidae). *J. Econ. Entomol.* 111, 1306–13123. doi:10.1093/jee/toy080

Noyes, P. D., and Lema, S. C. (2015). Forecasting the impacts of chemical pollution and climate change interactions on the health of wildlife. *Curr. Zool.* 61, 669–689. doi:10.1093/czoolo/61.4.669

Noyes, P. D., McElwee, M. K., Miller, H. D., Clark, B. W., Van Tiem, L. A., Walcott, K. C., et al. (2009). The toxicology of climate change: Environmental contaminants in a warming world. *Environ. Int.* 35, 971–986. doi:10.1016/j.envint.2009.02.006

Pei, X. Q., Liu, H. P., Zhao, F., and Ma, C. S. (2015). The influence of low temperature pretreatment on the lethal effect of imidacloprid to *Sitobion miscanthi*. *Plant Prot.* 41, 44–48. doi:10.3969/j.issn.0529-1542.2015.02.007

Rasmussen, J. J., Wiberg-Larsen, P., Baattrup-Pedersen, A., Bruus, M., Strandberg, B., Soerensen, P. B., et al. (2018). Identifying potential gaps in pesticide risk assessment: Terrestrial life stages of freshwater insects. *J. Appl. Ecol.* 55, 1510–1515. doi:10.1111/1365-2664.13048

Rohr, J. R., Sesterhenn, T. M., and Stieha, C. (2011). Will climate change reduce the effects of a insecticide on amphibians?: Partitioning effects on exposure and susceptibility to contaminants. *Glob. Change Biol.* 17, 657–666. doi:10.1111/j.1365-2486.2010.02301.x

Stoks, R., Verheyen, J., Van Dievel, M., and Tüzün, N. (2017). Daily temperature variation and extreme high temperatures drive performance and biotic interactions in a warming world. *Curr. Opin. Insect Sci.* 23, 35–42. doi:10.1016/j.cois.2017.06.008

Su, X. Y., Hu, F., Ren, X. X., Ye, Z. H., and Zhang, X. C. (2015). Research on the control effects of several insecticides on wheat aphids. *Agr. Sci. Tech.* 16, 1693–1695. doi:10.16175/j.cnki.1009-4229.2015.08.027

Tran, T. T., Janssens, L., Dinh, K. V., and Stoks, R. (2019). An adaptive transgenerational effect of warming but not of pesticide exposure determines how a pesticide and warming interact for antipredator behaviour. *Environ. Pollut.* 245, 307–315. doi:10.1016/j.envpol.2018.11.022

Tran, T. T., Janssens, L., Dinh, K. V., and Stoks, R. (2018). Transgenerational interactions between pesticide exposure and warming in a vector mosquito. *Evol. Appl.* 11, 906–917. doi:10.1111/eva.12605

Van den Brink, P. J., Boxall, A. B. A., Maltby, L., Brooks, B. W., Rudd, M. A., Backhaus, T., et al. (2018). Toward sustainable environmental quality: Priority research questions for europe. *Environ. Toxicol. Chem.* 37, 2281–2295. doi:10.1002/etc.4205

Van, K. D., Janssens, L., Debecker, S., and Stocks, R. (2014). Temperature and latitude specific individual growth rates shape the vulnerability of damselfly larvae to a widespread insecticide. *J. Appl. Ecol.* 51, 919–928. doi:10.1111/1365-2664.12269

Verheyen, J., Delnat, V., and Stoks, R. (2019). Increased daily temperature fluctuations overrule the ability of gradual thermal evolution to offset the increased pesticide toxicity under global warming. *Environ. Sci. Technol.* 53, 4600–4608. doi:10.1021/acs.est.8b07166

Verheyen, J., and Stoks, R. (2019b). Current and future daily temperature fluctuations make a pesticide more toxic: Contrasting effects on life history and physiology. *Environ. Pollut.* 248, 209–218. doi:10.1016/j.envpol.2019.02.022

Verheyen, J., and Stoks, R. (2019a). Temperature variation makes an ectotherm more sensitive to global warming unless thermal evolution occurs. *J. Anim. Ecol.* 88, 624–636. doi:10.1111/1365-2656.12946

Winder, L., Perry, J. N., and Holland, J. M. (1999). The spatial and temporal distribution of the grain aphid *Sitobion avenae* in winter wheat. *Entomol. Exp. Appl.* 93, 275–288. doi:10.1046/j.1570-7458.1999.00588.x

Wu, J. Y., Anelli, C. M., and Sheppard, W. S. (2011). Sub-lethal effects of pesticide residues in brood comb on worker honey bee (*Apis mellifera*) development and longevity. *PloS one* 6, e14720. doi:10.1371/journal.pone.0014720

Xing, K., Sun, D. B., Zhang, J. Z., and Zhao, F. (2021). Wide diurnal temperature amplitude and high population density can positively affect the life history of *Sitobion avenae* (Hemiptera: Aphididae). *J. Insect Sci.* 21, 6. doi:10.1093/jisesa/ieab011

Yang, Y., and Stamp, N. E. (1995). Simultaneous effects of night time temperature and an allelochemical on performance of an insect herbivore. *Oecologia* 104, 225–233. doi:10.1007/bf00328587

Yu, Y. L., Huang, L. J., Wang, L. P., and Wu, J. C. (2012). The combined effects of temperature and insecticide on the fecundity of adult males and adult females of the Brown planthopper *Nilaparvata lugens stål* (Hemiptera: Delphacidae). *Crop Prot.* 34, 59–64. doi:10.1016/j.cropro.2011.08.026

Zhao, F., Xing, K., Hoffmann, A. A., and Ma, C. S. (2019). The importance of timing of heat events for predicting the dynamics of aphid pest populations. *Pest Manag. Sci.* 75, 1866–1874. doi:10.1002/ps.5344

Zhao, F., Zhang, W., Hoffmannm, A. A., and Ma, C. S. (2014). Night warming on hot days produces novel impacts on development, survival and reproduction in a small arthropod. *J. Anim. Ecol.* 83, 769–778. doi:10.1111/1365-2656.12196

Zhu, L., Wang, L., and Ma, C. S. (2019). Sporadic short temperature events cannot be neglected in predicting impacts of climate change on small insects. *J. Insect Physiol.* 112, 48–56. doi:10.1016/j.jinsphys.2018.12.003

Zuo, T. Q., Zhang, B., Zhang, S. T., Zheng, C. Y., and Wang, F. H. (2015). Combined effects of high temperature and acetamiprid on life table parameters of the F_1 offspring of the treated *Frankliniella occidentalis* (Thysanoptera: Thripidae). *Acta Entomol. Sin.* 58, 767–775. doi:10.16380/j.kcxb.2015.07.009

frontiers | Frontiers in Physiology

TYPE Original Research
PUBLISHED 09 May 2023
DOI 10.3389/fphys.2023.1153913

OPEN ACCESS

EDITED BY
Yong Liu,
Shandong Agricultural University, China

REVIEWED BY
Yoshichika Baba,
UC-Berkeley, United States
Akira Sakurai,
Georgia State University, United States

*CORRESPONDENCE
Hiroto Ogawa,
hogawa@sci.hokudai.ac.jp

RECEIVED 30 January 2023
ACCEPTED 27 April 2023
PUBLISHED 09 May 2023

CITATION
Lu A, Fukutomi M, Shidara H and Ogawa H (2023), Persistence of auditory modulation of wind-induced escape behavior in crickets.
Front. Physiol. 14:1153913.
doi: 10.3389/fphys.2023.1153913

Persistence of auditory modulation of wind-induced escape behavior in crickets

Anhua Lu[1], Matasaburo Fukutomi[2], Hisashi Shidara[3,4] and Hiroto Ogawa[3]*

[1]Graduate School of Life Science, Hokkaido University, Sapporo, Japan, [2]Department of Biology, Washington University in St. Louis, St. Louis, MO, United States, [3]Department of Biological Sciences, Faculty of Science, Hokkaido University, Sapporo, Japan, [4]Department of Biochemistry, Graduate School of Medicine, Mie University, Tsu, Japan

Animals, including insects, change their innate escape behavior triggered by a specific threat stimulus depending on the environmental context to survive adaptively the predators' attack. This indicates that additional inputs from sensory organs of different modalities indicating surrounding conditions could affect the neuronal circuit responsible for the escape behavior. Field crickets, *Gryllus bimaculatus*, exhibit an oriented running or jumping escape in response to short air puff detected by the abdominal mechanosensory organ called cerci. Crickets also receive a high-frequency acoustic stimulus by their tympanal organs on their frontal legs, which suggests approaching bats as a predator. We have reported that the crickets modulate their wind-elicited escape running in the moving direction when they are exposed to an acoustic stimulus preceded by the air puff. However, it remains unclear how long the effects of auditory inputs indicating surrounding contexts last after the sound is terminated. In this study, we applied a short pulse (200 ms) of 15-kHz pure tone to the crickets in various intervals before the air-puff stimulus. The sound given 200 or 1000 ms before the air puff biased the wind-elicited escape running backward, like the previous studies using the longer and overlapped sound. But the sounds that started 2000 ms before and simultaneously with the air puff had little effect. In addition, the jumping probability was higher only when the delay of air puff to the sound was 1000 ms. These results suggest that the cricket could retain the auditory memory for at least one second and alter the motion choice and direction of the wind-elicited escape behavior.

KEYWORDS

escape behavior, cricket (*Gryllus bimaculatus*), multisensory integration, crossmodal interactions, contextual memory, behavioral choice

1 Introduction

Prey animals rely on escape responses to defend themselves against predators' attacks (Domenici et al., 2011a; b; LeDoux and Daw, 2018). These quick escape responses are not a simple reflex triggered by the presence of an approaching predator, but mediated via complex sensory-motor control, resulting in an action that maximizes the chances of survival for the animal. Many species of prey animals can change their innate escape behavior triggered by a specific threat stimulus depending on the surrounding contexts (Domenici, 2010; Domenici et al., 2011b). For example, the presence of refugees or burrows affects the escape trajectories in various species of prey animals (Hemmi, 2005; Ellard and Eller, 2009;

Zani et al., 2009; Kanou et al., 2014). This indicates that additional inputs from sensory organs of different modalities indicating surrounding conditions could affect the neuronal circuits to alter the escape strategies. In other words, multisensory integration in the nervous system may be involved in the context dependency of escape behavior.

Multisensory integration underlies the robust perception and appropriate action selection in various species of animals (Stein et al., 1989; Stein and Stanford, 2008; Ohyama et al., 2015). The temporal relationship among sensory inputs of different modalities is one of the crucial factors for multisensory perception. For example, the temporal coincidence of auditory and visual stimuli enhances the multisensory response in the superior colliculus neurons of cats, which mediates attentive and orientation behavior (Meredith et al., 1987). In humans, a preceding auditory cue improves the directionality of subsequent visual detection (McDonald et al., 2000). The temporal relationship should also play an important role in the multisensory integration for the context dependency of escape behavior because sensory information that informs of the surrounding context needs to be retained for some amount of time. Indeed, previous work shows that a specific timing of visual input increases the response probability of sound-evoked escape in larval zebrafish (Mu et al., 2012). However, it is unclear how the temporal relationship is involved in regulating escape strategies rather than responding or not responding.

Here we address this question by focusing on auditory modulation of wind-elicited escape behavior in field crickets *Gryllus bimaculatus* (Fukutomi et al., 2015; Fukutomi and Ogawa, 2017). Crickets exhibit an escape behavior in response to short air puff detected by the abdominal cercal sensory system (Oe and Ogawa, 2013; Sato et al., 2019). This escape behavior can be modulated by additional sensory inputs such as vision (Kanou et al., 2014), antennal mechanosensation (Ifere et al., 2022), and audition (Fukutomi et al., 2015; Fukutomi and Ogawa, 2017). We have reported that auditory stimuli can modulate the moving direction and response threshold of the wind-elicited escape behavior (Fukutomi et al., 2015; Fukutomi and Ogawa, 2017). This modulation is apparent with a high-frequency sound (15 kHz), which suggests approaching bats' call and triggers avoidance response during a flight but weakened with a 5-kHz sound corresponding to the carrier frequency of conspecific calling song, suggesting that crickets can alter their escape strategies depending on the acoustic context (Moiseff et al., 1978; Hoy et al., 1989; Pollack, 2015; Fukutomi and Ogawa, 2017). However, it remains unsolved what temporal relationship between these two stimuli is required for the auditory modulation of wind-elicited escape. In addition, crickets change their escape behavior, either running or jumping, depending on the intensity and duration of the air-puff stimuli (Sato et al., 2022a). It is, however, unknown whether this action selection is modulated by auditory input because it had been technically difficult to apply the quantitatively identical acoustic and air-puff stimuli to freely moving crickets from a specific angle. In this study, we used a newly developed servosphere treadmill system (Iwatani et al., 2019) and investigated the effects on the wind-elicited escape behavior in crickets when the high-frequency tone sound was given at various intervals to the air-puff stimulus.

2 Materials and methods

2.1 Animals

We used a wild-type strain of field crickets (*Gryllus bimaculatus*, Hokudai WT; Watanabe et al., 2018) that were bred in our laboratory. Adult male crickets, less than 14 days after the imaginal molting, were used throughout the experiments. They were reared under 12:12-h light/dark conditions at a constant temperature of 27°C. The guidelines of the Institutional Animal Care and Use Committee of the National University Corporation,

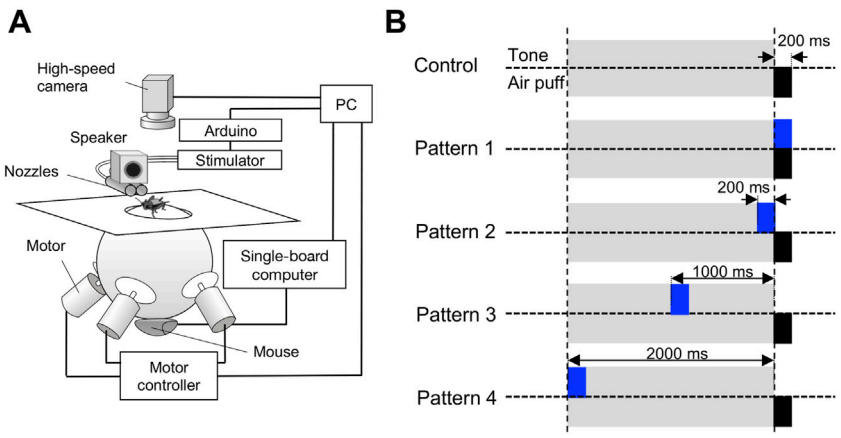

FIGURE 1
Experimental apparatus and stimulation patterns for behavioral tests. **(A)** Servo-sphere treadmill system for stimulation and monitoring of the freely moving cricket. The air-puff stimulus was applied from the right or left side of the cricket, which was specified by controlling the orientation of the cricket's body against the air nozzle with the servo-sphere treadmill system that was closed-loop controlled based on the high-speed camera image of the cricket. **(B)** Temporal arrangement of the air-puff and acoustic stimuli for the five different patterns. For the control pattern, only single air-puff stimuli were applied without the acoustic stimulus. For patterns 1-4, a 15-kHz pure tone sound of 200-ms duration was applied from a loudspeaker above the air nozzle, and the air-puff stimulus was initiated 0, 200, 1000, and 2000 ms after the onset of the acoustic stimulus, respectively.

Hokkaido University, Japan, specify no requirements for the treatment of insects in experiments.

2.2 Preparation and experimental condition

The antennae of the crickets were removed to eliminate the influence of mechanosensory inputs from the antennal organ, which enabled to focus on the interaction between the cercal and auditory systems. All behavioral experiments were conducted during the dark phase of the crickets at room temperature (26°C–28°C) under white LED illumination in a sound-attenuated room (AMC-3525, O'HARA and Co., Ltd., Tokyo, Japan) where anechoic foam sheets (F2-PF, Strider, Toyohashi, Japan) were attached to the ceiling and inner walls.

2.3 Treadmill system

To apply the quantitatively identical auditory and cercal stimuli to the free-moving cricket, we adopted a markerless visual feedback servo-sphere treadmill system (Iwatani et al., 2019). In this system, a Styrofoam ball (ø = 200 mm) was supported by three motor-driven omni-wheels. The treadmill system was installed within a sound-proofed wood box, and its top was covered with a white paper board of 500 mm × 500 mm except for the top 100-mm diameter of the ball. A region of 350 mm × 450 mm, including the ball top and whiteboard, was monitored by a high-speed digital video camera (acA 1920-155 um, BASLER, Ahrensburg, Germany), which was suspended at 800-mm height above the treadmill from a ceiling of the sound-attenuation room (resolution, 1,216 × 1,200 pixels; shutter speed, 1 ms; sampling rate, 160 frames/s, (Figure 1A). Full size of the captured image was used for tracking a cricket and a half size of them was stored for the offline analysis of escape behavior. While an animal was on the treadmill ball, the animal's location and head orientation were estimated automatically by an image processing technique proposed in a previous report from each captured image (Iwatani, 2021). The treadmill ball was regulated by rotation of the omni-wheels so that the center of the animal's body and its major axis were always kept at the center at the top of the treadmill ball and to a specific orientation, respectively. This negative feedback allowed the animal moving on the treadmill to be positioned in the specific location and head direction relative to the stimulus nozzle and loudspeaker. This system was feedback-controlled at a rate of 160 times per second. The escape movements caused by the airflow stimulus were recorded by the high-speed camera used for the feedback control of the treadmill. Spontaneous movement of the cricket before the air-current stimulation was detected as the rotation of the Styrofoam ball by an optical mouse placed under the treadmill.

2.4 Stimulation

An air-puff stimulus was provided to the stationary cricket by a short puff of nitrogen gas from a plastic nozzle (ø = 15 mm) connected to a pneumatic picopump (PV820, World Precision Instruments, Sarasota FL, USA). For the behavioral experiments using the treadmill system, two air-puff nozzles were arranged in parallel to align their center to the same horizontal plane as the top of the treadmill sphere (Figure 1A). Nozzle ends were placed at 200 mm from the animal. The velocity of the air puffs was controlled at 1.00 m/s, which was measured at the center of the arena with a 405-V1 thermal anemometer (Testo, Yokohama, Japan), by adjusting the delivery pressure of the picopump. The duration of the air-puff stimulus was 200 ms. By changing the cricket's body axis relative to the stimulus nozzle, the air puffs were applied to the right or left side of the cerci from one of the air nozzles, which was close to the posterior side of the crickets.

The acoustic stimuli were 15-kHz pure tones, synthesized using RPvdsEx software (Tacker Davis Technologies, Alachua FL, USA), and transduced and attenuated using an RM1 processor (TDT). The sounds were calibrated at an average of 70 dB SPL and delivered by a 1.5-inch (3.81 cm) full-range sealed loudspeaker (MM-SPS2, Sanwa Supply, Okayama, Japan), which was located just above the air-puff nozzles at 200 mm away from the animal (Figure 1A).

2.5 Stimulation protocols and experimental procedure

To test the cross-modal effects of temporal relationships between the acoustic and air-puff stimuli on the wind-elicited escape behavior, we designed five types of stimulation protocols, referred to as patterns 1-4, in which the air puff was combined with acoustic stimuli, and the control stimulated by the air puff without them (Figure 1B). For the control, only a single air puff of 200-ms duration stimulus was applied without the acoustic stimulation. For the stimulation protocols of patterns 1-4, a 15-kHz pure tone sound of 200-ms duration was started at 0, 200, 1000, or 2000 ms before the air-puff stimulus (Figure 1B). In all stimulation patterns, including the control for the behavioral experiments, a single air-puff stimulus was delivered alternatively from a nozzle to the left or right side of the cricket.

When a cricket was placed on the top of the treadmill, the feedback control of the servosphere was immediately started for the cricket to be positioned at the center of the treadmill and oriented on the left or right side relative to the stimulus nozzle. Every trial, regardless of with or without tone, started only when the cricket kept still for at least 1 s, defined by movement velocity < 10 mm/s measured with the optical mouse under the treadmill sphere. The air-puff stimulus was provided 2 s after the trial started. During these 2 s, the tone sound was played with a specific delay to the air puff. When the cricket moved during these 2 s, the air-puff stimulation was canceled, and the trial restarted after the cricket kept still for at least 1 s. At the onset of air-puff stimulation, the feedback control of the servosphere treadmill was stopped, allowing us to record the cricket's movement trajectory with the high-speed camera.

The crickets were divided into 4 groups for different stimulation patterns (patterns 1–4). As each experimental group consisted of 15 individuals, 60 crickets were used for the experiments in total. Each individual cricket was exposed to 4 different types of stimulation: control-right, control-left, with sound-right, with

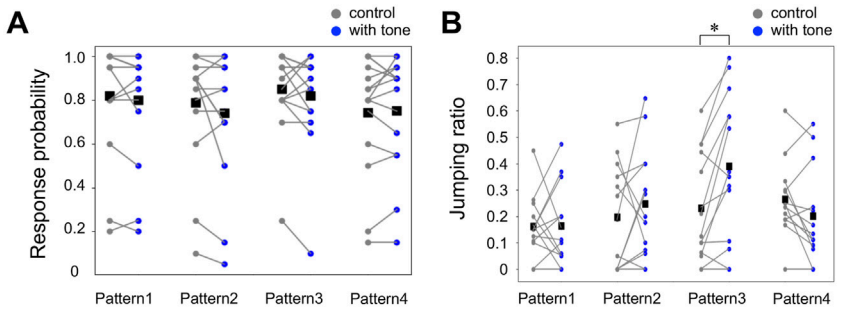

FIGURE 2
Auditory effects on the response probability and the action selection between running and jumping. **(A, B)** The probability of escape response in all trials **(A)** and the jumping probability in the responding trials **(B)** for the combined stimulation patterns (blue) and control (gray). Small dots connected by lines indicate the mean of the locomotion parameters for each individual. Black squares indicate the average of the data of all individuals. *$p < 0.05$, Wilcoxon rank-sum test. N = 15 individuals for each combined stimulation pattern.

sound-left. For "with sound," the airflow and sound were applied from the same side in any one of the combined stimulation patterns 1–4. The order of stimulation types was randomized, and this randomized stimulation set was repeated 10 times. Thus, 40 trials were conducted in succession for each individual in total. The inter-trial intervals were 1 min or more. The same pattern of the combined stimulation was used for one individual.

2.6 Image processing

To compensate for sample-by-sample errors in distance measurements due to angle of view and camera positions, only the area of 350 mm × 450 mm on the opposite side to the stimulus nozzle, which was indicated by four black spots on the white paper board, was cut out from the video image and transformed into a 406 × 522 pixels image. After approximating the contour of the cricket body as an ellipse based on a binarized image, the location and body axis of the cricket were determined by the centroid and the long axis of the ellipse, respectively. The head orientation was set manually on the first image for each sample.

2.7 Criteria for the wind-elicited escape responses

The wind-elicited responses of the cricket were analyzed in a manner similar to previous studies (Sato et al., 2017; Sato et al., 2019; Sato et al., 2022a; Sato et al., 2022b). Whether the cricket responded or not was determined based on the translational velocity of its movement. If the translational velocity exceeded 10 mm/s during the period from the stimulus onset to 250 ms after the stimulus onset and was greater in its maximum value than 50 mm/s, the cricket was considered to "respond" to the air current. If the cricket did not begin to move within 250 ms of the response definition period, the trial was considered as "no response." All the "responding" trials were further categorized into "jumping" or "running" according to leg movements during escape action, which was determined visually for all escaping trials by frame check of the video, as in the previous studies (Sato et al., 2017; Sato et al., 2019; Sato et al., 2022a; Sato et al., 2022b). If all six legs were off the ground simultaneously, that response was defined as "jumping." If any one of the six legs touched the ground during movement, that response was defined as "running" (see typical running and jumping responses shown in Supplementary Videos S1, S2 of Sato et al., 2022b). The initial response in which both jumping and running movements were observed, for example, the jumping followed by running and the jumping after running, was also defined as "jumping."

2.8 Quantification of escape responses

The selection ratio of running or jumping was calculated as the proportion of responses for all the responding trials. The jumping probability was calculated from the number of jumping responses per total responding trial for each stimulation pattern. The movements in the escape behavior were analyzed for the "initial response" in the responding trials as in previous studies (Oe and Ogawa, 2013; Sato et al., 2017; Sato et al., 2019; Sato et al., 2022a; Sato et al., 2022b). The start of the initial response was defined as when the translational velocity exceeded 10 mm/s for the first time just before reaching 50 mm/s. The finish was defined as when the velocity was less than 10 mm/s for the first time after the response started. Reaction time, maximum movement velocity, and movement distance were measured as metric parameters that characterized the escape movement. The definition of these parameters was the same as those in the previous studies (Oe and Ogawa, 2013; Sato et al., 2017; Sato et al., 2019; Sato et al., 2022a; Sato et al., 2022b). The reaction time was measured as the delay from opening the delivery valve in the picopump to the start of the initial response. The movement distance was measured as the entire path length of the 2-dimensional moving trajectory that was traced for the centroid of the approximated ellipse from the stimulated point to the termination point of the initial response on the video data. The movement direction as the angular parameter was measured as the angle between the body axis at the stimulated location and a line connecting the stimulated location and the response finish location.

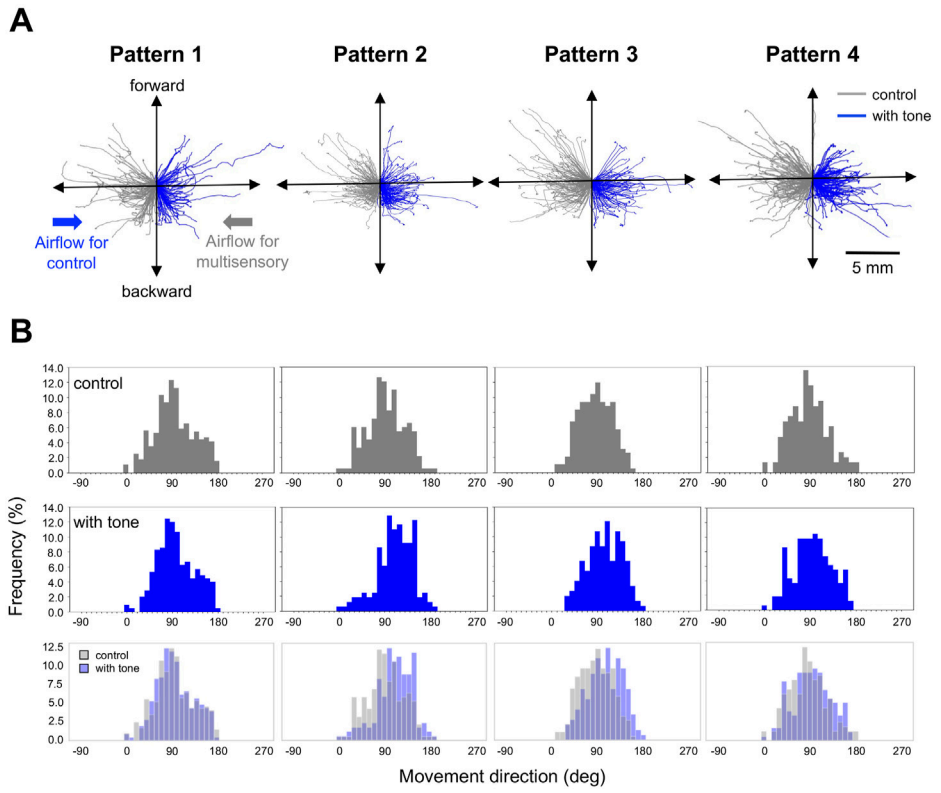

FIGURE 3
Movements in the running escape responses. **(A)** Typical running trajectories of given individuals in the running response to air puffs combined with and without acoustic stimulus. Gray traces indicate the response in control. Blue traces indicate the response to air-puff combined with tone sound, 0 ms (pattern 1), 200 ms (pattern 2), 1000 ms (pattern 3), and 2000 ms (pattern 4) before the air-puff onset. The trajectories were combined data of the responses to left and right stimuli. The trajectories for the control condition were displayed against the air puff from the right side, and those for the combined stimulation conditions were displayed against the air puff from the left side. **(B)** Distributions of running direction for different stimulation patterns. Gray bars represent the data for controls, and blue bars represent those for patterns 1, 2, 3, and 4. *N* = 15 individuals for control and each acoustic stimulation pattern.

2.9 Statistical methods

R programming software (ver. 4.0.2, R Development Core Team) was used for the statistical analysis. For analyses of the locomotion parameters measured in the behavioral experiment, such as movement direction, maximum movement velocity, movement distance, and reaction time, to avoid pseudo-replication, we used mean values of the data obtained in the responding trials for each individual as the representative values for the statistical tests. The movement direction is a circular parameter, but the mean angle of it for each individual ranged from 60° to 140°, so this parameter was analyzed as a metric parameter like other locomotion parameters. Prior to the statistical testing of the locomotion parameters, we checked the distribution of the datasets using the Shapiro-Wilk test. As the data of these parameters in the behavioral experiment were normally distributed, we used the paired *t*-test between the control and combined stimulation patterns to assess the significance of the effects on the running response of the acoustic stimulation. Since some individuals showed jumping responses to only one of the control or combined stimulations, we used the unpaired *t*-test to assess the auditory effects on the jumping responses. The Wilcoxon signed-rank test was used to assess the significance of the stimulation condition for the response and jumping probabilities those were not normally distributed.

3 Results

3.1 Preceding high-frequency sounds increased the choice of jumping response

To investigate how long the impact of the auditory stimuli on the wind-elicited escape behavior lasted, we designed four patterns of the stimulation pattern combining the acoustic stimulus and air puff, which differed in the delay (0, 200, 1000, or 2000 ms) from the onsets of the tone sound to that of the air puff (Figure 1B). The stimulation pattern in which only air puff was applied without the tone sound was used as a control. Crickets exhibit two distinct escape actions, running and jumping, in response to air-puff stimuli (Sato et al., 2017; Sato et al., 2019; Sato et al., 2022a; Sato et al., 2022b), but it is untested whether the auditory stimulus can affect this action selection. The servosphere treadmill system allowed the

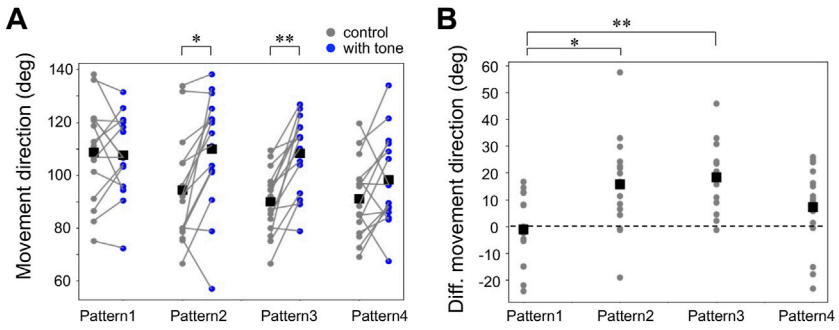

FIGURE 4
Auditory effects on the movement direction in the running response. **(A)** Movement direction for control (gray) and combined stimulation patterns (blue). Small dots connected by lines indicate the mean angle of the movement directions for each individual. Black squares indicate the average of the data of all individuals. The direction opposite to the air puff is indicated as positive. *$p < 0.05$, **$p < 0.01$, paired t-test. **(B)** Changes in movement direction by acoustic stimulation. Small gray dots represent the mean of the data of each individual. *$p < 0.05$, **$p < 0.01$ unpaired t-test with Bonferroni correction. N = 15 individuals for each acoustic stimulation pattern.

crickets to escape not only by running but also by jumping in response to the air-puff stimulus, unlike the tethered treadmill system (Oe and Ogawa, 2013; Fukutomi et al., 2015; Fukutomi and Ogawa, 2017). In all stimulation patterns, most of the crickets exhibited wind-elicited escape behaviors, either running or jumping, as reported in the previous study of free-moving crickets (Sato et al., 2017; Sato et al., 2019; Sato et al., 2022a; Sato et al., 2022b).

Firstly, we examined the probability that the crickets exhibited the escape response, including running and jumping. The preceding tone did not modify the probability of responses to the airflow stimuli of the velocity we used in this study (Figure 2A, Supplementary Datasheet S1). The behavioral responses that we recorded were classified into either running or jumping based on the cricket's leg movements. Then, we compared the selection ratio of the running and jumping in all responding trials among different stimulation patterns (Figure 2B, Supplementary Datasheet S1). In control, jumping was observed in 21% of all responding trials. When the sound stimulus was applied 1000 ms before the air puff in Pattern 3, the jumping ratio to all responding trials was 39%, which was significantly higher than that in the control. In contrast, the jump ratios for other stimulation patterns 1, 2, and 4 were 19%, 25%, and 22%, respectively, and were almost the same as the control. These results indicated that the crickets chose the jumping more frequently in the wind-elicited escape behavior when they heard the high-frequency sound applied 1000-ms before the air-puff stimulus.

3.2 Auditory effect on the motor parameters of the escape behavior

Next, we focused on the auditory effects of the running escape that have been reported in previous studies on the crickets tethered on an air-lifted treadmill (Fukutomi et al., 2015; Fukutomi and Ogawa, 2017). It has been confirmed that the 15-kHz tone sound we used alone does not induce any locomotion in crickets (Fukutomi and Ogawa, 2017). The running trajectories in all trials responding to the air puff applied from the side of the crickets indicated that they moved toward the side opposite to the stimulus (Figure 3A). When the 15-kHz tone sounds were applied simultaneously with the air puff, referred as Pattern 1, there was no difference in the trajectories compared to the control (gray traces in Figure 3A). In contrast, when the tone sound was given 200–2000 ms before the air puff as in Patterns 2, 3, and 4, the trajectories seemed to be extended more backward (Figure 3A). The distributions of running direction, therefore, for the stimulation patterns 2-4 were likely shifted to backward compared to that for control (Figure 3B). The statical analysis indicated that the running direction for the pattern 2 and 3, in which the air puffs were applied 200 ms and 1000 ms after the sound started, was significantly greater than that for the control (Figure 4A, Supplementary Datasheet S1). In contrast, there was no significant difference in the running direction for patterns 1 and 4 (Figure 4A), indicating that the sounds given 0 ms or 2000 ms before the air puff had little effect on the movement direction in the running escape. These results suggest that the auditory modulation of movement direction requires the tone sounds preceding the air puff, not simultaneous to it. In addition, the magnitude of the auditory effect on the movement direction was measured as the difference between the control condition without acoustic stimulus and the test condition with tone and was examined for delay times from acoustic to airflow stimuli (Figure 4B, Supplementary Datasheet S1). The high-frequency sound starting 1000 ms before the airflow onset seemed to be still as effective as that immediately before the airflow, even though there was a silent period of 800 ms before the airflow onset. And the sound given 2000 ms before the airflow onset (the silent period between the sound and airflow was 1800 ms) appeared less effective. These results indicated that the auditory effect on the movement direction lasted at least 800 ms after the end of the sound stimulus but was not maintained for 1800 ms.

Although the previous works did not detect auditory effects on the other locomotion parameters, it was possible that the different temporal relationships of tone and air puff could

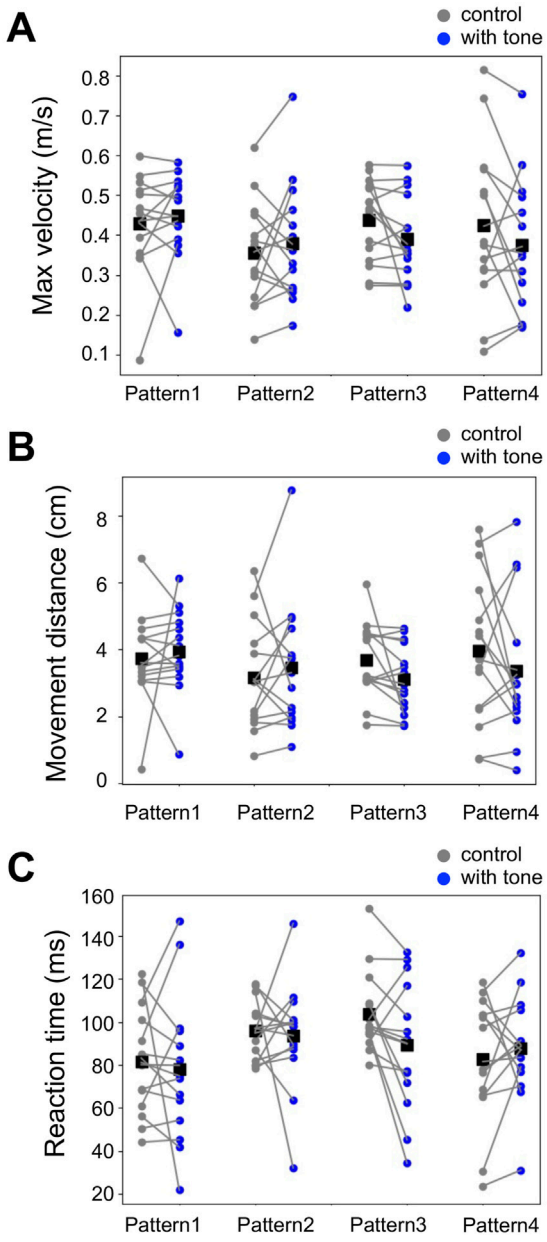

FIGURE 5
No effects of acoustic stimulation on other locomotion parameters for the running response. **(A–C)** Maximum movement velocity **(A)**, movement distance **(B)**, and reaction time **(C)** in the escape running responses for the different patterns of combined stimulation (blue) and control (gray). Small dots connected by lines indicate the mean of the locomotion parameters for each individual. Black squares indicate the average of the data of all individuals. There was no significant difference in these parameters between combined stimulation patterns (1–4) and control (paired *t*-test). *N* = 15 individuals for control and each acoustic stimulation pattern.

modulate them (Fukutomi et al., 2015; Fukutomi and Ogawa, 2017). Then, we examined the auditory modulation of locomotion parameters in the running escape, including the maximum movement velocity, the movement distance, and the reaction time (Figure 5, Supplementary Datasheet S1). The measured values of these parameters varied among the different groups of crickets but were not significantly different for any stimulation patterns compared to the controls. This result indicated that these parameters are not affected by sound regardless of the temporal relationship.

Then, we also investigated the auditory modulation of the locomotion parameters in the jumping response, which were movement direction, movement distance, maximum velocity, and reaction time (Figure 6, Supplementary Datasheet S1). As in the running response, there was no significant difference in any of the parameters of the running response between the control and combined stimulation for all 4 patterns. Taken together, the high-frequency sound applied before the air-puff stimulus did not affect locomotor parameters in both running and jumping escape.

4 Discussion

4.1 Auditory effect on the behavioral choice

An identical stimulus does not always cause animals to engage in the same behavior. They determine the appropriate response based on the situation, the external stimulus, and their internal state. Crickets exhibit several escape actions, including running and jumping in response to a short air current detected as a predator approaches (Tauber and Camhi, 1995; Dupuy et al., 2011). Recently our study of freely moving crickets in an experimental arena revealed that crickets change the behavioral choice in the wind-elicited escape behavior, either running or jumping, according to the airflow speed and duration (Sato et al., 2022a). Using quantitatively identical acoustic stimulation with the servosphere treadmill system, we succeeded in examining the auditory effect on this behavioral choice in the freely moving crickets. Our results showed that the high-frequency sound applied 1000 ms before the air-puff stimulus increased the choice of jumping. This suggests that the additional auditory input could bias the decision of running or jumping. In addition, unlike the auditory effect on the running direction, this effect on the behavioral choice was not observed when the acoustic stimulus was given 200 ms before the air puff. This indicates that 200 ms is too short for crickets to reflect the auditory information of the context in the behavioral choice.

The behavioral choice includes not only running or jumping but also escaping or not. Previous works showed that the preceding sound elevated the response threshold, i.e., decreased the response probability of the wind-elicited escape (Fukutomi et al., 2015; Fukutomi and Ogawa, 2017). However, we could not find the auditory effect on response probability from the present results. This may have been due to a difference in the airflow intensity used. In this study, to examine the behavioral choice between jumping and running, we used large-velocity air-puff stimuli (1.0 m/s). The response probability curve against air-puff velocity shows that response probability is saturated at around 1.1 m/s (Fukutomi et al., 2015). Thus, it may be difficult to detect the auditory effect on the response probability at that velocity. The lower velocity of the air-puff stimulus should be used to detect the auditory modulation of response probability.

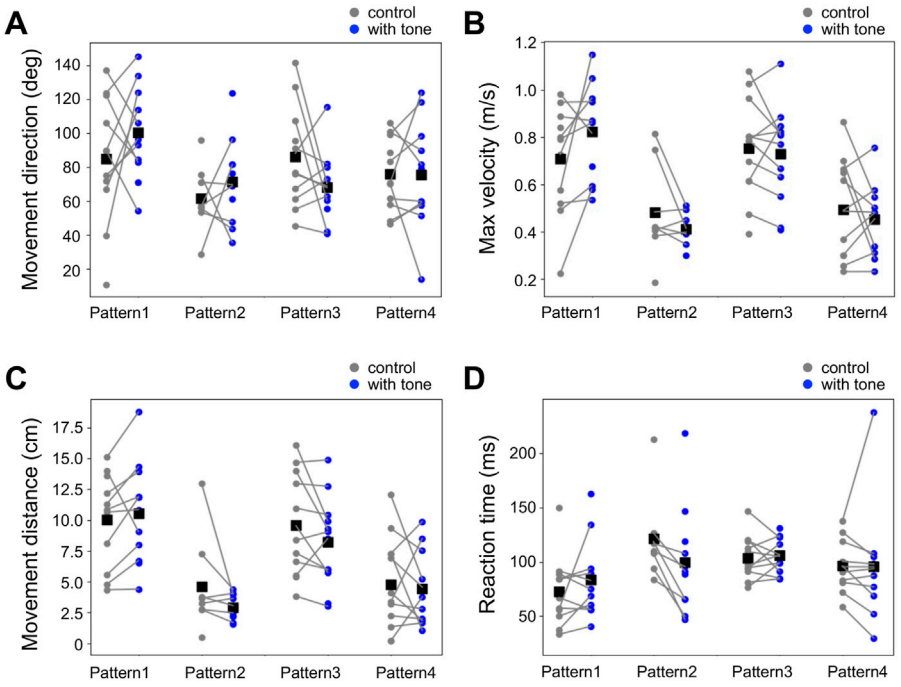

FIGURE 6
No effects of acoustic stimulation on the locomotion in the jumping response. **(A–D)** Movement direction **(A)**, maximum movement velocity **(B)**, movement distance **(C)**, and reaction time **(D)** in the escape jumping responses for the different patterns of combined stimulation (blue) and control (gray). Small dots connected by lines indicate the mean of the locomotion parameters for each individual. Black squares indicate the average of the data of all individuals. There was no significant difference in these parameters between combined stimulation patterns (1–4) and control (unpaired *t*-test). *N* = 11 and 11 (pattern 1), 8 and 11 (pattern 2), 12 and 12 (pattern 3), and 12 and 11 (pattern 4) individuals for control and each combined stimulation, respectively.

4.2 Auditory effects on the running direction lasted at least 1 s

Directional control is one of the most important aspects of the initial phase in escape behavior (Domenici et al., 2011a; b; Nair et al., 2017; Kimura and Kawabata, 2018). Crickets can control the direction of their wind-induced escape according to the angle of the stimulus, as in the escape behaviors of flies and cockroaches (Domenici et al., 2008; Card, 2012). Crickets flee in the opposite direction from which the air-puff stimulus comes, as in the control condition observed in our experiments (Oe and Ogawa, 2013; Sato et al., 2019). The previous study reported that crickets moved more backward in response to the air puff from their side when they heard a high-frequency sound for 800 ms before that threat stimulus (Fukutomi et al., 2015). This modulation is considered to be a behavioral modulation adapting to the presence of echolocating bats, which are a predator of crickets (Fukutomi and Ogawa, 2017). In these previous studies, however, a final part of the preceding tone sound temporally overlapped with the air-puff stimulus. Therefore, it has been unknown whether the temporal coincidence of the acoustic and air-puff stimuli is necessary for the modulation of the escape behavior. In other words, it remains unclear whether the acoustic stimulus terminating before the air-puff stimulus also modulates the escape behavior. If so, how long does the auditory effect last? The present results indicated that the running direction was biased backward when the 200-ms sound pulse was applied 200 or 1000 ms before the air-puff stimulus started. In contrast, the acoustic stimuli that were given simultaneously or 2000 ms before the air puff had little impact on the escape direction. These results demonstrated that preceding auditory inputs rather than simultaneous ones with the air-puff stimulus were necessary for the behavioral modulation.

Interestingly, even when the sound pulse of 200-ms duration was applied 1000-ms before the air-puff stimulus, it also biased the running direction backward. This result also suggested that the acoustic contextual information could be retained for at least 800 ms after the loss of auditory inputs. Temporal relationships between conditioning stimulus (CS) and unconditioned stimulus (US) were crucial rules for classical conditioning to induce associative learning (Mazur, 2006; Mazur, 2012). In classical eye-blink conditioning in mammals, successful learning requires that the sound stimulus as CS precedes the air puff as US, and that simultaneous exposure to both CS and US does not induce the learning. That is because it takes some time for the animals to recognize the CS and to associate the CS with the following US. Probably, this reason accounts for our results that auditory modulation of the running direction required precursor time. The neurophysiological study on eye-blink conditioning in rabbits reported that rostral medial prefrontal cortex (rmPFC) neurons detect CS-US time intervals with dominant firing peaks (Caro-Martín et al., 2015). In the cricket brain, LN3 neuron has been identified as a coincidence detector to recognize the interval of an acoustic pulse of a male's calling song (~20 ms) (Schöneich et al., 2015), although the interval is much shorter than 800 ms. Future studies will explore what neural

mechanisms could perceive the auditory context and sustain that "memory" to modulate wind-elicited escape behavior.

5 Conclusion

Crickets modulate wind-elicited escape behavior depending on acoustic context mediated by cross-modal integration (Fukutomi et al., 2015; Fukutomi and Ogawa, 2017). Here we showed that the auditory modulations of movement direction and jumping probability require preceding auditory input but not simultaneous input. Furthermore, the effect of this contextual information was found to persist for at least 0.8 s after the acoustic stimulus ceased. Future works will examine what neural mechanism supports the persistence of contextual information that influence the behavior.

Data availability statement

The raw data supporting the conclusion of this article will be made available by the authors, without undue reservation.

Author contributions

All authors edited and approved the final version of the manuscript; AL and MF wrote the paper; HS and HO reviewed and edited the paper; All authors conceptualized and designed the work; AL performed experiments and analyzed data; MF, HS, and HO supervised the work. All authors listed have made a substantial, direct, and intellectual contribution to the work and approved it for publication. All authors contributed to the article and approved the submitted version.

Funding

This work was supported by funding to HO from JSPS and MEXT KAKENHI grants 16H06544, 21K06259, and 21H05295.

Acknowledgments

The authors thank Dr. Yasushi Iwatani for developing and manufacturing the servo-sphere treadmill system and his helpful advice.

Conflict of interest

The authors declare that the research was conducted in the absence of any commercial or financial relationships that could be construed as a potential conflict of interest.

Publisher's note

All claims expressed in this article are solely those of the authors and do not necessarily represent those of their affiliated organizations, or those of the publisher, the editors and the reviewers. Any product that may be evaluated in this article, or claim that may be made by its manufacturer, is not guaranteed or endorsed by the publisher.

Supplementary material

The Supplementary Material for this article can be found online at: https://www.frontiersin.org/articles/10.3389/fphys.2023.1153913/full#supplementary-material

References

Card, G. M. (2012). Escape behaviors in insects. *Curr. Opin. Neurobio.* 22, 180–186. doi:10.1016/j.conb.2011.12.009

Caro-Martín, C., Leal-Campanario, R., Sánchez-Campusano, R., Delgado-García, J. M., and Gruart, A. (2015). A variable oscillator underlies the measurement of time intervals in the rostral medial prefrontal cortex during classical eyeblink conditioning in rabbits. *J. Neurosci.* 35, 14809–14821. doi:10.1523/JNEUROSCI.2285-15.2015

Domenici, P., Turesson, H., Brodersen, J., and Brönmark, C. (2008). Predator-induced morphology enhances escape locomotion in crucian carp. *Proc. R. Soc. B* 275, 195–201. doi:10.1098/rspb.2007.1088

Domenici, P., Blagburn, J. M., and Bacon, J. P. (2011a). Animal escapology I: Theoretical issues and emerging trends in escape trajectories. *J. Exp. Biol.* 214, 2463–2473. doi:10.1242/jeb.029652

Domenici, P., Blagburn, J. M., and Bacon, J. P. (2011b). Animal escapology II: Escape trajectory case studies. *J. Exp. Biol.* 214, 2474–2494. doi:10.1242/jeb.053801

Domenici, P. (2010). Context-dependent variability in the components of fish escape response: Integrating locomotor performance and behavior. *J. Exp. Zool. A Ecol. Genet. Physiol.* 313, 59–79. doi:10.1002/jez.580

Dupuy, F., Casas, J., Body, M., and Lazzari, C. R. (2011). Danger detection and escape behaviour in wood crickets. *J. Insect Physiol.* 57, 865–871. doi:10.1016/j.jinsphys.2011.03.020

Ellard, C. G., and Eller, M. C. (2009). Spatial cognition in the gerbil: Computing optimal escape routes from visual threats. *Anim. Cogn.* 12, 333–345. doi:10.1007/s10071-008-0193-9

Fukutomi, M., and Ogawa, H. (2017). Crickets alter wind-elicited escape strategies depending on acoustic context. *Sci. Rep.* 7, 15158. doi:10.1038/s41598-017-15276-x

Fukutomi, M., Someya, M., and Ogawa, H. (2015). Auditory modulation of wind-elicited walking behavior in the cricket *Gryllus bimaculatus*. *J. Exp. Biol.* 218, 3968–3977. doi:10.1242/jeb.128751

Hemmi, J. M. (2005). Predator avoidance in fiddler crabs: 2. The visual cues. *Anim. Behav.* 69, 615–625. doi:10.1016/j.anbehav.2004.06.019

Hoy, R., Nolen, T., and Brodfuehrer, P. (1989). The neuroethology of acoustic startle and escape in flying insects. *J. Exp. Biol.* 146, 287–306. doi:10.1242/jeb.146.1.287

Ifere, N. O., Shidara, H., Sato, N., and Ogawa, H. (2022). Spatial perception mediated by insect antennal mechanosensory system. *J. Exp. Biol.* 225, jeb243276. doi:10.1242/jeb.243276

Iwatani, Y., Ogawa, H., Shidara, H., Sakura, M., Sato, T., Hojo, M. K., et al. (2019). Markerless visual servo control of a servosphere for behavior observation of a variety of wandering animals. *Adv. Robot.* 33, 183–194. doi:10.1080/01691864.2019.1570334

Iwatani, Y. (2021). "High-speed servosphere," in Proceedings of IEEE/SICE International Symposium on System Integration, Iwaki, Fukushima, Japan, January 2021 (IEEE), 613–618.

Kanou, M., Matsuyama, A., and Takuwa, H. (2014). Effects of visual information on wind-evoked escape behavior of the cricket, *Gryllus bimaculatus*. *Zool. Sci.* 31, 559–564. doi:10.2108/zs130218

Kimura, H., and Kawabata, Y. (2018). Effect of initial body orientation on escape probability of prey fish escaping from predators. *Biol. Open* 7, bio023812. doi:10.1242/bio.023812

LeDoux, J., and Daw, N. D. (2018). Surviving threats: Neural circuit and computational implications of a new taxonomy of defensive behaviour. *Nat. Rev. Neurosci.* 19, 269–282. doi:10.1038/nrn.2018.22

Mazur, J. E. (2006). *Learning and behavior*. 6th ed. Prentice-Hall, Englewood Cliffs, NJ: Pearson Education, Inc.

Mazur, J. E. (2012). *Learning and behavior: Instructor's review copy*. 7th ed. New York: Psychology Press.

McDonald, J. J., Teder-Sälejärvi, W. A., and Hillyard, S. A. (2000). Involuntary orienting to sound improves visual perception. *Nature* 407, 906–908. doi:10.1038/35038085

Meredith, M. A., Nemitz, J. W., and Stein, B. E. (1987). Determinants of multisensory integration in superior colliculus neurons. I. Temporal factors. *J. Neurosci.* 7, 3215–3229. doi:10.1523/JNEUROSCI.07-10-03215.1987

Moiseff, A., Pollack, G. S., and Hoy, R. R. (1978). Steering responses of flying crickets to sound and ultrasound: Mate attraction and predator avoidance. *Proc. Nat. Acad. Sci. U. S. A.* 75, 4052–4056. doi:10.1073/pnas.75.8.4052

Mu, Y., Li, X.-Q., Zhang, B., and Du, J.-L. (2012). Visual input modulates audiomotor function via hypothalamic dopaminergic neurons through a cooperative mechanism. *Neuron* 75, 688–699. doi:10.1016/j.neuron.2012.05.035

Nair, A., Changsing, K., Stewart, W. J., and McHenry, M. J. (2017). Fish prey change strategy with the direction of a threat. *Proc. R. Soc. B* 284, 20170393. doi:10.1098/rspb.2017.0393

Oe, M., and Ogawa, H. (2013). Neural basis of stimulus-angle-dependent motor control of wind-elicited walking behavior in the cricket *Gryllus bimaculatus*. *PLoS One* 8, e80184. doi:10.1371/journal.pone.0080184

Ohyama, T., Schneider-Mizell, C. M., Fetter, R. D., Aleman, J. V., Franconville, R., Rivera-Alba, M., et al. (2015). A multilevel multimodal circuit enhances action selection in Drosophila. *Nature* 520, 633–639. doi:10.1038/nature14297

Pollack, G. S. (2015). Neurobiology of acoustically mediated predator detection. *J. Comp. Physiol. A* 201, 99–109. doi:10.1007/s00359-014-0948-5

Sato, N., Shidara, H., and Ogawa, H. (2017). Post-molting development of wind-elicited escape behavior in the cricket. *J. Insect Physiol.* 103, 36–46. doi:10.1016/j.jinsphys.2017.10.003

Sato, N., Shidara, H., and Ogawa, H. (2019). Trade-off between motor performance and behavioural flexibility in the action selection of cricket escape behaviour. *Sci. Rep.* 9, 18112. doi:10.1038/s41598-019-54555-7

Sato, N., Shidara, H., and Ogawa, H. (2022a). Action selection based on multiple-stimulus aspects in wind-elicited escape behavior of crickets. *Heliyon* 8, e08800. doi:10.1016/j.heliyon.2022.e08800

Sato, N., Shidara, H., Kamo, S., and Ogawa, H. (2022b). Roles of neural communication between the brain and thoracic ganglia in the selection and regulation of the cricket escape behavior. *J. Insect Physiol.* 139, 104381. doi:10.1016/j.jinsphys.2022.104381

Schöneich, S., Kostarakos, K., and Hedwig, B. (2015). An auditory feature detection circuit for sound pattern recognition. *Sci. Adv.* 1, e1500325. doi:10.1126/sciadv.1500325

Stein, B. E., and Stanford, T. R. (2008). Multisensory integration: Current issues from the perspective of the single neuron. *Nat. Rev. Neurosci.* 9, 255–266. doi:10.1038/nrn2331

Stein, B. E., Meredith, M. A., Huneycutt, W. S., and McDade, L. (1989). Behavioral indices of multisensory integration: Orientation to visual cues is affected by auditory stimuli. *J. Cogn. Neurosci.* 1, 12–24. doi:10.1162/jocn.1989.1.1.12

Tauber, E. R. A. N., and Camhi, J. (1995). The wind-evoked escape behavior of the cricket *Gryllus bimaculatus*: Integration of behavioral elements. *J. Exp. Biol.* 198, 1895–1907. doi:10.1242/jeb.198.9.1895

Watanabe, T., Ugajin, A., and Aonuma, H. (2018). Immediate-early promoter-driven transgenic reporter system for neuroethological research in a hemimetabolous insect. *eNeuro* 5, e0061. doi:10.1523/ENEURO.0061-18.2018

Zani, P. A., Jones, T. D., Neuhaus, R. A., and Milgrom, J. E. (2009). Effect of refuge distance on escape behavior of side-blotched lizards (*Uta stansburiana*). *Can. J. Zool.* 87, 407–414. doi:10.1139/z09-029

frontiers | Frontiers in Physiology

TYPE Original Research
PUBLISHED 15 May 2023
DOI 10.3389/fphys.2023.1148129

OPEN ACCESS

EDITED BY
Feng Shang,
Southwest University, China

REVIEWED BY
Jia Fan,
Institute of Plant Protection (CAAS), China
Tian-Xing Jing,
Yangzhou University, China

*CORRESPONDENCE
Chao Li,
lichaoyw@xjau.edu.cn

RECEIVED 19 January 2023
ACCEPTED 24 April 2023
PUBLISHED 15 May 2023

CITATION
Liu X, Yang H, Niu F, Sun H and Li C (2023), Impact of water stress on the demographic traits and population projection of Colorado potato beetle. *Front. Physiol.* 14:1148129. doi: 10.3389/fphys.2023.1148129

Impact of water stress on the demographic traits and population projection of Colorado potato beetle

Xia Liu[1], Hangxin Yang[1], Fushuai Niu[1], Hanhan Sun[1] and Chao Li[1,2]*

[1]Key Laboratory of Prevention and Control of Invasive Alien Species in Agriculture and Forestry of the North-western Desert Oasis (Co-construction by Ministry and Province), Ministry of Agriculture and Rural Affairs, College of Agronomy, Xinjiang Agricultural University, Urumqi, China, [2]Western Agricultural Research Center, Chinese Academy of Agricultural Sciences, Changji, China

Introduction: The Colorado potato beetle is one of the famous quarantine pests in China which is extremely destructive to Solanaceae crops and causes serious losses to the potato industry.

Methods: In this experiment, the host plant potato was subjected to different degrees of water stress to observe the oviposition selection, growth and development, survival, reproduction and population growth of Colorado potato beetles.

Results: The results showed that adult Colorado potato beetles laid more eggs on potato plants suitable for water treatment, but fewer eggs on potato plants treated with water stress. The developmental duration of Colorado potato beetles in light drought treatment was shorter than that in control treatment, and the survival rate was higher than that in control treatment. With the aggravation of water stress, the developmental duration was prolonged, survival rate was decreased, and the number of eggs was decreased. Under different water stress levels, the intrinsic rate of increase (r), finite rate of increase (λ), net reproductive rate (R_0), and mean generation time (T) of the Colorado potato beetle population were significantly lower than those of control treatment, but there was no significant difference between light drought and control treatment. The TIMING-MS Chart program was used to predict the population dynamics of Colorado potato beetle for 110 days, which showed the fastest population growth in CK treatments and the slowest in HD treatments. The reduced water content of the leaves also reduces the survival rate of adult Colorado potato beetles. The growth, development, survival, and reproduction of Colorado potato beetles are affected by water stress of host plants. Moderate and heavy droughts have negative effects on the development and reproduction of Colorado potato beetles.

Discussion: This information can be used to clarify the impact of water stress on the growth, development and population dynamics of Colorado potato beetle, to provide a theoretical basis for the control of this pest.

KEYWORDS

Leptinotarsa decemlineata **(Say), water stress, oviposition selection, growth and development, reproduction**

1 Introduction

Colorado potato beetle (*Leptinotarsa decemlineata* (Say)) is a famous quarantine pest in China. It is a world-wide pest that seriously harms solanaceous crops (Zhang et al., 2020); it originated in the United States, and in China, the quarantine pest Colorado potato beetle was first found in Yili Valley and the Tacheng area of Xinjiang in 1993 (Amanulla, 2015). Both adults and larvae feed on the blade, and when the damage is serious, the entire leaf can be eaten up, leaving only the stems of the plant, which is extremely destructive to potatoes (Alyokhin et al., 2008; Li et al., 2014), causing serious losses to the local potato industry (Li et al., 2013; Zhang et al., 2018).

Xinjiang is located in the northwest of China, a typical temperate continental climate zone. Water is one of the main problems faced by Xinjiang's planting industry. Potato is a crop with strong suitability, high yield, and rich nutrition. With the proposal of the strategy of potato as a staple grain, potato, wheat, corn, and rice are called the four staple grains (Wang et al., 2019). Due to the unique geographical location and soil climate of Xinjiang, potato crops grown in Xinjiang have high yields. At the same time, Xinjiang is located in the core area of the "Silk Road Economic Belt" and has frequent trade exchanges with countries along the belt, which will increase the likelihood of the Colorado potato beetle spreading more widely (Liu et al., 2018; Liao et al., 2022a).

In recent years, the acceleration in global warming has had a significant impact on the natural ecosystem, and the corresponding changes of insect populations have also taken place (Cao et al., 2011). The interaction between plants and plant-feeding insects is a common phenomenon in nature; plants are the main food source and oviposition grounds for insects, and in general, the choice of the host is important for the growth and development of its offspring, The relationship between female insect selection on host plants and the survival and development of their offspring generally supports the preference–performance hypothesis (Jaenike, 1978; Clark et al., 2011). In the process of plant growth and development, plants will often suffer from some adverse stresses. Common abiotic stresses include high temperature, salt, and water. Water is a very important factor, which can independently affect each part of this interaction relationship and also through the interaction relationship between indirectly affect various parts. However, insects are more susceptible to water stress due to their small size (Addo-Bediako et al., 2001). Plants are the places for growth, development, reproduction, and habitation of insects, and the changes of their external morphology and internal organizational structure directly affect the living environment of herbivorous insects and then affect the behavior, growth, and reproduction of insects. Cabrera et al. (1995) found that the growth rate and relative growth rate of *Schizaphis graminum* Rondani decreased to a certain extent after feeding on wheat subjected to persistent water stress. Dang et al. (2009) found in the study of *Holotrichia oblita* Fald that when the environmental humidity was high, the larval mortality of *H. oblita* increased greatly. Water stress will also affect the fecundity of insects, and too low environmental humidity will affect the oviposition rate and emergence rate of insects. For example, the egg carrying rate and egg hatching rate of *Cnaphalocrocis medinalis* Guenee are significantly reduced under a low-humidity environment (Xu et al., 1999), and high humidity will have an adverse effect on the attachment of eggs. At low humidity, the pupal weight of *Spodoptera litura* Fabricius was lower and female adult spawn ability decreased (Zhong et al., 2001). Water stress will also lead to a decrease in the weight of *Nilaparvata lugens* Stal adults, and both egg laying and egg hatching rates also decreased (Luo et al., 2012). In addition, water stress also indirectly affected natural enemies. After potato drought treatment, the fecundity and life parameters of Colorado potato beetles were adversely affected, and the life and survival rate of adults of natural enemies of *Arma chinensis* Fallou were also reduced (Liu et al., 2022).

With the global climate change, the frequency and intensity of drought events may increase, so it is important to study the effects of plant-mediated herbivorous insect interactions under water stress. At present, although there are many studies on the impact of water stress on potatoes (Wu et al., 2022; Zhang et al., 2022), the impact of water stress on Colorado potato beetles and other pests is rarely reported. This experiment was conducted to study the oviposition preference, growth, development, and reproduction characteristics of Colorado potato beetle under different water stress conditions in the host plant potato, in order to clarify the impact of water stress on the growth, development, and population dynamics of Colorado potato beetle, to provide a theoretical basis for the control of this pest.

2 Materials and methods

2.1 Test materials

Potted potato plants were planted under the same management conditions (one plant is retained), the variety is "Holland 15," and the experiment will be started after the plant growth is stable. Insects tested: Adult Colorado potato beetles were collected from the potato field in Jimsar County, Changji Hui Autonomous Prefecture, Xinjiang, and placed in an artificial climate box (RXM-168C-1 climate chamber, Ningbo Jiangnan Instrument Factory, Ningbo, China). The feeding was performed under the following conditions: ambient temperature 27 °C ± 1 °C, relative humidity 70% ± 5%, and photoperiod 16L:8D. The adults collected outdoors are the first generation. The eggs laid by the outdoor adults develop into second-generation adults. The second generation of Colorado potato beetle larvae was collected from the potato leaves planted in the earlier stage for feeding.

2.2 Experiment method

2.2.1 Drought treatment of potato

The experiment adopted the potting soil cultivation method, planting potatoes in plastic pots (diameter 27 cm, bottom diameter 17 cm, and height 19 cm), three holes were punched at the bottom of the plastic pot to prevent water accumulation, each pot was filled with 4 kg of nutrient soil, and the potted seedlings were placed outdoors in a rain-sheltered place, which could cover from rain on rainy days and normal light on sunny days. On 28 March 2022, seed potato chunks with basically the same size and full buds were selected for sowing, and one plant per pot was planted. The pots

were kept at a distance to avoid interference caused by the canopy of the grown potatoes. After sowing, they were watered enough to ensure normal emergence, and when the potato plants grow to about 10 cm (May 22), different degrees of water stress tests were carried out. According to the soil water content to determine the water stress intensity, the test set up a total of four treatments, normal irrigation (CK): the soil water content is more than 80%; light drought (LD): a soil moisture content of 55%–65%; moderate drought (MD): a soil moisture content of 35%–45%; and heavy drought (HD): 15%–25% soil water content. During the test, the soil moisture meter was used to determine the soil moisture content, and the soil water content was controlled by the weighing method, and the control group was irrigated every 4 days and the drought group was irrigated every 2 days, and the experiment was started after plant stress for 21 days (Jiao et al., 2011; Liu et al., 2022).

2.2.2 Oviposition selection of Colorado potato beetles

When the potato plant grows to 10 cm, a canopy shall be set up, two pots of CK, light-drought, moderate-drought, and heavy-drought potato plants shall be placed in each canopy for the selection of the Colorado potato beetle adult egg laying host, and each pot of potato in the canopy shall be placed in a fixed position. The Colorado potato beetle adults were paired, and four Colorado potato beetle adults were placed (2♀ + 2♂); after they laid eggs on the potato plant, the number of egg pieces and eggs at 10 o'clock every morning for 7 consecutive days was recorded, and each treatment was repeated five times.

2.2.3 Effects of water stress on the growth and development of Colorado potato beetles

The first instar larvae of Colorado potato beetle hatched on the same day from the indoor Colorado potato beetle population were collected and divided into four groups, CK, LD, MD, and HD; each group of 30 first instar larvae were transferred in a 9 cm plastic culture dish, with 10 replicates for each group, and the larvae used the potato leaves treated with different water in the early stage for feeding. When the larvae grow to the fourth instar and no longer feed, they are placed in a 500 mL insect rearing box to pupate and emerge. Sand is filled in the insect box to 3 cm of the mouth of the bowl, and a proper amount of distilled water is sprayed to ensure that the soil has a certain humidity so that it can emerge into adults (Li, 2013). The top is tied with gauze to prevent Colorado potato beetles from escaping. Potato leaves are placed in the insect box and replaced regularly every day. After the adults emerge, they are paired according to the ratio of male to female 1:1. Survival of each pest state of Colorado potato beetles and the oviposition of adults is recorded every day.

2.2.4 Life parameter analysis

The population dynamic parameters are intrinsic rate of increase (r), finite rate of increase (λ), net reproductive rate (R_0), and mean generation time (T). The calculation formula of the main population growth parameters is as follows (Chi and Liu, 1985; Liao et al., 2022b):

$$\text{Intrinsic rate of increase } (r): \sum_{x=0}^{\infty} e^{-r(x+1)} l_x m_x, \quad (1)$$

$$\text{Finite rate of increase } (\lambda): \lambda = e^{r}, \quad (2)$$

$$\text{Net reproductive rate } (R_0): R_0 = \sum_{X=0}^{\infty} l_x m_x, \quad (3)$$

$$\text{Mean generation time } (T): T = \frac{\ln(R_0)}{r}. \quad (4)$$

2.2.5 Population projection

The population size and stage composition were projected from an initial population of 10 eggs on all four treatments using the TIMING-MS Chart program in 110 days (Chi, 2019). This computer program is available for download at http://140.120.197.173/ecology/.

2.3 Data analysis

The data for the Colorado potato beetles were analyzed using SPSS 26.0. The one-way ANOVA was used to analyze the test of between-subject effects of different water stresses. The data on the oviposition selection, development, and population parameters of Colorado potato beetles on different treatments were tested for normality and variance homogeneity. The LSD multiple mean comparison method was used to compare significant differences among different treatments that met the assumptions. Nonparametric tests were used for the data that did not meet the assumptions, the Kruskal–Wallis test was used, the pairwise comparison method was used to compare significant differences among different treatments, and the p-value is the value after Holm–Bonferroni correction. Survival data were analyzed by constructing survival curves using the Kaplan–Meier estimator, and comparison was performed using the log-rank test. The figures were drawn using GraphPad Prism 9.0.

3 Results and analysis

3.1 Effect of water stress on oviposition selection of Colorado potato beetle

There were significant differences in the egg laying capacity of Colorado potato beetles on potato plants treated with different water stresses (p = 0.000) (Figures 1A, B). The number of egg mass of adult Colorado potato beetles in potato plants under CK and LD treatment was significantly higher than that under MD and HD treatment. Studies on egg number and egg mass have similar results.

3.2 Effect of water stress on the development duration of Colorado potato beetle

Water stress has a clear effect on the development of Colorado potato beetle (Figure 2). Under different water stress treatments, the development duration of the second instar larvae (p = 0.000) and the fourth instar larvae (p =

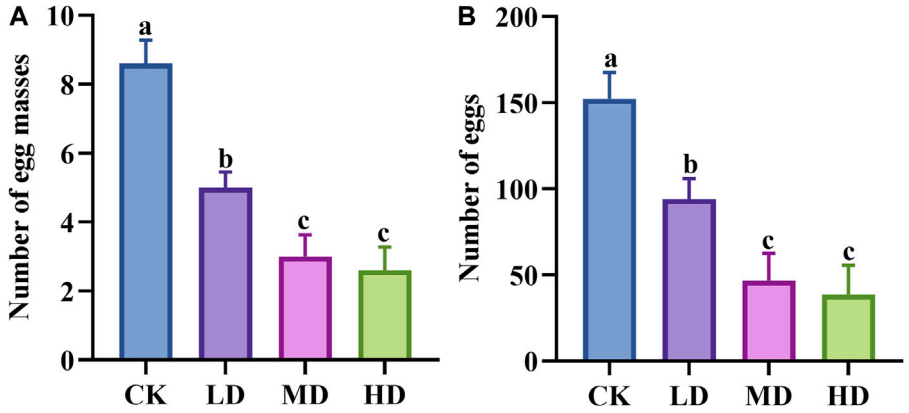

FIGURE 1
Effects of water stress on Colorado potato beetle oviposition. **(A)** Number of egg masses. **(B)** Number of eggs. CK: control group; LD: light drought; MD: moderate drought; and HD: heavy drought. After one-way ANOVA, the data were analyzed by LSD (p<0.05), and the letters a/b/c were used to indicate significance; data were presented as mean ± SE, N = 5.

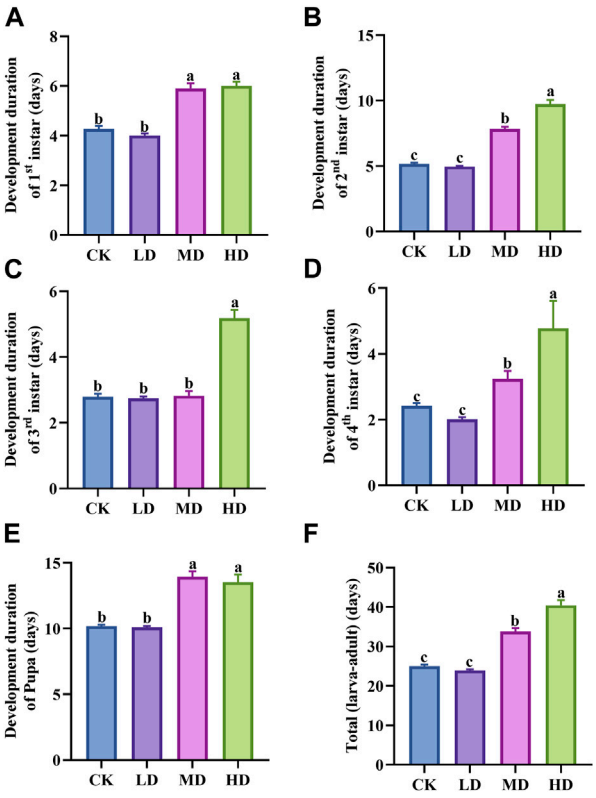

FIGURE 2
Override for the duration of Colorado potato beetle under water stress. **(A)** Development duration of first instar larva, **(B)** development duration of second instar larva, **(C)** development duration of third instar larva, **(D)** development duration of fourth instar larva, **(E)** development duration of pupa, and **(F)** total development duration refers to the sum of the development period from the first instar larva to the pupa of Colorado potato beetle. After one-way ANOVA, the data were analyzed by LSD (p<0.05), and the letters a/b/c were used to indicate significance; data were presented as mean ± SE, N = 10.

0.000) of Colorado potato beetles was significantly different (Figures 2B, D). Among them, the development duration of second and fourth instar larvae under MD and HD treatment was significantly longer than that of CK and LD, and there was no significant difference between CK and LD treatment. The development duration of first instar larvae (p = 0.000), third instar larvae (p = 0.000), and pupae (p = 0.000) was also significantly different (Figures 2A, C, E). The developmental duration of first instar larvae, third instar larvae, and pupae treated with MD and HD was significantly longer than that of CK and LD. The total development duration (p = 0.000) under MD and HD treatment is significantly longer than under CK and LD, and there is no significant difference between the two treatments (Figure 2F).

3.3 Effects of water stress on the survival rate of Colorado potato beetle

The survival rate of Colorado potato beetle under water stress was significantly different. There were differences between CK and LD (p = 0.033) and MD (p = 0.000) and HD (p = 0.000) and no difference between MD and HD (Figure 3). Under water stress, the survival rate of all treatments decreased with the increase in stress time. At the 5th day of water stress, the survival rate of CK treatment and LD treatment was basically the same. After this period, the survival rate of LD treatment showed a downward trend and was always higher than that of CK treatment. After the 5th day of water stress, the survival rate of MD treatment showed a downward trend and was always higher than that of HD treatment, but on the 57th day, the survival rate of both treatments was basically unchanged and significantly lower than that of CK and LD treatment. In general, the survival rate of Colorado potato beetles decreased after water stress, but the survival rate of Colorado potato beetles on LD-treated plants was significantly higher than that of other water stress treatments after the 5th day. In conclusion, the survival rate of Colorado potato beetles decreased with the increase in water stress, and LD was beneficial to the survival of Colorado potato beetles.

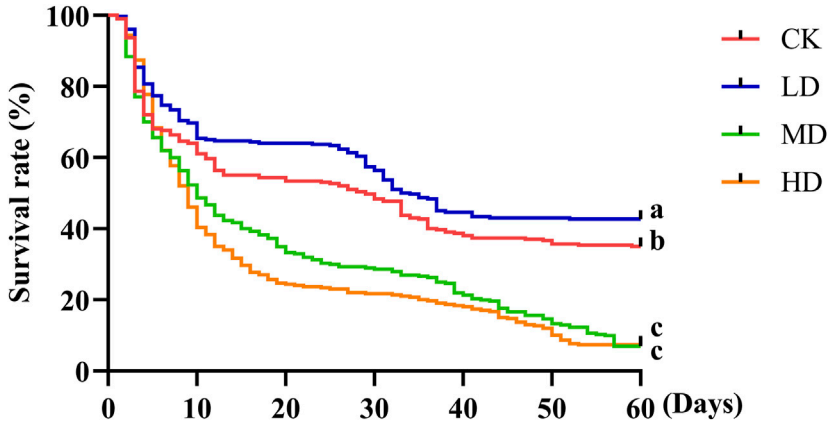

FIGURE 3
Survival rate of Colorado potato beetle under water stress. Kaplan–Meier survival curves of Colorado potato beetle fed with potato leaves that had been under water stress. The log-rank test was used to assess the significance of differences between the two survival curves.

TABLE 1 Population parameters of Colorado potato beetle under water stress.

Water stress	(Intrinsic rate of increase) r	(Finite rate of increase) λ	(Net reproductive rate) R_0	(Mean generation time) T
CK	0.0436 ± 0.01 a	1.0449 ± 0.01 a	14.6300 ± 4.09 a	48.9156 ± 0.68 a
LD	0.0234 ± 0.01 a	1.0238 ± 0.01 a	3.3467 ± 0.72 a	44.4931 ± 2.49 a
MD	0.0058 ± 0.00 ab	1.0059 ± 0.00 ab	0.9367 ± 0.33 ab	25.5648 ± 8.55 a
HD	0.0011 ± 0.00 b	1.0011 ± 0.00 b	0.5567 ± 0.19 b	25.0868 ± 8.39 a

Data were presented as mean ± SE; different lowercase letters in the same column indicate significant difference ($p < 0.05$).

3.4 Effect of water stress on the demographic parameters of Colorado potato beetle

There were significant differences in intrinsic rates of increase (r) ($p = 0.000$), finite rates of increase (λ) ($p = 0.000$), and net reproductive rates (R_0) ($p = 0.000$) of Colorado potato beetle under different treatments. There were no significant differences in mean generation time (T) ($p = 0.355$) of Colorado potato beetle under different treatments (Table 1). Among them, the Colorado potato beetles under CK treatment net reproductive rates were the highest and the mean generation times was the longest, while the net reproductive rates under HD treatment were the lowest and the mean generation times were the shortest.

3.5 Effect of water stress on the population projection of Colorado potato beetle

The population projection showed the stage sizes and the emergence of different stages (Figure 4). The growth of the Colorado potato beetle population was faster and the population size was larger on CK and LD than on the MD and HD treatments. The total adult population sizes on CK and LD were 235.4 and 52.2 individuals, respectively, while the populations barely increased on MD (1.6 individuals) and HD (0.7 individuals).

4 Discussion

The effects on insects after host plant water stress may be either positive or negative (Dai, 2016). A large number of studies have shown that water stress is not conducive to insect oviposition. Salgado and Saastamorinen (2019) found that *Melitaea cinxia* L. under water stress before the *Plantago lanceolata* L. spawning preference is weak. This study found a similar conclusion that water stress was not favorable for Colorado potato beetle laying eggs, with adults laying more eggs on the potato plants suitable for water treatment and fewer eggs on the water-treated potato plants. Awmack and Leather. (2002) found that insect selection for their host plants includes adult oviposition selection and larval feeding selection. Generally, adults will choose host plants that are more suitable for the growth and development of their offspring to lay eggs. The oviposition selection of Colorado potato beetles adults is beneficial to the survival and development of larvae; that is, the growth and development of Colorado potato beetles larvae are better when they feed on potato plants with appropriate water treatment and LD. Hahn and Maron. (2018) found that feeding on water-

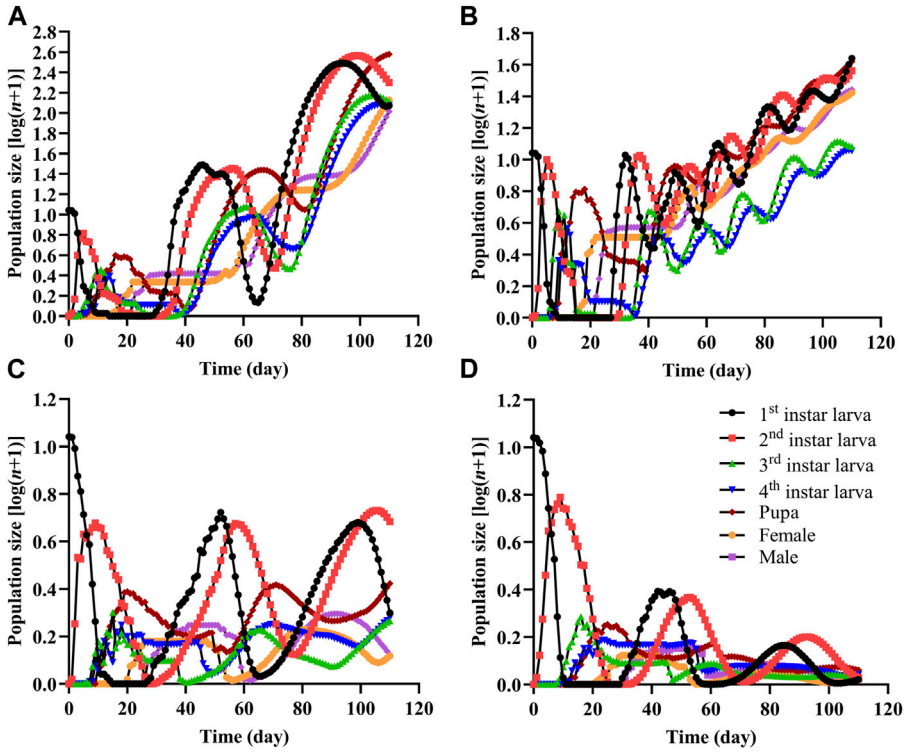

FIGURE 4
Population projection of Colorado potato beetle under water stress. An initial population of 10 eggs was used in each projection. **(A)** CK, **(B)** LD, **(C)** MD, and **(D)** HD.

stressed plants was beneficial to the growth and development of *Danaus plexippus* L. larvae. However, Showler and Moran (2003) found that *Spodoptera exigua* Hübner larvae had poorer growth and higher mortality after feeding on cotton treated with water stress. Valim et al. (2016) fed drought-stressed cabbage to *Plutella xylostella* L. and found that larval survival, pupa weight, reproductive rate, and population growth rate were reduced. In this experiment, LD had a positive effect on the growth and development of Colorado potato beetle, and feeding on leaves under LD was beneficial to the survival and pupation of Colorado potato beetle. Moderate and heavy drought negatively affected the growth and development of Colorado potato beetle, and feeding on leaves treated with water stress was not beneficial for survival and pupation of Colorado potato beetle, and the number of adults was low. Studies have found that the water content in plant leaves has a direct impact on the feeding and growth of plant-feeding insects, and water stress reduces the water content of plant leaves. If plants are in a state of water shortage for a long time, insects will have not only a longer development period after feeding but also a lower survival rate (Connor, 1988; Lower and Orians, 2003; Bisigato et al., 2015), and the results of this study are similar to those of previous studies.

This study also found the reduced Colorado potato beetle population growth under water stress, and when Colorado potato beetles were fed on leaves after water stress treatment, the net reproductive rates, intrinsic rates of increase, and finite rates decreased significantly compared with CK, which is consistent with the previous study showing that *Sitobion avenae* Fabricius showed a lower net reproductive rates, intrinsic rates of increase, and finite rates of increase on plants grown under water stress (Xie et al., 2020). Demographic parameters can be used to predict population growth: the intrinsic rate of increase reflects the growth ability of the population and can be used to measure the trend of population growth and decline at that time or in the future (Ahn et al., 2020; Liao et al., 2022a). In this experiment, the intrinsic rate of increase of Colorado potato beetles under CK treatment of 0.0436 was significantly higher than that of LD, MD, and HD treatments, indicating that water stress was not conducive to the growth of the Colorado potato beetle population.

This paper analyzed the oviposition selection and growth development of Colorado potato beetles reared in groups after water stress treatment of the host plant potato. It showed that moderate and heavy drought had adverse effects on Colorado potato beetles, delaying and reducing the population growth of Colorado potato beetles. However, this study only discussed the effects of water stress of host plants on the egg laying selection, growth, development, and reproduction of Colorado potato beetles. However, in actual production, temperature and natural enemies can affect the population growth of Colorado potato beetles. Therefore, the effects of water stress on the population growth and survival of natural enemies of Colorado potato beetles under experimental conditions need further study.

5 Conclusion

Water stress affects the oviposition behavior, growth and development, survival, and reproduction of insects. In this study, it was found that water stress significantly affected the developmental duration, reproduction, and the population growth of Colorado potato beetles, and they laid more eggs on potato plants suitable for water treatment. The development period of Colorado potato beetles was prolonged with the increase in water stress, and the survival rate and the amount of eggs were reduced. The intrinsic rates of increase (r), finite rates of increase (λ), and net reproductive rates (R_0) of the Colorado potato beetles decreased. There was no significant difference between the LD and the control. The MD and severe drought had adverse effects on the growth and reproduction of the Colorado potato beetles. Adult egg laying preference in Colorado potato beetles is consistent with offspring performance, so the relationship between oviposition preference and offspring performance in Colorado potato beetles under water stress supports the "preference–performance hypothesis."

Data availability statement

The original contributions presented in the study are included in the article/Supplementary Material; further inquiries can be directed to the corresponding author.

Author contributions

Conceptualization: CL and XL; methodology: XL and HY; formal analysis and investigation: XL, HY, HS, and FN; writing—original draft preparation: XL; writing—review and editing: CL; funding acquisition: CL; and resources: CL. All authors read and agreed to the published version of the manuscript All authors contributed to the article and approved the submitted version.

Funding

This research was supported by the National Key R&D Program of China (2021YFD1400200) and Xinjiang Agricultural University Graduate Research Innovation Project, Grant/Award Number XJAUGRI2022040.

Acknowledgments

The authors are very thankful to Liu Juan and Liao Jianghua who helped in data analysis and preparing the figures.

Conflict of interest

The authors declare that the research was conducted in the absence of any commercial or financial relationships that could be construed as a potential conflict of interest.

Publisher's note

References

Addo-Bediako, A., Chown, S. L., and Gaston, K. J. (2001). Revisiting water loss in insects: A large scale view. *J. Insect Physiol.* 47, 1377–1388. doi:10.1016/S0022-1910(01)00128-7

Ahn, J. J., Cho, J. R., Kim, J. H., and Seo, B. Y. (2020). Thermal effects on the population parameters and growth of *Acyrthosiphon pisum* (Harris) (Hemiptera: Aphididae). *Insects* 11, 481. doi:10.3390/insects11080481

Alyokhin, A., Baker, M., Mota-Sanchez, D., Dively, G., and Grafius, E. (2008). Colorado potato beetle resistance to insecticides. *Am. J. Potato Res.* 85, 395–413. doi:10.1007/s12230-008-9052-0

Amanulla, E. (2015). *Effect of* Solanum rostratum *Invasion on distribution, life history and habits of* Leptinotarsa decemlineata. Xinjiang: Xinjiang Agricultural University.

Awmack, C. S., and Leather, S. R. (2002). Host plant quality and fecundity in herbivorous insects. *Annu. Rev. Entomol.* 47, 817–844. doi:10.1146/annurev.ento.47.091201.145300

Bisigato, A. J., Saín, C. L., Campanella, M. V., and Cheli, G. H. (2015). Leaf traits, water stress, and insect herbivory: Is food selection a hierarchical process? *Arthropod-Plant Interact.* 9, 477–485. doi:10.1007/s11829-015-9387-7

Cabrera, H. M., Argandona, V. H., Zúñiga, G. E., and Corcuera, L. J. (1995). Effect of infestation by aphids on the water status of barley and insect development. *Phytochemistry* 40, 1083–1088. doi:10.1016/0031-9422(95)00325-2

Cao, L., Diana, J. S., Keoleian, G. A., and Lai, Q. M. (2011). Life cycle assessment of Chinese shrimp farming systems targeted for export and domestic sales. *Environ. Sci. Technol.* 45, 6531–6538. doi:10.1021/es104058z

Chi, H., and Liu, H. (1985). Two new methods for the study of insect population ecology. *Acad. Sin.* 24, 225–240.

Chi, H. (2019). *TIMING-MSChart: A computer program for the population projection based on age-stage, two-sex life table*. Taichung, Taiwan: National Chung Hsing University. Avaliable At: http://140.120.197.173/Ecology/Download/TIMING-MSChart-exe.rar.

Clark, K. E., Hartley, S. E., and Johnson, S. N. (2011). Does mother know best? The preference-performance hypothesis and parent-offspring conflict in aboveground-belowground herbivore life cycles. *Ecol. Entomol.* 36, 117–124. doi:10.1111/j.1365-2311.2010.01248.x

Connor, E. F. (1988). Plant water deficits and insect responses: The preference of *Corythucha arcuata* (heteroptera: Tingidae) for the foliage of white oak, *Quercus alba*. *Ecol. Entomol.* 13, 375–381. doi:10.1111/j.1365-2311.1988.tb00369.x

Dai, P. (2016). *The response of* Sitobion avenae *(Fabricius) to water-deficit stress and its genetic mechanisms*. Yangling: Northwest A&F University.

Dang, Z. H., Li, Y. F., Gao, Z. L., and Pan, W. L. (2009). Influence of soil moisture on growth and development of *Holotrichia oblita*. *Chin. J. Appl. Entomology* 46, 135–138.

Hahn, P. G., and Maron, J. L. (2018). Plant water stress and previous herbivore damage affect insect performance. *Ecol. Entomol.* 43, 47–54. doi:10.1111/een.12468

Jaenike, J. (1978). On optimal oviposition behavior in phytophagous insects. *Theor. Popul. Biol.* 14, 350–356. doi:10.1016/0040-5809(78)90012-6

Jiao, Z. L., Li, Y., Lv, D. Q., and Wang, J. Y. (2011). Effect of different drought treatments on growth indicators and physiological characters of potato seedlings. *Chin. Potato J.* 25, 329–333.

Li, C., Cheng, D. F., Liu, H., Zhang, Y. H., and Sun, J. R. (2013). Effect of temperature on the distribution of the Colorado potato beetle (*Leptinotarsa decemlineata*)-effect of high temperature on its emergence in Turpan, Xinjiang. *Sci. Agric. Sin.* 46, 737–744. doi:10.3864/j.issn.0578-1752.2013.04.008

Li, C., Peng, H., Cheng, D. F., Guo, W. C., Liu, H., Zhang, Y. H., et al. (2014). Diffusion of colorado potato beetle, *Leptinotarsa decemlineata*, adults in field. *Acta Ecol. Sin.* 34, 359–366. doi:10.5846/stxb201304180743

Li, C. (2013). *Research on diffusion rule of* Leptinotarsa decemlineata *based on GIS in Xinjiang, China*. Chongqing: Southwest University.

Liao, J. H., Liu, J., and Li, C. (2022b). Effects of repeated short-term heat exposure on life history traits of Colorado potato beetle. *Insects* 13, 455. doi:10.3390/insects13050455

Liao, J. H., Liu, J., Liu, X., Hu, H. Z., Niu, P., Han, L. L., et al. (2022a). Effects of short-term low temperature on the population growth of the Colorado potato beetle, *Leptinotarsa decemlineata* (Coleoptera: Chrysomelidae). *Acta Entomol. Sin.* 65, 112–118. doi:10.16380/j.kcxb.2022.01.012

Liu, C. H., Su, W. J., and Tong, S. L. (2018). Brief analysis of potato planting and production in Xinjiang. *Seed Sci. Technol.* 36, 20.

Liu, J., Liao, J. H., and Li, C. (2022). Bottom-up effects of drought on the growth and development of potato, *Leptinotarsa decemlineata* Say and *Arma chinensis* Fallou. *Pest Manag. Sci.* 78, 4353–4360. doi:10.1002/ps.7054

Lower, S. S., and Orians, C. M. (2003). Soil nutrients and water availability interact to influence willow growth and chemistry but not leaf beetle performance. *Entomol. Exp. Appl.* 107, 69–79. doi:10.1046/j.1570-7458.2003.00037.x

Luo, D., Xu, H. X., Yang, Y. J., Zheng, X. X., and Lv, Z. X. (2012). Feeding behavior and oviposition preference of Brown planthoppers, *Nilaparvata lugens*, on different rice varieties under drought stress stimulated by polythylene glycol (PEG6000). *Chin. J. Rice Sci.* 26, 731–736. doi:10.3969/j.issn.1001-7216.2012.06.013

Salgado, A. L., and Saastamoinen, M. (2019). Developmental stage-dependent response and preference for host plant quality in an insect herbivore. *Anim. Behav.* 150, 27–38. doi:10.1016/j.anbehav.2019.01.018

Showler, A. T., and Moran, P. J. (2003). Effects of drought stressed cotton, *Gossypium hirsutum* L., on beet armyworm, *Spodoptera exigua* (Hübner), oviposition, and larval feeding preferences and growth. *J. Chem. Ecol.* 29, 1997–2011. doi:10.1023/A:1025626200254

Valim, J. O. S., Teixeira, N. C., Santos, N. A., Oliveira, M. G. A., and Campos, W. G. (2016). Drought-induced acclimatization of a fast-growing plant decreases insect performance in leaf-chewing and sap-sucking guilds. *Arthropod-Plant Inte.* 10, 351–363. doi:10.1007/s11829-016-9440-1

Wang, J. X., Wang, Z. H., Zhang, S. X., Jing, Y. C., Wang, Y., Bai, J., et al. (2019). Current situation and development stragegy of potato staple food in China. *J. Shanxi Agric. Sci.* 47, 1667–1669. doi:10.3969/j.issn.1002-2481.2019.09.41

Wu, X., Liu, J., Mu, C. Y., He, Q. L., Wang, S. M., Wang, Z. W., et al. (2022). Effect of drought stress on starch accumulation and yield composition of main potato varieties in Yunnan. *China Veg.* 11, 70–79. doi:10.19928/j.cnki.1000-6346.2022.2036

Xie, H. C., Shi, J. Q., Shi, F. Y., Xu, H. Y., He, K. L., and Wang, Z. Y. (2020). Aphid fecundity and defenses in wheat exposed to a combination of heat and drought stress. *J. Exp. Bot.* 71, 2713–2722. doi:10.1093/jxb/eraa017

Xu, R. Q., Zeng, C. X., Huang, Y. B., Huang, R. F., and Jiang, S. C. (1999). Relation between the occurrence amount of the major pestilent generation of *Cnaphalocrocis medinalis* Guenee and rainfall. *Fujian J. Agric. Sci.* 3, 23–25. doi:10.19303/j.issn.1008-0384.1999.03.006

Zhang, R. J., Ma, H., Ji, L. J., Ren, D. Z., Li, S. D., Zhang, Y. H., et al. (2022). Effects of drought stress on growth and physiological and biochemical indexes of potato varieties. *Chin. Agric. Sci. Bull.* 38, 34–39.

Zhang, S., Fang, G. Q., Gao, Y. L., Zhang, W., Qiu, C. L., Shen, Y., et al. (2018). Co-evolution of Colorado potato beetles with host plants and their controls. *Chin. Potato J.* 32, 367–373.

Zhang, S., Luo, Q. Y., Ma, L. Y., Yu, J. Q., and Wang, X. F. (2020). BTB-BACK-TAZ domain protein MdBT2-mediated MdMYB73 ubiquitination negatively regulates malate accumulation and vacuolar acidification in apple. *J. China Agric. Univ.* 25, 151–160. doi:10.1038/s41438-020-00384-z

Zhong, G. H., Liang, G. W., Mo, M. Y., and Zeng, L. (2001). Effects of temperature and humidity on development of experimental cotton leafworm population. *J. South China Agric. Univ.* 3, 29–32.

frontiers | Frontiers in Physiology

TYPE Original Research
PUBLISHED 28 June 2023
DOI 10.3389/fphys.2023.1186804

OPEN ACCESS

EDITED BY
Jia Fan,
Institute of Plant Protection (CAAS), China

REVIEWED BY
LinQuan Ge,
Yangzhou University, China
Shuai Zhang,
Yangzhou University, China

*CORRESPONDENCE
Man Zhao,
zhaoman821@henau.edu.cn

†These authors have contributed equally to this work

RECEIVED 15 March 2023
ACCEPTED 05 June 2023
PUBLISHED 28 June 2023

CITATION
Yuan X, Li H, Guo X, Jiang H, Zhang Q, Zhang L, Wang G, Li W and Zhao M (2023), Functional roles of two novel P450 genes in the adaptability of *Conogethes punctiferalis* to three commonly used pesticides.
Front. Physiol. 14:1186804.
doi: 10.3389/fphys.2023.1186804

Functional roles of two novel P450 genes in the adaptability of *Conogethes punctiferalis* to three commonly used pesticides

Xingxing Yuan[1†], Han Li[1†], Xianru Guo[1], He Jiang[2], Qi Zhang[1], Lijuan Zhang[1], Gaoping Wang[1], Weizheng Li[1] and Man Zhao[1*]

[1]Henan International Laboratory for Green Pest Control, College of Plant Protection, Henan Agricultural University, Zhengzhou, China, [2]State Key Laboratory of Integrated Management of Pest Insects and Rodents, Institute of Zoology, Chinese Academy of Sciences, Beijing, China

Introduction: Insect cytochrome P450 (CYP450) genes play important roles in the detoxification and metabolism of xenobiotics, such as plant allelochemicals, mycotoxins and pesticides. The polyphagous *Conogethes punctiferalis* is a serious economic pest of fruit trees and agricultural crops, and it shows high adaptability to different living environments.

Methods: The two novel P450 genes *CYP6CV1* and *CYP6AB51* were identified and characterized. Quantitative real-time PCR (qRT-PCR) technology was used to study the expression patterns of the two target genes in different larval developmental stages and tissues of *C. punctiferalis*. Furthermore, RNA interference (RNAi) technology was used to study the potential functions of the two P450 genes by treating RNAi-silenced larvae with three commonly used pesticides.

Results: The *CYP6CV1* and *CYP6AB51* genes were expressed throughout various *C. punctiferalis* larval stages and in different tissues. Their expression levels increased along with larval development, and expression levels of the two target genes in the midgut were significantly higher than in other tissues. The toxicity bioassay results showed that the LC_{50} values of chlorantraniliprole, emamectin benzoate and lambda-cyhalothrin on *C. punctiferalis* larvae were 0.2028 μg/g, 0.0683 μg/g and 0.6110 mg/L, respectively. After treating with different concentrations of chlorantraniliprole, emamectin benzoate and lambda-cyhalothrin (LC_{10}, LC_{30}, LC_{50}), independently, the relative expressions of the two genes *CYP6CV1* and *CYP6AB51* were significantly induced. After the dsRNA injection, the expression profiles of the two CYP genes were reduced 72.91% and 70.94%, respectively, and the mortality rates of the larvae significantly increased when treated with the three insecticides independently at LC_{10} values.

Discussion: In the summary, after interfering with the *CYP6CV1* and *CYP6AB51* in *C. punctiferalis*, respectively, the sensitivity of *C. punctiferalis* to chlorantraniliprole, emamectin benzoate and lambda-cyhalothrin was significantly increased, indicating that the two CYP6 genes were responsible for the adaptability of *C. punctiferalis* to the three chemical insecticides in *C. punctiferalis*. The results from this study demonstrated that *CYP6CV1* and *CYP6AB51* in *C. punctiferalis* play crucial roles in the detoxification of chlorantraniliprole, emamectin benzoate and lambda-cyhalothrin.

KEYWORDS

Conogethes punctiferalis, cytochrome P450, adaptability, chemical pesticides, RNA interference

1 Introduction

The yellow peach moth, *Conogethes punctiferalis* (Guenée), is widely distributed in East Asia, South Asia, Australia and Papua New Guinea (Shwe et al., 2021a). It is one of the few polyphagous borer pests that not only damage woody plants, such as peach, apple, hawthorn and chestnut, but also feed on herbaceous plants, including maize, soybeans and cotton (Stanley et al., 2009; Chen et al., 2018). In recent years, *C. punctiferalis* has caused severe damage, and it is now considered a dominant economic lepidopteran pest of summer corn fields in the Huanghuaihai Region of China (Shwe et al., 2021b). Currently, chemical control is commonly used to control lepidopteran pests in corn fields, including the widely used pesticides chlorantraniliprole, emamectin benzoate and lambda-cyhalothrin. However, the excessive and frequent use of insecticides has caused a series of serious problems, including the evolution of pesticide resistance (Gao, 2010; Siegwart et al., 2017; Wang et al., 2020). Some lepidopteran pests have developed high resistance levels to pesticides commonly used in corn fields. For example, the field population of *Plutella xylostella* is more than 2,000 times resistant to chlorantraniliprole (Wang and Wu, 2012). *Spodoptera frugiperda* has a high risk of developing resistance to emamectin benzoate (Muraro et al., 2021), and field populations of *Spodoptera exigua* have developed a high level of resistance to lambda-cyhalothrin insecticides (Su and Sun, 2014). The increased metabolic activity levels of detoxification enzymes are main causes of insect resistance, including the cytochrome P450 monooxygenase (P450)-mediated detoxification of insecticides (Elzaki et al., 2015). The overexpression of P450 genes plays important roles in insecticide resistance. For example, overexpression of *CYP6BG1* may contribute to chlorantraniliprole resistance in *P. xylostella* (Li et al., 2018), *CYP337B3* in *Helicoverpa armigera* is involved in the resistance to cypermethrin (Rasool et al., 2014), and *CYP6AY1* of *Nilaparvata lugens* is involved in resistance to imidacloprid (Ding et al., 2013).

P450 is a common and important detoxification enzyme in all living organisms, including animals, plants and microorganisms (Cui et al., 2016; Elfaki et al., 2018). Insect P450 can be divided into four main branches: CYP2, CYP3, CYP4 and mitochondrial P450s. The CYP3 family is a large group of insect P450s, which can be subdivided into CYP6, CYP9, CYP28 and several other families (Wang et al., 2018; Ullah et al., 2020). To date, the identified insect cytochrome P450s mainly have two functions. They catalyze the formation and decom position of endogenous substances (such as ecdysone, juvenile hormone and fatty acid) to maintain the normal functions of the organism (Helvig et al., 2004; Iga and Kataoka, 2012). In addition, they metabolize many exogenous substances (such as pesticides, plant secondary substances and other environmental chemicals), and this has detoxification and activation effects (Yang and Liu, 2011; Giraudo et al., 2015). Many insect P450 genes, especially in the families of CYP3 and CYP4, participate in the detoxification of, and metabolic resistance to, several insecticides (Amenya et al., 2008; Balabanidou et al., 2016; Wang et al., 2019; Jing et al., 2022).

Previous reports found that the mRNA expression levels of CYP6CV1 and CYP6AB51 in CYP6 family from *C. punctiferalis* were upregulated when larvae fed on resistant plant, and in other lepidopteran insects, the CYP6 family genes also played important role in the insect resistance to some pesticides (Chen et al., 2015; Jing et al., 2022). To examine whether CYP6CV1 and CYP6AB51 in *C. punctiferalis* also are involved in the detoxification of the commonly used pesticides, they were identified and characterized by molecular technologies. The results provide significant insights into the functions of *CYP6CV1* and *CYP6AB51* from *C. punctiferalis* in the detoxification of chlorantraniliprole, emamectin benzoate and lambda-cyhalothrin, which are three commonly used pesticides for the control of *C. punctiferalis* and other lepidopteran insects in corn fields (Siegwart et al., 2017; Wang et al., 2020).

2 Materials and methods

2.1 Insects and chemical insecticides

C. punctiferalis used in this study was collected from corn fields in 2019 at the Xuchang campus of Henan Agricultural University (Henan, China), and then, they were maintained in the laboratory under the follow conditions: 27°C ± 1°C and a 75% ± 5% relative humidity, with a 14-h light: 10-h dark photoperiod. The larvae were fed fresh maize ears, and the adults were provided a 10% sucrose solution without exposure to any insecticides.

Three chemical pesticides, 95% chlorantraniliprole, 91% emamectin benzoate and 96.9% lambda-cyhalothrin were kindly provided by the Insect Physiology, Biochemistry and Molecular Biology Group of Henan Agricultural University.

2.2 Molecular cloning of CYP6CV1 and CYP6AB51 from *C. punctiferalis*

The total RNA of fourth-instar larvae of *C. punctiferalis* was extracted using TRIzol reagent in accordance with the instructions (Invitrogen, Carlsbad, CA, United States). After the RNA quality and concentration were verified using 1.5% agarose gel electrophoresis and a NanoDrop 1,000 spectrophotometer (Thermo Scientific, Waltham, MA, United States), respectively. cDNA was synthesized using a FastKing RT Kit (with gDNase) (Tiangen Biotech, Beijing, China).

The gene-specific primers were designed to clone *CYP6CV1* and *CYP6AB51* (Table 1), and the above synthesized cDNA was used as the template for PCR amplification. The PCR reaction was performed in a total volume of 25 μL, containing 12.5 μL of PrimeSTAR® Max DNA Polymerase (TaKaRa, Dalian, China), 1 μL of each primer (10 μM), 1 μL of cDNA template and 9.5 μL

TABLE 1 Sequences of primers used in this study.

Primer name	Base sequence (5′–3′)
cDNA full-length amplification	
CYP6CV1-F	ATGGCGTCGCTTGTTTGTGTCGCGA
CYP6CV1-R	TCACCTTTTCGATATCTTCACCCAT
CYP6AB51-F	ATGATTGCTCTCATTTTGATTACA
CYP6AB51-R	TTAAATCTTCCGTTCTCGGAATAT
Quantitative real-time PCR	
CYP6CV1-Q-F	TTCTACTCGGCTGGTTTC
CYP6CV1-Q-R	TGCCCATTACATTTCTCG
CYP6AB51-Q-F	AATCGCTGGCTGGGTTGGC
CYP6AB51-Q-R	CCGTTCTCGGAATATCAGTGGC
GAPDH-F	CTGCCTCTTACGACGCTATCA
GAPDH-R	ATCGTTCAGGGAGATGCCG
dsRNA synthesis	
ds*CYP6CV1*-F	CGTCTGCTGCTACAATGTCTTT
ds*CYP6CV1*-R	CAATTACGCGGTCCTTCC
ds*CYP6AB51*-F	CGAAATGACGTACCTTGATTGGAC
ds*CYP6AB51*-R	CCGTTCTCGGAATATCAGTGGC
ds*EGFP*-F	CACAAGTTCAGCGTGTCCG
ds*EGFP*-R	GTTCACCTTGATGCCGTTC
T7-ds*CYP6CV1*-F	GATCACTAATACGACTCACTATAGGGAGACGTCTGCTGCTACAATGTCTTT
T7-ds*CYP6CV1*-R	GATCACTAATACGACTCACTATAGGGAGACAATTACGCGGTCCTTCC
T7-ds*CYP6AB51*-F	GATCACTAATACGACTCACTATAGGGAGACGAAATGACGTACCTTGATTGGAC
T7-ds*CYP6AB51*-R	GATCACTAATACGACTCACTATAGGGAGACCGTTCTCGGAATATCAGTGGC
T7-ds*EGFP*-F	GATCACTAATACGACTCACTATAGGGAGACACAAGTTCAGCGTGTCCG
T7-ds*EGFP*-R	GATCACTAATACGACTCACTATAGGGAGAGTTCACCTTGATGCCGTTC

T7 sequence: GATCACTAATACGACTCACTATAGGGAGA.

of ddH_2O, and the amplification conditions were as follows: 98°C for 5 min; 40 cycles of 98°C for 10 s, 55°C for 10 s and 72°C for 30 s; and a final extension step at 72°C for 7 min. After detecting the target band using 1.5% agarose gel electrophoresis, the gel was cut and then purified using a DNA gel extraction kit (Axygen Scientific, Union City, CA, United States). Afterwards, the product was inserted into the pClone 007 vector (Tsingke Biotech, Beijing, China) and then transformed into *Escherichia coli* DH5α competent cells (Sangon Biotech, Shanghai, China). Finally, the selected positive clones were cultured in LB liquid medium containing Amp (50 mg/ml) at 37°C and 180 r/min for 12 h. The positive clones were confirmed by PCR and sequencing (Sangon Biotech). The sequencing results were compared with the previously obtained transcriptome sequences.

2.3 Sequence analysis and phylogenetic analysis

ORF finder (https://www.ncbi.nlm.nih.gov/orffinder/) was used to determine the open reading frames (ORFs) of the genes. The online website ExPASy (http://web.expasy.org/compute_pi/) was used to predict the isoelectric points and molecular weights of the proteins encoded by the genes. The Neighbor-Joining method in MEGA 7.0 was used to analyze the phylogenetic relationships between the target genes and other amino acid sequences of the CYP6 family in lepidopteran insects. The ClustalX was used to align the sequences of *C. punctiferalis* CYP6CV1 and CYP6AB51 with the related lepidopteran cytochrome P450.

2.4 Analysis of the CYP6CV1 and CYP6AB51 expression patterns in *C. punctiferalis*

Larval samples of *C. punctiferalis* at different developmental stages were collected, including first- (80 individuals), second- (40 individuals), third- (10 individuals), fourth- (5 individuals) and fifth-instar (3 individuals) larvae, to analyze the expression levels of the two genes. Samples of different larval tissues, including head, salivary gland, midgut, fat body, cuticle and hemolymph from 20 fourth-instar larvae, were also dissected and collected. Each insect sample had three replicates. The total RNA extraction and synthesis of cDNA were the same as in section 2.2.

On the basis of the cloned cDNA sequences of *CYP6CV1* and *CYP6AB51*, Primer 5.0 was used to design qRT-PCR primers (Table 1), and glyceraldehyde 3-phosphate dehydrogenase (*GAPDH*; GenBank accession no: KX668532.1) was used as the internal reference gene to normalize the qRT-PCR data. qRT-PCR experiments were performed using a QuantStudio™ three Real-Time PCR System (Thermo Scientific) in a total volume of 20 μL, which contained 10 μL of 2 × SuperReal PreMix Plus, 0.6 μL of each primer (10 μM), 0.4 μL of 50× ROX Reference Dye, 1 μL of cDNA template (200 ng) and 7.4 μL of RNase-Free ddH_2O. The qRT-PCR

program conditions were as follows: 95°C for 15 min; 40 cycles of 95°C for 10 s and 60°C for 32 s. To assess the specificity of each PCR amplification, a dissociation-curve analysis was performed at the end of the run. Each sample had three technical replicates.

2.5 The susceptibility of *C. punctiferalis* larvae to the three insecticides

The toxicity levels of 95% chlorantraniliprole and 91% emamectin benzoate to the third-instar larvae of *C. punctiferalis* were evaluated independently using the feed-mixing method (Yu et al., 2015). The two insecticides were dissolved and diluted with 0.1% TritionX-100 independently (Solarbio, Beijing, China) to obtain a series of different concentrations. Then, 1 ml of each different diluted solution was incorporated into 100 g of the artificial diet to obtain six concentration-gradient mixed insecticide feeds, and 0.1% TritionX-100 was used as a control. Then, the diets were cut into small pieces and provided to third-instar larvae of *C. punctiferalis* that had been starved for 12 h. The toxicity of 96.9% lambda-cyhalothrin to the third-instar larvae of *C. punctiferalis* was evaluated using the topical application method (Brewer and Trumble, 1989). The 96.9% lambda-cyhalothrin was diluted into a series of different concentrations using acetone (Fuyu Chemical, Tianjin, China), and 1 μL of the diluted solution was placed on the thoracic dorsum of the larvae using a microdropper (Envta Technology, Beijing, China). Three biological replicates were used for each concentration, and 20 larvae were treated per replicate. The number of dead insects was counted after 24 h or 48 h (24 h for 96.9% lambda-cyhalothrin and 48 h for both 95% chlorantraniliprole and 91% emamectin benzoate).

2.6 Effects of exposure to the three insecticides on the mRNA expression levels of the target genes

On the basis of the toxicity levels of the three chemical insecticides on the third-instar larvae, LC_{10}, LC_{30} and LC_{50} were used to evaluate the effects of chlorantraniliprole, emamectin benzoate and lambda-cyhalothrin on the *CYP6CV1* and *CYP6AB51* expression levels in *C. punctiferalis*. The third-instar larvae were treated with the above concentrations of the three insecticides as described in section 2.5, and the surviving larvae were collected at 3, 6, 12, 24 and 48 h after treatment. Each replication included 10 larvae, with three biological replicates per concentration. The total RNA extraction, cDNA synthesis and qRT-PCR were performed as described above in section 2.2 and 2.4.

2.7 RNAi silencing of *CYP6CV1* and *CYP6AB51* and interference efficiency detection

On the basis of the obtained gene sequences of *CYP6CV1* and *CYP6AB51* in *C. punctiferalis*, gene-specific primers containing the T7 promoter were designed, and the enhanced green fluorescent protein gene (*EGFP*) was used as a control (Table 1). ds*CYP6CV1*, ds*CYP6AB51* and ds*EGFP* were synthesized using a T7 RiboMAX™ Express RNAi System kit (Promega, Madison, WI, United States) in accordance with the instructions. The dsRNA products were diluted with nuclease-free water to a final concentration of 3 μg/μL and then maintained at −80°C for later use.

The third-instar larvae of *C. punctiferalis* were injected with 2 μL (3 μg/μL) of gene-specific dsRNA (ds*CYP6CV1* and ds*CYP6AB51*) at the second internode membrane of the abdomen using a manual microinjector. Larvae injected with same amount of ds*EGFP* (*EGFP* control) or nuclease-free water (DEPC control) were used as negative controls, and the non-injection treatment was used as a blank control (CK). At 24, 36 and 48 h after injection, 10 surviving larvae per treatment were collected, and qRT-PCR was used to detect the interference efficiency with the target gene. Three biological replicates were used per treatment, and each biological replicate had three technical replicates.

2.8 The susceptibility of *C. punctiferalis* to the three insecticides after target gene interference

The third-instar larvae of *C. punctiferalis* were injected with 2 μL (3 μg/μL) of the target gene dsRNA, ds*EGFP* or DEPC. At 36 h after injection, the surviving larvae were fed diets treated with chlorantraniliprole or emamectin benzoate at the LC_{10} dose, and another group of *C. punctiferalis* larvae were subjected to the topical application of lambda-cyhalothrin at the LC_{10} dose. After 6 h, the mortality of each treatment was recorded. Every treatment was performed in triplicate, and each replicate included 20 larvae.

2.9 Statistical analysis

The relative expression levels of the genes as assessed by qRT-PCR were analyzed using the $2^{-\Delta\Delta CT}$ method (Livak and Schmittgen, 2001). Excel was used to sort the data, and SPSS 20.0 was used for the statistical analysis. After a one-way ANOVA, Duncan's multiple range tests ($p < 0.05$) were used to analyze the significant differences between different treatments. The bioassay used the Probit function of SPSS 20.0 for the statistical regression analysis.

3 Results

3.1 Identification of *CYP6CV1* and *CYP6AB51* in *C. punctiferalis*

The cDNA sequences of *CYP6CV1* and *CYP6AB51* in *C. punctiferalis* were obtained through molecular cloning and sequencing. The ORF lengths, number of encoded amino acids, protein molecular weights and isoelectric points of CYP6CV1 and CYP6AB51 in *C. punctiferalis* were determined using the online tools of the NCBI and ExPASY, and then, the data were submitted to NCBI to obtain the GenBank accession numbers. The basic

TABLE 2 Sequence characteristics of *CYP6CV1* and *CYP6AB51* in *C. punctiferalis*.

Gene name	ORF length (bp)	Number of coded amino acids	Protein molecular weight (kDa)	Isoelectric point (pI)	GenBank accession number
CYP6CV1	1,503	500	57.045	8.93	MT740277
CYP6AB51	1,536	511	59.343	8.38	MW402840

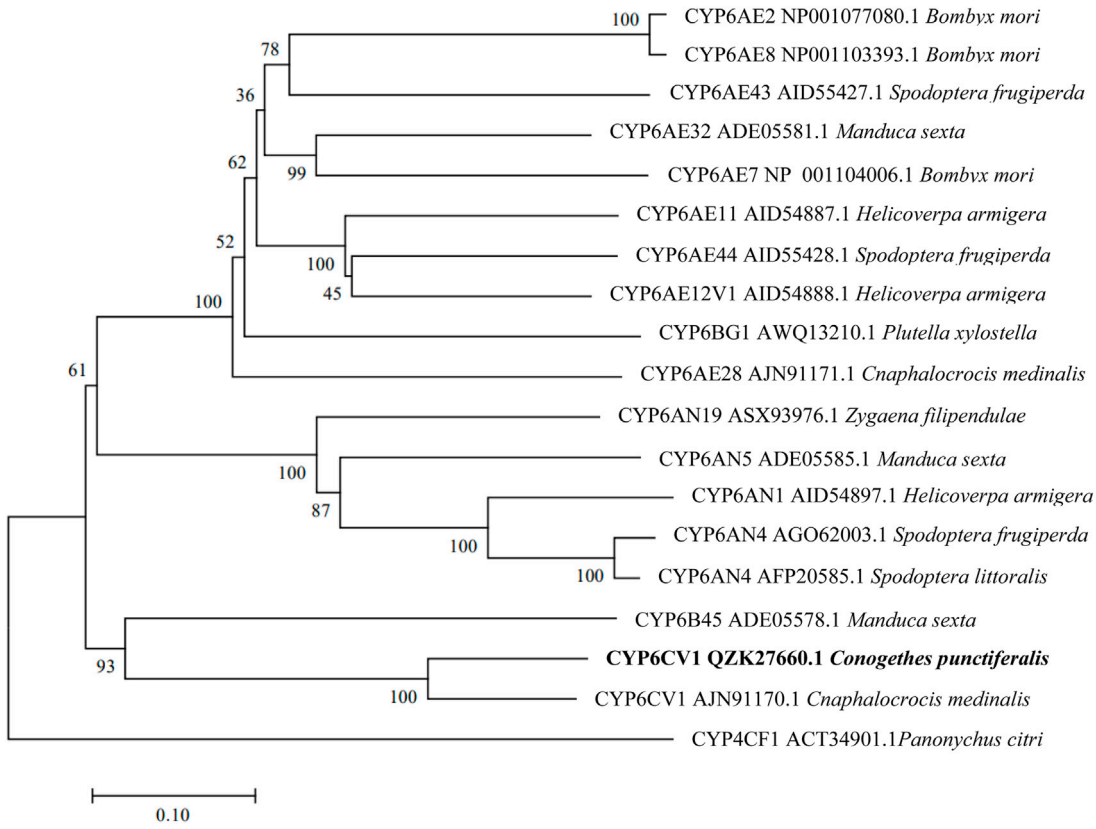

FIGURE 1
Phylogenetic relationships between CYP6CV1 from *C. punctiferalis* and homologs from other lepidopteran insects. The phylogram was generated by MEGA 7.0 using the neighbor-joining method, and the inferred phylogeny was tested using a bootstrap analysis with 1,000 pseudoreplicate datasets.

sequence characteristics of *CYP6CV1* and *CYP6AB51* from *C. punctiferalis* are shown in Table 2.

The constructed phylogenetic tree showed that *C. punctiferalis* CYP6CV1 was closely related to CYP6CV1 in *Cnaphalocrocis medinalis*, with a homology of 78.45% (Figure 1), whereas there was a close relationship between CYP6AB51 from *C. punctiferalis* and CYP6AB51 from *Chilo suppressalis*, with a homology of 61.36% (Figure 2). The predicted amino acid sequences encoded by the two genes contained five typical conserved structural regions of insect P450 proteins (Graham and Peterson, 1999; Deng et al., 2007), a C-helix region ($W_{XXX}R$), I-helix region (AG_XETS), K-helix region ($E_{XX}R$), meander sequence ($P_{XX}F_XP_{XX}F$) and heme-binding sequence ($F_{XX}G_XR_XC_XG$) (where X represents any amino acid) (Figure 3).

3.2 Expression profiles of *CYP6CV1* and *CYP6AB51* in different larval developmental stages and different tissues

qRT-PCR was used to detect the gene expression levels of *CYP6CV1* and *CYP6AB51* at different larval developmental stages and in different tissues of *C. punctiferalis*. The two target genes were expressed throughout the *C. punctiferalis* larval growth period and in different tissues. As the larvae developed, the expression levels of the two genes increased. The maximum expression levels of *CYP6CV1* and *CYP6AB51* genes were detected in the fifth-instar larvae stage, and they were 385.96 and 12.42 times higher than in the first-instar larvae, respectively. Among the different tissues, the expression levels of the two genes in the midgut were the highest, and they were significantly higher than in other larval

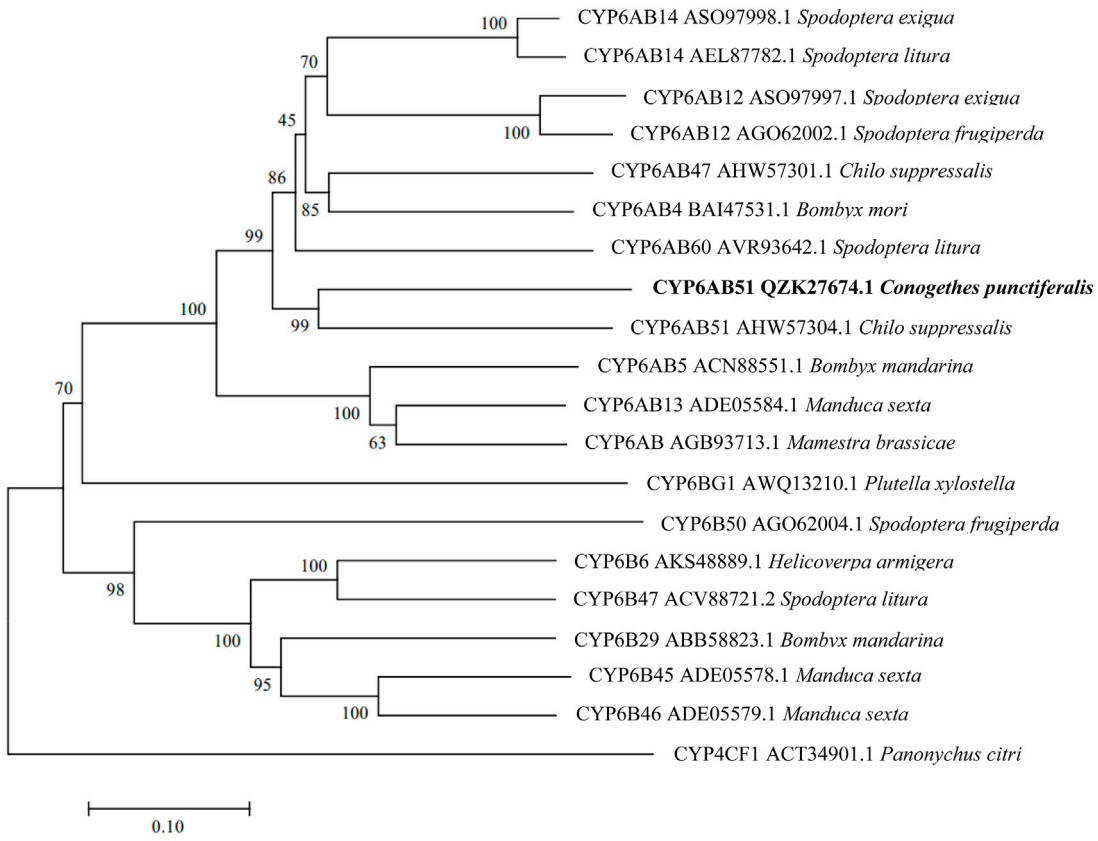

FIGURE 2
Phylogenetic relationships between CYP6AB51 from *C. punctiferalis* and homologs from other lepidopteran insects. The phylogram was generated by MEGA 7.0 using the neighbor-joining method, and the inferred phylogeny was tested using a bootstrap analysis with 1,000 pseudoreplicate datasets.

tissues. The transcript levels in the head and cuticle were the lowest among the tested tissues (Figure 4).

3.3 Toxicity of the three insecticides on *C. punctiferalis*

The toxicity of the three chemical insecticides, chlorantraniliprole, emamectin benzoate and lambda-cyhalothrin, on *C. punctiferalis* larvae are shown in Table 3.

3.4 Effects of insecticide exposure on the mRNA expression levels of *CYP6CV1* and *CYP6AB51*

Three pesticides commonly used in the control of *C. punctiferalis* were selected to evaluate their effects on the expression levels of *C. punctiferalis CYP6CV1* and *CYP6AB51* as assessed by qRT-PCR. When *C. punctiferalis* larvae were exposed to chlorantraniliprole at LC_{10}, the expression of *CYP6CV1* increased significantly and peaked at 3 h, whereas the expression of *CYP6AB51* peaked at 6 h. When treating with chlorantraniliprole at LC_{30}, the expression levels of *CYP6CV1* in *C. punctiferalis* were obviously different from the control group at 3 h and 48 h, and the transcript levels of *CYP6AB51* at different time points were all higher than in the control. Compared with the control group, the expression of *CYP6CV1* in the LC_{50} treatment increased significantly at 3 h, and the expression of *CYP6AB51* was induced notably at all the time points (Figures 5A,B).

Emamectin benzoate at LC_{10} obviously induced the expression of *CYP6CV1* and *CYP6AB51* at 3 h and 6 h. In addition, emamectin benzoate at LC_{30} also significantly increased the expression levels of the two genes relative to the control treatment. However, when *C. punctiferalis* larvae were exposed to emamectin benzoate at LC_{50}, the expression of *CYP6CV1* was significantly increased at 3 h and then decreased slowly, whereas the transcript levels of *CYP6AB51* peaked at 48 h (Figures 5C,D).

In response to lambda-cyhalothrin exposure, the expression levels of *CYP6CV1* at the three concentrations all peaked at 24 h, whereas the expression of *CYP6AB51* was upregulated at all time points and peaked at 3 h compared with the control (Figures 5E,F).

3.5 The sensitivity of *C. punctiferalis* larvae to the three insecticides after target gene silencing

After the silencing of *CYP6CV1* and *CYP6AB51* independently in *C. punctiferalis* by injecting ds*CYP6CV1* and ds*CYP6AB51*,

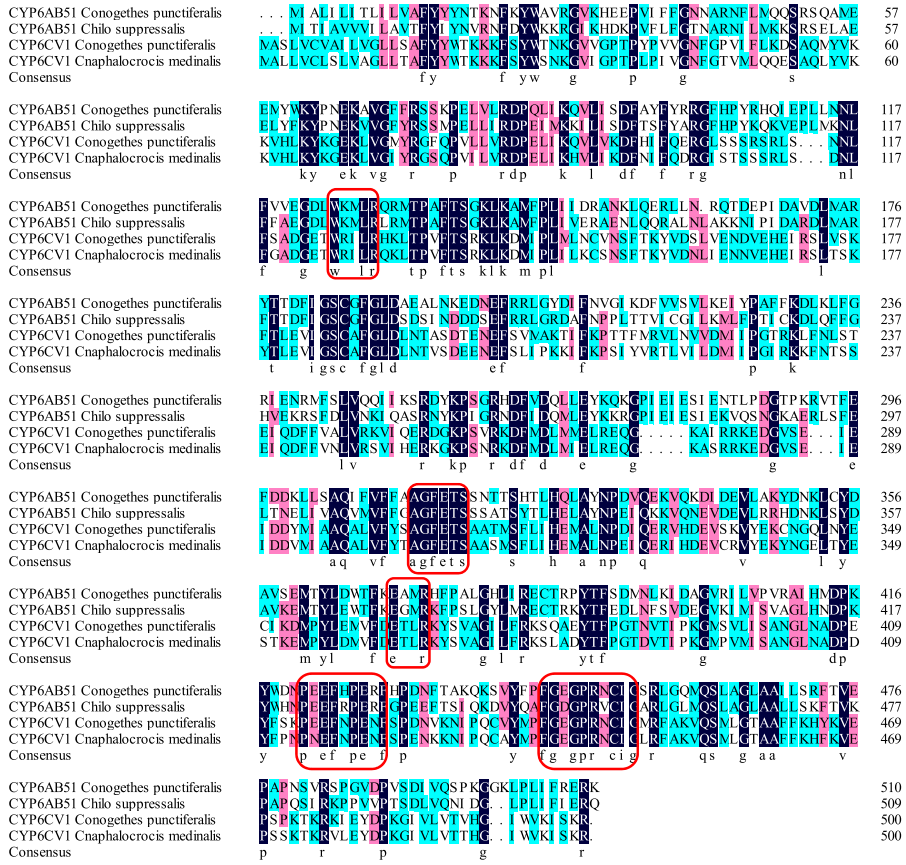

FIGURE 3
Alignment of *C. punctiferalis* CYP6CV1 and CYP6AB51 with related lepidopteran cytochrome P450s. The sequences of *C. punctiferalis* CYP6AB51, *C. suppressalis* CYP6AB51, *C. punctiferalis* CYP6CV1 and *C. medinalis* CYP6CV1 were aligned using ClustalX. The dark blue indicates a shared amino acid identity of 100%, the pink indicates a shared amino acid identity greater than or equal to 75%, and the green indicates a shared amino acid identity greater than or equal to 50%. The five conserved domains of the cytochrome P450 genes are marked with red boxes.

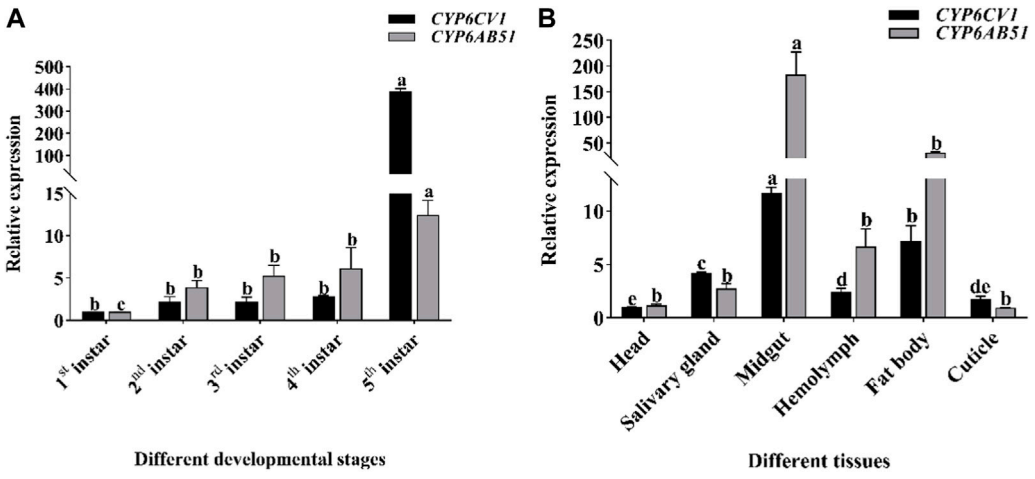

FIGURE 4
The transcription levels of *CYP6CV1* and *CYP6AB51* in different larval developmental stages **(A)** and tissues [**(B)**, fourth-instar larvae] of *C. punctiferalis*. All the transcript levels were normalized using *GAPDH* as the internal reference gene. The values are represented as the means ± SEs. Significant differences among treatments are indicated by lowercase letters above each bar ($p < 0.05$).

10.3389/fphys.2023.1186804

TABLE 3 Toxicity levels of the three tested chemical insecticides on the third-instar larvae of *C. punctiferalis*.

Pesticides	LC_{10} (CI_{95})	LC_{30} (CI_{95})	LC_{50} (CI_{95})	Toxicity regression equation	Correlation coefficient
Chlorantraniliprole	0.0248 (0.0137–0.0371)	0.0858 (0.0622–0.11055)	0.2028 (0.1605–0.2595)	y = 0.9724 + 1.4033x	0.956
Emamectin benzoate	0.0238 (0.0180–0.0293)	0.0444 (0.0371–0.0517)	0.0683 (0.0590–0.0794)	y = 3.2646 + 2.8015x	0.986
Lambda-cyhalothrin	0.0237 (0.0110–0.0417)	0.1616 (0.1024–0.2393)	0.6110 (0.4167–0.9263)	y = 0.1943 + 0.9078x	0.981

LC_{10}, lethal concentration at 10%; LC_{30}, lethal concentration at 30%; LC_{50}, lethal concentration at 50%; CI, confidence intervals.

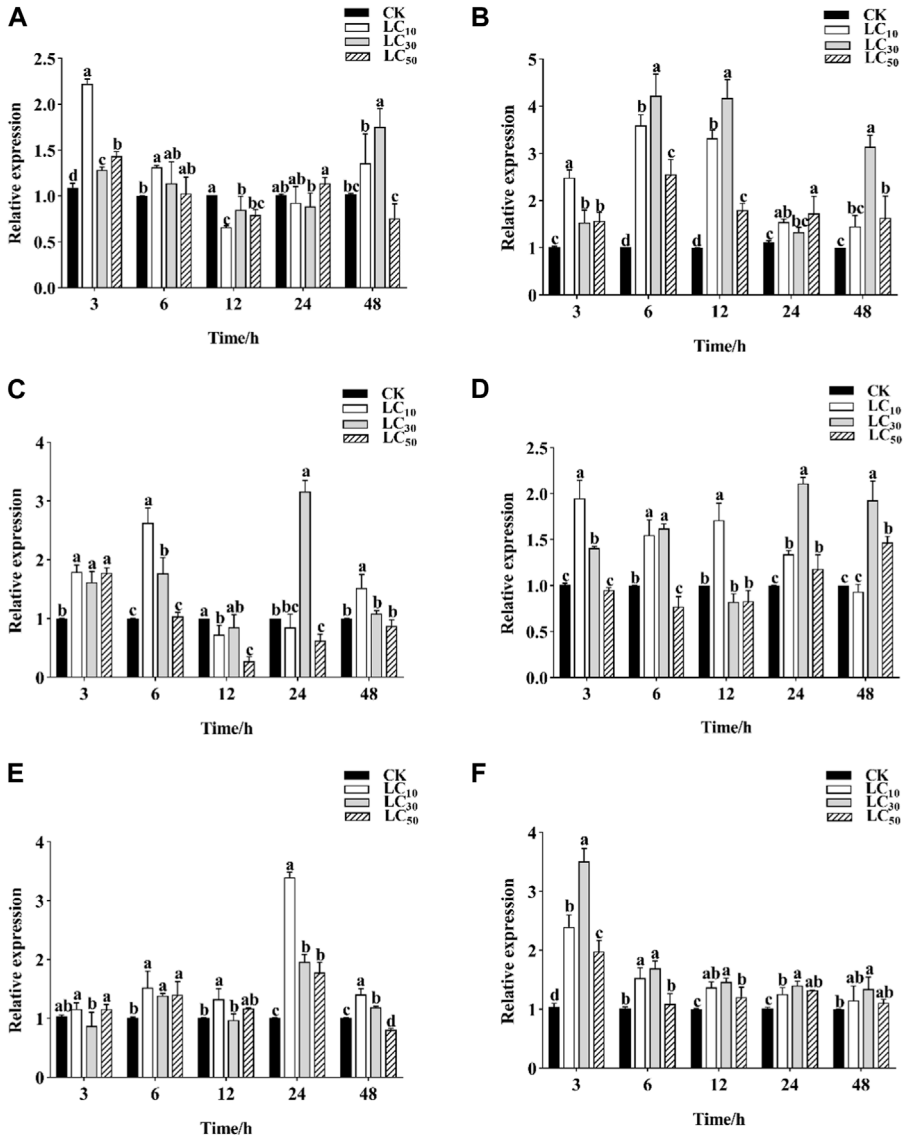

FIGURE 5
Effects of three different pesticides treatments on *CYP6CV1* and *CYP6AB51* expression level in *C. punctiferalis*. The relative transcription levels of **(A)** *CYP6CV1* and **(B)** *CYP6AB51* in the chlorantraniliprole treatment **(C)** *CYP6CV1* and **(D)** *CYP6AB51* in the emamectin benzoate treatment; and **(E)** *CYP6CV1* and **(F)** *CYP6AB51* in the lambda-cyhalothrin treatment. Values are represented by means ± SEs. Significant differences among groups are indicated by lowercase letters above each bar ($p < 0.05$).

respectively, the expression levels of *CYP6CV1* and *CYP6AB51* were both decreased most at 36 h, with reductions of 72.91% and 70.94%, respectively, when compared with the control groups (Figure 6).

After dsRNA injection, the mortality of *CYP6CV1*-silenced larvae and *CYP6AB51*-silenced larvae treated independently with LC_{10} values of chlorantraniliprole, emamectin benzoate and

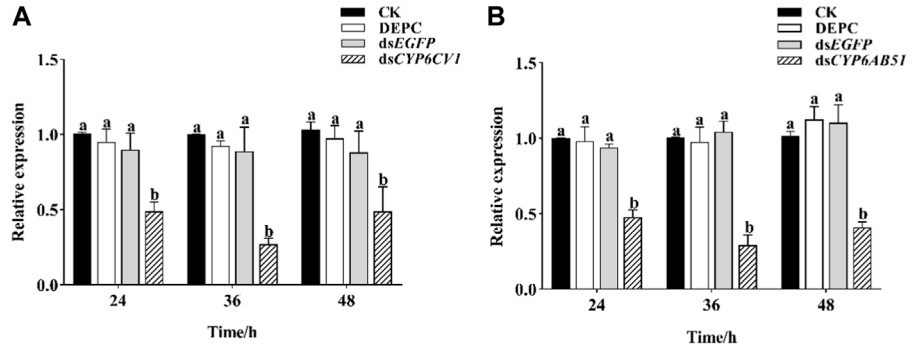

FIGURE 6
Effects of RNAi on the transcript levels of *CYP6CV1* **(A)** and *CYP6AB51* **(B)** in *C. punctiferalis*. Values represent means ± SEs for three independent replicates. Significant differences among groups are indicated by lowercase letters above each bar ($p < 0.05$).

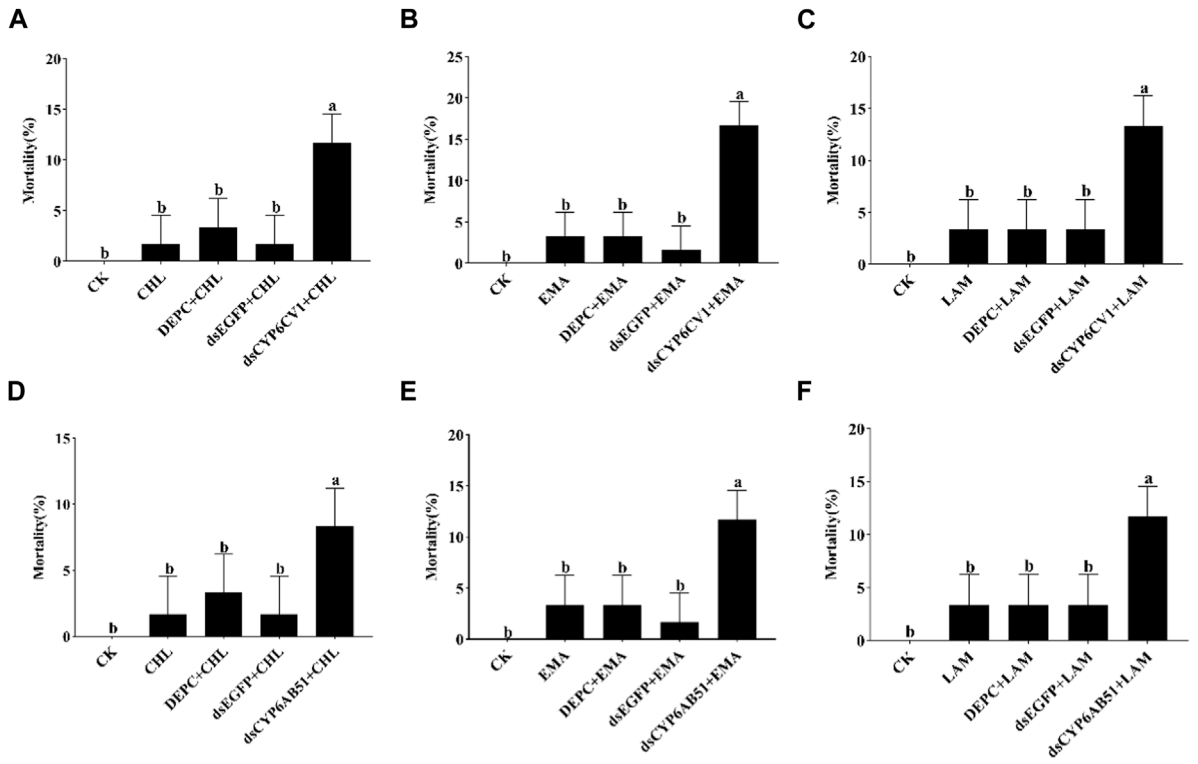

FIGURE 7
Silencing *CYP6CV1* **(A–C)** and *CYP6AB51* **(D–F)** to the sensitivity of *C. punctiferalis* larvae treat with three pesticides. Data shown are means ± SEs, and significant differences among groups are indicated by lowercase letters above each bar ($p < 0.05$). CK: uninjected larvae fed with normal artificial diets; CHL/EMA/LAM: uninjected larvae treated with chlorantraniliprole, emamectin benzoate or lambda-cyhalothrin at the LC_{10} value; DEPC + CHL/EMA/LAM: larvae injected with DEPC-treated water and then treated with chlorantraniliprole, emamectin benzoate or lambda-cyhalothrin at the LC_{10} value; ds*EGFP* + CHL/EMA/LAM: larvae injected with ds*EGFP* and then treated with chlorantraniliprole, emamectin benzoate or lambda-cyhalothrin at the LC_{10} value; ds*CYP6CV1*/ds*CYP6AB51* + CHL/EMA/LAM: larvae injected with ds*CYP6CV1* or ds*CYP6AB51* and then treated with chlorantraniliprole, emamectin benzoate or lambda-cyhalothrin at the LC_{10} value.

lambda-cyhalothrin were recorded. The results indicated that the delivery of ds*CYP6CV1* increased the larval mortality caused by chlorantraniliprole (from 1.67% to 11.67%), emamectin benzoate (from 3.33% to 16.67%) and lambda-cyhalothrin (from 3.33% to 13.33%), and injection with ds*CYP6AB51* significantly increased the larval mortality caused by chlorantraniliprole (from 1.67% to 8.33%), emamectin benzoate (from 3.33% to 11.67%) and lambda-cyhalothrin (from 3.33% to 11.67%) (Figure 7).

4 Discussion

The number of CYP genes carried by insect genomes range from 36 for *Pediculus humanus* to 170 for *Culex quinquefasciatus* (Arensburger et al., 2010; Lee et al., 2010). The first identified insect P450 gene was *CYP6A1* cloned from *Musca domestica* (Feyereisen et al., 1989), and since then, more and more novel insect P450 genes have been identified with the development of molecular biology-related technology (Li F. et al., 2019). Some P450 genes, especially CYP3 (including CYP6 and CYP9) and CYP4 are involved in the detoxification and metabolism of exogenous compounds (Feyereisen, 2011). In *Mamestra brassicae*, the *CYP4M51* and *CYP6AB56* genes have potential roles in the detoxification of deltamethrin (Zhou et al., 2017). In addition, the *CYP9A105* gene may play an important role in the detoxification of α-cypermethrin, deltamethrin and fenvalerate in *Spodoptera exigua* (Wang et al., 2018). In this study, the obtained P450 CYP6 genes, *CYP6CV1* and *CYP6AB51* in *C. punctiferalis*, also contained the five conserved domains of insect P450s. The phylogenetic analysis showed that CYP6CV1 and CYP6AB51 in *C. punctiferalis* were closely related to *C. medinalis* CYP6CV1 and *C. suppressalis* CYP6AB51, respectively.

Analyses of P450 gene expression patterns provide useful information on the potential roles of these genes in biological functions (Lyu et al., 2020). Insect P450 genes have a diverse distribution. Some genes are expressed throughout all the developmental stages and distributed widely in all the tissues, whereas some genes are only expressed in specific developmental stages and specific tissues (Scott et al., 1999; Feyereisen, 2015; Xu et al., 2009). Larval midguts and fat bodies play important roles in the metabolism of xenobiotics; therefore, the P450 genes associated with the detoxification of xenobiotics may be highly expressed in these tissues (Hou et al., 2021). Consequently, the expression profiles of *CYP6CV1* and *CYP6AB51* in *C. punctiferalis* at different developmental stages and in different larval tissues were assessed by qRT-PCT. As the larvae developed, the gene expression levels increased. The expression levels of *CYP6CV1* and *CYP6AB51* in fifth-instar larvae were 385.96 and 12.42 times higher than in first-instar larvae, respectively. This expression pattern is similar to the larval expression pattern of *CYP6CV1* in *C. medinalis* (Chen et al., 2015). A tissue-specific expression analysis showed that *CYP6CV1* and *CYP6AB51* are highly expressed in the larval midguts of *C. punctiferalis*, with expression levels being approximately 11.60-fold and 156.96-fold higher than in the head, respectively, and a similar result was also found for the *CYP6AB60* expression levels in *Spodoptera litura* (Sun et al., 2019). The detoxification system of the midgut responds quickly to the ingestion of xenobiotics (plant secondary substances and pesticides), indicating that the detoxification enzymes of midguts play important roles in the metabolism of xenobiotics (Li Q. et al., 2019; Huang et al., 2021).

An important feature of the P450 enzyme system is its inducibility (Yang et al., 2013). The expression of insect P450 can be induced by a broad range of xenobiotics, thereby enhancing their ability to metabolize the xenobiotics after exposure (Feyereisen, 2015). *CYP6B8* in *Helicoverpa zea* metabolizes plant allelochemicals, such as xanthotoxin, quercetin and flavone, as well as three insecticides, diazinon, cypermethrin and aldrin (Li et al., 2004). The upregulation of *CYP6CM1* in *Bemisia tabaci* is related to its resistance to neonicotinoid insecticides (Jones et al., 2011). In *Leptinotarsa decemlineata*, six CYP6 genes (*CYP6BH2*, *CYP6BJ1*, *CYP6BQ17*, *CYP6EG1*, *CYP6EH1* and *CYP6EJ1*) are involved in cyhalothrin detoxification (Wan et al., 2013). In this study, the expression of *CYP6CV1* and *CYP6AB51* was significantly induced by chlorantraniliprole, emamectin benzoate and lambda-cyhalothrin treatments, which indicated that *CYP6CV1* and *CYP6AB51* may participate in the detoxification and metabolism of the three pesticides in *C. punctiferalis*.

RNAi is a commonly used gene silencing technology that inhibits the expression of target genes in the test organisms. It has been widely used to study the functional roles of insect P450s (Bautista et al., 2009; Shi et al., 2016). Furthermore, it is a promising bioengineering technology that can be applied to pest control (Zhu and Palli, 2020). It has been successfully used in the functional studies of a variety of insect P450 genes (Zhao et al., 2021). In the current study, independent injections with dsRNA targeting *CYP6CV1* and *CYP6AB51* significantly increased the mortality of *C. punctiferalis* larvae treated with chlorantraniliprole, emamectin benzoate or lambda-cyhalothrin, which suggested the potential roles of *CYP6CV1* and *CYP6AB51* in the detoxification of the three pesticides. Similarly, after the injection of dsRNA targeting *CYP6B7*, the sensitivity of *H. armigera* larvae significantly increases after fenvalerate exposure (Tang et al., 2012). In addition, the gene silencing of *CYP6B6* in *H. armigera* significantly reduces the survival rate and development of larvae (Zhang et al., 2013). After injecting the dsRNA of *CYP6AB14*, the transcription level of *CYP6AB14* in *S. litura* is significantly reduced, and the mortality of larvae significantly increases (Wang et al., 2015).

5 Conclusion

In this study, it was found that after interfering with the *CYP6CV1* and *CYP6AB51* in *C. punctiferalis*, respectively, the sensitivity of *C. punctiferalis* to chlorantraniliprole, emamectin benzoate and lambda-cyhalothrin was significantly increased, indicating that the two CYP6 genes were responsible for the adaptability of *C. punctiferalis* to the three chemical insecticides in *C. punctiferalis*. The results from this study demonstrated that *CYP6CV1* and *CYP6AB51* in *C. punctiferalis* play crucial roles in the detoxification of chlorantraniliprole, emamectin benzoate and lambda-cyhalothrin.

Data availability statement

The datasets presented in this study can be found in online repositories. The names of the repository/repositories and accession number(s) can be found in the article/supplementary material.

Author contributions

Formal analysis, QZ; Investigation, XY and HL; Supervision, XG and HJ; Writing—original draft, LZ, GW, WL, and MZ. All authors contributed to the article and approved the submitted version.

Funding

This study was supported by the National Natural Science Foundation of China (Grant No. 31801735) and the State Key Laboratory of Integrated Management of Pest Insects and Rodents (Grant No. IPM2117).

Conflict of interest

The authors declare that the research was conducted in the absence of any commercial or financial relationships that could be construed as a potential conflict of interest.

Publisher's note

All claims expressed in this article are solely those of the authors and do not necessarily represent those of their affiliated organizations, or those of the publisher, the editors and the reviewers. Any product that may be evaluated in this article, or claim that may be made by its manufacturer, is not guaranteed or endorsed by the publisher.

References

Amenya, D. A., Naguran, R., Lo, T. C., Ranson, H., Spillings, B. L., Wood, O. R., et al. (2008). Over expression of a cytochrome P450 (CYP6P9) in a major African malaria vector, *Anopheles funestus*, resistant to pyrethroids. *Insect Mol. Biol.* 17, 19–25. doi:10.1111/j.1365-2583.2008.00776.x

Arensburger, P., Megy, K., Waterhouse, R. M., Abrudan, J., Amedeo, P., Antelo, B., et al. (2010). Sequencing of *Culex quinquefasciatus* establishes a platform for mosquito comparative genomics. *Science* 330, 86–88. doi:10.1126/science.1191864

Balabanidou, V., Kampouraki, A., MacLean, M., Blomquist, G. J., Tittiger, C., Juárez, M. P., et al. (2016). Cytochrome P450 associated with insecticide resistance catalyzes cuticular hydrocarbon production in *Anopheles gambiae*. *Proc. Natl. Acad. Sci. U. S. A.* 113, 9268–9273. doi:10.1073/pnas.1608295113

Bautista, M. A. M., Miyata, T., Miura, K., and Tanaka, T. (2009). RNA interference-mediated knockdown of a cytochrome P450, *CYP6BG1*, from the diamondback moth, *Plutella xylostella*, reduces larval resistance to permethrin. *Insect Biochem. Mol. Biol.* 39, 38–46. doi:10.1016/j.ibmb.2008.09.005

Brewer, M. J., and Trumble, J. T. (1989). Field monitoring for insecticide resistance in beet armyworm (Lepidoptera: Noctuidae). *J. Econ. Entomol.* 82, 1520–1526. doi:10.1093/jee/82.6.1520

Chen, J., Li, C., and Yang, Z. (2015). Identification and expression of two novel cytochrome P450 genes, *CYP6CV1* and *CYP9A38*, in *Cnaphalocrocis medinalis* (Lepidoptera: Pyralidae). *J. Insect Sci.* 15, 50. doi:10.1093/jisesa/ieu174

Chen, G. M., Chi, H., Wang, R. C., Wang, Y. P., Xu, Y. Y., Li, X. D., et al. (2018). Demography and uncertainty of population growth of *Conogethes punctiferalis* (Lepidoptera: Crambidae) reared on five host plants with discussion on some life history statistics. *J. Econ. Entomol.* 111, 2143–2152. doi:10.1093/jee/toy202

Cui, S., Wang, L., Ma, L., and Geng, X. (2016). P450-mediated detoxification of botanicals in insects. *Phytoparasitica* 44, 585–599. doi:10.1007/s12600-016-0550-1

Deng, J., Carbone, I., and Dean, R. A. (2007). The evolutionary history of cytochrome P450 genes in four filamentous Ascomycetes. *BMC Evol. Biol.* 7, 30–22. doi:10.1186/1471-2148-7-30

Ding, Z., Wen, Y., Yang, B., Zhang, Y., Liu, S., Liu, Z., et al. (2013). Biochemical mechanisms of imidacloprid resistance in *Nilaparvata lugens*: Over-expression of cytochrome P450 CYP6AY1. *Insect biochem. Mol. Biol.* 43, 1021–1027. doi:10.1016/j.ibmb.2013.08.005

Elfaki, I., Mir, R., Almutairi, F. M., and Duhier, F. M. A. (2018). Cytochrome P450: Polymorphisms and roles in cancer, diabetes and atherosclerosis. *Asian pac. J. Cancer Prev.* 19, 2057–2070. doi:10.22034/APJCP.2018.19.8.2057

Elzaki, M. E. A., Zhang, W., and Han, Z. (2015). Cytochrome P450 CYP4DE1 and CYP6CW3v2 contribute to ethiprole resistance in *Laodelphax striatellus* (Fallén). *Insect Mol. Biol.* 24, 368–376. doi:10.1111/imb.12164

Feyereisen, R., Koener, J. F., Farnsworth, D. E., and Nebert, D. W. (1989). Isolation and sequence of cDNA encoding a cytochrome P450 from an insecticide-resistant strain of the house fly, *Musca domestica*. *Proc. Natl. Acad. Sci. U. S. A.* 86, 1465–1469. doi:10.1073/pnas.86.5.1465

Feyereisen, R. (2011). Arthropod CYPomes illustrate the tempo and mode in P450 evolution. *Biochim. Biophys. Acta, Proteins Proteomics* 1814, 19–28. doi:10.1016/j.bbapap.2010.06.012

Feyereisen, R. (2015). Insect P450 inhibitors and insecticides: Challenges and opportunities. *Pest Manage. Sci.* 71, 793–800. doi:10.1002/ps.3895

Gao, X. W. (2010). Current status and development strategy for chemical control in China. *Plant Prot.* 36, 19–22.

Giraudo, M., Hilliou, F., Fricaux, T., Audant, P., Feyereisen, R., and Le Goff, G. (2015). Cytochrome P450s from the fall armyworm (*Spodoptera frugiperda*): Responses to plant allelochemicals and pesticides. *Insect Mol. Biol.* 24, 115–128. doi:10.1111/imb.12140

Graham, S. E., and Peterson, J. A. (1999). How similar are P450s and what can their differences teach us? *Arch. Biochem. Biophys.* 369, 24–29. doi:10.1006/abbi.1999.1350

Helvig, C., Tijet, N., Feyereisen, R., Walker, F. A., and Restifo, L. L. (2004). *Drosophila melanogaster* CYP6A8, an insect P450 that catalyzes lauric acid (ω-1)-hydroxylation. *Biochem. Biophys. Res. Commun.* 325, 1495–1502. doi:10.1016/j.bbrc.2004.10.194

Hou, W. T., Staehelin, C., Elzaki, M. E. A., Hafeez, M., Luo, Y. S., and Wang, R. L. (2021). Functional analysis of *CYP6AE68*, a cytochrome P450 gene associated with indoxacarb resistance in *Spodoptera litura* (Lepidoptera: Noctuidae). *Pestic. Biochem. Physiol.* 178, 104946. doi:10.1016/j.pestbp.2021.104946

Huang, Y., Luo, Y., Wu, P., Zheng, J., Qiu, L., and Hou, L. (2021). Effects of three insecticides on the expression of cytochrome P450 CYP6B7 in *Helicoverpa armigera*. *J. Appl. Entomol.* 145, 440–447. doi:10.1111/iwj.13544

Iga, M., and Kataoka, H. (2012). Recent studies on insect hormone metabolic pathways mediated by cytochromeP450 enzymes. *Biol. Pharm. Bull.* 35, 838–843. doi:10.1248/bpb.35.838

Jing, D. P., Huang, X. D., Zhang, T. T., and Wang, Z. Z. (2022). Involvement of *CYP6AE76* gene in detoxifying the Cry1Ab protein in *Conogethes punctiferalis* (Lepidoptera: Crambidae). *Acta Entomol. Sin.* 65, 1136–1143.

Jones, C. M., Daniels, M., Andrews, M., Slater, R., Lind, R. J., Gorman, K., et al. (2011). Age-specific expression of a P450 monooxygenase (*CYP6CM1*) correlates with neonicotinoid resistance in *Bemisia tabaci*. *Pestic. Biochem. Physiol.* 101, 53–58. doi:10.1016/j.pestbp.2011.07.004

Lee, S. H., Kang, J. S., Min, J. S., Yoon, K. S., Strycharz, J. P., Johnson, R., et al. (2010). Decreased detoxification genes and genome size make the human body louse an efficient model to study xenobiotic metabolism. *Insect Mol. Biol.* 19, 599–615. doi:10.1111/j.1365-2583.2010.01024.x

Li, X., Baudry, J., Berenbaum, M. R., and Schuler, M. A. (2004). Structural and functional divergence of insect CYP6B proteins: From specialist to generalist cytochrome P450. *Proc. Natl. Acad. Sci. U. S. A.* 101, 2939–2944. doi:10.1073/pnas.0308691101

Li, X., Li, R., Zhu, B., Gao, X., and Liang, P. (2018). Overexpression of cytochrome P450 *CYP6BG1* may contribute to chlorantraniliprole resistance in *Plutella xylostella* (L). *Pest Manag. Sci.* 74, 1386–1393. doi:10.1002/ps.4816

Li, F., Zhao, X., Li, M., He, K., Huang, C., Zhou, Y., et al. (2019). Insect genomes: Progress and challenges. *Insect Mol. Biol.* 28, 739–758. doi:10.1111/imb.12599

Li, Q., Sun, Z., Shi, Q., Wang, R., Xu, C. C., Wang, H., et al. (2019). RNA-seq analyses of midgut and fat body tissues reveal the molecular mechanism underlying *Spodoptera litura* resistance to tomatine. *Front. Physiol.* 10, 8. doi:10.3389/fphys.2019.00008

Livak, K. J., and Schmittgen, T. D. (2001). Analysis of relative gene expression data using real-time quantitative PCR and the $2^{-\Delta\Delta CT}$ method. *Methods* 25, 402–408. doi:10.1006/meth.2001.1262

Lyu, Z., Kong, D., Cheng, J., and Lin, T. (2020). Identification and expression analysis of cytochrome P450 genes in *Plecoptera oculata* (Lepidoptera: Noctuidae). *Entomol. Res.* 50, 90–99. doi:10.1111/1748-5967.12412

Maïbèche-Coisne, M., Jacquin-Joly, E., François, M. C., and Nagnan-Le Meillour, P. (2002). cDNA cloning of biotransformation enzymes belonging to the cytochrome P450 family in the antennae of the noctuid moth *Mamestra brassicae*. *Insect Mol. Biol.* 11, 273–281. doi:10.1046/j.1365-2583.2002.00335.x

Muraro, D. S., de Oliveira Abbade Neto, D., Kanno, R. H., Kaiser, I. S., Bernardi, O., and Omoto, C. (2021). Inheritance patterns, cross-resistance and synergism in *Spodoptera frugiperda* (Lepidoptera: Noctuidae) resistant to emamectin benzoate. *Pest Manage. Sci.* 77, 5049–5057. doi:10.1002/ps.6545

Rasool, A., Joußen, N., Lorenz, S., Ellinger, R., Schneider, B., Khan, S. A., et al. (2014). An independent occurrence of the chimeric P450 enzyme CYP337B3 of *Helicoverpa armigera* confers cypermethrin resistance in Pakistan. *Insect Biochem. Mol. Biol.* 53, 54–65. doi:10.1016/j.ibmb.2014.07.006

Scott, J. G., Liu, N., Wen, Z., Smith, F. F., Kasai, S., and Horak, C. E. (1999). House-fly cytochrome P450 CYP6D1: 5′ flanking sequences and comparison of alleles. *Gene* 226, 347–353. doi:10.1016/s0378-1119(98)00545-9

Shi, L., Zhang, J., Shen, G., Xu, Z., Xu, Q., and He, L. (2016). Collaborative contribution of six cytochrome P450 monooxygenase genes to fenpropathrin resistance in *Tetranychus cinnabarinus* (Boisduval). *Insect Mol. Biol.* 25, 653–665. doi:10.1111/imb.12251

Shwe, S. M., Wang, Y., Gao, Z., Li, X., Liu, S., Bai, S., et al. (2021a). Toxicity of Cry1-Class, Cry2Aa, and Vip3Aa19 Bt proteins and their interactions against yellow peach moth, *Conogethes punctiferalis* (Guenée) (Lepidoptera: Crambidae). *J. Invertebr. Pathol.* 178, 107507. doi:10.1016/j.jip.2020.107507

Shwe, S. M., Prabu, S., Chen, Y., Li, Q., Jing, D., Bai, S., et al. (2021b). Baseline susceptibility and laboratory selection of resistance to Bt Cry1Ab protein of Chinese populations of yellow peach moth, *Conogethes punctiferalis* (Guenée). *Toxins* 13, 335. doi:10.3390/toxins13050335

Siegwart, M., Thibord, J. B., Olivares, J., Hirn, C., Elias, J., Maugin, S., et al. (2017). Biochemical and molecular mechanisms associated with the resistance of the European corn borer (Lepidoptera: Crambidae) to lambda-cyhalothrin and first monitoring tool. *J. Econ. Entomol.* 110, 598–606.

Stanley, J., Chandrasekaran, S., and Preetha, G. (2009). *Conogethes punctiferalis* (Lepidoptera: Pyralidae) its biology and field parasitization. *Indian J. Agric. Sci.* 79, 906–909. doi:10.1093/jee/tow267

Su, J., and Sun, X. X. (2014). High level of metaflumizone resistance and multiple insecticide resistance in field populations of *Spodoptera exigua* (Lepidoptera: Noctuidae) in Guangdong Province, China. *Crop Prot.* 61, 58–63. doi:10.1016/j.cropro.2014.03.013

Sun, Z., Shi, Q., Li, Q., Wang, R., Xu, C., Wang, H., et al. (2019). Identification of a cytochrome P450 CYP6AB60 gene associated with tolerance to multi-plant allelochemicals from a polyphagous caterpillar tobacco cutworm (*Spodoptera litura*). *Pestic. Biochem. Physiol.* 154, 60–66. doi:10.1016/j.pestbp.2018.12.006

Tang, T., Zhao, C., Feng, X., Liu, X., and Qiu, L. (2012). Knockdown of several components of cytochrome P450 enzyme systems by RNA interference enhances the susceptibility of *Helicoverpa armigera* to fenvalerate. *Pest Manage. Sci.* 68, 1501–1511. doi:10.1002/ps.3336

Ullah, F., Gul, H., Tariq, K., Desneux, N., Gao, X., and Song, D. (2020). Functional analysis of cytochrome P450 genes linked with acetamiprid resistance in melon aphid, Aphis gossypii. *Aphis Gossypii. Pestic. Biochem. Physiol.* 170, 104687. doi:10.1016/j.pestbp.2020.104687

Wan, P. J., Shi, X. Q., Kong, Y., Zhou, L. T., Guo, W. C., Ahmat, T., et al. (2013). Identification of cytochrome P450 monooxygenase genes and their expression profiles in cyhalothrin-treated 549 Colorado potato beetle, *Leptinotarsa decemlineata*. *Pestic. Biochem. Physiol.* 107, 360–368. doi:10.1016/j.pestbp.2013.10.004

Wang, X., and Wu, Y. (2012). High levels of resistance to chlorantraniliprole evolved infield populations of *Plutella xylostella*. *J. Econ. Entomol.* 105, 1019–1023. doi:10.1603/ec12059

Wang, R. L., Xia, Q. Q., Baerson, S. R., Ren, Y., Wang, J., Su, Y. J., et al. (2015). A novel cytochrome P450 CYP6AB14 gene in *Spodoptera litura* (Lepidoptera: Noctuidae) and its potential role in plant allelochemical detoxification. *J. Insect Physiol.* 75, 54–62. doi:10.1016/j.jinsphys.2015.02.013

Wang, R. L., Liu, S. W., Baerson, S. R., Qin, Z., Ma, Z. H., Su, Y. J., et al. (2018). Identification and functional analysis of a novel cytochrome P450 gene CYP9A105 associated with pyrethroid detoxification in *Spodoptera exigua* Hübner. *Int. J. Mol. Sci.* 19, 737. doi:10.3390/ijms19030737

Wang, Z. G., Jiang, S. S., Mota-Sanchez, D., Wang, W., Li, X. R., Gao, Y. L., et al. (2019). Cytochrome P450-mediated λ-cyhalothrin-resistance in a field strain of *Helicoverpa armigera* from Northeast China. *J. Agric. Food Chem.* 67, 3546–3553. doi:10.1021/acs.jafc.8b07308

Wang, R., Liu, J., Zhu, X., Pang, Y., Wang, Y., Liu, X., et al. (2020). Screening of insecticides for controlling yellow peach moth, *Conogethes Punctiferalis* (Guenée) on maize. *Pestic. Sci. Adm.* 41, 42–49. doi:10.1093/gastro/goz055

Xu, Y. Q., Wang, J. J., Jiang, H. B., Wei, D., Tang, P. A., and An, F. M. (2009). Identification, characterization, and expression of P450 gene encoding CYP6BQ13v2 from the red flour beetle, *Tribolium castaneum* (Herbst) (Coleoptera: Tenebrionidae). *Agric. Sci. China.* 8, 1210–1218. doi:10.1016/s1671-2927(08)60331-4

Yang, T., and Liu, N. (2011). Genome analysis of cytochrome P450s and their expression profiles in insecticide resistant mosquitoes, *Culex quinquefasciatus*. *PloS One* 6, e29418. doi:10.1371/journal.pone.0029418

Yang, X., Li, X., and Zhang, Y. (2013). Molecular cloning and expression of *CYP9A61*: A chlorpyrifos-ethyl and lambda-cyhalothrin-inducible cytochrome P450 cDNA from *Cydia pomonella*. *Int. J. Mol. Sci.* 14, 24211–24229. doi:10.3390/ijms141224211

Yu, H. L., Xiang, X., Yuan, G. X., Chen, Y. Q., and Wang, X. G. (2015). Effects of sublethal doses of cyantraniliprole on the growth and development and the activities of detoxifying enzymes in *Spodoptera exigua* (Lepidoptera: Noctuidae). *Acta Entomol. Sin.* 58, 634–641.

Zhang, X., Liu, X., Ma, J., and Zhao, J. (2013). Silencing of cytochrome P450 *CYP6B6* gene of cotton bollworm (*Helicoverpa armigera*) by RNAi. *B. Entomol. Res.* 103, 584–591. doi:10.1017/S0007485313000151

Zhao, P., Xue, H., Zhu, X., Wang, L., Zhang, K., Li, D., et al. (2021). Silencing of cytochrome P450 gene *CYP321A1* effects tannin detoxification and metabolism in *Spodoptera litura*. *Int. J. Biol. Macromol.* 194, 895–902. doi:10.1016/j.ijbiomac.2021.11.144

Zhou, X., Fan, X., Gao, Y., Yang, J., Qian, J., and Fan, D. (2017). Identification of two novel P450 genes and their responses to deltamethrin in the cabbage moth, *Mamestra brassicae* Linnaeus. *Pestic. Biochem. Physiol.* 141, 76–83. doi:10.1016/j.pestbp.2016.12.001

Zhu, K. Y., and Palli, S. R. (2020). Mechanisms, applications, and challenges of insect RNA interference. *Annu. Rev. Entomol.* 65, 293–311. doi:10.1146/annurev-ento-011019-025224

frontiers | Frontiers in Physiology

TYPE Original Research
PUBLISHED 31 July 2023
DOI 10.3389/fphys.2023.1153249

OPEN ACCESS

EDITED BY
Jia Fan,
Institute of Plant Protection (CAAS), China

REVIEWED BY
Haicui Xie,
Hebei Normal University of Science and Technology, China
Chao Li,
Xinjiang Agricultural University, China
Zhaohuan Xu,
Jiangxi Agricultural University, China

*CORRESPONDENCE
Lanlan Han,
hanll_neau@aliyun.com

RECEIVED 29 January 2023
ACCEPTED 26 June 2023
PUBLISHED 31 July 2023

CITATION
Zhang A, Dou N, Qu Z, Guo Y, Zhou W, Wu D, Lin Z, Feng M, Cui H and Han L (2023), Effects of the termination of LC_{30} imidacloprid stress on the multigeneration adaptive strategies of *Aphis glycines* population. *Front. Physiol.* 14:1153249. doi: 10.3389/fphys.2023.1153249

Effects of the termination of LC_{30} imidacloprid stress on the multigeneration adaptive strategies of *Aphis glycines* population

Aonan Zhang[1], Nan Dou[1], Zhongcheng Qu[2], Yongxia Guo[3], WenJing Zhou[1], Dongxue Wu[1], Zhiying Lin[1], Min Feng[1], Hengjia Cui[1] and Lanlan Han[1]*

[1]College of Plant Protection, Northeast Agricultural University, Harbin, Heilongjiang, China, [2]Qiqihar Branch of Heilongjiang Academy of Agricultural Sciences, Qiqihar City, Heilongjiang, China, [3]National Coarse Cereals Engineering Research Center, Key Laboratory of Low-Carbon Green Agriculture in Northeastern China, Ministry of Agriculture and Rural Affairs China and Heilongjiang Provincial Key Laboratory of Crop Pest Interaction Biology and Ecological Control, Daqing, China

Aphis glycines Matsumura (Hemiptera: Aphididae) is a major soybean pest that often poses a serious threat to soybean production. Imidacloprid is one of the commonly used insecticides to control the soybean aphid. To investigate the effect of termination of imidacloprid stress on the adaptive strategies of soybean aphid populations, we studied the growth, development, and related metabolism changes when the stress was terminated after 24 generations of imidacloprid stress on *A. glycines*. The results show that the *A. glycines* population accelerated its recovery and expanded its population size across generations. The longevity of the adults of the recovering population in the F12, F18, and F24 generations, respectively, was 1.11, 1.15, and 1.11 times longer than the control, while the fecundity was 10.38%, 11.74%, and 11.61% higher than that of the control. The net reproductive rate (R_0) of the recovering population was always significantly higher than that of the control in the F1 to F24 generations. In addition, metabolisms related to the regulation of cell proliferation and oocyte meiosis were significantly upregulated in the recovering population. Even when the imidacloprid pressure disappeared, intergenerational stimuli still affected the adaptive strategies of soybean aphid populations. This effect was manifested as inhibiting the growth and development of the soybean aphid in the early generations and improving the fecundity of the soybean aphid in the later generations. Adaptive soybean aphid populations would surge in the absence of imidacloprid pressure. This study provides an important reference for exploring the adaptability of the *A. glycines* population under termination of stress from low lethal concentrations of imidacloprid across generations. It also provides important data for monitoring the population dynamics of *A. glycines* in the field and analyzing the degree of pharmacodynamic stress.

KEYWORDS

***Aphis glycines*, imidacloprid, recovering population, life table, transcriptome**

1 Introduction

The soybean aphid, *Aphis glycines* Matsumura is native to Asia and mainly distributed in the soybean growing regions of the Far East. It was discovered in North America in 2000 (Ragsdale et al., 2011; Hopper et al., 2017). It is one of the major pests that damages cultivated soybeans through piercing and sucking (Hullé et al., 2020). It has become a worldwide agricultural pest (Todd et al., 2022).

Insecticide application remains an effective management strategy for preventing outbreaks of soybean aphids (Mokbel, 2019; Aseperi et al., 2020; Valmorbida et al., 2022). The first generation of neonicotinoids imidacloprid had an excellent control effect on the soybean aphid, and rapidly dominated the insecticide market since its production (Stamm et al., 2016; Hesler and Beckendorf, 2021; Zhang et al., 2022). Although imidacloprid is effective against piercing–sucking pests, its frequent application still has negative effects. For example, *Myzus persicae* populations from different regions were reported to have shown some adaptability to imidacloprid (Devine et al., 1996). The adaptation of field aphids to neonicotinoids might be related to long-term exposure to low doses of insecticides. Plant, animal, fungal, and bacterial interactions cause concentrations of neonicotinoids to decrease gradually from the initial field application levels. Chronic exposure of aphids to neonicotinoids at lower-than-recommended concentrations, across multi-generations has been reported. Also, low doses of insecticides promote the development of resistance in heterozygotes, which can cause rapid fixation of resistance genes in the population. This results in the rapid development of resistant populations and the enhancement of population adaptability (Desneux et al., 2005; Desneux et al., 2007; Fenner et al., 2013). Also, exposures of *A. gossypii* to low doses of thiamethoxam had an intergenerational stimulative effect on the adaptability of its population. The reproduction rate of the aphid population accelerated, which peaked in a shorter time (Ullah et al., 2020a). At present, many researchers have focused on the effects of low-dose neonicotinoids stress on the growth and development of populations. Few researchers have reported on the changes in adaptive strategies of populations after the termination of low-dose insecticide stress. Will the intergenerational stimulative effect continue to affect the adaptive strategies of populations after termination of low-dose insecticide stress? Do adaptive pest populations proliferate without insecticide pressure? These are urgent questions to address for which studies are required.

The insect population life table is an effective tool in population ecology theory to describe population dynamics and analyze population adaptability (Bevill and Louda, 1999). In agricultural production, the acquisition of life table data on a species is important for the efficient management of agricultural pests (Rajotte, 2022). The age–stage life table model has the advantage of considering the relationships and differences between individuals at different developmental stages when predicting population dynamics. It also adopts a systematic identification method and relies on the model to manage population data and estimate the transfer probability between different developmental stages (Chi and Liu, 1985; Chi, 1988; Chi et al., 2020). For example, the basic data and derived parameters provided by the age–stage life table were used to predict the population adaptability of *Bactrocera cucurbitae* (Huang and Chi, 2012). Zhang et al. (2021) found that low-dose thiamethoxam reduced the adaptability of the soybean aphid population by studying the age–stage life table data. Ullah et al. (2019) also used the age–stage life table to analyze the effects of acetamiprid on the adaptive strategies of *Aphis gossypii* and found that the negative effects from the mother still inhibited the development of the offspring.

The regulation of the adaptation strategy of insect populations involves not only changes in population parameters but also changes in the corresponding metabolic regulation. Transcriptome sequencing enables the generation of a large amount of RNA expression data, screens differential genes, analyzes changes in metabolic pathways, and thus reveals the factors that influence the regulation of the adaptive strategy of insect populations (Ma et al., 2016). In this study, the effects of the termination of LC_{30} imidacloprid stress on the multigenerational adaptation strategy of the soybean aphid population were evaluated by analyzing the population parameters and development-related transcription expressions. The results serve as an important reference for understanding the changes in adaptation strategy of soybean aphid populations after the termination of imidacloprid stress. It also provides important information for monitoring the soybean aphid population dynamics in the field and analyzing the degree of pharmacodynamic stress.

2 Materials and methods

2.1 Soybean aphid populations and chemical reagents

All populations were fed dongnong bean 252 soybean plants in the laboratory with 25°C ± 1°C, a relative humidity of 65%–70%, and a photoperiod of 14:10 (L:D).

2.1.1 Laboratory population

The laboratory population of *A. glycines* used in this study was originally collected from a soybean field in Xiangyang farm, Harbin, Heilongjiang, China. The population was cultured separately in the laboratory of Northeast Agricultural University since 2014 and was never exposed to any insecticides.

2.1.2 Field population

The field population used in this study was also collected from a soybean field in Xiangyang in mid-July 2019. The F1–F24 generations were used in this experiment.

2.1.3 Resistant population

The resistant population was derived from the laboratory population subjected to imidacloprid. The laboratory population was exposed to LC_{30} (30% lethal concentration) imidacloprid for F1–F24 generations, from which the resistant population was obtained.

2.1.4 Recovering population

The recovering population used in this study was slowly recovered from the abovementioned resistant soybean aphid across generations. Specifically, exposure of the resistant population at the F24 to imidacloprid was stopped, and they were fed fresh soybean leaves for development and reproduction.

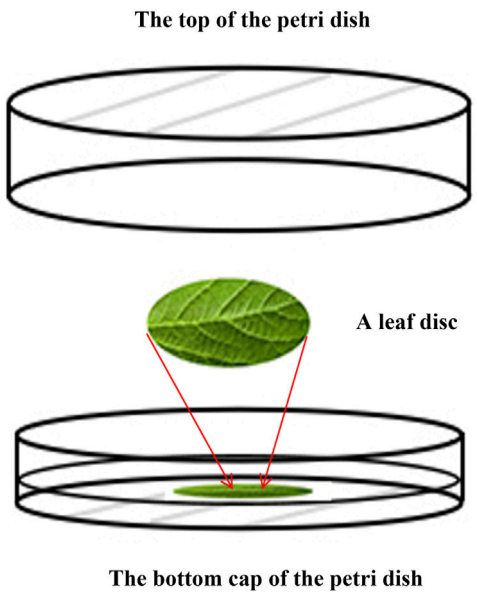

FIGURE 1
Diagram of Petri dish.

Water dispersible granules of 70% imidacloprid were purchased from North China Pharmaceutical Group Corporation, Hebei, China. Calcium nitrate, potassium nitrate, potassium dihydrogen phosphate, magnesium sulfate, disodium ethylenediaminetetraacetic acid (disodium EDTA), and streptomycin sulfate were all purchased from Shanghai Alighting Biochemical Technology Co., Ltd., Shanghai, China.

2.2 Feeding methods of soybean aphids in the laboratory

Dongnong bean 252 soybean plants were grown in pots (15 cm diameter × 17 cm depth), with six plants in each pot that were kept at 25°C ± 1°C, a relative humidity of 65%–70%, and a photoperiod of 14:10 h (L:D). The laboratory aphid colony was maintained in the same environmental conditions as that of the chamber which was used for plant germination. A total of 12 pots with soybean plants were placed in a large tray (L × W = 70 × 60 cm). Then, twice a week, one-third of the old aphid-infested soybean plants (i.e., the four oldest pots with an aphid infestation) were removed and replaced with new aphid-free ones. Aphids were transferred by placing infested leaves on non-infested plants. This prevented the accumulation of excessive honeydew and sooty mold and ensured the provision of a homogeneous soybean plant for the aphids to feed on (James et al., 2020).

2.3 Preparation of culture medium

Non-toxic, transparent plastic Petri dishes (6 cm diameter × 1.5 cm height) were used to perform the bioassays involving newly hatched nymphs of *A. glycines* as well as to perform the life table study. The components of the plant nutrient concentrate used to prepare the medium were calcium nitrate (4.1 g), potassium nitrate (2.5 g), potassium dihydrogen phosphate (0.7 g), magnesium sulfate (0.6 g), 1.54% disodium EDTA aqueous solution (5.0 mL), one million units of streptomycin sulfate (0.05 g), and distilled water (5.0 L). The diluent was obtained by mixing the nutrient concentrate with distilled water at a ratio of 1:3. Agar was prepared by mixing 1% w/w agar powder with diluent and was boiled while constantly mixing. After cooling for approximately 10 min, the warm agar was poured into the Petri dishes to a depth of at least 3–4 mm. At least 10 mm distance was allowed between the top of the agar and the rim of the Petri dishes. A metal tube was used to cut leaf discs from clean, untreated leaves. The leaf discs were attached topside down on the agar medium. *A. glycines* on leaf discs fed on the bottom surface (Figure 1). Each Petri dish was then placed upside down to keep *A. glycines* in a natural feeding state.

2.4 Dose–response bioassay and resistance ratios

The dose–response bioassays were conducted with adults from the laboratory population, resistant population, and recovering population using the leaf dip method recommended by the Insecticide Resistance Action Committee (IRAC; http://www.irac-online.org/resources/methods.asp). Insecticidal stock solutions were prepared in 1% acetone and further diluted to different concentrations using distilled water containing 0.05% (v/v) Triton X-100, before being used in the dose–response bioassay. Fresh soybean leaf discs were immersed in solutions of a series of imidacloprid; each leaf disc was immersed in a specific concentration for 10 s and then removed from the solution to air dry. The control leaf disc was immersed in a solution of distilled water containing 0.05% (v/v) Triton X-100% and 1% acetone. The air-dried leaf discs were attached to the agar medium with the top-side facing down, and the newly hatched nymphs were placed on them. Treatment details (insecticide, concentration, and date) were recorded for each Petri dish. A small drop of distilled water was placed on the surface of the agar prior to laying the leaf on the surface to ensure that the leaf stuck to the agar surface. A total of 60 adults were used for the dose–response bioassays at each concentration; three replicates were used per concentration, and each replicate had 20 adults. Mortality was determined 24 h after exposure. The nymphs were considered dead if they were found upside down and not moving or if they did not move when prodded with a small paint brush. The toxicity of imidacloprid to adults were statistically analyzed using the concentration–mortality regression line and a log-probit model of SPSS (version 23.0, SPSS Inc., Chicago, IL, United States), and the LC_{50} and LC_{30} values were obtained. The resistance ratios of the resistant population were calculated as LC_{50} ratios between the resistant population and laboratory population. The resistance ratio of the recovering population was calculated as LC_{50} ratios between the recovering population and laboratory population. LC_{50} and LC_{30} concentrations of imidacloprid to adults of laboratory population in supplementary information (Supplementary Table S1).

2.5 Life table construction

The method that was followed for the construction of the life table for the laboratory population (control group) is as follows:

100 apterous adults (F0) were transferred onto 10 leaf discs using a small paint brush, with 10 apterous adults placed on each leaf disc. Each Petri dish containing a leaf disc was sealed with a close-fitting ventilated lid. After 24 h, the newly hatched nymphs (F1) produced by the selected aphid were placed in a new Petri dish with a leaf disc. Leaf discs were pre-soaked in distilled water solution containing 0.05% (v/v) Triton X-100% and 1% acetone. A newly hatched nymph was placed on each leaf disc, which served as a replicate, for a total of 100 replicates. Leaf discs were replaced every 24 h. Growth, survival, and death of individuals were observed and recorded every 24 h until all individuals died. The numbers of newly hatched aphids were recorded and then discarded to avoid repeated recording the next day. After that, the construction of the life table for the laboratory population in each generation was repeated using newly hatched aphids produced in the previous generation.

The construction of the life table for the resistant population, which followed the aforementioned method, is as follows: 100 apterous adults (F0) were transferred onto 10 leaf discs using a small paint brush, with 10 apterous adults placed on each leaf disc. A leaf disc pre-impregnated with LC_{30} imidacloprid was placed on each Petri dish. After 24 h, the surviving aphids were placed on a new leaf disc free of the chemical and pre-impregnated with distilled water solution containing 0.05% (v/v) Triton X-100% and 1% acetone; they were allowed to continue feeding to produce the next generation of adults (F1). The process of constructing the life table of the soybean aphid in each generation was similar. The concentration of LC_{30} imidacloprid used in each generation was 30% lethal for adults. The adults of each generation were fed with chemical-free leaf discs 24 h after insecticide stress.

The construction of the life table for the recovering population is as follows: the initial hatchlings of the resistant population produced by the F24 generation were recorded as the recovering F1 generation population. A single hatchling was then reared in separate Petri dishes, each of which was pre-impregnated with a distilled water solution containing 0.05% (v/v) Triton X-100% and 1% acetone for 100 replicates. Growth, survival, and death of the individuals were observed and recorded every 24 h until all individuals died. Data were recorded in the same manner as for the laboratory population.

The construction of the life table for the field population is as follows: the method of constructing the life table of the field population was similar to that of the laboratory population. They differed only in the source of the tested insects.

Preliminary results showed that there was no significant difference in the life table parameters of adjacent generations. We therefore compared and analyzed the changes in the life table parameters of F1, F6, F12, F18, and F24.

2.6 Life table data analysis

The age–stage–specific survival rate (s_{xj}, x = age, j = stage), age-specific survival rate (l_x), age–stage and age-specific fecundity (m_x) were calculated as follows (Chi and Liu, 1985):

$$s_{xj} = \frac{n_{xj}}{n_{01}}, \tag{1}$$

$$l_x = \sum_{j=1}^{k} s_{xj}, \tag{2}$$

$$m_x = \frac{\sum_{j=1}^{k} s_{xj} f_{xj}}{\sum_{j=1}^{k} s_{xj}}, \tag{3}$$

where n_{01} is the number of newly hatched nymphs, and k is the number of stages. The net reproductive rate (R_0), intrinsic rate of increase (r), finite rate of increase (λ), and mean generation time (T) were calculated as follows (Goodman, 1982):

$$R_0 = \sum_{x=0}^{\infty} l_x m_x, \tag{4}$$

$$\sum_{x=0}^{\infty} e^{-r(x+1)} l_x m_x = 1, \tag{5}$$

$$\lambda = e^r, \tag{6}$$

$$T = \frac{\ln R_0}{r}. \tag{7}$$

The life expectancy (e_{xj}), i.e., the time that an individual of age x and stage j is expected to live, was calculated according to Chi and Su (2006) as

$$e_{xj} = \sum_{i=x}^{\infty} \sum_{y=j}^{k} s'_{iy} \tag{8}$$

where s_{iy}' is the probability that an individual of age x and stage j would survive to age i and stage y. Tuan et al. (2014) defined the reproductive value (v_{xj}) as the contribution of individuals of age x and stage j to the future population. It was calculated as follows:

$$v_{xj} = \frac{e^{r(x+1)}}{s_{xj}} \sum_{i=x}^{\infty} e^{-r(i+1)} \sum_{y=j}^{k} s'_{iy} f_{iy}. \tag{9}$$

The mean values and standard errors of the population parameters, mean longevity of the first to fourth instar nymphs and adults, adult and total pre-reproductive period, and mean fecundity were analyzed using the TWOSEX-MSChart software. The paired bootstrap test (B = 100,000), which was based on the percentile of differences and 95% CI of normalized distribution of differences, was used to compare the differences among treatments. The toxicity of imidacloprid to the adults was analyzed using the log-probit model of SPSS 23.0 and the concentration–mortality regression line. Graphs were generated using SigmaPlot 12.0.

2.7 Transcriptome sequencing

Total RNA was extracted from whole adults using TRIzol according to the method of Wu et al. (2017). The adults for transcriptome sequencing were independently obtained from the F24 generation of the laboratory, field, resistant, and recovering populations. The mRNA of poly-A tail was enriched from the total RNA of adults using Oligo dT magnetic beads. The enriched RNA was then fragmented with a fragmentation buffer, about 200 bp. The cDNA was then synthesized and purified several times using AMPure XP beads to remove small non-target segments from the reaction system. Each qualified cDNA library was sequenced and the

TABLE 1 Toxicity of imidacloprid to adults of the resistant population in different generations.

Generation	Resistant population				
	LC_{50} (CI_{95})[a] (mg/L)	LC_{30} (CI_{95}) (mg/L)	Slope ± SE	χ^2 (df)	*p*
F1	5.636 (0.513–9.590)	3.469 (0.115–6.985)	2.489 ± 0.865	0.444 (5)	0.994
F6	11.832 (5.025–15.773)	8.314 (2.295–12.303)	3.422 ± 0.982	0.505 (5)	0.992
F12	26.504 (24.239–28.987)	22.098 (19.600–24.168)	6.642 ± 0.946	0.481 (5)	0.993
F18	36.761 (31.486–42.354)	26.706 (20.564–31.224)	3.779 ± 0.683	0.451 (5)	0.994
F24	42.247 (36.839–47.540)	32.216 (25.358–36.928)	4.455 ± 0.832	0.39 (5)	0.996

[a]CI_{95} is 95% confidence interval.

TABLE 2 Toxicity of imidacloprid to adults of the recovering population in different generations.

Generation	Recovering population				
	LC_{50} (CI_{95})[a] (mg/L)	LC_{30} (CI_{95}) (mg/L)	Slope ± SE	χ^2 (df)	*P*
F1	41.015 (36.174–45.630)	32.095 (25.735–36.355)	4.924 ± 0.927	0.262 (5)	0.998
F6	39.564 (34.410–44.566)	30.036 (23.281–34.513)	4.382 ± 0.859	0.503 (5)	0.992
F12	33.629 (29.203–37.937)	25.5 (18.694–29.331)	4.363 ± 1.028	0.512 (5)	0.992
F18	27.644 (23.123–32.191)	19.483 (13.155–23.256)	3.451 ± 0.813	0.512 (5)	0.992
F24	23.684 (19.378–28.113)	15.976 (10.280–19.495)	3.067 ± 0.721	0.515 (5)	0.992

[a]CI_{95} is 95% confidence interval.

sequencing company was Wuhan Kangce Technology Co., Ltd. The expression quantity was calculated using the SMEM algorithm of Salmon (v.0.9.1) software with the Perl script abundance_estimates_to_matrix.pl in Trinity (v.2.4.0) software. The threshold was set to | log2 (a fold changes) | > 1 and *p*-value < 0.01. KEGG enrichment analysis was performed using ClusterProfiler (v.3.8.1).

3 Results

3.1 Toxicity of imidacloprid to adults in different generations

The LC_{50} and LC_{30} values of the resistant population in F24 increased by 36.611 and 28.747 when compared with F1, respectively (Table 1). The LC_{50} and LC_{30} values of the recovering population in F24 decreased by 17.331 and 16.119 when compared with F1, respectively (Table 2).

3.2 Tolerance of soybean aphids after termination of imidacloprid stress

After termination of LC_{30} imidacloprid stress, the tolerance of the soybean aphid population decreased, and the resistance ratio of the recovering population in F1 was 18.69; 0.57 lower than that in F24 of the resistant population. The resistance ratio of the recovering population in F24 decreased to 10.79; 8.47 lower than the highest resistance ratio of the resistant population (Figure 2).

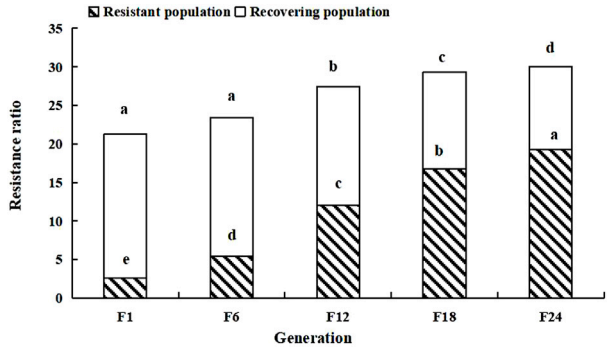

FIGURE 2
Resistance ratio of the soybean aphid population. Different lowercase letters indicate significant difference, and the significance level is 0.05.

3.3 Effects of termination of long-term imidacloprid stress on life history parameters of soybean aphid population

The termination of LC_{30} imidacloprid stress had effects on the developmental duration, lifespan of adults, and fecundity in the recovering population of the F1 generation (Table 3). The developmental time of fourth instar nymphs and the total pre-reproductive period (TPOP) of the F1 recovering population were significantly longer than that of the control, while the developmental

10.3389/fphys.2023.1153249

TABLE 3 Effects of termination of LC_{30} imidacloprid stress on life history parameters of soybean aphid population.

Generation	Stage	Laboratory population control (mean ± SE)	Field population (mean ± SE)	Resistant population (mean ± SE)	Recovering population (mean ± SE)
F1	L1 developmental time (d)	1.22 ± 0.04 a	1.14 ± 0.03 a	1.18 ± 0.04 a	1.20 ± 0.04 a
F1	L2 developmental time (d)	1.2 ± 0.04 b	1.14 ± 0.03 b	1.44 ± 0.06 a	1.17 ± 0.04 b
F1	L3 developmental time (d)	1.13 ± 0.04 b	1.07 ± 0.03 b	1.63 ± 0.11 a	1.12 ± 0.03 b
F1	L4 developmental time (d)	1.01 ± 0.01 c	1.29 ± 0.05 b	1.53 ± 0.10 a	1.32 ± 0.05 b
F1	Mean longevity of adult (d)	11.49 ± 0.56 a	11.92 ± 0.44 a	8.22 ± 0.74 b	11.92 ± 0.44 a
F1	Adult pre-reproductive period (APOP) (d)	0.15 ± 0.04 a	0.08 ± 0.01 a	0.07 ± 0.05 a	0.08 ± 0.03 a
F1	Total pre-reproductive period (TPOP) (d)	4.62 ± 0.07 c	4.73 ± 0.01 bc	5.58 ± 0.12 a	4.86 ± 0.07 b
F1	Fecundity	43.30 ± 1.72 a	44.11 ± 1.46 a	20.14 ± 2.29 b	43.90 ± 1.41 a
F6	L1 developmental time (d)	1.22 ± 0.04 a	1.16 ± 0.04 a	1.18 ± 0.05 a	1.13 ± 0.03 a
F6	L2 developmental time (d)	1.23 ± 0.04 b	1.12 ± 0.03 c	1.48 ± 0.08 a	1.10 ± 0.03 c
F6	L3 developmental time (d)	1.10 ± 0.03 b	1.07 ± 0.03 b	1.46 ± 0.08 a	1.08 ± 0.03 b
F6	L4 developmental time (d)	1.01 ± 0.01 b	1.29 ± 0.05 a	1.34 ± 0.07 a	1.28 ± 0.05 a
F6	Mean longevity of adult (d)	11.86 ± 0.51 a	11.85 ± 0.44 a	9.89 ± 0.74 b	12.25 ± 0.42 a
F6	Adult pre-reproductive period (APOP) (d)	0.14 ± 0.04 a	0.10 ± 0.03 a	0.06 ± 0.03 b	0.04 ± 0.02 b
F6	Total pre-reproductive period (TPOP) (d)	4.66 ± 0.07 b	4.73 ± 0.06 b	5.33 ± 0.13 a	4.64 ± 0.06 b
F6	Fecundity	45.34 ± 1.93 a	46.19 ± 1.44 a	27.48 ± 2.57 b	44.14 ± 1.41 a
F12	L1 developmental time (d)	1.20 ± 0.04 ab	1.14 ± 0.03 b	1.28 ± 0.05 a	1.12 ± 0.03 b
F12	L2 developmental time (d)	1.27 ± 0.04 a	1.15 ± 0.04 b	1.29 ± 0.05 a	1.12 ± 0.03 b
F12	L3 developmental time (d)	1.09 ± 0.03 b	1.07 ± 0.03 b	1.27 ± 0.05 a	1.06 ± 0.02 b
F12	L4 developmental time (d)	1.01 ± 0.01 c	1.29 ± 0.05 a	1.16 ± 0.05 b	1.26 ± 0.04 a
F12	Mean longevity of adult (d)	11.7 ± 0.51 b	11.97 ± 0.42 ab	11.12 ± 0.49 b	13.03 ± 0.41 a
F12	Adult pre-reproductive period (APOP) (d)	0.17 ± 0.04 a	0.08 ± 0.03 b	0.04 ± 0.02 bc	0.02 ± 0.01 c
F12	Total pre-reproductive period (TPOP) (d)	4.70 ± 0.07 b	4.73 ± 0.06 b	5.03 ± 0.08 a	4.59 ± 0.06 b
F12	Fecundity	42.95 ± 1.71 b	44.61 ± 1.47 ab	33.19 ± 1.32 c	47.41 ± 1.44 a
F18	L1 developmental time (d)	1.18 ± 0.04 a	1.14 ± 0.03 ab	1.23 ± 0.05 a	1.11 ± 0.03 b
F18	L2 developmental time (d)	1.29 ± 0.05 a	1.14 ± 0.04 b	1.20 ± 0.05 ab	1.13 ± 0.03 b
F18	L3 developmental time (d)	1.10 ± 0.03 a	1.09 ± 0.03 a	1.16 ± 0.05 a	1.07 ± 0.03 a
F18	L4 developmental time (d)	1.01 ± 0.01 c	1.29 ± 0.05 b	1.44 ± 0.06 a	1.26 ± 0.04 b
F18	Mean longevity of adult (d)	11.57 ± 0.50 b	11.88 ± 0.39 ab	11.40 ± 0.36 b	13.27 ± 0.40 a
F18	Adult pre-reproductive period (APOP) (d)	0.18 ± 0.04 a	0.07 ± 0.03 b	0.09 ± 0.04 b	0.06 ± 0.02 b
F18	Total pre-reproductive period (TPOP) (d)	4.73 ± 0.07 b	4.73 ± 0.06 b	5.15 ± 0.09 a	4.64 ± 0.06 b
F18	Fecundity	42.68 ± 1.64 b	44.17 ± 1.39 a	35.61 ± 1.44 c	47.69 ± 1.40 a
F24	L1 developmental time (d)	1.18 ± 0.04 ab	1.12 ± 0.03 b	1.28 ± 0.05 a	1.14 ± 0.04 b

(Continued on following page)

TABLE 3 (*Continued*) Effects of termination of LC_{30} imidacloprid stress on life history parameters of soybean aphid population.

Generation	Stage	Laboratory population control (mean ± SE)	Field population (mean ± SE)	Resistant population (mean ± SE)	Recovering population (mean ± SE)
F24	L2 developmental time (d)	1.28 ± 0.04 a	1.17 ± 0.04 ab	1.22 ± 0.05 ab	1.16 ± 0.04 b
F24	L3 developmental time (d)	1.11 ± 0.03 a	1.09 ± 0.03 a	1.19 ± 0.05 a	1.09 ± 0.03 a
F24	L4 developmental time (d)	1.01 ± 0.01 b	1.27 ± 0.05 a	1.36 ± 0.06 a	1.26 ± 0.04 a
F24	Mean longevity of adult (d)	12.19 ± 0.49 b	11.94 ± 0.37 b	11.38 ± 0.40 b	13.48 ± 0.40 a
F24	Adult pre-reproductive period (APOP) (d)	0.15 ± 0.04 ab	0.07 ± 0.03 b	0.18 ± 0.04 a	0.11 ± 0.03 ab
F24	Total pre-reproductive period (TPOP) (d)	4.72 ± 0.07 b	4.73 ± 0.05 b	5.23 ± 0.08 a	4.77 ± 0.07 b
F24	Fecundity	43.31 ± 1.71 bc	44.08 ± 1.36 b	39.45 ± 1.38 c	48.34 ± 1.33 a

Standard errors were estimated using 100,000 bootstrap resampling. A paired bootstrap test at the 5% significance level was used to detect differences between treatments. *Note*: L1 is the first instar nymph, L2 is the second instar nymph, L3 is the third instar nymph, and L4 is the fourth instar nymph.

TABLE 4 Effects of termination of LC_{30} imidacloprid stress on the reproductive parameters of soybean aphid population.

Generation	Parameters	Laboratory population control (mean ± SE)	Field population (mean ± SE)	Resistant population (mean ± SE)	Recovering population (mean ± SE)
F1	r	0.438 ± 0.008 a	0.445 ± 0.006 a	0.239 ± 0.015 b	0.440 ± 0.006 a
F1	λ	1.549 ± 0.012 a	1.560 ± 0.009 a	1.271 ± 0.019 b	1.552 ± 0.009 a
F1	R_0	37.24 ± 2.109 b	41.9 ± 1.686 a	11.68 ± 1.651 c	42.14 ± 1.600 a
F1	T	8.26 ± 0.080 c	8.40 ± 0.083 bc	10.26 ± 0.215 a	8.51 ± 0.095 b
F6	r	0.425 ± 0.007 a	0.452 ± 0.005 a	0.288 ± 0.014 b	0.451 ± 0.005 a
F6	λ	1.529 ± 0.011 a	1.571 ± 0.008 a	1.333 ± 0.019 b	1.570 ± 0.008 a
F6	R_0	39.45 ± 2.267 b	44.34 ± 1.649 a	17.86 ± 2.111 c	42.82 ± 1.559 a
F6	T	8.66 ± 0.099 b	8.40 ± 0.084 cd	10.02 ± 0.213 a	8.33 ± 0.079 d
F12	r	0.429 ± 0.007 a	0.443 ± 0.006 a	0.366 ± 0.010 b	0.461 ± 0.005 a
F12	λ	1.536 ± 0.011 a	1.557 ± 0.009 a	1.441 ± 0.014 b	1.585 ± 0.007 a
F12	R_0	37.80 ± 2.050 b	42.83 ± 1.664 a	24.89 ± 1.744 c	46.94 ± 1.505 a
F12	T	8.47 ± 0.096 b	8.49 ± 0.084 b	8.79 ± 0.109 a	8.36 ± 0.076 b
F18	r	0.430 ± 0.007 a	0.438 ± 0.005 a	0.368 ± 0.011 b	0.457 ± 0.005 a
F18	λ	1.537 ± 0.011 a	1.550 ± 0.008 a	1.445 ± 0.015 b	1.579 ± 0.008 a
F18	R_0	37.56 ± 2.000 c	42.40 ± 1.592 b	24.93 ± 1.919 d	47.21 ± 1.463 a
F18	T	8.43 ± 0.103 b	8.55 ± 0.082 ab	8.74 ± 0.126 a	8.44 ± 0.080 b
F24	r	0.426 ± 0.007 a	0.439 ± 0.005 a	0.373 ± 0.009 b	0.449 ± 0.005 a
F24	λ	1.531 ± 0.011 a	1.551 ± 0.008 a	1.453 ± 0.013 b	1.567 ± 0.008 a
F24	R_0	38.11 ± 2.058 b	42.32 ± 1.564 b	29.19 ± 2.008 c	47.37 ± 1.470 a
F24	T	8.54 ± 0.099 b	8.54 ± 0.075 b	9.04 ± 0.103 a	8.59 ± 0.009 b

Standard errors were estimated using 100,000 bootstrap resampling. A paired bootstrap test at the 5% significance level was used to detect differences between treatments. *Note*: r is intrinsic rate of increase, λ is finite rate of increase, R_0 is net reproductive rate, and T is mean generation time.

time of the second to fourth instar nymphs and the total pre-reproductive period (TPOP) were significantly shorter than that of the resistant population. Also, the lifespan of the adults was significantly longer and the fecundity significantly higher than those of the resistant population ($p < 0.05$). The effects of termination of imidacloprid stress on the developmental duration of the soybean aphid, lifespan, and pre-reproductive period of F6 were similar to those of F1. In F12, the longest lifespan of the

adults in the recovering population was 13.03 days, which was 11.37% longer than that of the control group. The fecundity of the recovering population was 1.1, 1.06, and 1.43 times higher than that of the control, field population, and resistant population, respectively. In F18, the minimum adult pre-reproductive period (APOP) of the recovering population was 0.06 days, which was 33.33%, 85.71%, and 66.67% of the control, field population, and resistant population, respectively. The fecundity of the recovering population in F24 continued to increase and was 1.12, 1.1, and 1.23 times higher than that of the control, field population, and resistant populations, respectively (Table 3).

3.4 Effects of termination of long-term imidacloprid stress on reproductive parameters of soybean aphid population

The termination of LC_{30} imidacloprid stress affected related reproductive parameters of the recovering population in F1 (Table 4). The intrinsic rate of increase (r) and finite rate of increase (λ) of the recovering population were significantly higher than those of the resistant population. The net reproductive rate (R_0) of the recovering population was 1.13 and 3.61 times higher than that of the control and resistant populations, respectively. After termination of imidacloprid stress, the mean generation time (T) of the recovering population was significantly shorter than that of the resistant population, but significantly longer than that of the control. The intrinsic rate of increase (r), the finite rate of increase (λ), and net reproduction rate (R_0) of the recovering population increased by 2.50%, 1.16%, and 1.61%, respectively, when compared with the corresponding parameter values of the F1. The intrinsic rate of increase (r), the finite rate of increase (λ), and net reproduction rate (R_0) of the recovering population in F12 increased by 2.22%, 0.96%, and 9.62% when compared with the F6 generation, respectively. The net reproductive rate (R_0) of the recovering population in F18 was the highest, which was 1.26, 1.11, and 1.89 times higher than that of the control, field, and resistant populations, respectively. The net reproductive rate (R_0) of the recovering population in F24 was significantly higher than that of the control group and field population (Table 4).

3.5 Effects of termination of long-term imidacloprid stress on age–stage survival rate (s_{xj}) and fertility of soybean aphid population

Results showed that the age–stage survival rate (s_{xj}) of the aphids overlapped (Figure 3). The probability of newly hatched nymphs reaching the adult stage for the recovering population in F1 was 0.96, while that for the control, field, and resistant populations was 0.86, 0.95, and 0.58, respectively. In F1, the peak of adults in the recovering population appeared on the seventh day, 1 day later than that of the control. The age–stage survival rate (s_{xj}) of the recovering population in F12 was higher than that in F1. The probability of the soybean aphid of the recovering population successfully entering the adult stage was 0.99, which was 0.03 higher than that in the F1. In F24, the probability of the recovering population successfully entering the adult stage was 0.98, 0.1, 0.02, and 0.24 higher than that of the control, field, and resistant populations, respectively.

The survival curves of the control, field, and recovering populations showed a convex trend. However, the daily survival rate curve of the resistant population decreased sharply within 24 h, with the curve following a concave trend (Figure 4). The age-specific fecundity peak (m_x) of the recovering population in F1 was 5.69, 2.57 and 0.33 higher than that of the resistant and field populations, respectively, but 1.72 lower than that of the control. The m_x peak of the recovering population in F24 was 5.32, which was 0.58 higher than that of the resistant population, but 0.75 and 0.02 lower than that of the control and field population, respectively (Figure 4). In addition, termination of LC_{30} imidacloprid stress significantly improved the reproductive value (v_{xj}) (Supplementary Figure S1) and life expectancy (e_{xj}) (Supplementary Figure S2) of the recovering population.

3.6 Differentially expressed genes

We found that the number of differentially expressed genes between the recovering population and the laboratory population was the largest, which was 3,573. There were 581 different genes between the recovering population and resistant population, and 764 different genes between the recovering population and field population (Figure 5).

3.7 KEGG pathway enrichment analysis of differentially expressed genes

The enrichment analysis of KEGG pathways between the recovering population and laboratory population showed that all differentially expressed genes were distributed in 119 metabolic pathways. The significantly upregulated pathways related to population development and reproduction were longevity-regulating pathway—worm (ko04015), oocyte meiosis (ko04114), valine, leucine, and isoleucine degradation (ko00280), steroid hormone biosynthesis (ko00140), progesterone-mediated oocyte maturation (ko04914), and Rap1 signaling pathway (ko04015), Hedgehog signaling pathway (ko04340), and Notch signaling pathway (ko04330), all involved in the regulation of cell proliferation. The downregulated pathway was the Hippo signaling pathway (ko04391), which could inhibit cell growth and apoptosis (ko04214) (Figure 6A). All differentially expressed genes between the recovering population and field population were distributed in 40 metabolic pathways. The significantly upregulated pathways related to population development and reproduction were lysine degradation (ko00310), valine, leucine, and isoleucine degradation (ko00280), oocyte meiosis

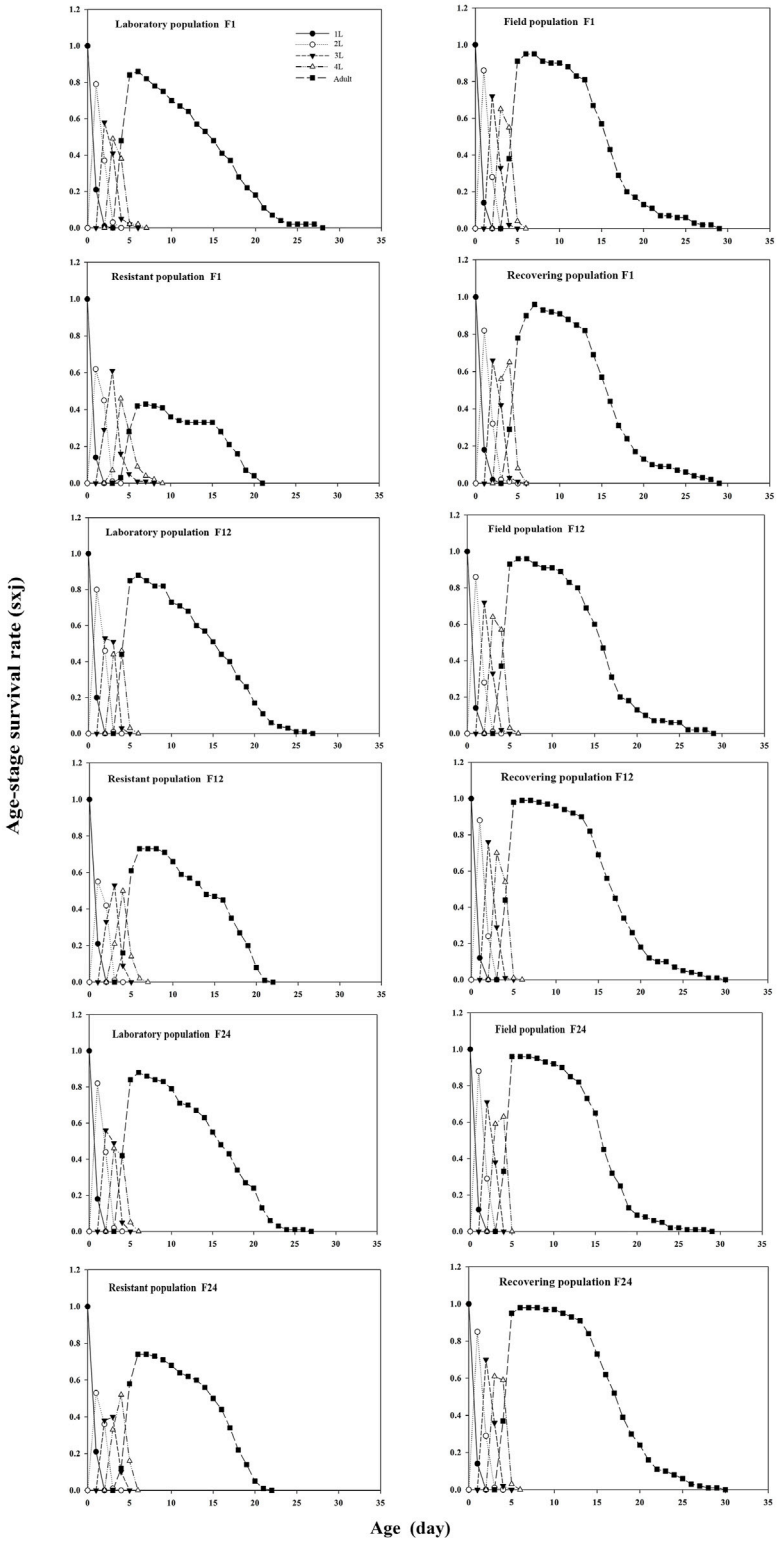

FIGURE 3
Effects of termination of LC_{30} imidacloprid stress on the age–stage survival rate (s_{xj}) of the soybean aphid population. *Note*: 1L is the first instar nymphs, 2L is the second instar nymphs, 3L is the third instar nymphs, and 4L is the fourth instar nymphs.

(ko04114), and cell cycle (ko04110). The downregulated pathways were glycine, serine, and threonine metabolism (ko00260), estrogen signaling pathway (ko04915), and retinol metabolism (ko00830) (Figure 6B). All differentially expressed genes between the recovering and resistant populations were distributed in 41 metabolic pathways, among which significantly upregulated

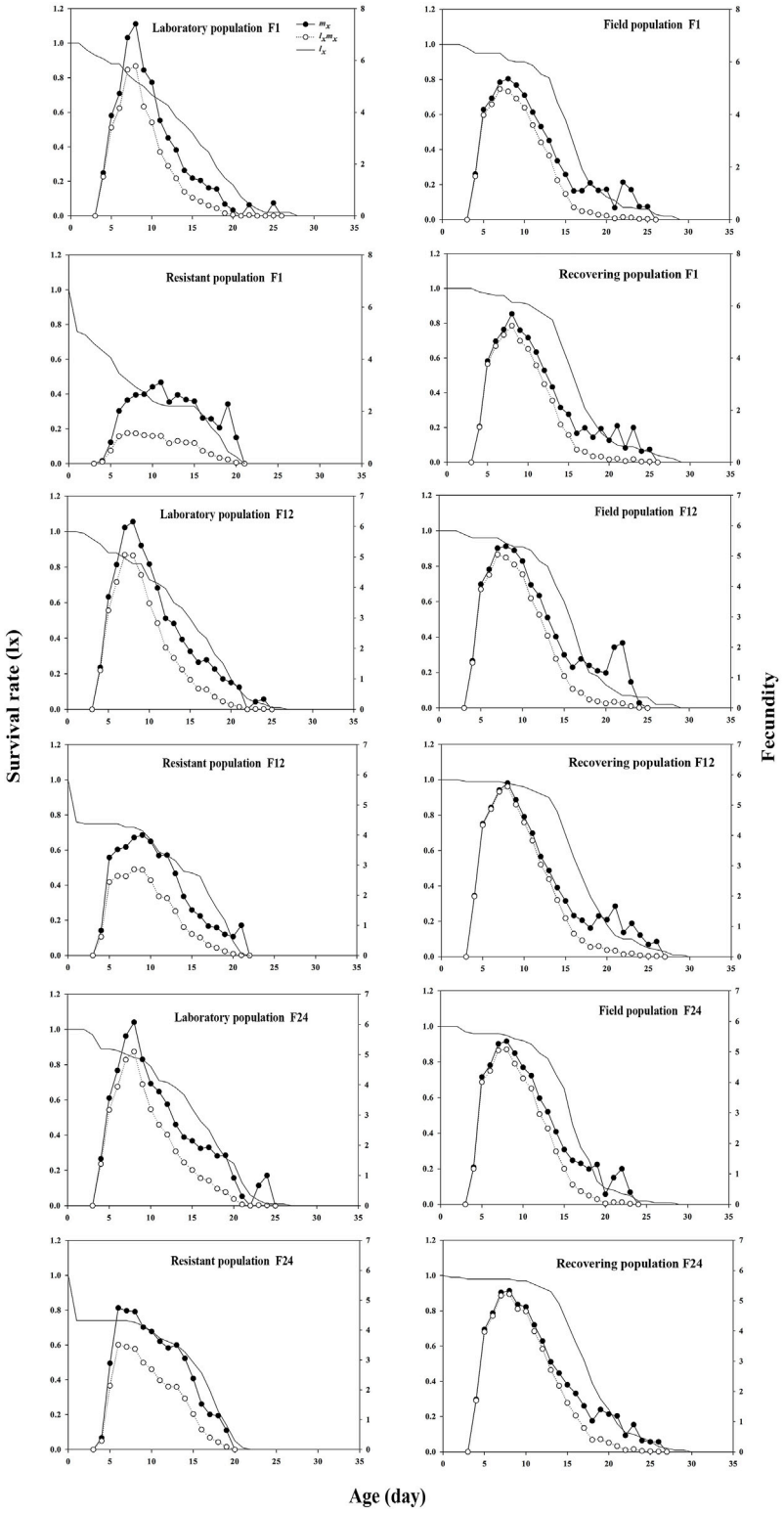

FIGURE 4
Effects of termination of LC_{30} imidacloprid stress on the age specific survival rate (l_x) and fecundity (m_x) of soybean aphid.

pathways related to population development and reproduction were oocyte meiosis (ko04114), cell cycle (ko04110), glycine, serine, and threonine metabolism, and longevity regulating pathway—worm (ko04015). The downregulated pathway was the Hippo signaling pathway (ko04391) that inhibited cell growth (Figure 6C).

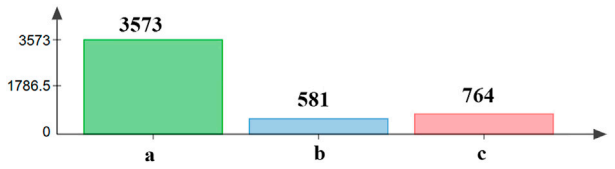

FIGURE 5
Analysis of differentially expressed genes between the recovering population and other populations. a—differentially expressed genes between the recovering population and laboratory population. b—differentially expressed genes between the recovering population and resistant population. c—differentially expressed genes between the recovering population and field population.

4 Discussion

Multi-generations of pests frequently exposed to insecticides could lead to a decrease in sensitivity (Pathan et al., 2008; Mansoor et al., 2017). In this study, results showed that the tolerance of the soybean aphid to imidacloprid of resistant populations increased over generations, while that of recovering populations decreased after termination of LC_{30} imidacloprid stress. A study found that the ability of parents to cope with stress was limited, and once the stress intensity exceeded the limit, the negative effects of the stress were passed on to offspring. These negative effects were reflected in the effects on the developmental time of the individual, fertility, and longevity of the offspring (Cao et al., 2021). We found that the termination of LC_{30} imidacloprid stress prolonged the developmental time and the total pre-reproductive period (TPOP) of the recovering population in F1 when compared to that of the control. It indicated that even in the absence of imidacloprid stress, the negative effects of the stress on soybean aphid parents were still transmitted to the offspring, which weakened the biological fitness of the population. A similar finding on the effects of acetamiprid stress on the biological fitness of the *Aphis gossypii* was reported (Ullah et al., 2020b). Our results showed that the longevity of adults and fecundity of the recovering population exceeded those of the laboratory population, from the F12. These results showed that the soybean aphid population accelerated its recovery after removal of imidacloprid stress, indicated by an increase in the population size across generations. This might be because the soybean aphid parents no longer required to use more energy to improve its tolerance to stress, and the offspring could obtain more resources for development and reproduction (Rugno et al., 2016; Tang et al., 2019; Cao et al., 2021).

The physiological and behavioral changes in the recovering population occurred after the removal of low-dose imidacloprid stress. The soybean aphids shortened the time required to enter the reproductive stage and quickly produced offspring, which promoted their recovery and adaptability. In addition, the life history parameters of the recovering population were similar to those for the field population, which might be related to the long-term exposure of the field population to low doses of imidacloprid.

Insecticides are degraded by bacteria, fungi, microorganisms, animals, and the natural environment in the field after application, which results in the lowering of the initial concentrations applied (Desneux et al., 2005; Desneux et al., 2007). Exposure of the soybean aphids to low doses of insecticides in the field was aided by the drifting and degradation of insecticides (Rix et al., 2016). Our results showed that low-dose imidacloprid had a stimulating effect on soybean aphids from the F12 generation, as the reproductive capacity of the recovering population was significantly higher than that of the laboratory population. This faster increase of the population may hinder the control of the soybean aphid in the field, seriously threaten the production of soybean and other crops, and might lead to an early outbreak of the soybean aphids in the field. Therefore, it is necessary to monitor the dynamics of soybean aphid populations and determine the type and dosage of insecticides to be applied, according to their developmental and reproductive characteristics (Rugno et al., 2015; Gordy et al., 2021; Holland et al., 2021).

We found out that the mean generation time (T) of the recovering population in F1 was still longer than that of the control even after the removal of imidacloprid stress, indicating that the low dose of imidacloprid inhibited the development of the soybean aphid population, but the inhibitory effect gradually weakened over generations. The ability of the recovering population to reproduce increased dramatically, and as generations passed, it diverged further from the laboratory population. This was probably related to the intergenerational effect of low-dose imidacloprid on the soybean aphid population (Peng et al., 2019). The soybean aphid recovered its adaptability across generations after the removal of imidacloprid stress. The time required for soybean aphids to enter the adult stage gradually advanced in each generation, and the proportion of soybean aphid individuals increased across generations.

The results also showed that the probability of a newly born nymph reaching the adult stage of the recovering population was the highest in F1. This indicated that removal of the low-dose imidacloprid stress accelerated the adaptive recovery of the soybean aphid population. In F24, the reproductive value in the recovering population exceeded that of the field and resistant populations. The fertility of the soybean aphid population increased slowly across generations after removal of imidacloprid stress. The reproductive value of the recovering population fluctuated in the late life history of the soybean aphid, which was probably related to their longevity. In addition, the reproductive value (v_{xj}) and life expectancy (e_{xj}) of the recovering population were very similar to those of the field soybean aphid population, which may be due to the effect of pharmacodynamic stress on the field population. When imidacloprid stress was terminated, the adaptive strategies of the soybean aphid population were adjusted across generations. The growth and development of the soybean aphid in the earlier generation were still inhibited, but the fecundity and population growth rate increased greatly in later generations. The stimulation of early generations of insects plays an important role in the induction of individual phenotypes and even intergenerational types in offspring. These phenotypes are mainly related to development, longevity, and fecundity (Xing et al., 2019; Zhao et al., 2019). Insects with frequent generations and relatively short life cycle, such as soybean aphids, are easily stimulated during their development. Meanwhile, maternal stress not only affects contemporary individuals but also affects the differential expression of developmental pathways in offspring through intergenerational effects (Zhao et al., 2017; Tran et al., 2018; Peng et al., 2019).

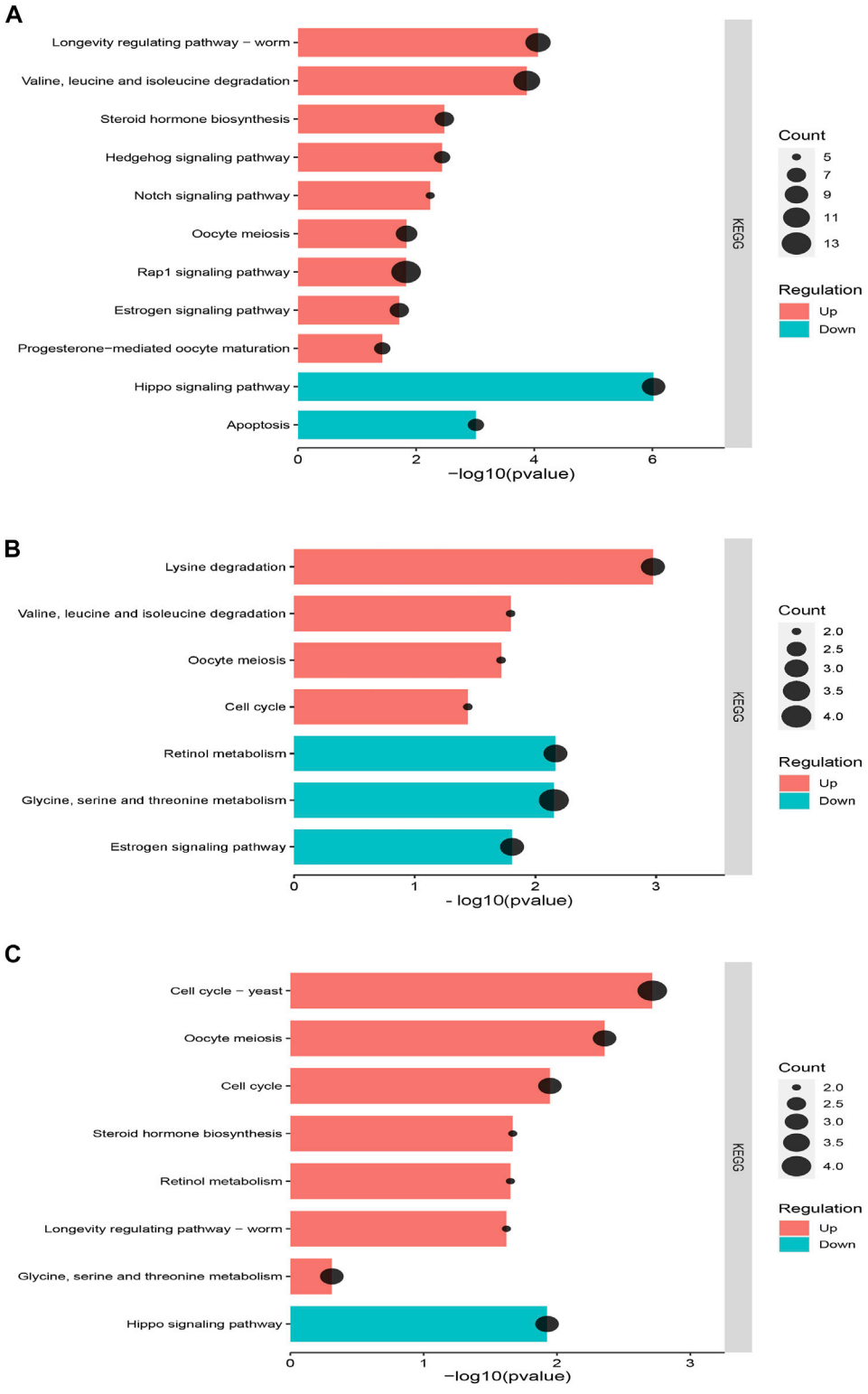

FIGURE 6
KEGG pathway enrichment analysis of differentially expressed genes between the recovering population and other populations. **(A)** KEGG pathway enrichment analysis between the recovering population and laboratory population. **(B)** KEGG pathway enrichment analysis between the recovering population and field population. **(C)** KEGG pathway enrichment analysis between the recovering population and resistant population. The horizontal axis represents the enrichment significance, which is represented by –log10 (*p*-value). The vertical axis represents the enriched KEGG pathway. The dot size indicates the number of differential genes contained in the KEGG pathway.

Compared with the other populations after termination of imidacloprid stress, a large number of upregulated pathways in the recovering population were mainly related to cell division, cell proliferation, oocyte meiosis and maturation, and amino acid metabolism. Cell division and proliferation are fundamental to the growth and reproduction of organisms (Belluccini et al., 2021). The Hedgehog signaling pathway, Notch signaling pathway, and Rap1 signaling pathway co-regulate cell fate, proliferation, and differentiation in the recovering population (Wang et al., 2010). The activation of these signaling pathways might promote the rapid proliferation of oocytes and the development and maturation of embryos, which might be the reason why the fertility of the recovering population was higher than that of the other populations. In the absence of imidacloprid stress, the activated amino acid metabolism in the recovering population is indicated by the significant upregulation of the metabolic pathways of valine, leucine, and isoleucine. These play important roles in the energy supply for population reproduction and the synthesis of large amounts of growth hormones (Hurley and Bryson, 2022), which ensures that the soybean aphid has sufficient energy to resist the negative effects from the mother. The nutrients and energy that offspring received from their mothers were also used more for development and reproduction, which might be one of the reasons for the increased fertility of the recovering population. In addition, the longevity of adults of the recovering populations was significantly higher than that of the other populations, which might be related to the upregulated expression of the longevity regulation pathway in the recovering population.

Our study serves as an important reference for understanding the changes in adaptation strategies of soybean aphids across generations when their exposure to low-dose imidacloprid stress is terminated. It also provides important data for monitoring the population dynamics of the soybean aphid in the field and analyzing the degree of pharmacodynamic stress.

5 Conclusion

This study investigated the effects of termination of imidacloprid stress on the development, reproduction, and metabolism of the soybean aphid. We found that despite the absence of imidacloprid pressure, intergenerational stimuli still affected the adaptive strategies of the recovering population. This effect was manifested as inhibiting the growth and development of individuals in the early generations and improving the fecundity in the later generations. Adaptive soybean aphid populations would surge in the absence of imidacloprid pressure. This study provides an important reference for exploring the adaptability of the *A. glycines* population under termination of stress from low lethal concentrations of imidacloprid, across generations.

Data availability statement

The raw data supporting the conclusion of this article will be made available by the authors, without undue reservation.

Author contributions

AZ, ND, LH, and ZQ designed the research. AZ and WZ conceived the experiments. YG and DW analyzed the data. AZ drafted the manuscript. ZL, MF, HC, and LH revised and finalized the manuscript. All authors contributed to the article and approved the submitted version.

Funding

This work was supported by the National key research and development program (2021YFD1201103), the Heilongjiang Science Foundation Project (grant number C2018011), Special Fund for Construction of Modern Agricultural Industry Technology System (grant number CARS-04), and Research and Development of Technology and Products on Nature Enemy Insects Prevent and Control (No: 2017YFD0201000).

Conflict of interest

The authors declare that the research was conducted in the absence of any commercial or financial relationships that could be construed as a potential conflict of interest.

Publisher's note

Supplementary material

The Supplementary Material for this article can be found online at: https://www.frontiersin.org/articles/10.3389/fphys.2023.1153249/full#supplementary-material

References

Aseperi, A. K., Busquets, R., Hooda, P. S., Cheung, P. C. W., and Barker, J. (2020). Behaviour of neonicotinoids in contrasting soils. *J. Environ. Manag.* 276, 111329. doi:10.1016/j.jenvman.2020.111329

Belluccini, G., López-García, M., Lythe, G., and Molina-París, C. (2021). A multi-stage model of cell proliferation and death: Tracking cell divisions with erlang distributions. arXiv e-prints.

Bevill, R. L., and Louda, S. M. (1999). Comparisons of related rare and common species in the study of plant rarity. *Conserv. Biol.* 13, 493–498. doi:10.1046/j.1523-1739.1999.97369.x

Cao, J. Y., Xing, K., and Zhao, F. (2021). Complex delayed and transgenerational effects driven by the interaction of heat and insecticide in the maternal generation of the wheat aphid, *Sitobion avenae*. *Pest Manag. Sci.* 77, 4453–4461. doi:10.1002/ps.6480

Chi, H. (1988). Life-table analysis incorporating both sexes and variable development rates among individuals. *Environ. Entomol.* 17, 26–34. doi:10.1093/ee/17.1.26

Chi, H., and Liu, H. (1985). Two new methods for the study of insect population ecology. *Bull. Inst. Zool.* 24, 225–240.

Chi, H., and Su, H. Y. (2006). Age-stage, two-sex life tables of Aphidius gifuensis (Ashmead) (Hymenoptera: Braconidae) and its host *Myzus persicae* (Sulzer) (Homoptera: Aphididae) with mathematical proof of the relationship between female fecundity and the net reproductive rate. *Environ. Entomol.* 35, 10–21. doi:10.1603/0046-225x-35.1.10

Chi, H., You, M., Atlihan, R., Smith, C. L., Kavousi, A., Ozgokce, M. S., et al. (2020). Age- Stage, two-sex life table: An introduction to theory, data analysis, and application. *Entomol. Gen.* 40, 103–124. doi:10.1127/entomologia/2020/0936

Desneux, N., Decourtye, A., and Delpuech, J. M. (2007). The sublethal effects of pesticides on beneficial arthropods. *Annu. Rev. Entomol.* 52, 81–106. doi:10.1146/annurev.ento.52.110405.091440

Desneux, N., Fauvergue, X., Dechaume-Moncharmont, F. X., Kerhoas, L., Ballanger, Y., and Kaiser, L. (2005). Diaeretiella rapae limits *Myzus persicae* populations after applications of deltamethrin in oilseed rape. *J. Econ. Entomol.* 98, 9–17. doi:10.1093/jee/98.1.9

Devine, G. J., Harling, Z. K., Scarr, A. W., and Devonshire, A. L. (1996). Lethal and sublethal effects of imidacloprid on nicotine-tolerant Myzus nicotianae and *Myzus persicae*. *Pest Manag. Sci.* 48, 57–62. doi:10.1002/(sici)1096-9063(199609)48:1<57::aid-ps435>3.0.co;2-9

Fenner, K., Canonica, S., Wackett, L. P., and Elsner, M. (2013). Evaluating pesticide degradation in the environment: Blind spots and emerging opportunities. *Science* 341, 752–758. doi:10.1126/science.1236281

Goodman, D. (1982). Optimal life histories, optimal notation, and the value of reproductive value. *Am. Nat.* 119, 803–823. doi:10.1086/283956

Gordy, J. W., Seiter, N. J., Kerns, D. L., Reay-Jones, F., Bowling, R. D., Way, M. O., et al. (2021). Field assessment of aphid doubling time and yield of sorghum susceptible and partially resistant to sugarcane aphid (Hemiptera: Aphididae). *J. Econ. Entomol.* 5, 2076–2087. doi:10.1093/jee/toab135

Hesler, L. S., and Beckendorf, E. A. (2021). Soybean aphid infestation and crop yield in relation to cultivar, foliar insecticide and insecticidal seed treatment in South Dakota. *Phytoparasitica* 7, 971–981. doi:10.1007/s12600-021-00914-y

Holland, J. M., Mchugh, N. M., and Salinari, F. (2021). Field specific monitoring of cereal yellow dwarf virus aphid vectors and factors influencing their immigration within fields. *Pest Manag. Sci.* 77, 4100–4108. doi:10.1002/ps.6435

Hopper, K. R., Lanier, K., Rhoades, J. H., Hoelmer, K. A., Meikle, W. G., Heimpel, G. E., et al. (2017). Host specificity of Aphelinus species collected from soybean aphid in Asia. *Biol. Control.* 115, 55–73. doi:10.1016/j.biocontrol.2017.09.004

Huang, Y. B., and Chi, H. (2012). Age-stage, two-sex life tables of *Bactrocera cucurbitae* (Coquillett) (Diptera: Tephritidae) with a discussion on the problem of applying females age-specific life tables to insect populations. *Insect Sci.* 19, 263–273. doi:10.1111/j.1744-7917.2011.01424.x

Hullé, M., Chaubet, B., Turpeau, E., and Simon, J. C. (2020). Encyclop'Aphid: A website on aphids and their natural enemies. *Entomol. Gen.* 40, 97–101. doi:10.1127/entomologia/2019/0867

Hurley, W. L., and Bryson, J. M. (2022). *Mammary gland metabolism of amino acids in the lactating sow: An* in vitro *study*. Berlin, Germany: Springer.

James, M., Patrick, B., Anitha, C., Cole, D., John, G., Phillip, G., et al. (2020). Implementation of a diagnostic-concentration bioassay for detection of susceptibility to pyrethroids in soybean aphid (Hemiptera: Aphididae). *J. Econ. Entomol.* 113, 932–939. doi:10.1093/jee/toz351

Ma, J., Wang, R., Li, X., Gao, B., and Chen, S. (2016). Transcriptome and gene expression analysis of *Cylas formicarius* (Coleoptera: Brentidae) during different development stages. *J. Insect Sci.* 63, 63. doi:10.1093/jisesa/iew053

Mansoor, M. M., Raza, A. B., Abbas, N., Aqueel, M. A., and Afzal, M. (2017). Resistance of green lacewing, *Chrysoperla carnea* Stephens to nitenpyram: Cross-resistance patterns, mechanism, stability, and realized heritability. *Pestic. Biochem. Physiol.* 135, 59–63. doi:10.1016/j.pestbp.2016.06.004

Mokbel, E. (2019). Resistance risk assessment: Realized heritability, cross resistance and resistance stability of acetamiprid in the cotton aphid, *Aphis gossypii* Glover (Homoptera: Aphididae). *J. Plant Prot. Res.* 58, 328–334. doi:10.24425/jppr.2018.124641

Pathan, A. K., Sayyed, A. H., Aslam, M., Razaq, M., Jilani, G., and Saleem, M. A. (2008). Evidence of field-evolved resistance to organophosphates and pyrethroids in *Chrysoperla carnea* (Neuroptera: Chrysopidae). *J. Econ. Entomol.* 101, 1676–1684. doi:10.1603/0022-0493(2008)101[1676:eofrto]2.0.co;2

Peng, X., Zhao, Q., Guo, X., Su, S., Chen, M., Li, Y., et al. (2019). Effects of variable maternal temperature on offspring development and reproduction of *Rhopalosiphum padi*, a serious global pest of wheat. *Ecol. Entomol.* 45, 269–277. doi:10.1111/een.12796

Ragsdale, D. W., Landis, D. A., Brodeur, J., Heimpel, G. E., and Desneux, D. (2011). Ecology and management of the soybean aphid in North America. *Annu. Rev. Entomol.* 56, 375–399. doi:10.1146/annurev-ento-120709-144755

Rajotte, E. G., and Rosa, C. (2022). The effect of species soybean vein necrosis orthotospovirus (svnv) on life table parameters of its vector, soybean thrips (*Neohydatothrips variabilis* Thysanoptera: Thripidae). *Insects* 13, 632. doi:10.3390/insects13070632

Rix, R. R., Ayyanath, M. M., and Cutler, G. C. (2016). Sublethal concentrations of imidacloprid increase reproduction, alter expression of detoxification genes, and prime *Myzus persicae* for subsequent stress. *J. Pest Sci.* 89, 581–589. doi:10.1007/s10340-015-0716-5

Rugno, G. R., Zanardi, O. Z., Cuervo, J. B., Morais, M. R., and Yamamoto, P. T. (2016). Impact of insect growth regulators on the predator *Ceraeochrysa cincta* (Schneider) (Neuroptera: Chrysopidae). *Ecotoxicology* 25, 940–949. doi:10.1007/s10646-016-1651-9

Rugno, G. R., Zanardi, O. Z., and Yamamoto, P. T. (2015). Are the pupae and eggs of the lacewing *Ceraeochrysa cubana* (Neuroptera: Chrysopidae) tolerant to insecticides? *J. Econ. Entomol.* 108, 2630–2639. doi:10.1093/jee/tov263

Stamm, M. D., Heng-Moss, T. M., Baxendale, F. P., Siegfried, B. D., Blankenship, E. E., and Nauen, R. (2016). Uptake and translocation of imidacloprid, clothianidin and flupyradifurone in seed-treated soybeans. *Pest Manag. Sci.* 72, 1099–1109. doi:10.1002/ps.4152

Tang, Q., Ma, K., Chi, H., Hou, Y., Gao, X., and Desneux, N. (2019). Transgenerational hormetic effects of sublethal dose of flupyradifurone on the green peach aphid, *Myzus persicae* (Sulzer) (Hemiptera: Aphididae). *PLoS One* 14, e0208058. doi:10.1371/journal.pone.0208058

Todd, J. C., Stewart, L. R., Redinbaugh, M. G., and Wilson, J. R. (2022). Soybean aphid (Hemiptera: Aphididae) feeding behavior is largely unchanged by soybean mosaic virus but significantly altered by the beetle-transmitted bean pod mottle virus. *J. Econ. Entomol.* 4, 1059–1068. doi:10.1093/jee/toac060

Tran, T. T., Janssens, L., Dinh, K. V., and Stoks, R. (2018). Transgenerational interactions between pesticide exposure and warming in a vector mosquito. *Evol. Appl.* 11, 906–917. doi:10.1111/eva.12605

Tuan, S. J., Li, N. J., Yeh, C. C., Tang, L. C., and Chi, H. (2014). Effects of green manure cover crops on *Spodoptera litura* (Lepidoptera: Noctuidae) populations. *J. Econ. Entomol.* 107, 897–905. doi:10.1603/ec13435

Ullah, F., Gul, H., Desneux, N., Qu, Y., Xiao, X., Khattak, A. M., et al. (2019). Acetamiprid-induced hormetic effects and vitellogenin gene (*Vg*) expression in the melon aphid, *Aphis gossypii*. *Entomol. Gen.* 39, 259–270. doi:10.1127/entomologia/2019/0887

Ullah, F., Gul, H., Tariq, K., Desneux, N., and Song, D. (2020b). Acetamiprid resistance and fitness costs of melon aphid, *Aphis gossypii*: An age-stage, two-sex life table study. *Pestic. Biochem. Phys.* 171, 104729. doi:10.1016/j.pestbp.2020.104729

Ullah, F., Gul, H., Tariq, K., Desneux, N., and Song, D. (2020a). Thiamethoxam induces transgenerational hormesis effects and alteration of genes expression in Aphis gossypii. *Pestic. Biochem. Phys.* 165, 104557. doi:10.1016/j.pestbp.2020.104557

Valmorbida, I., Coates, B. S., Hodgson, E. W., Ryan, M., and O'Neal, M. E. (2022). Evidence of enhanced reproductive performance and lack-of-fitness costs among soybean aphids, Aphis glycines, with varying levels of pyrethroid resistance. *Pest Manag. Sci.* 5, 2000–2010. doi:10.1002/ps.6820

Wang, Z., Li, Y., Kong, D., and Sarkar, F. H. (2010). The role of notch signaling pathway in epithelial-mesenchymal transition (emt) during development and tumor aggressiveness. *Curr. Drug Targets.* 11, 745–751. doi:10.2174/138945010791170860

Wu, S., Huang, Z., Rebeca, C. L., Zhu, X., Zhang, F., Lin, Q., et al. (2017). De novo characterization of the pine aphid *Cinara pinitabulaeformis* Zhang et Zhang transcriptome and analysis of genes relevant to pesticides. *Plos One* 12 (6), e0178496. doi:10.1371/journal.pone.0178496

Xing, K., Hoffmann, A. A., Zhao, F., and Ma, C. (2019). Wide diurnal temperature variation inhibits larval development and adult reproduction in the diamondback moth. *J. Therm. Biol.* 84, 8–15. doi:10.1016/j.jtherbio.2019.05.013

Zhang, A., Han, L., Zhao, K., Zhu, L., and Liu, T. (2021). Effects of imidacloprid and thiamethoxam on the development and reproduction of the soybean aphid *Aphis glycines*. *Plos One* 16, e0250311. doi:10.1371/journal.pone.0250311

Zhang, A., Xu, L., Liu, Z., Zhang, J., Zhao, K., and Han, L. (2022). Effects of acetamiprid at low and median lethal concentrations on the development and reproduction of the soybean aphid *Aphis glycines*. *Insects* 13, 87. doi:10.3390/insects13010087

Zhao, F., Hoffmann, A. A., Xing, K., and Ma, C. S. (2017). Life stages of an aphid living under similar thermal conditions differ in thermal performance. *J. Insect Physiol.* 99, 1–7. doi:10.1016/j.jinsphys.2017.03.003

Zhao, F., Xing, K., Hoffmann, A. A., and Ma, C. S. (2019). The importance of timing of heat events for predicting the dynamics of aphid pest populations. *Pest Manag. Sci.* 75, 1866–1874. doi:10.1002/ps.5344

Frontiers in Physiology

Understanding how an organism's components work together to maintain a healthy state

The second most-cited physiology journal, promoting a multidisciplinary approach to the physiology of living systems - from the subcellular and molecular domains to the intact organism and its interaction with the environment.

Discover the latest Research Topics

See more →

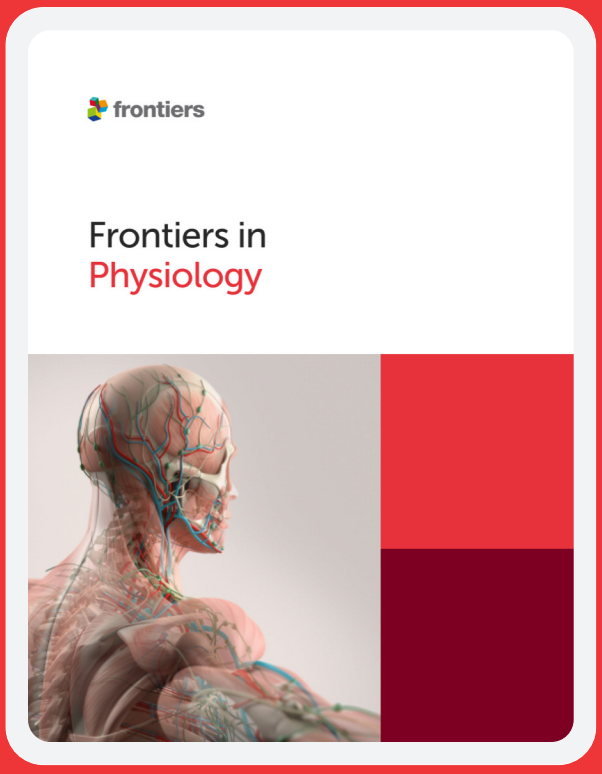

Frontiers

Avenue du Tribunal-Fédéral 34
1005 Lausanne, Switzerland
frontiersin.org

Contact us

+41 (0)21 510 17 00
frontiersin.org/about/contact